ZINC FINGER TEMPLATE MEDIATED DNA RECOGNITION

SYNTHESIS AND DNA INTERACTION STUDIES WITH TEMPLATE PROTOTYPES

A Thesis Submitted
in Partial Fulfilment of the Requirements
for the Degree of

DOCTOR OF PHILOSOPHY

by

NARAYANASWAMY JAYARAMAN

to the

DEPARTMENT OF CHEMISTRY

INDIAN INSTITUTE OF TECHNOLOGY KANPUR

July, 1993

TO MY PARENTS

STATEMENT

I hereby declare that the matter embodied in this thesis is the result of investigations carried out by me in the Department of Chemistry, Indian Institute of Technology, Kanpur, India, under the supervision of Professor S. Ranganathan.

In keeping with the general practice of reporting scientific observations due acknowledgements have been made wherever the work embodied is based on the findings of other investigators.

N. JAYARAMAN

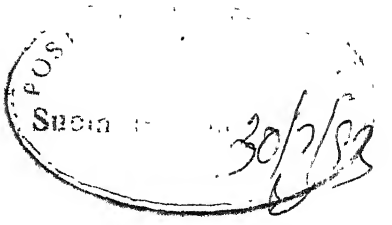

CERTIFICATE

Certified that the work contained in this thesis, entitled, "ZINC FINGER MEDIATED DNA RECOGNITION: SYNTHESIS AND DNA INTERACTION STUDIES WITH TEMPLATE PROTOTYPES" has been carried out by Mr. Narayanaswamy Jayaraman, under my supervision and the same has not been submitted elsewhere for a degree.

Kanpur
July 1993.

(S. Ranganathan)
Thesis Supervisor
Professor of Chemistry
IIT, Kanpur

DEPARTMENT OF CHEMISTRY
INDIAN INSTITUTE OF TECHNOLOGY, KANPUR, INDIA

CERTIFICATE OF COURSE WORK

This is to certify that Mr. Narayanaswamy Jayaraman has satisfactorily completed all the course requirement for the Ph.D. degree programme. The course include:

Chm. 502	Advanced Organic Chemistry
Chm. 505	Principles of Organic Chemistry
Chm. 524	Modern Physical Methods in Chemistry
Chm. 525	Principles of Physical Chemistry
Chm. 545	Principles of Inorganic Chemistry
Chm. 581	Basic Biological Chemistry
Chm. 800	General Seminar
Chm. 801	Graduate Seminar
Chm. 900	Research

Mr. Narayanaswamy Jayaraman has successfully completed his Ph.D. qualifying examinations in September, 1989. He has also successfully presented his open seminar of the work embodied in this thesis.

(P.K. Ghosh)
Professor and Head
Department of Chemistry
IIT, Kanpur

(Y.D. Vankar)
Convenor
Departmental Post-Graduate Committee
IIT, Kanpur

ACKNOWLEDGEMENTS

With great admiration and appreciation, I acknowledge my supervisor Professor S. Ranganathan. Above all, his deeply rooted insight into the art of science of organic chemistry has inculcated in me a strong appealing and adoration for this exotic human endeavour. I am highly indebted to him in introducing me into this challenging field of chemistry, filled with powerful themes on protein engineering with organic chemistry as their neural networks and in allowing me to work in a free style. Throughout the course, every aspect of my advancement has inevitably become a part of his deep interest, involvement and encouragement. His perspicacity for science and the pervasiveness of it become the cornerstones to transcendent my mind for determinism in science. It is my immense fortune to be under his tutelage and I am grateful and thankful to him with no words in dearth.

Equally, I acknowledge my close association with Dr. Darshan Ranganathan for her interest throughout every aspect of my project. I am highly indebted for her valuable comments and criticisms that became the necessary checks for furthering the project. Her affectionate enquiries, at many instances, were boosting my moral for continuing the project with high spirits. I am most thankful for all her invaluable helps throughout the programme.

I take pleasure in acknowledging Dr. Dipankar Chatterji and Professor D. Balasubramanian of CCMB, Hyderabad for their interest in my project. I am grateful to them in allowing me to work in CCMB for the part of the study presented in this thesis, without which the project would not have seen its interesting aspects. Especially, the support and encouragement accorded on me by Dr. Dipankar Chatterji was quite instrumental in giving a shape to the project. I place in record my sincere thankfulness to both of them.

With immense gratitude and respect, I thank Professor S. Radhakrishnan of Khadir Mohideen College, Adirampattinam and Professor N. Sathyamurthy, IIT, Kanpur for their very keen interest in my academic progress. Their inspiration alone led me to take-up the academic path. To their support and encouragement at times of utmost need, I am highly indebted with my words become boundless to express at. My sincere thanks are due to them. Equally, I am most grateful to Mrs. Suguna Sathyamurthy for her interest in my welfare and academic progress and particularly for their delicious dinner during each Friday of my stay here!

To my teachers Professor S. Chandrasekaran, Professor Javed Iqbal, Professor S. Manogaran, Professor Robin Mukherji and Professor P.K. Bharadhwaj I am grateful and thankful. Their classes at the initial stages of my studentship here gave me a great momentum to start my research project. My sincere gratitude to all of them.

My sincere thanks are due to Dr. Raja Roy and Dr. K.P. Madhusudanan of CDRI, Lucknow for their all efforts in bringing life to my research in terms of extensively helping to analyse nmr and FAB mass of many of research samples. Their continued interest and efforts, I place in record with gratitude.

For all unstinted and unreserved helps I have taken freely from my collegues and friends, I acknowledge them individually with a "Thank you very much":
My senior collegues Dr. Mukund Mehrotra, Dr. P.V. Ramachandran, Dr. Sanjiv Mehrotra, Dr. Shio Kumar Singh, Dr. Girij Pal Singh, Dr. Ramesh Rathi, Dr. Sujata Saini and Dr. Kavita Shah.
My colleagues Messrs. Bhisma, Shaji, Tamil, Dinu and Narend
My friends at CDRI, Lucknow: Messrs. Harsh Guniyal, Samson and Adiraj
My friends at CCMB, Hyderabad: Dr. Purnima Bhargava, Dr. Vijaya Gopal, Mrs. Kumaran, Mayalagu, Nagesh, Ms. Padma, Ms. Jyoti, Ms. Manni Luthra, Messrs. Purnanand, Nambi, Dhople, Thennarasu, Sukhaswamy and Rams.
Each of them have helped at times of my need and, at many instances, were essential for getting ahead with my benchwork. Dr. Girij Pal Singh, Mr. Kumaran, Mr. Nambi, Ms. Manni Luthra and Ms. Padma find a special place for their interest in my research work. I deeply appreciate their assistance.

I take pleasure in acknowledging Dr. V. Balasubramanian for his affection and for helping extensively in the production of the thesis. The production of the thesis finds a difinite contribution from him and sincerely thank him for helping me in this regard. I thank Mr. Sanjay Kumar for his assistance in getting me DTMM plots.

But for the pleasant association of Messsrs. Kalyanaraman, Raghu, Siva, Murali, Srinivasan and Pramod, the hostel life would not have been all the same. My deep appreciation to all of them.

I appreciate with thanks the staff of the Chemistry department, especially Mr. Bajpai, for all their assistance. I am thankful to Mr. Rajagopalan and Mr. Nayab Ahemad for spectral analyses. For the skillful sketches of drawings presented in this thesis, I appreciate and acknowledge Mr. B.K. Jain. I thank Mr. Om Prakash for his help the lab. The services rendered by the Central Library, the Central Glass Blowing Fecility and the Liquid Nitrogen Fecility find a place of deep appreciation.

A very special mention to Mr. Anand Ranganathan, my association and friendship with him is quite rememberable.

Finally, to all my family members, for their constant encouragement and moral support, my deepest sense of feelings that does not find the limit. I rever them with my deep affection and love.

ZINC FINGER TEMPLATE MEDIATED DNA RECOGNITION SYNTHESIS AND DNA INTERACTION STUDIES WITH TEMPLATE PROTOTYPES

ABSTRACT

The recognition of the information system represented by DNA, is essential for all cellular functions. Considering the complexity of genomic information, the specific recognition of regions for transcription is a highly sophisticated process. Proteins that perform this important task rely heavily on their secondary structural features. In the very recent past, tetrahedrally coordinated Zn^{II} has emerged as a highly versatile motif responsible for DNA recognition.

The focus of the thesis is the synthesis of zinc finger template prototypes involved in DNA recognition and the study of their interaction with DNA and oligonucleotides.

A brief account of Zn^{II} containing motifs that are known to be involved in DNA recognition, form the background of the thesis.

The first synthesis of a metal template which incorporates the essential features of zinc finger motif associated with transcription, has been achieved from precursor tripeptide using a novel thiol-disulfide exchange and complexation (Chart C.19).

Templates wherein Zn^{II} is terahedrally coordinated to four cysteines -the recognition motif associated with DNA-glucocorticoid receptor proteins - has been prepared from the novel 20 membered cyclo[bis-oxalyl cystine] (Chart C.11) via PDT reduction and metal complexation (Chart C.28).

A novel methodology, that would enable the preparation of individual zinc finger modules having predetermined recognition elements from the appropriate precursor

peptides, has been accomplished (Chart C.25). Thus, the basic zinc finger template prototype is prepared in a single step from precursor dipeptide and $ZnCl_2$, by a tandem complexation - deprotection sequence (Chart C.26).

The methodology delineated for zinc finger template prototypes (Chart C.19) has been applied to insulin hexa methyl ester leading to the incorporation of the template, thus transforming a hormone to a potentially DNA binding system (Chart C.31).

DNA interaction studies with the synthetic minimal zinc finger structural motif was deemed essential not only with respect to the understanding of the structural aspects involved, but also to provide the cornerstone for construction of finger modules, so designed as to recognize specific DNA triplet sequences. In retrospect, this notion was amply justified, since, although it has been established that zinc finger proteins bind DNA, as tandem modules, leading to remarkable specificity in interaction, *the present study has established that even the simple monomeric unit, [$(CH)_2Zn^{II}$](A) [Chart C.23] binds to DNA specifically and with appreciable stability.*

Analysis of large data set of zinc finger - DNA recognition domain sequences showed that there lies a preference for guanine-rich sequences and thus three recognition templates, namely, poly d(G-C), poly dG and 5' AGCGTGGGCGTT 3' (oligo-1) were used in this study with appropriate controls. Poly d(A-T) was also studied for comparison. Substrates used in the DNA binding studies are, the zinc finger motifs [$(CH)_2Zn^{II}$] (A) (52), its "antisense" analog [$(HC)_2Zn^{II}$] (B)(Chart C.23) (53) and as blanks, the tripeptides $(CH)_2$ [Chart C. 14 (33)] and $(HC)_2$ [Chart C. 14 (34)] devoid of Zn^{II}, co-valent $Zn^{II}(acac)_2$ and the ionic $Zn^{II}(NO_3)_2$.

The UV profile of poly d(G-C) at various [$(CH)_2Zn^{II}$] (A), [$(HC)_2Zn^{II}$] (B)/ DNA (Figure C.7) clearly shows that both (A) and (B) exhibit remarkable co-operative transition with the mid-point of transition close to a molar ratio of 1:1 between DNA and the ligands. A pronounced hypochromicity is seen on increasing the ratio of (A) and (B) to DNA. Also an $\sim$ 8 nm bathochromic effect is observed with (A). Whereas the motifs (A) and (B) showed nearly equivalent hypochromicity corresponding to a Δ O.D of $\sim$ 0.3, the precursor peptides alone showed no influence on DNA. Addition of zinc as ionic $Zn(NO_3)_2$ or as covalent $Zn(acac)_2$ did not result in co-operative DNA binding. In sharp contrast, the UV hypochromicity profile on addition of either (A) or (B) to poly d(A-T) was quite comparable to those mediated by either $Zn(NO_3)_2$ or $Zn(acac)_2$. The precursor peptides $(CH)_2$ and $(HC)_2$ had no influence in the UV spectrum of poly d(A-T).

These findings are of considerable interest, since a large conformational change in DNA structure which might occur as a consequence of DNA-motif complex formation is reflected as a spectral change in this region. The coopertive nature of transition in the UV profile, which occurs with a mid-point of transition close to a molar ratio of 1:1 between poly d(G-C) and the motifs is consistent with a notion that there exists a strong interaction between poly d(G-C) with (A) and (B) and that this interaction contributes positively to the helix stabilisation and to the structural rigidity.

Upon Scatchard analysis [of the data of Figure C.17], pertaining to $(CH)_2Zn^{II}$ (A)(52) and poly d(G-C), a binding curve was obtained with two distinct types of binding. The first phase of binding had more number of binding sites (n) ($\sim$ 14-15 DNA(phosphates)/(A)) and perhaps is due to the phosphate binding. The second phase was characterized by a binding constant having a value of $\sim$ $1.80 \times 10^7 M^{-1}$ (

n = ~ 2-3 DNA(phosphates)/(A)), strongly suggestive of specific interaction with DNA base. All additional probes (*vide infra*) support the notion.

The conformational changes induced upon DNA as a consequence of binding is further demonstrated by CD studies which is extremely sensitive even to small changes in mutual orientation of neighbouring bases in a polynucleotide. The progressive increase in ordering of bases in poly d(G-C) on addition of (A) (Figure C. 18) is indicated by decreasing magnitude of the positive long wave length band. The most dramatic one is reflected at approximately 1:1 ratio of ligand and DNA, where seemingly a reversal of conformation occurs. No noteworthy effects were observed with parallel studies with poly d(A-T). The tripeptide $(CH)_2$ and $(HC)_2$, devoid of metal, had no appreciable effect on the CD profile of poly d(G-C).

The oligo-1, the sequence used to make complex with 96 amino acid residue fragment in crystal studies, strongly interacts with $[(CH)_2Zn^{II}](A)(\underline{52})$ and, considerable ellipticity decrease, denoting order, is observed (Figure C.26). Similar profile is exihibited with $[(HC)_2Zn^{II}](B)$. In contrast, templates without zinc did not show any significant change. These spectral changes in oligo-1 are delightful, and reflect the pronounced ordering induced on DNA, with preference for guanine bases.

Gel retardation studies were carried out in order to observe complex formation between oligo-1 and $[(CH)_2Zn^{II}](A)(\underline{52})$. The oligonucleotide was specifically end labeled with γ ^{32}P-ATP using standard protocols. The complex formation was examined by electrophoresis in 20% polyacrylamide gel and autoradiography (Figure C.31). The results clearly showed marked retardation for oligo-1 - template adduct compared to the control.

Thermal denaturation studies have provided significant insight pertaining to the role of $[(CH)_2Zn^{II}](A)(\underline{52})$ in DNA re-structuring. The addition of (A) resulted in

a marked stabilisation of DNA structure. The T_m, which represents helix→Coil transition, of poly d(G-C) was enhanced from 62.5° to 70.5° C at a (A)/DNA ratio of 0.04. A unique property of this interaction is that it is cooperative and reversible, with an ideal profile, changing to the native state on cooling. Here the heating and cooling curves are nearly superimposable (Figure C.33). This finding is in sharp contrast to early report of T_m studies of DNA with Zn ions, where the cooling profile was out of phase , the likely reason being that in this type of transition the complementary base pairs in the strands are out of register. It is clear therefore that (A) not only binds to poly d(G-C) but also maintains the complementary bases in register in the denatured state enabling ideal reversal upon cooling. The T_m was independent of the concentration of (A) suggesting *specific binding* to poly d(G-C). This property is responsible for the fact that when the (A)/DNA ratio increases towards unity, whilst the T_m is hardly affected, the reversibility is completely lost. In comparison, poly d(A-T) showed a concentration dependent denaturation behaviour. At the lowest concentration the T_m is somewhat lowered, with increasing ratio the T_m gradually shifts along the temperature axis. Thus T_m studies with poly d(G-C) and $[(CH)_2Zn^{II}]$ (A) (52) are fairly consistent with a model for interaction having characteristics of reversibility, fairly well-defined stoichiometry, cooperativeness, and selectivity .

The UV of poly dG arising from addition of increasing amounts of (A) as well as its 'anti sense' analog (B) exhibit a profile remarkably similar to that with poly d(G-C), strongly suggesting that the specific binding of (A) with DNA arises from interaction with guanine residues.

Perhaps the most direct experimental evidence for the interaction of (A) with guanine residues was secured by competitive binding assay through ethidium bro-

mide flourescence quenching. The changes in the profile of ethidium bromide bound poly dG on addition of increasing amounts of (A) is shown in Figure C.45 - C.48. It is clear that initial addition of (A) brings about an order in poly dG, arising from non-specific interactions as seen by enhanced flourescence. Subsequent additions quenches the ethidium bromide flourescence, eventually effectively quenching the induced fluorescence of ethidium bromide, thus suggesting that the specific interaction of template with guanine residues leads to displacement of ethidium bromide.

From the studies outlined above and based on the known interaction of zinc finger template with major groove of DNA, a model for (A) - DNA interaction involving two types of binding is proposed. First of these is the recognition of the sugar-phosphate backbone by one of the imidazoles present and the second, a specific interaction involving the appropriately positioned amino group with guanine of the DNA (Figure C.49).

CONTENTS

ABBREVIATIONS

Acm	acetamidomethyl
aq	aqueous
Boc	t-butyloxycarbonyl
Bz	benzoyl
CD	circular dichroism
COSY	correlated specroscopy
Cys	cysteine
DCC	dicyclohexylcarbodiimide
DCU	dicylclohexylurea
DMF	dimethylformamide
DMSO	dimethylsulfoxide
DNA	deoxyribonucleic acid
EDTA	ethylene diamine tetra-acetic acid
ETB	ethidium bromide
dG	2'- deoxyguanosine
dT	2'- deoxythymidine
FAB	fast atom bombardment
His	histidine
ir	infra red
ms	mass spectroscopy
NOe	nuclear overhauser effect
NOESY	nuclear overhauser spectroscopy

Np-OH	p-nitrophenol
nmr	nuclear magnetic resonance
O-^{t}Bu	t-butyl ester
OD	optical density
OMe	methyl ester
PDT	Propane-1,3-dithiol
ppm	parts per million
poly dG.poly dC	poly 2'-deoxyguanosine.poly 2'- deoxy-cytidine - double strand homopolymer
poly d(G-C)	poly (2'-deoxyguanosine.2'-deoxycytidine) - double strand heteropolymer
poly d(A-T)	poly (2'-deoxyadenosine.2'-deoxythymidine) -double strand heteropolymer
rt	room temperature
SDS-PAGE	sodium dodecyl sulfate polyacrylamide gel electrophoresis
TEMED	N,N,N',N'- tetramethylethylenediamine
TMG	tetramethylguanidine
TMS	tetramethylsilane
TOCSY	totally correlated spectroscopy
Trp	tryptophan
VT	variable temperature
uv	ultraviolet spectroscopy
Z	carbobenzoxy (benzyloxycarbonyl)

A. INTRODUCTION

The myriads of multifaceted, diverse, prolific, spontaneous and ever so pervasive manifestation of nature are designed by the phenomenon of recognition which when logically extrapolated to the microscopic domain lead to the link between information and function which when expressed in molecular terms signify DNA - protein interactions. Such interactions are involved in many of the fundamental processes that occur inside cells including packaging, replication, recombination, restriction and transcription. The understanding of the nature of such interactions, as they are so intimately linked to the control of gene expression, cell division and differentiation is an endeavour that is significant pertaining to the very basic features involved in life systems. The sophistication with which the DNA - protein recognition takes place, as could be expected, is varied. Many proteins particularly those involved in packaging, for example, the histones, or in replication, as with DNA polymerase, have low or no sequence specificity, whereas others which reflect the art of extremely sophisticated molecular complementarity is shown in repressors, transcriptional activators and restriction endonucleases. Indeed, these proteins are so designed that they are able to and must recognise short stretches of information spanning 10 - 20 base pairs in a background ranging from a million to a billion similar sites. In the last decade there has been a virtual explosion in our understanding of molecular intricacies associated with targeted protein - DNA recognition. These endeavours have shown much diversity, at the same time also, an unifying principle. The recognition can be traced to modules whether they are helices or templates or a combination of many such subsystems.

Transcription factors regulate cell development, differentiation and cell growth by binding to a specific DNA sites and regulating gene expression. It appears that the strategy used here to specifically identify a small set of DNA sequences amongst a milieu is different in the procaryotic (bacterial) and eucaryotic (animal) domain. It is of interest to note that whereas in procaryotic systems the recognition is achieved largely on the basis of secondary and tertiary protein structures, typical ones being the helix turn helix motif, those in the eucaryotic realm uses more versatile molecular assembly, notably using metal templates.

Eucaryotic genes are regulated differentially in response to a complex set of environmental and developmental queue. In terms of transcriptional regulation, small autonomous domains containing less than 100 amino acid residues are sufficient for this purpose. Sustained activity in eucaryotic gene recognition factors have so far brought out typical recognition ensembles such as, extended helical homeodomains, leucine zippers and zinc template motifs. The focus of the present work reported in the thesis pertains to the understanding of the role of such template motifs in recognition, particularly with reference to their interaction with the DNA structure in general and the DNA backbone in particular.

A tetrahedrally coordinated zinc as a structural element in DNA recognition has been established in three different classes. The first is the zinc finger motif, an approximately 30 amino acid residue module with one zinc ion liganded to two cysteines and two histidines. The second, an approximately 70 amino acid residue domain found in the receptors for the steroid and related hormone like molecules, the two zinc ions each liganded to four cysteines and finally the third is found in a set of yeast activators including GAL4, with two closely spaced zinc ions sharing 6 cysteines in a small peptide segment scaffold. Architecturally these three,

although achieving the same function, namely, the recognition of DNA sequences, are constructed in radically different ways.

The focus of the work reported in this thesis is the syntheis of zinc templates that are prototypes of the first two mentioned catagories and a detailed study of specific interaction between minimal zinc finger protein and DNA.

A brief account of zinc(II) containing motifs that are known to be involved in DNA recognition, comprising an appropriate background pertaining to the present work, is given in the next section.

B. BACKGROUND

Familial relationships are powerful unifying themes in the study of DNA binding proteins, since they relate evolution, structure, recognition, gene regulation and design. Thinking about these motifs can at least in a schematic fashion give a satisfying general picture of protein - DNA recognition. In some way, which is entirely logical, the number of members in a particular family of DNA binding proteins may measure the relative evolutionary success of that particular DNA binding motif. It would not be a hyperbole to state that these families constitute nature's most successful designs for DNA binding proteins. As stated in the earlier section, the eucaryotic DNA recognition factors are closely associated with what is termed as a recognition motif, a relatively small construct that is pivotal in bringing about the desired interaction. These constructs invariably contain a much smaller sub-system. Consequently, it is entirely logical, as a starting point towards the understanding of DNA binding proteins in molecular terms, how these small sub-systems - which in the present study are metal templates - interact with the DNA molecule. The templates undoubtedly are scaffolds in the construction of recognition systems and their interaction with DNA will surely be useful in the design of newer, better, more efficient and versatile chemical models pertaining to the recognition. The most important interactions for specificity are hydrogen bonding between protein side chains and functional groups exposed in the major groove of DNA[1]. The reasons for concentrating on hydrogen bonding pattern derives from structural considerations which would clearly show, as shown in Chart B.1, that discrimination of base pairs by hydrogen bonding is possible in the major groove[2]. Whilst the recognition system is able to decipher the concerned DNA sequence, this interaction is critical for the proper orientation of the protein subsystems. This, in all cases involve what

Chart B.1

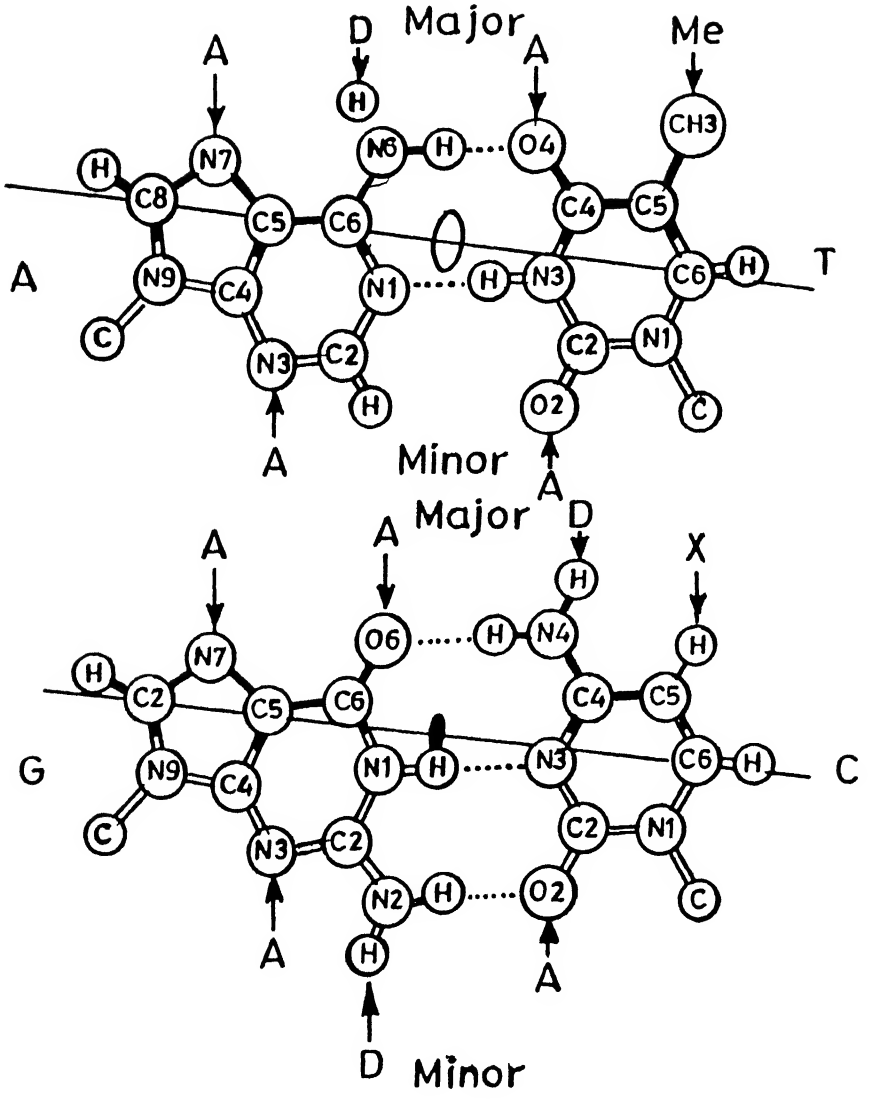

Hydrogen-bonding patterns in protein-DNA interactions

A - An atom acting as a hydrogen-bond acceptor, D - an atom acting as a hydrogen-bond donor, X - position at which no interaction persists, and Major and Minor refer to the two grooves of DNA.

could be termed as a docking mechanism. In this, the DNA backbone plays an integral part and, by and large, the metal template is able to be docked to the DNA via hydrogen bonding, largely with the sugar phosphate backbone in a non-specific manner.

Amongst the eucaryotic zinc templated DNA recognition systems, the earliest one to be identified and designed is commonly termed as the zinc finger motif. The discovery of this unusual motif as responsible for a pivotal function pertaining to the DNA transcription constitutes one of the most exciting discoveries in molecular biology in recent times.

Transcription factor IIIA (TFIIIA) is required for the correct initiation of transcription of Xenopus 5S RNA genes by RNA polymerase. This 40 kDa protein binds to a 50 base pair region located within the coding sequences of 5S RNA genes, (the internal control region). TFIIIA is found in large quantities in the ovaries of immature frogs stored as a 7S complex with its own gene product 5S RNA. TFIIIA therefore binds to both DNA and RNA. This presented an intriguing structural problem as to how such a small protein interacts with a long tract of DNA[3]. The stability of the 7S complex was greatly improved by excluding chelating agents such as DTT and EDTA, thus suggesting that a metal was involved in the binding of the protein to RNA and to DNA. Analysis by atomic absorption spectroscopy revealed that preparation of 7S particles purified to homogeneity in the absence of chelating agents contain 7 - 11 atoms of zinc per mole of particle. This result was consistent with the fact that the protein contains a large number of cysteine and histidine residues, the commonest ligands for zinc enzymes and other proteins. It also explained why zinc was necessary for transcription of 5S RNA genes[4]. Careful and painstaking proteolytic studies of the 40 kDa protein showed that it consists of atleast 10 domains, each of $\sim$ 3 kDa , each and everyone of these containing

one zinc atom. This novel idea of a small zinc stabilised domains was obvious from DNA sequence clone derived from TFIIIA. A rigorous computation analysis showed that of the 344 amino acids of the TFIIIA sequence residues, 13 to 270 formed a continuous run of tandemly repeated, similar units of $\sim$ 30 amino acids containing two invarient pairs of cysteines and histidines (Chart B.2)[5].

Thus a very pretty picture emerged pertaining to the secondary structure of TFIIIA arising from 3 different lines of evidence, namely, a 30 amino acid repeats in sequence, the matching of the number of zinc atoms with these modules and the fact that they are aligned in tandem. This led to the proposal that the protein has a repeating structure in which each of the nine 30 amino acid units folds around a zinc atom to form a small independent structural domain (Chart B.3)[6]. Thus for the very first time in molecular biology a modular design on the basis of tandemly aligned modules harbouring a metal template for DNA recognition came into vogue. This development logically led to proliferation of endeavours in this domain to find answers to basic questions, such as the role played by the template, the nature of the recognition system and the minimal number of the 30 residue modular fingers that can recognise a DNA sequence. Many of these questions were answered by subsequent experimentation. It was soon found that whereas a single module is not capable of specific DNA recognition, the higher ones starting from two and above can achieve this, suggesting that the domains at least in a neighbourly manner are inter-related[7].

Within a short span of 5 years, the zinc finger motif has emerged as one of the major structural motifs, involved in eucaryotic protein - nucleic acid interacti Thus, sequence motif or profile $X_3CysX_{2-4}CysX_{12}HisX_{3-4}HisX_4$ and hundreds similar finger sequences were reported. They were shown to be involved in ma aspects of eucaryotic gene regulation, such as, in proteins induced by differentiati

Chart B.2

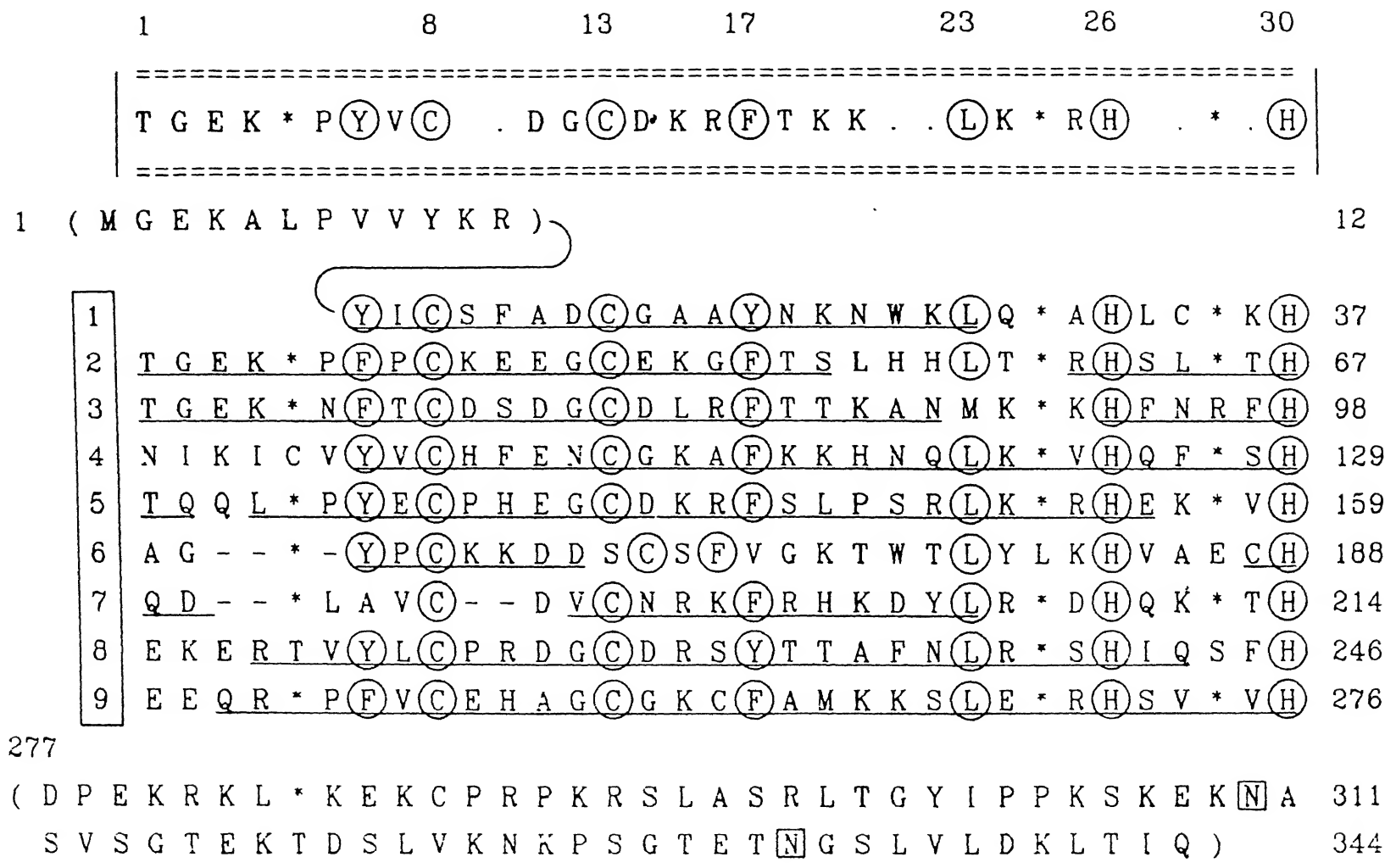

Amino acid sequence of TFIIIA. Sequences are aligned to highlight conserved residues (Circles)

Chart B.3

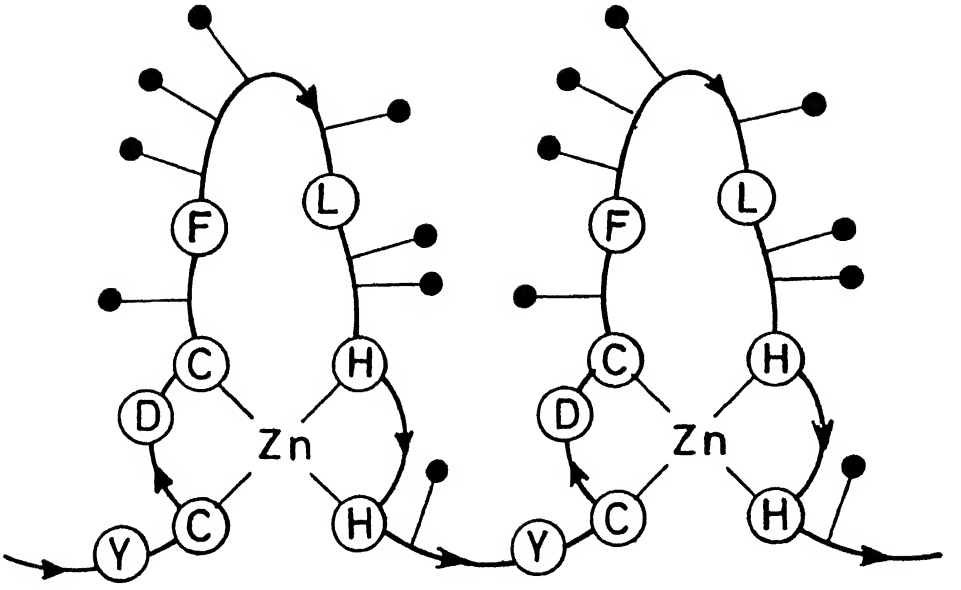

Folding scheme for a linear arrangement of repeated zinc finger domains

Residues circled are the conserved amino acids, black circles indicate most probable DNA-binding side chains.

and growth signals, in proto-oncogenes, Wilms' tumor genes, in general transcription factors, in Drosophila segmentation genes and in regulatory genes of lower organisms.

Model building predicted[8] and 2-D nmr studies confirmed[9] that the TFIIIA like zinc fingers contain an antiparallel β-sheet and an α-helix. Two cysteines which are near the turn in the β-sheet and two histidines which are near the α-helix coordinate a central zinc ion and hold these secondary structure together to form a compact globular domain. The determination of the crystal structure reported in 1991 of a complex, containing three zinc fingers from Zif-268, a mouse immediate early protein and a consensus DNA binding site, has provided the precise structural interactions involved in DNA recognition or recognition of DNA sequences by the zinc finger modules[10]. The structural description of the protein and the nucleotide segment involved in cocrystallisation is shown in Chart B.4. Above all, the X-ray structure determination showed the interactions that lead to such efficient protein - DNA recognition. The three zinc fingers here are arranged in a semicircular structure that fit snugly into the major groove of B-DNA (Chart B.5). As expected from nmr studies of individual fingers, each zinc finger domain consists of an antiparallel β-sheet and an α-helix held together by a zinc ion and by a set of hydrophobic residues. Two cysteines from β-sheet region and two histidines from the α-helix coordinate the zinc ion.

The crystallographic studies show that the α-helix of each zinc finger fits directly into the major groove and that residues from the amino terminal portion of each α-helix contact the base pairs in the major groove. Each of the three Zif-268 zinc finger uses its α-helix in similar fashion and each fingers make its primary contact with a three base pair sites. The overall structure of the complex exhibit periodicity with neighbouring fingers related in way that reflects the three base pair periodicity

Chart B.4

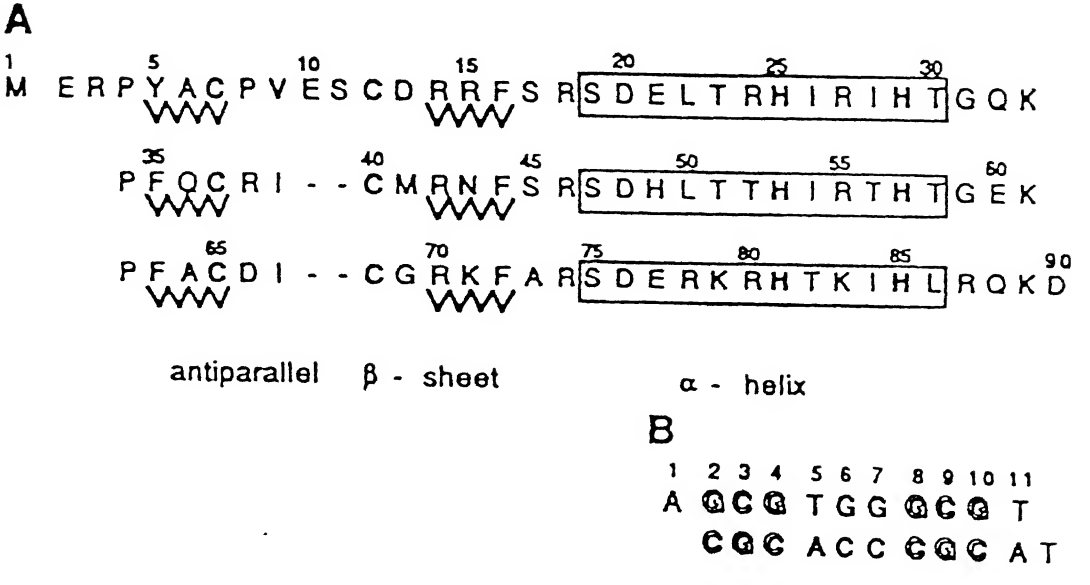

The sequences of protein (A) and nucleic acid (B) used in co-crystallisation studies of Zif-268 - DNA complex[10]

Chart B.5

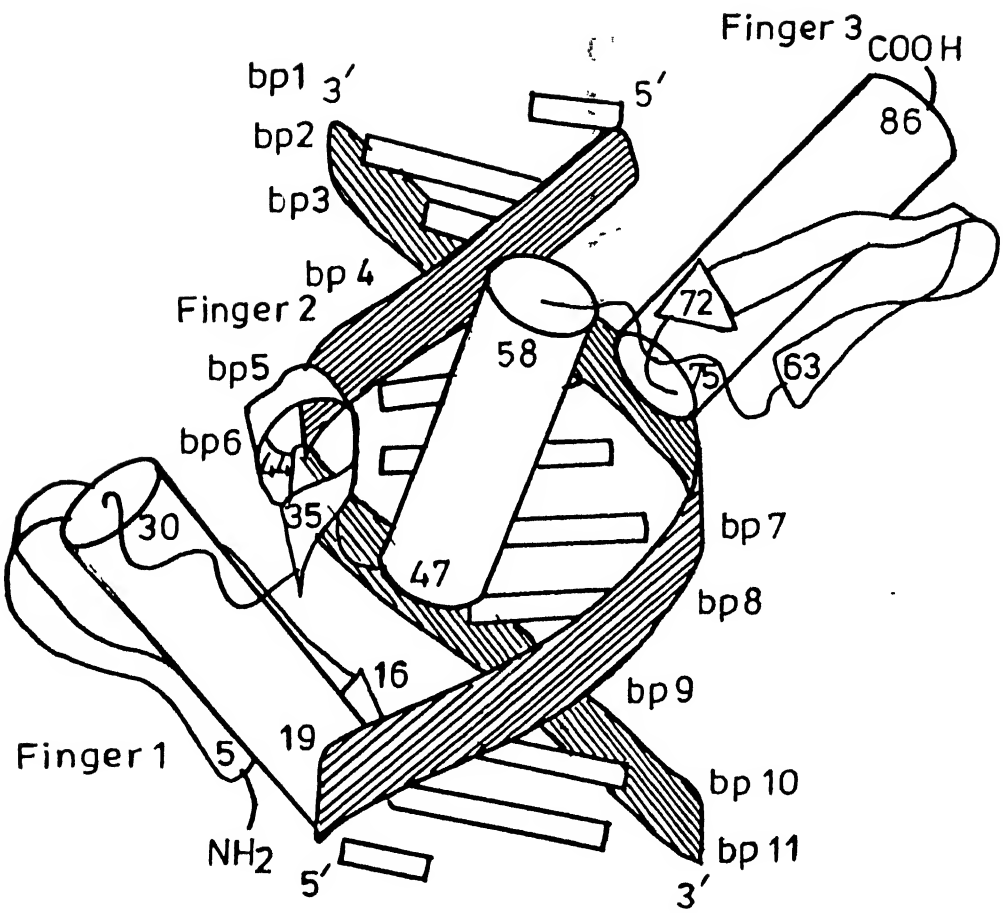

The overall structure of the Zif268-DNA complex

of the subsites. A rotation of $\sim 96^o$ around the DNA axis and a translation of $\sim 10^o$ along the DNA axis move one finger onto the next. Although the α-helix fits into the major groove, its axis is only approximately aligned with the groove. The β-sheet is back on the α-helix, away from the base pair and is shifted toward one side of the major groove. The two strands of the β-sheet have very different role in the complex. The first β-strand does not make any contacts with the DNA whereas the second β-strand contacts the sugar phosphate backbone along one strand of the DNA.

The Zif-268 zinc finger peptide makes eleven critical hydrogen bonds with the bases in the major groove. The important side chains include an arginine that immediately preceeds the α-helix, in each of the three fingers and also include the second, the third and the sixth residue in the α-helix. All these hydrogen bonds involve bases rich on the guanine strand (G - rich strand) of the consensus binding sites (5' GCG TGG GCG 3'). Using the 5'$\rightarrow$ 3' convention for the direction of the DNA strand and the N $\rightarrow$ C convention for the direction of polypeptide strand, we may say that the overall arrangement of the peptide is antiparallel to the DNA strand and that has most of the contacts. The peptide is arranged so that finger 1 binds near the 3' end of the primary strand (5' GCG TGG GCG 3'), finger 2 binds near the center (5' GCG TGG GCG 3') and finger 3 binds near the 5' end (5' GCG TGG GCG 3'). The general profile of the interaction of the recognition element in each of the zinc finger modules with the appropriate triplet base sequences is shown in a general manner in Chart B.6 and in structural details in Chart B.7. A detailed analysis of the molecular interactions, involved with reference to DNA recognition is possible from consideration of Charts B.6 and B.7. As stated previously, the first coded amino acid side chain that makes contact with the DNA is invariably the one prece ding the α-helix, which is in the present case arginine placed at respectively

18, 46 and 74 positions. Interestingly they act in concert with the second residue of the α-helix which is invariably an aspartic acid, placed at 20, 48 and 76 locations. As could be seen from Chart B.7 the arginine-aspartic acid combination makes a splendid guanine recognition system, involving hydrogen bonding contacts as well as ionic stabilisation. This motif should turn out to be universal pertaining to the recognition and will find use in the domain of molecular recognition and specificity. The third residue in the α-helix serves as a recognition element only in the case of histidine pertaining to finger number two. In the other two cases this site is occupied by glutamic acid which is devoid of sequence recognition. The histidine recognition of the guanine residue is via hydrogen bonding as illustrated in Chart B.7. It is also possible that this histidine residue could have a stacking interaction with the proximal thymine residue (Chart B.6). The sixth residue of the α-helix involved in base contacts in fingers 1 and 3 is again arginine placed at locations 24 and 80. In the case of finger 2 the corresponding site is occupied by a threonine which does not seem to participate in recognition.

Pivotal to the sequence recognition is the precise alignment of the recognition loop of each of the modules. This has been demonstrated to be achieved principally by nonspecific contacts with sugar phosphate backbone where the template plays a very crucial role. In each of 3 fingers it is seen that the first histidine that coordinate zinc ion also hydrogen bonds to a phosphate on the primary strand of the DNA. This histidine which is the seventh residue in each of the α helices coordinate the zinc ion through its N^{ϵ} and contacts the phosphodiester oxygen with its N^{δ}. This interaction is analogous to the zinc-histidine-carboxylate interaction observed in carboxypeptidase A. These histidine-phosphate contacts are remarkable in the sense that the zinc makes an unexpected and direct contribution to the overall binding energy and the invarient positioning of the histidines brings out the importance of

Chart B.6

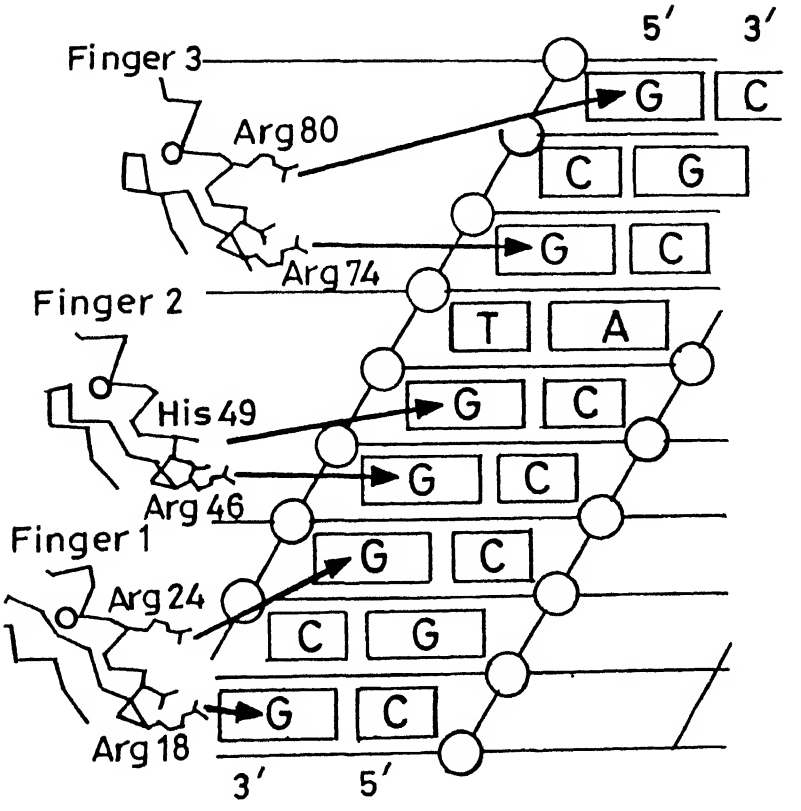

Summary of all the base contacts made by the Zif268 peptide

The DNA is represented as a cylindrical projection.

Chart B.7

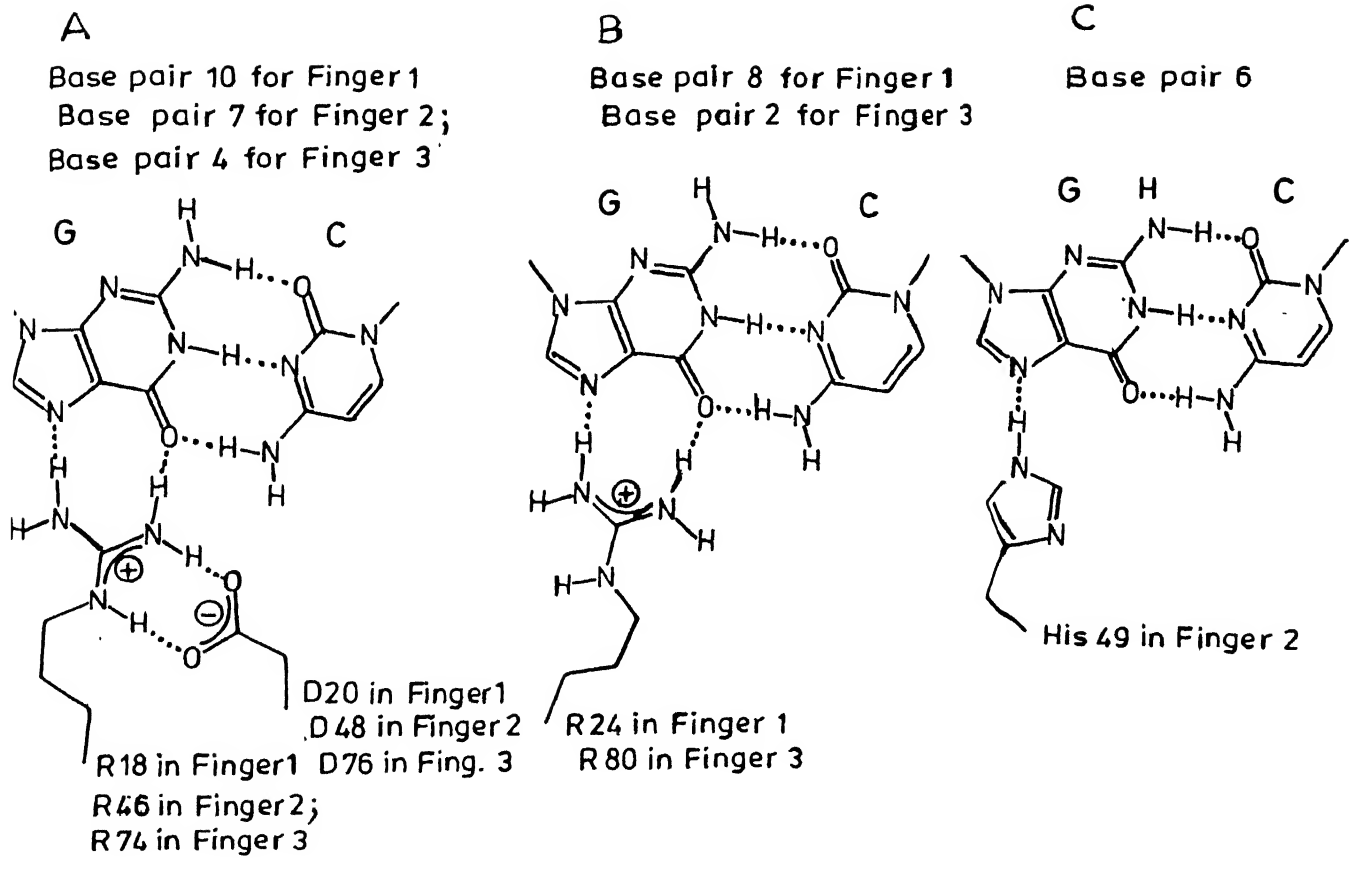

Zinc finger contacts with the bases (primarily the guanine-rich DNA strand)

(**A**) The Asp-Arg-guanine interaction; (**B**) The Arg-guanine interaction; (**C**) The His-guanine interaction.

the tetrahedral zinc finger template to orient the finger for site specific recognition. The zinc finger mediated DNA recognition, above all, attests to the dictum that Nature uses versatility to design the simplest of structures to bring about seemingly the most complex functions. From a conceptual and design vantage, the most attractive feature of the zinc finger motif is that it is amenable to adaptation to suit contingencies that are quite unrelated. It also shows that redundancies in the finger can be done away with-in the structuring of far simpler systems that could be equally effective. Perhaps the most attractive facet of the zinc finger module is that since each finger makes its primary contacts along a three base pair region, it should be possible to design fingers that could recognise each of the 64 base pair triplets, which, by judicial combination, could lead to the design of proteins with any desired sequence specificity[10].

The concept of zinc finger modules as a motif for sequence specific DNA recognition has been established by detailed studies on several similar systems. Some of which are outlined below:

The yeast transcription activator (ADR1) is a positive activator of the glucose respressible alcohol dehydrogenase gene in the yeast *saccharomyces cerevisiae.* This activator codes for a 1322 protein and sequence analysis has revealed two zinc finger domains between residues 100 and 160. A 30 residue peptide containing residues 130 to 159 corresponding to one of the fingers named as ADR1a was synthesised by normal peptide methods. Addition of zinc ion and monitoring by detailed nmr spectroscopic studies clearly showed that the 30 residue peptide folded neatly into a zinc finger arising from a tetrahedral coordination of the zinc(II) with pairs of cysteines and histidines present in ADR1a (Chart B.8)[9]. Interestingly, the single finger domain although showed interaction with DNA, was not sequence specific. A reason for this may be that although they possess determinants for binding

Chart B.8

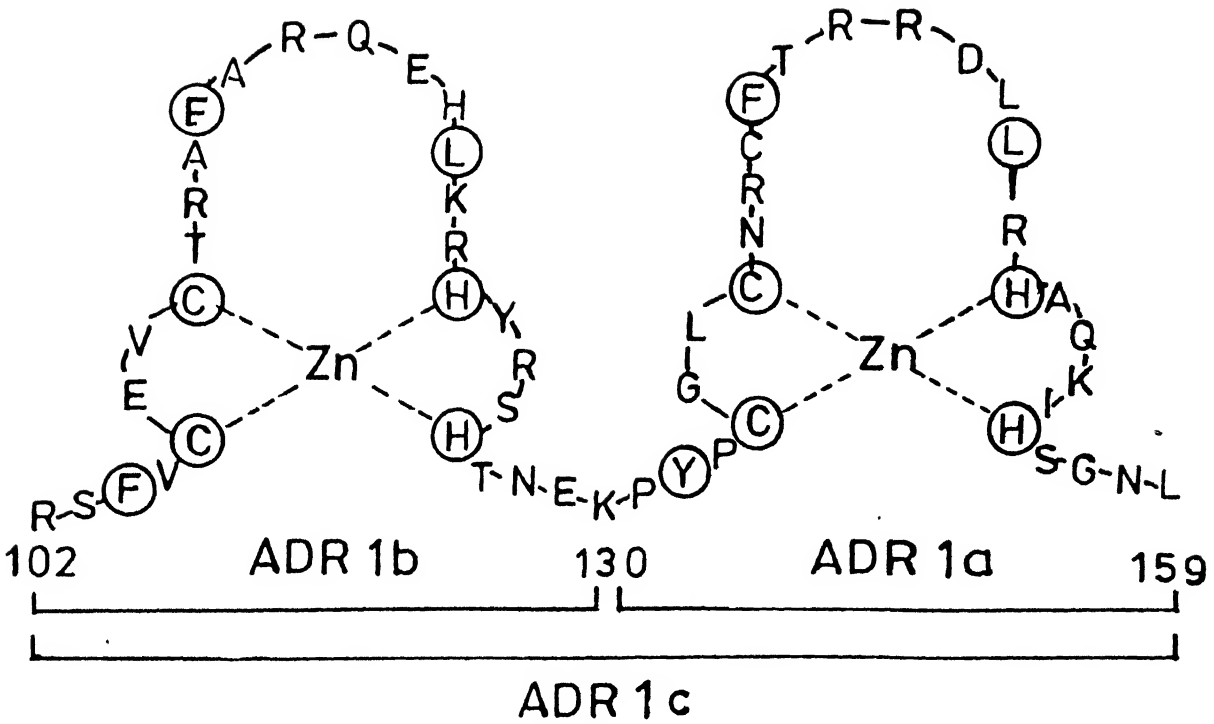

Amino acid sequence of ADR1 zinc fingers

Circled residues are conserved.

specificity, a single domain may not contain enough DNA contacts for high affinity binding.

However when the number of fingers is increased to three, base specific contacts do take place as demonstrated with a protein fragment containing only the three zinc finger domains from the yeast protein SW15[7]. The fact that a three finger domain can bind to DNA in a sequence specific manner has been shown by studies with transcription factor SP1. Transcription factor SP1 is a 105kDa protein containing 778 amino acids which activates a reasonably large subsets of mammalian genes " GC box upstream promoter elements ". The carboxy terminal 168 amino acid residues of SP1 contain 3 contiguous zinc finger motifs $CysX_4CysX_{12}HisX_3His$ which are believed to bind zinc(II). The carboxy terminal domain has been shown to constitute the DNA binding domain, while the amino terminal 610 amino acid residues form the trans activating domain. These two domains function independently. A DNA sequence corresponding to the codons from 614 to 778 of SP1, the carboxy terminal end encompassing the three zinc finger motif was cloned, overproduced and the protein corresponding to the 165 residues of Sp1 plus two from the cloning vector designated Sp1(167*) was isolated and purified. This protein neatly folded in the presence of zinc(II), conforming to three zinc finger modules. These modules specifically recognised the GC box sequence in the presence of a large excess of calf thymus DNA. These studies clearly established that a synthetic three finger module can recognise the appropriate DNA sequences in a correct manner[11].

As stated previously, the modular concept inherent in zinc finger motifs can be used in the construction of totally synthetic modules that could even exhibit enhanced DNA sequence binding properties. This has been recently demonstrated from a synthetic sequence derived as a result of consensus analysis of 131 established naturally occurring zinc finger sequences. Thus a single zinc finger peptide

PYLCTECGKSHSQKSDLVKHQRTHTG was designed from the data base and the compound synthesised. Studies with these peptides clearly showed that they fold precisely as predicted, in the presence of Zn^{II} and Co^{II} ions with greater affinity for metal ions than normal zinc finger modules. NMR studies clearly confirmed the nature of these modules as predicted and observed for other zinc finger domains[12].

The use of the zinc finger motif in the development of a code that correlates the side chains of coded amino acids with that of corresponding DNA recognition sequences has great appeal so far in terms of our understanding of protein - DNA interactions and also, most importantly, in the design of novel recognition systems. Whilst it is possible to visualise such a correlation that extends to all the 64 triplets in the genetic code, such a goal is still far away with many of the problems pertaining to this not clear. A beginning has been made towards this goal, taking advantage of permuting the recognition peptide of the zinc finger module on the one hand and the corresponding nucleotide sequence on the other. Painstaking experiments involving the preparation and interaction studies with a large number of mutants has led to the beginnings in this direction.

The zinc finger proteins typified by the human transcription factor SP1 contain tandem arrays or domains each of which approach the 28 sequence namely $TY(F)X_{aa}CX_{aa}X_{aa}CX_{aa}X_{aa}X_{aa}FX_{aa}\ X^{13}_{aa}X_{aa}X_{aa}X^{16}_{aa}LX_{aa}X^{19}_{aa}HX_{aa}X_{aa}X_{aa}$ HTGEK. Each domain is associated with three base pairs of DNA,the triplet subsites from adjacent domains being contiguous, but not overlapping. The predominant sequence specific contacts are made by residues X^{13}_{aa}, X^{16}_{aa} and X^{19}_{aa} which are in the helical regions of the structure and whose variations pertain to the evolution of the code described above. Through systematic variations at two of the three contact positions in 5' GGG N(G or T) GGG 3', the underlined positions signifying variations,

Two kinds of codes, a design code and a prediction code might exist for zinc finger - DNA recognition. The simpler of these, the design code, would allow for the construction of a zinc finger protein that would bind with appropriate specificity to a given DNA sequence. In contrast, a prediction code, translating information in the other direction would enable the prediction of the DNA sequence to which a given zinc finger protein would optimally bind. Beginning the development of a design code, the results discussed here can be combined in the form of a set of rules that correlate the sequence of amino acids in the recognition regions of a zinc finger domain with the triplet base pairs to which it is capable of binding. Because of the three base pair per zinc finger domain relationship, these rules can be tabulated as shown in Chart B.9, in the format of the well-known genetic code. The rules illustrated in Chart B.9 are more useful as a part of design code than as a part of prediction code. The three key zinc finger recognition residues that would be used to optimally recognise a given base pair triplet is clearly denoted in Chart B.9. The smaller lettering for 2 sets of residues indicates that these exhibit relatively low affinity when used in Sp1 base systems and further work is required to establish the appropriateness of these placements[13].

Hormones, located at cell surfaces turn on the genes present in the cell nucleus. This super family of hormones include glucocorticoids, steroids, retinoids, thyroids and several others. Members of this elite class have a common amino acid sequence organisation composed of discrete functional domain for ligand binding, DNA binding and transcriptional regulation. The DNA binding domain is highly selective for interaction. The hormones allosterically modulate the DNA recognition. They activate the cellular form of the receptor, which in the absence of the ligand is complexed with a heat shock protein chaeperon. Ligand binding dissociates the complex whereupon the receptor ligand complex can dimerise and move to the nu-

Chart B.9

II

I	A	C	G	T	III
5′-G	$R_{19}N_{16}R_{13}$	$R_{19}E_{16}R_{13}$	$R_{19}H_{16}H_{13}$	$R_{19}L_{16}R_{13}$	G-3′
	$R_{19}N_{16}Q_{13}$	$R_{19}D_{16}Q_{13}$	$R_{19}H_{16}Q_{13}$	$R_{19}A_{16}Q_{13}$	T-3′

A set of rules for zinc finger-DNA recognition

The small letter two sets of residues indicate low affinity binding to the corresponding base triplets in Sp1-based systems.

cleus. In the case of glucocorticoid receptors, the DNA binding domain contain $\sim$ 70 residues possessing eight conserved cysteines (Chart B.10). An 86 amino acid fragment of the rat glucocorticoid receptor encompassing amino acid residues 440 - 525 of the DNA binding region was expressed in E.Coli and co-crystallised with self complementary oligonucleotide. The X-ray structure solved to moderate resolution presented a very novel and unusal structural profile. The interaction of the protein with the DNA is on the basis of a dimer. Each of the two units contain two loop helix elements, each with a zinc ion liganded by two cysteines at the beginning of the loop and two others at the N-terminus of the α helix. Two helices in the domain are packed against each other at nearly right angles. Interestingly, the configuration of cysteine ligands around the zinc has opposite handedness in the two elements that belongs to each of the units (Chart B.11).

The protein assumes a compact globular fold divided into two substructures or modules each being nucleated by a zinc coordination center and followed by an amphipathic α-helix. The two substructures are joined together mainly through the interaction of aromatic side chain of the amphipathic helices which together with tyrosine 452 from the large loop of the first finger and tyrosine 474 on the β strand linking the two modules form an aromatic cluster. A shell of hydrophobic residues sorrounds the aromatic cluster. The resulting hydrophobic core stabilises the globular fold and fixes the relative orientation of the two substructures. The two subdomains differ structurally and functionally. Whereas the main loop of the amino terminal finger has a short segment of anti parallel β structure, the carboxy terminus has a distorted α-helix. The β-sheet of the amino terminal finger helps to orient the residues that make phosphate contacts and its second pair of zinc coordinating cysteines begin in an α-helix that provides all of the base contacts in the major groove. The carboxy terminal subdomain provides phosphate contacts,

Chart B.10

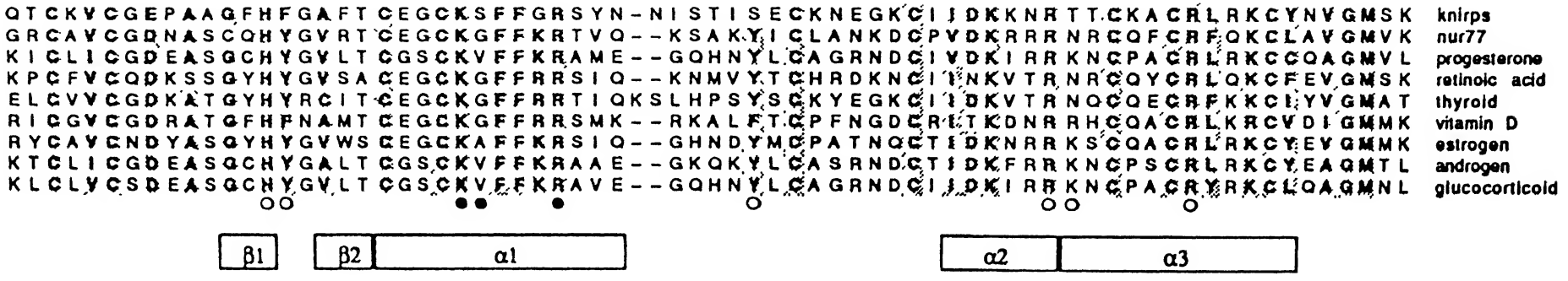

Alignment of steroid receptor sequences.

Positions of the conserved cysteines (C) are shaded, as are the positions that are acidic (D, E), basic (H, R, K), hydrophobic (A, C, V, I, L, M, F, Y), or small (G, A). The positions of secondary structure, backbone contacts (o), and major groove contacts (●) are from the structure of the glucocorticoid complex

Chart B.11

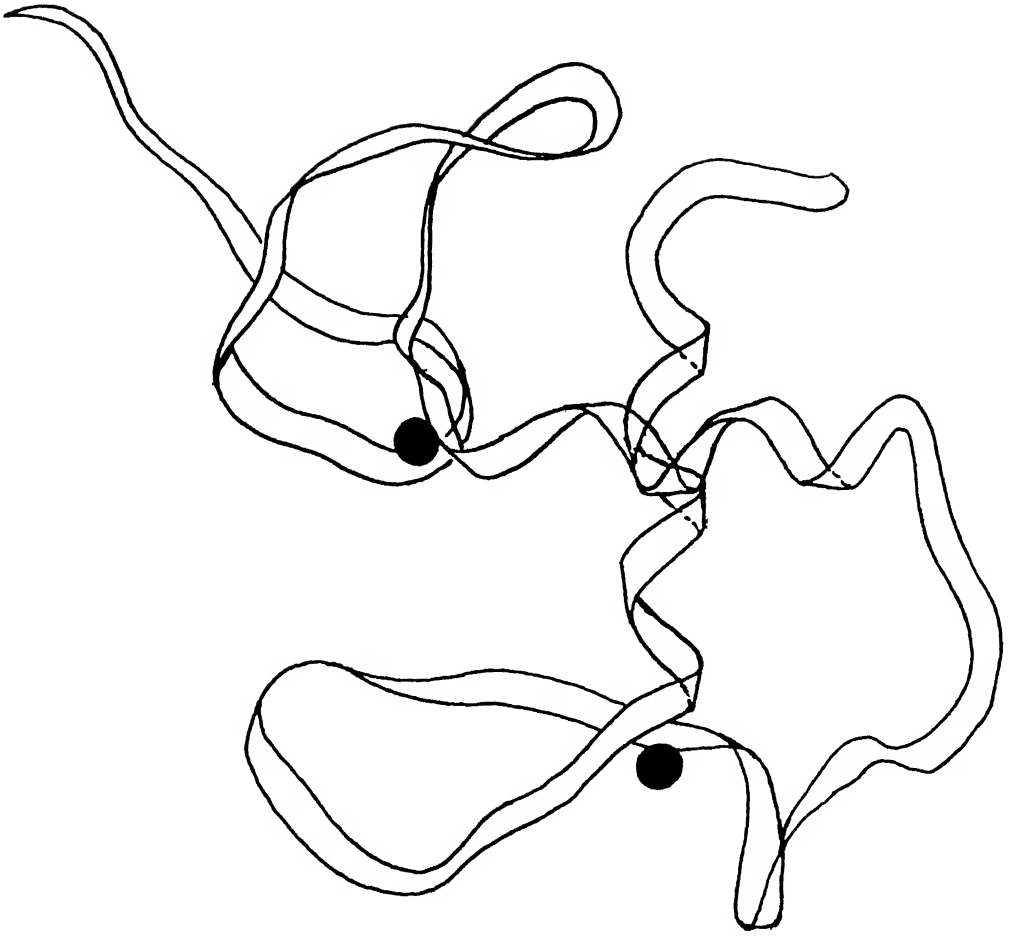

Structure of the oestrogen receptor protein DNA-binding domain

The protein backbone is shown as a ribbon sturucture; the filled circles indicate the zinc atoms.

the entire dimerisation interface as well as site implicated in positive control of transcription. Most of the inter subunit contacts are made by residues in the loop between Cys476 and Cys482, a region referred to as the D-box for its postulated role in dimerisation. The conformation of this loop is a reverse β-turn and is maintained by the R configuration of the zinc center. The role of carboxy terminus substructure in providing all of the known protein - protein interactions may be the underlying reason for the distinctive chirality of the metal center. There is a β strand in the main loop of the carboxy terminal finger which exposes the hydrophobic residues to the solvent, a situation which is sufficiently unusual in protein structures to suggest a potential role for these residues in contacting other domains of the receptor or even other proteins.

Two molecules or fragments 445 to 525 bind to one face of the 18 base pair DNA, as a two fold, rotationally symmetric dimer (Chart B.12). The interactive surface of each subunit engages successive major grooves. There are no other protein contacts to the bases in the intervening minor groove. Backbone contacts are made by strand farthest from the diad by the large loop of the amino terminal finger to the strand closest to the diad by the carboxy terminal modules. At both specific and nonspecific half sites the amino terminal α-helix lies in the major groove and its side chains form the only contacts to the bases. Thus only one subunit of the protein complex faces the target half site sequence. The second subunit is forced out of register. Zinc coordination has more than functional role. In the glucocorticoid receptor DNA binding it stabilises not only the helices at the carboxy terminal end of both fingers but also fold the carboxy terminal module that is essential for dimerisation. The use of zinc(II) to nucleate substructures in the folding motifs of many transcription factors may be an evolutionary reflection of the structural economy and versatility provided by metal coordination[14].

The DNA recognition associated with transcriptional activation in the yeast have a common profile which can be exemplified with GAL4, whose crystal structure with the DNA complex was reported recently[15].

The yeast protein - GAL4 activates transcription of genes required for catabolism of galactose and mellibiose. The DNA sequence recognised by GAL4 are 17 base pairs in length and each site binds a dimer of the protein. Four such sites similar but not identical in sequence are found in the upstream activating sequence that mediates several GAL genes. Functions have been assigned to various parts of the 881 amino acid GAL4 protein (Chart B.13).

Chart B.14 provides the rich details pertaining to GAL4 organisation, the function of each of the subsystems involved, structural profile of the binding region, the consensus GAL4 binding sites and the oligonucleotide which was used in co-crystallographic studies with the DNA recognition element. Thus, in the GAL4, amino acids 1-65 are involved in DNA recognition, 65-94 in DNA independent dimerisation and most of the others for transcriptional activation and other function. Chart B.14 shows, also in detail, the structural and functional profile of the DNA recognition element. As could be seen here, this consists of three subsystems namely metal binding domain, linker region and dimerisation element. A specific DNA complex of the 65 residue recognition fragment was analysed at 2.7 A resolution by X-ray crystallography. The overall profile shows that the protein binds as a dimer to a symmetrical 17 base pair sequence, a small zinc(II) containing domain recognises a conserved CCG triplet at each of the sites through direct contacts with the major groove. A short coiled-coil dimerisation element imposes two fold symmetry. A segment of polypeptide chain links the metal binding module to the dimerisation element and specifies the length of the site, Chart B.14.

The protein fragment binds to its DNA site as a symmetrical dimer. Each

Chart B.13

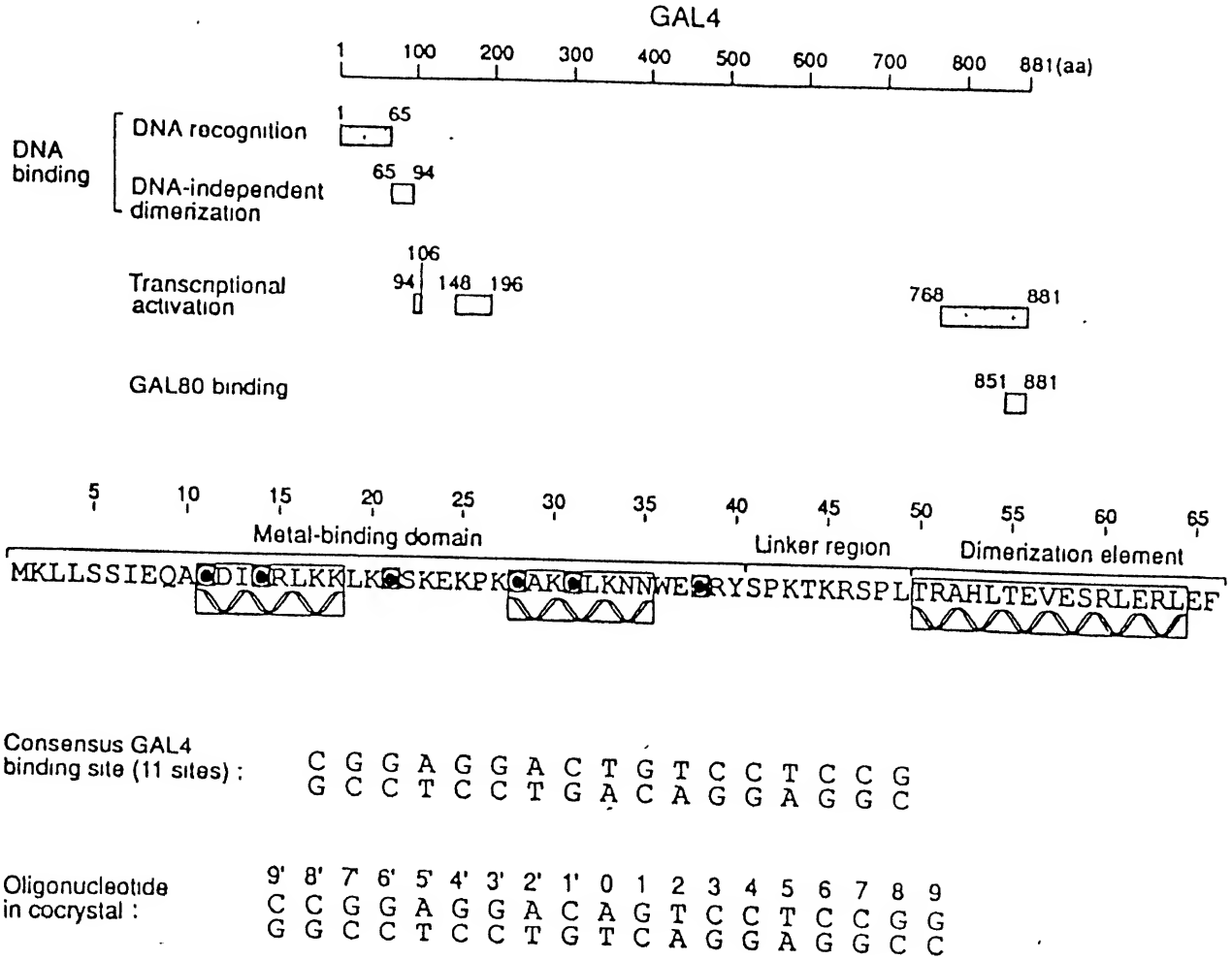

GAL4 (B) and its DNA binding site (C) used for co-crystallisation studies of GAL4 - DNA complex (A)

subunit folds into three distinct module; a compact metal binding domain (8-40), an extended linker (41-49) and an α helical dimerisation element (50-64). The overall view of the complex (Chart B.14) would show that a large part of the DNA major groove is not contacted by the protein. In this the GAL4 motif is very much different from the earlier two that were discussed in length. The DNA is relatively straight. A metal domain lies in the major groove near each end of the DNA fragment. The paired parallel helices of the dimerisation element project away from the DNA, along the two fold axis of the complex. The metal binding domain contacts three DNA base pairs in the major groove and therefore could be rightly called as the recognition module. This motif is held together by two metal ions tetrahedrally coordinated by 6 cysteines, two of the cysteines 11 and 28 ligate both metals creating a binuclear cluster (Chart B.15).

Residues 50 - 64 form an amphipathic α helix. The coiled-coil is positioned over the DNA minor groove perpendicular to the DNA helix axis. The linker region (41 - 49) forms an extended segment connecting the recognition module with the dimerisation element, the whole concept very much reminiscent of the leucine zipper motif.

The DNA in the complex has only small deviation from a standard B structure. The consensus GAL4 binding site is roughly symmetrical, the 17 base pair element with a highly conserved CCG sequence at either end reading outwards 5' $\rightarrow$ 3' from the diad which is recognised by the metal cluster (Chart B.14). The two recognition modules lie in the major groove separated by about one and one half turns of the DNA helix and centered over the conserved CCG triplets. Additionally, they are anchored to the sugar phosphate backbone by hydrogen bonds. In summary, the crystal structure shows that recognition of DNA by a GAL4 dimer combines 3 components: (i) specificity for the conserved CCG triplets, provided by direct

Chart B.14

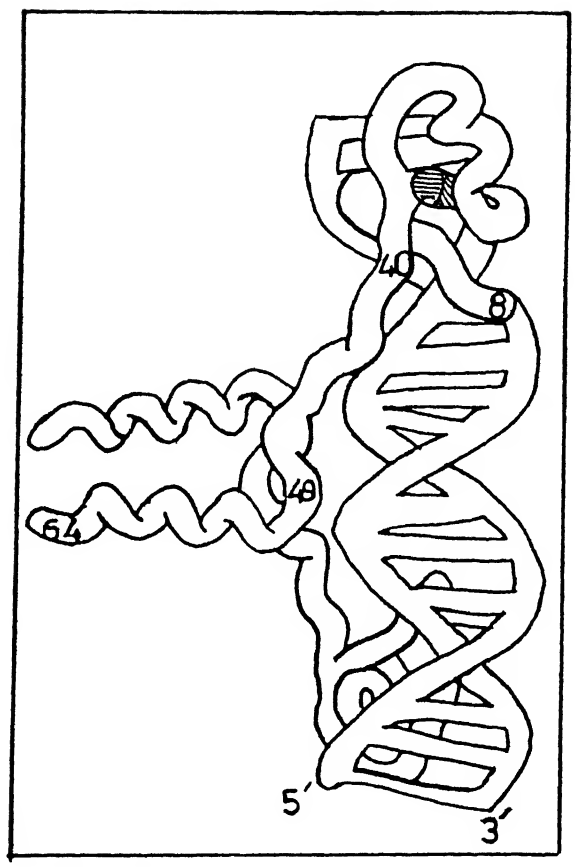

Structure of the GAL4/DNA complex

The protein is represented as a ribbon structure; the zinc atoms as shaded circles

Chart B.15

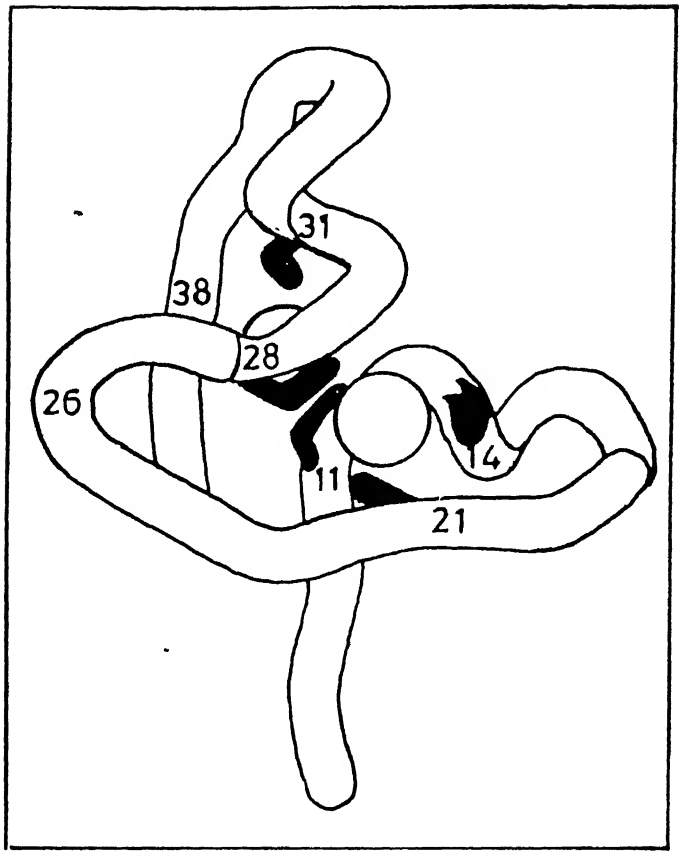

Structure of the metal binding DNA recognition module of the GAL4 protein

The filled sticks represent the Cys residues that chelate the two zinc ions (circles); cysteines 11, 14, 21 and 28 are the ligands for one zinc ion, and 11, 28, 31 and 38 the ligands for the other; residues at 11 and 28 are shared by both ions.

contact with the recognition modules in the major groove ; (ii) requirement for a symmetrical site provided by a coiled-coil dimerisation region that lies over the minor groove and (iii) preference for the number of intervening base pairs provided by the conformation of the linker.

A most interesting aspect of GAL4 recognition is that the intervening 11 central base pairs are exposed and are accessible to major groove contacts. Thus the possibility of additional protein recognition in this region is very much a possibility. Indeed there are indications that this exposed region is used for secondary recognition processes[15].

The background above provides a very clear picture of 3 motifs which uses zinc(II) coordination for DNA recognition. Above all, they illustrate the versatility of the metal template which can be used under varied environments and yet result in the unified purpose, namely the recognition of the DNA sequence. The modular profile of these 3 systems are illustrated in Chart B.16.

The importance of zinc in the formation of tetrahedral templates pertaining to specific folding of long stretches of proteins has received, in the very recent past, wide recognition. These developments, few of which are illustrated below, hopefully would demonstrate that the identification and characterisation of potential zinc template motifs in natural and synthetic environments would lead to the understanding of innumerous facets pertaining to protein - DNA interaction.

Shortly after the discovery of the pattern of cysteine and histidine residues in TFIIIA, a systematic search method was developed for identifying patterns of Cys and His residues in proteins of known sequence[16]. Prominent among the proteins discovered by this method are the retroviral nucleocapsid protein and some viruses typified by rauscher murine leukamia virus. These contain a single sequence of the form $CysX_2CysX_4HisX_4Cys$. Others, such as human immunodeficiency virus con-

Chart B.16

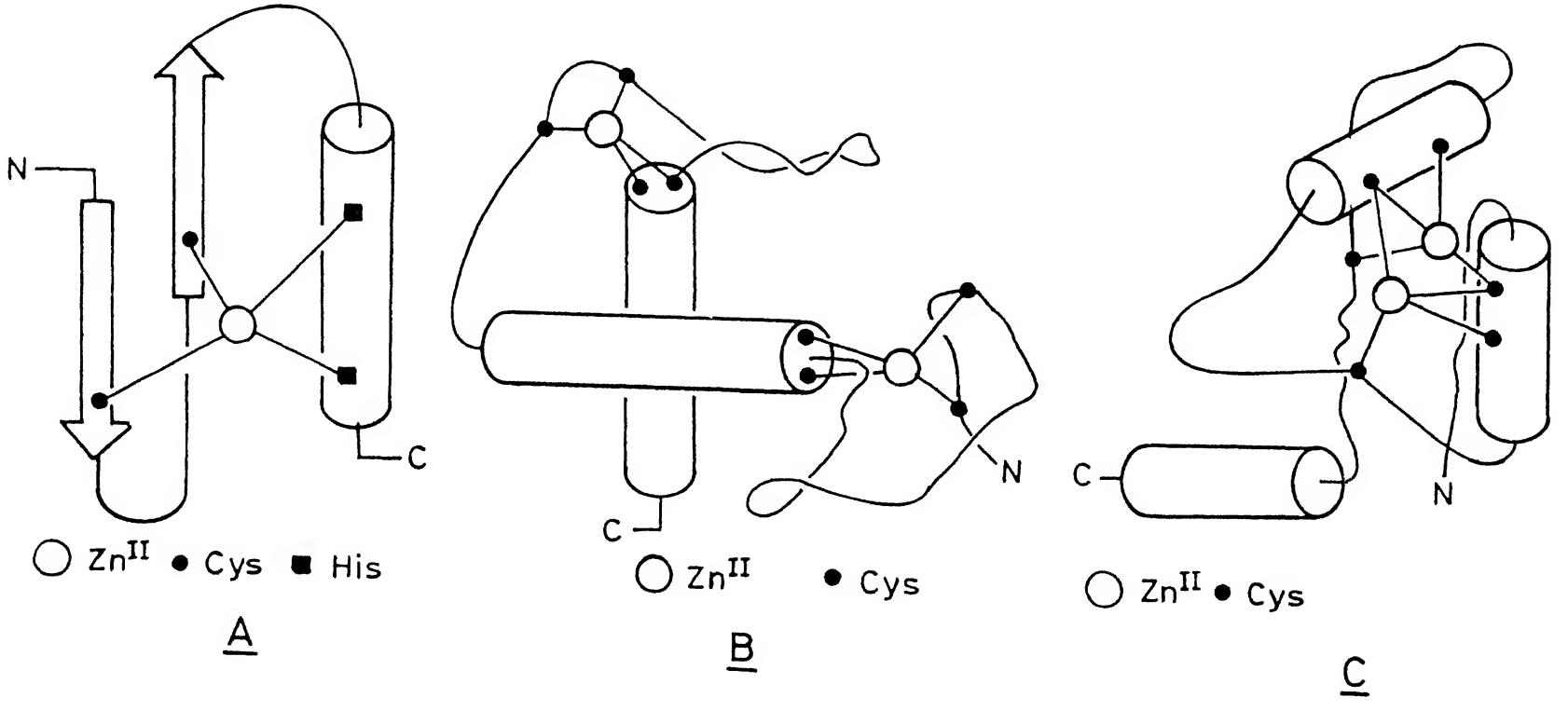

Zinc containing protein modules for DNA recognition

A : The Zinc Finger ; B : The Glucocorticoid Receptors ; C : The GAL4

tain, two such sequences. Because of their importance such sequences are referred to as "CCHC" box. Studies with synthetic peptides derived from several viruses and with synthetic proteins from rauscher murine leukamia virus have revealed that reduced materials containing these patterns bind metal ions such as zinc and cobalt with high affinity. Moreover the presence of such ions have profound effects on the structure of the metal binding domain as determined by nmr studies[17]. The structure of one such retroviral CCHC box has been determined fairly precisely by nmr methods[18] (Chart B.17).

The 18 residue peptide DQCAYCKQKGHWAKDCPK, derived from the core nucleic acid binding protein from rauscher murine leukamia virus binds metal ions such as zinc(II) and cobalt(II). A detailed 3-D structure for this domain has been obtained by comparison of crystallographically characterised metalloproteins of similar domains and on detailed nmr analysis[19].

The potential of the zinc template motifs in protein engineering is truly enormous. This aspect has been forcefully illustrated in recent studies pertaining to dimerisation of human growth hormone (HGH) in presence of zinc(II) ions leading to the box HHDE as shown in Chart B.18. Needless to say the biological profile of such modified hormones would prove interesting[20]. In this regard, the complexation of zinc porphyrins with adenine as shown in Chart B.19 reported recently is noteworthy[21].

It is curious that in those organisms most noted for genomic economy, the procaryotes, no zinc bearing transcription factors have yet been identified. Thus it is reasonable to conclude that the identification of zinc in DNA recognition is synonymous with evolution leading to multifaceted cellular assembly. It is becoming increasingly clear that the mechanism of transcription is remarkably conserved throughout the eucaryotic kingdom. Such functional conservation undoubtedly in-

dicates that the basic mechanism of transcriptional initiation has existed since the first eucaryotic organism. In addition to the conservation of the basic transcriptional activation mechanisms, eucaryotic cells from yeast to human contain structurally similar and functionally analogous transcription factors that recognise essentially identical sequences. By analogy, the genetic code is essentially universal and eucaryotic TATA elements and procaryotic ten base sequences are similar though transcriptional mechanisms are quite different.

The past few years have brought exciting progress in the study of protein - DNA recognition, but important questions remain. Although many of the problems are interrelated, some of the most critical questions involving issues of structure, energy, evolution, gene regulation and protein design await clear-cut answers.

Chart B.17

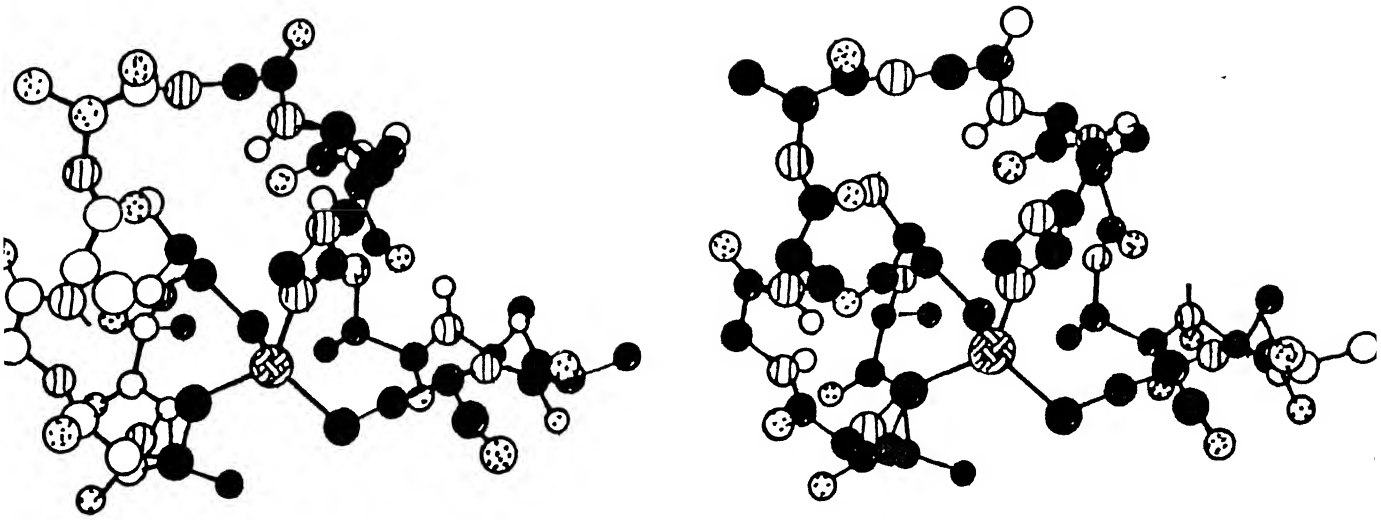

The stereo pair showing the structure of a retroviral CCHC box peptide bound to zinc

Chart B.18

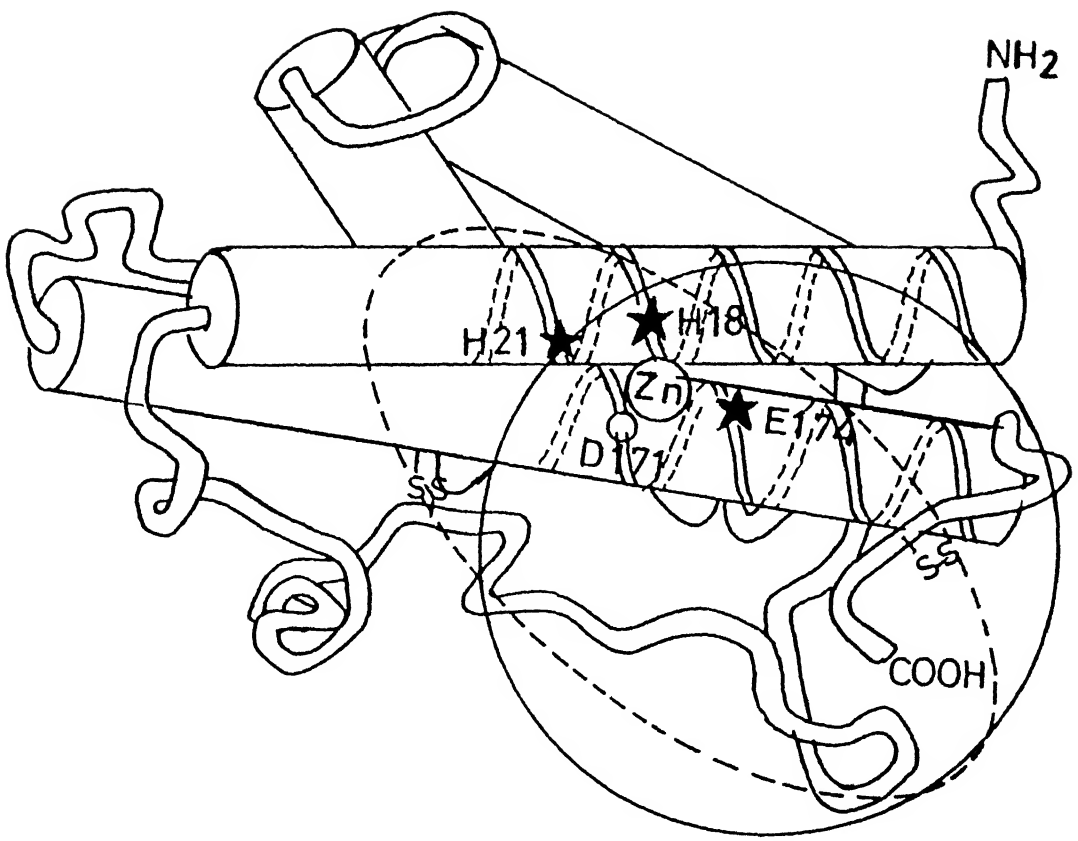

Location and structure of the Zn^{2+} binding site in hGH

Stars are the putative location of the Zn^{2+} ligands; large solid circle denote the metal binding regions for the hGH receptor; the open circle shows the non-ligand Asp^{174}.

Chart B.19

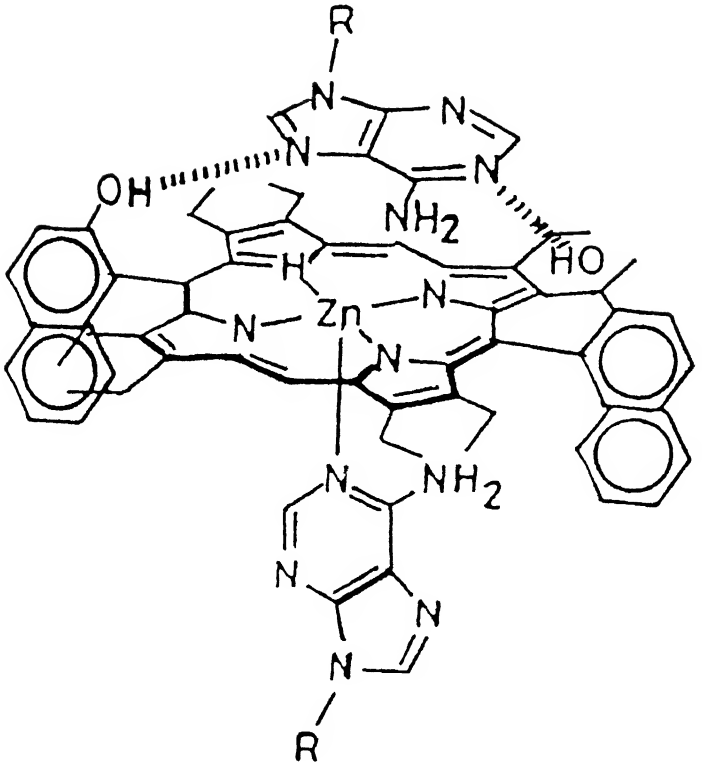

New mode of porphyrin complexation with nucleobase adenine

C. PRESENT WORK: SYNTHESIS

Transcriptional factors regulate cell development, differentiation and cell growth by binding to specific DNA sites, the first event of which is the direct DNA sequence recognition by a relatively small autonomous region. Sustained activity in the eucaryotic genome recognition factors have so far brought out typical ensembles, such as, extended helical homeodomains leucine zipper, zinc finger, gluco-corticoid receptor and GAL-4 activators [22]. Zinc finger, originally encountered as tandem modules constituting transcription factor IIIA[6], is now considered, for transcriptionally regulating proteins, one of the rare generalised conformation through which sequence specific recognition can occur and, logically, the zinc finger template - tetrahedral Zn^{II} in a $(thiolate)_2(imidazole)_2$ environment - is emerging as a major structural motif involved in protein- DNA recognition. Recent crystallographic studies[10] tend to show that the binding energy contribution of this template plays a pivotal role in properly orienting the peptide recognition loop of the finger towards the major groove of the B-DNA.

We felt that the synthesis and DNA interaction studies of a minimal zinc finger structural motif is essential not only with respect to the understanding of the structural interaction involved with DNA but also to provide the cornerstone for construction of finger modules so designed as to recognise specific DNA triplet sequences.

The role of the basic zinc template in zinc finger protein is confirmed and crystallographically proven to be essential for DNA recognition. Central to this is the fact that $zinc^{II}$ forms well oriented tetrahedral complexes, thus providing the appropriate anchor for construction of the actual DNA recognition systems. This notion

has been further strenghthened by the more recent understanding of the nature of gluco-corticoid receptor protein - DNA interaction . Crystallographic studies here have shown that the DNA recognition takes place on the basis of a dimer, each unit of which contains two zinc atoms, tetrahedrally coordinated to four cysteines. This template motif, namely, Zn-(thiolate)$_4$, performs, within each of the units two different functions. One of the template is involved in DNA recognition and the other in the formation of the dimer. Thus, the role of the basic templates pertaining to the zinc finger motif and the gluco-corticoid receptor in DNA recognition should be different. In this context, it was considered very attractive to synthesise the basic template associated with gluco-corticoid receptor for DNA recognition studies.

Approaches to zinc finger template has been shown in a retrosynthetic manner in Scheme C-1. In this, the ultimate synthetic objective, namely, a single unit of zinc finger comprising of $\sim$ 30 residues, can be easily made from the metal free precursor. The minimal zinc finger template would arise from zinc^{II} complexation of pairs of cysteines and histidines. This can be, as shown in Scheme C-1, accomplished either from His-Cys-Cys-His precursor or from S-protected Cys-His units. Both approaches has been successfully illustrated in the present work. In Scheme C-2 is shown, by retrosynthetic analysis, the possible route to the tripeptide which on reduction and complexation would lead to the zinc finger template. In Scheme C-3 is shown by a retrosynthetic analysis approach to the basic zinc finger template involving the alternate strategy of using S-protected cysteine.

L-Cystine on treatment with anhydrous methanolic HCl afforded cystine diOMe. 2HCl (1)[23] in 73% yields. Alternatively, treatment of cystine with isobutene in THF - H_2SO_4 afforded cystine di-O^{t}Bu (2)[24] (32% yield). N-Protection of cystine was achieved via treatment with either benzoyl chloride or benzyloxy carbonyl chloride

Scheme C-1

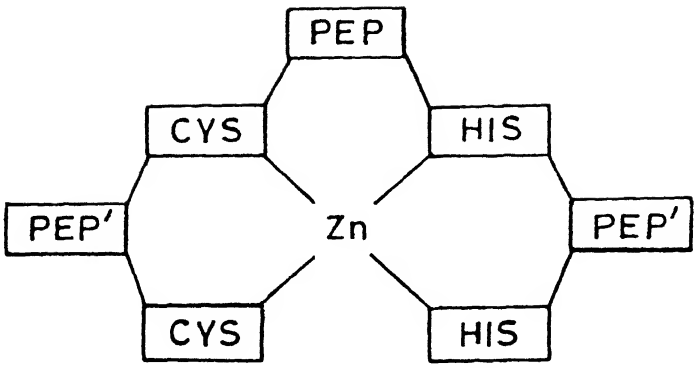

CYS : CYSTEINE HIS : HISTIDINE PEP′: LINKER (~4 RESIDUES)
PEP: RECOGNITION ELEMENT (~12 RESIDUES)

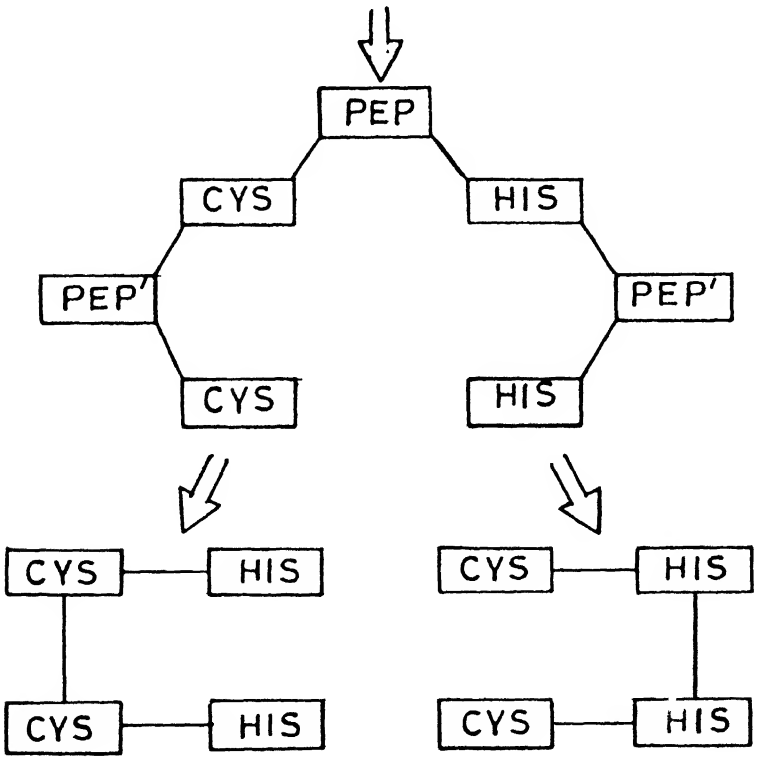

Scheme C-2

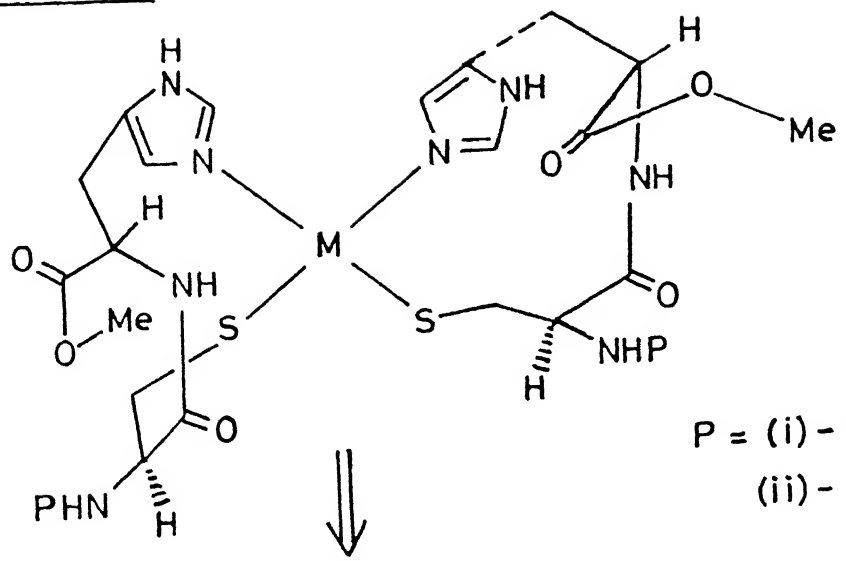

P = (i) - $COOCH_2C_6H_5$ (Z)
(ii) - $COOC(CH_3)_3$ (BOC)

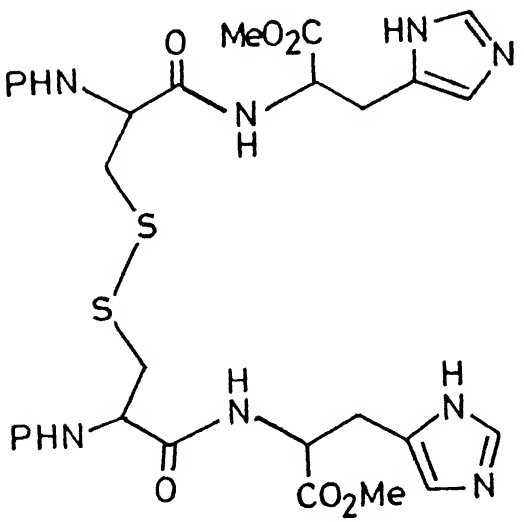

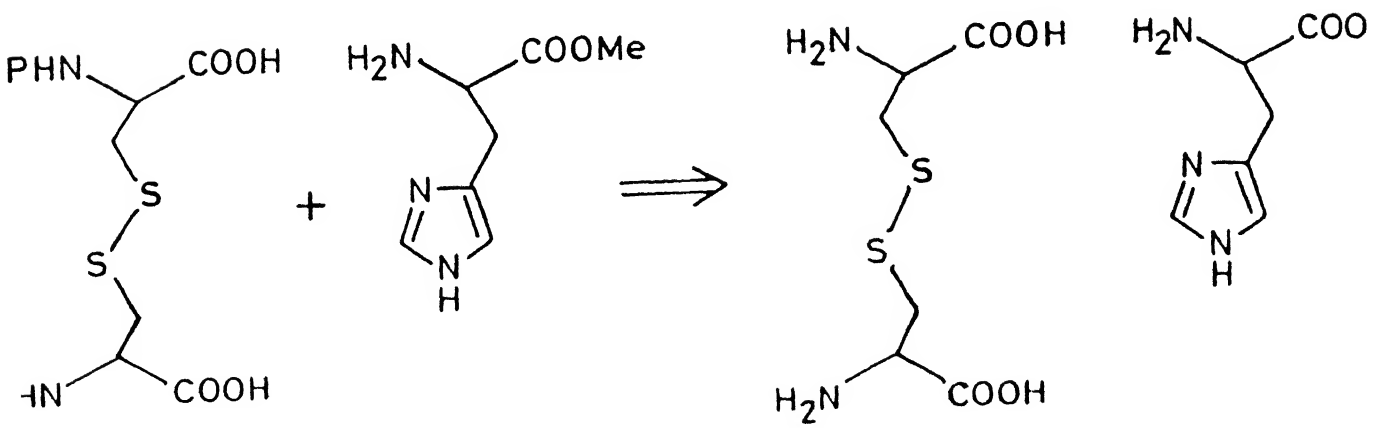

Scheme C.3

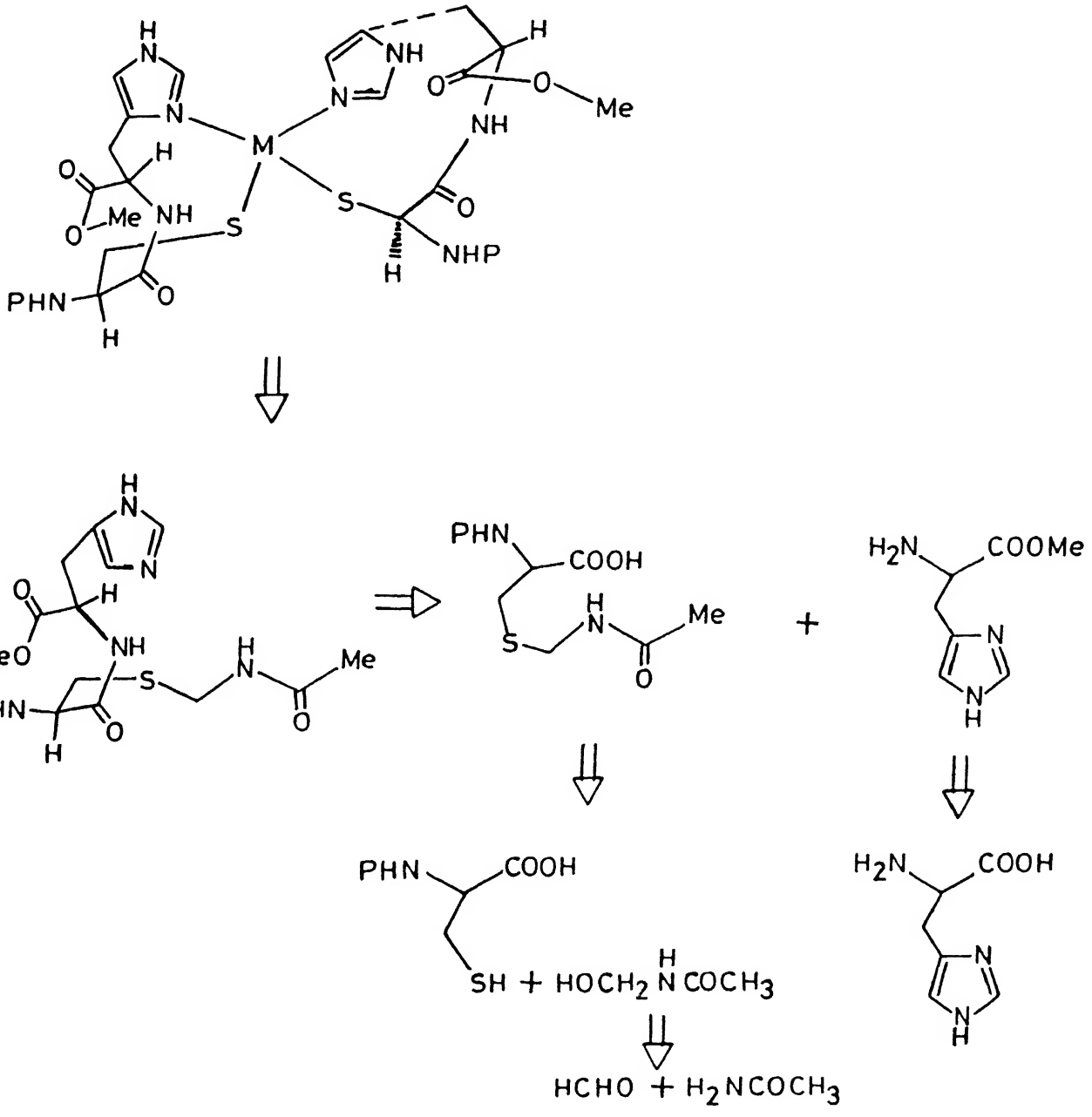
PHN
COOH
SH + HOCH2 N COCH3
H
HCHO + H2NCOCH3
H2N
COOMe
COOH
MeO
Me
NHP

by Schotton-Bouman procedure leading to, respectively, bis-Z-cystine (3)[25] (68.9%) and bis-Bz-cystine (5)[26] (84% yield). Finally, N-protection by ^{t}butyloxy carbonyl residue was accomplished with di-tertiary butyl di carbonate in presence of anhydrous NaOH, leading to bis-Boc-cystine (4)[27] (63.9%) (Chart C.1).

As substrates for further studies, the fully N,C - protected cystine was also prepared. Reaction of cystine di-OMe 2HCl (1) with either benzyloxy carbonyl chloride or benzoyl chloride in aqueous bicarbonate afforded, respectively, bis-Z-cystine di-OMe (6)[23] (34.5% yield) and bis-Bz-cystine di-OMe (7)[23] (52%). Compounds (6) and (7) were also prepared via reaction of their appropriate precursors, namely, (3) and (5), with CH_2N_2-MeOH, in respectively, 85% and $\sim$ 100% yields (Chart C-2).

Cystine-di-O^{t}Bu (2):

ir: ν_{max} (neat) cm^{-1} : 3376, 1730, 1155, 1035.

nmr: δ ($CDCl_3$) (60MHz) : 1.50(s, 18H, t-butyl), 2.95(t, 4H, β-CH_2-), 3.65(b, 2H, α-CH).

Bis-Z-cystine (3):

mp 112^o-115^{o}C (lit.[25] 114^{o}C).

ir:ν_{max} (KBr) cm^{-1}: 3310, 1690, 1530, 1060.

nmr : δ ($CDCl_3$) (80MHz) : 3.22(d, 4H, β-CH_2), 4.59 (q, 2H, α-CH), 5.13(s, 4H, $ArCH_2$), 6.00(d, 2H, -CONH-), 7.41(s, 10H, Ar-).

Bis-Boc-cystine (4):

mp 145^o-146^{o}C (lit.[27] 143^o - 145^{o}C).

ir: ν_{max} (KBr) cm^{-1}: 3370, 2980, 1720, 1680, 1510.

nmr: δ($CDCl_3$)(80MHz): 1.4(s, 18H, $(CH_3)_3$, 3 1(d, 4H, β-CH_2), 4.6(b, 1H, α-CH),

CHART C.1

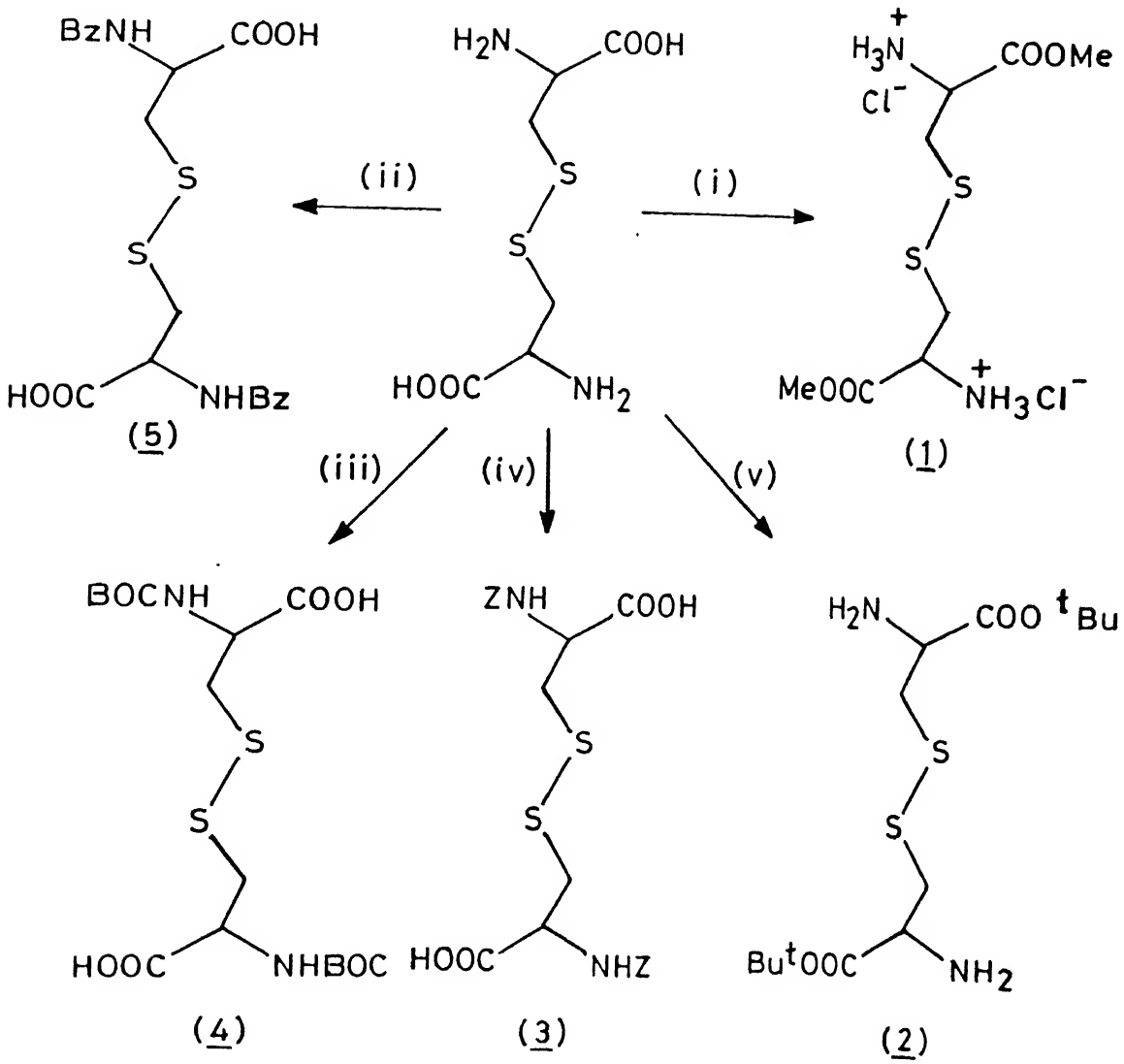

(i): HCl - MeOH (ii): BzCl - NaOH - H_2O

(iii): $(^tBuO)_2CO$ - MeOH - NaOH - H_2O (iv): ZCl - NaOH - H_2O

(v): $(Me)_2C=CH_2 - H_2SO_4$ - THF

CHART C.2

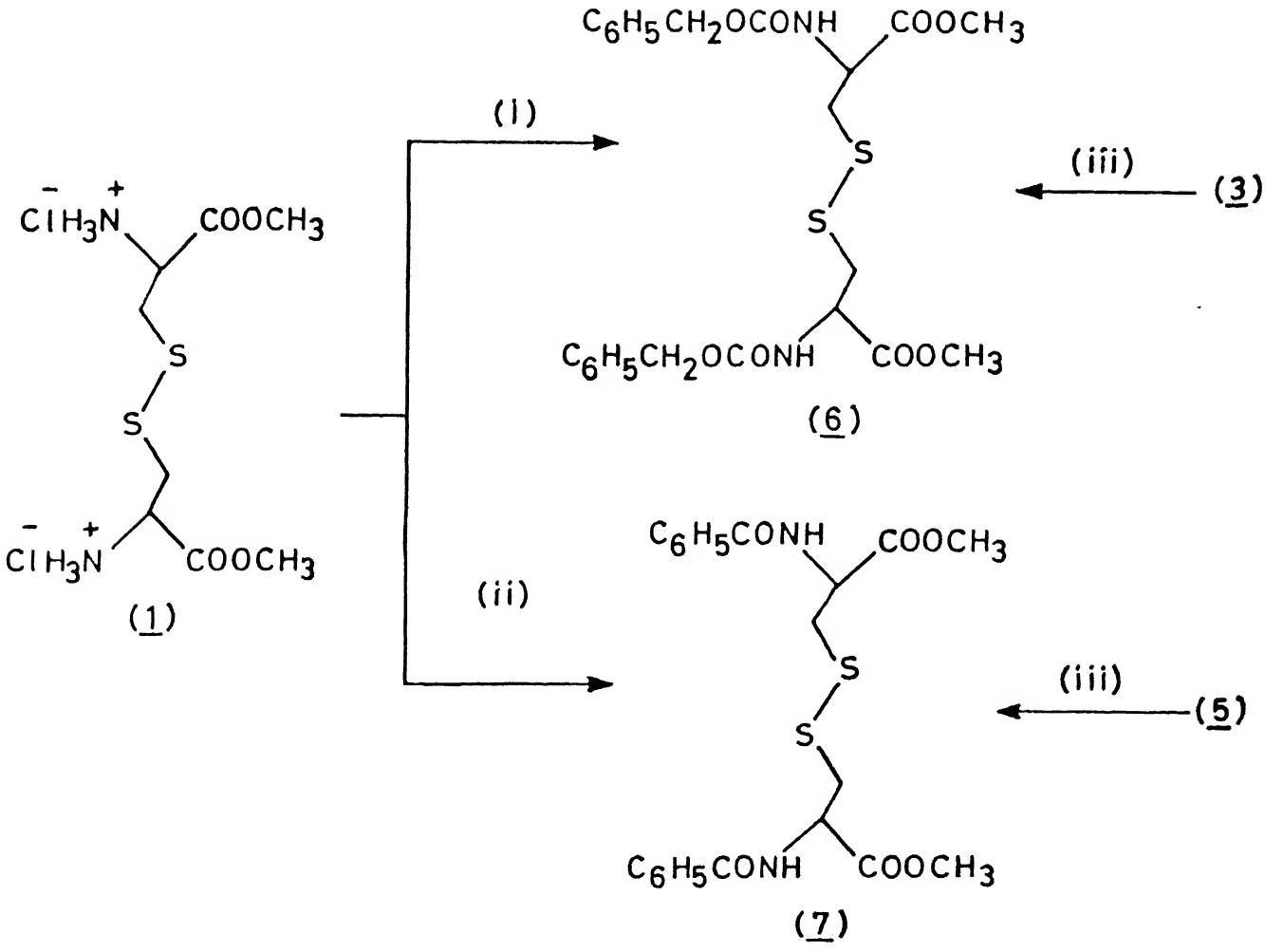

(i) $ZCl-NaHCO_3-H_2O$ (ii) $BzCl-NaHCO_3-H_2O$ (iii) CH_2N_2-MeOH

5.5(b, 1H, -CONH-).

Bis-Bz-cystine (5):

mp 197°-198°C (lit.[26] 196°-197°).

Bis-Z-cystine di-OMe (6):

mp 66°-68° (lit.[23] 73°-75° C).

ir:ν_{max} (KBr) cm^{-1}: 3340, 1735, 1695, 1540, 1240.

nmr: $\delta(CDCl_3)$ (80MHz): 3.15 (d, 4H, β-CH_2), 3.75 (s, 6H, ester), 4.62 (q, 2H, α-CH), 5.13 (s, 4H, $ArCH_2$), 5.59 (b, 2H, -CONH-), 7.33(s, 10H, Ar-).

Bis-Bz-cystine di-OMe (7):

mp 169°-171°C, (lit.[23] 177°-178°C).

ir:ν_{max} (KBr) cm^{-1}: 3340, 1750, 1640, 1528.

nmr:δ ($CDCl_3$) (80MHz): 3.30 (d, 4H, β-CH_2), 3.76 (s, 6H, ester), 5.0 (q, 2H, α-CH), 7.74 (m, 10H, Ar-), 8.45 (d, 2H, -CONH-).

The substrates used for coupling studies, bis-Z-cystine di-ONp (8) and bis-Boc-cystine di-ONp (9) were prepared, in respectively, 62% and 64% yields from bis-Z-cystine (3) and bis-Boc-cystine (4) by reaction with p-nitrophenol and DCC in EtOAc (Chart C-3).

Bis-Z-Cystinyl di-ONp (8):

mp 125°-127°C.

nmr: δ ($CDCl_3$) (80 MHz) : 3.34(d, J=5Hz, 4H), 4.88(q,2H), 5.12 (s, 4H), 5.72(d, 2H), 7.38(br, 14H), 8.25(d, 4H, J=9Hz).

CHART C.3

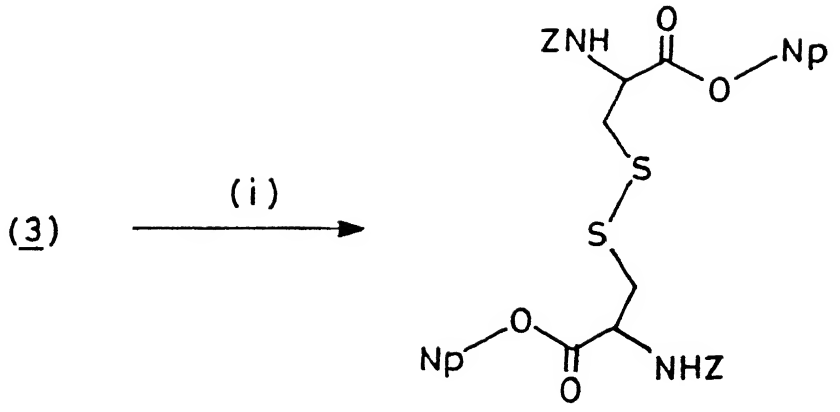

(8)

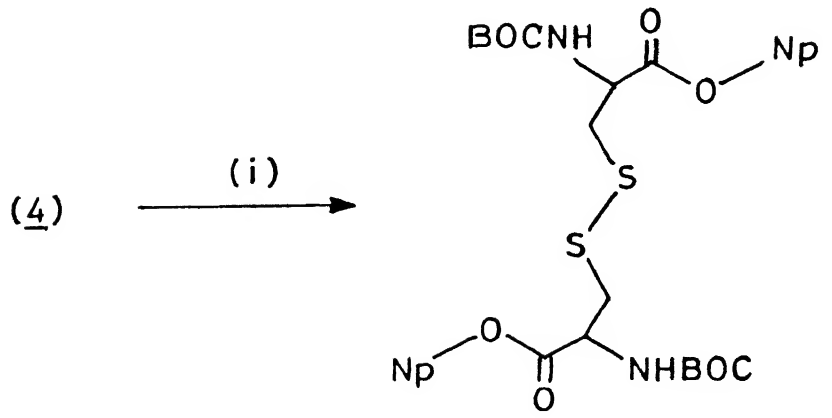

(9)

(i) Np-OH-DCC-EtOAc

Bis-Boc-Cystine di-ONp (9):

mp 133°-136°C.

ir:ν_{max} (KBr) cm^{-1} : 3373, 1772, 1755, 1681, 1520, 1253, 1054.

nmr: δ ($CDCl_3$) (80MHz): 1.47(s, 18H), 3.35(d, 4H), 4.83(q, 2H), 5.51(d 2H), 7.32, 8.38(d,d 8H).

Cysteine.HCl was S-protected to acetamidomethyl cysteine HCl (10) in 35.4% yields by reaction with hydroxymethyl acetamide in presence of aqueous HCl. The hydroxymethyl acetamide, in turn, was prepared by condensation of acetamide with formalin in aqueous K_2CO_3[28].

S-Acetamidomethyl cysteine hydrochloride (10) on treatment with benzyloxy-carbonyl chloride in aqueous NaOH afforded Z acetamidomethyl cysteine (Z-S-Acm Cys)(11) (91.4% yields) [29]. N-Boc protection was achieved by treatment of (10) with Boc-azide using TMG - DMF leading to Boc acetamidomethyl cysteine (Boc-S-Acm Cys) (12) in 32% yields [29] (Chart C-4).

As an intermediate for the synthesis of gluco-corticoid receptor template, acetamidomethyl cysteine methyl ester (S-Acm Cys-OMe) (13) was prepared by treatment of (10) with $SOCl_2$ - MeOH (Chart C-4).

S-Acm Cys.mono H_2O (10):

mp 187°-190°C (dec.) (lit.[28] 187°C (dec.)).

ir:ν_{max} (KBr) cm^{-1} : 3238, 1727, 1602, 1560.

nmr: (D_2O) (80MHz): 2.0(s, 3H, Ac-), 3.09(m, 2H, cys β- CH_2), 3.92(m, 1H, cys

CHART C.4

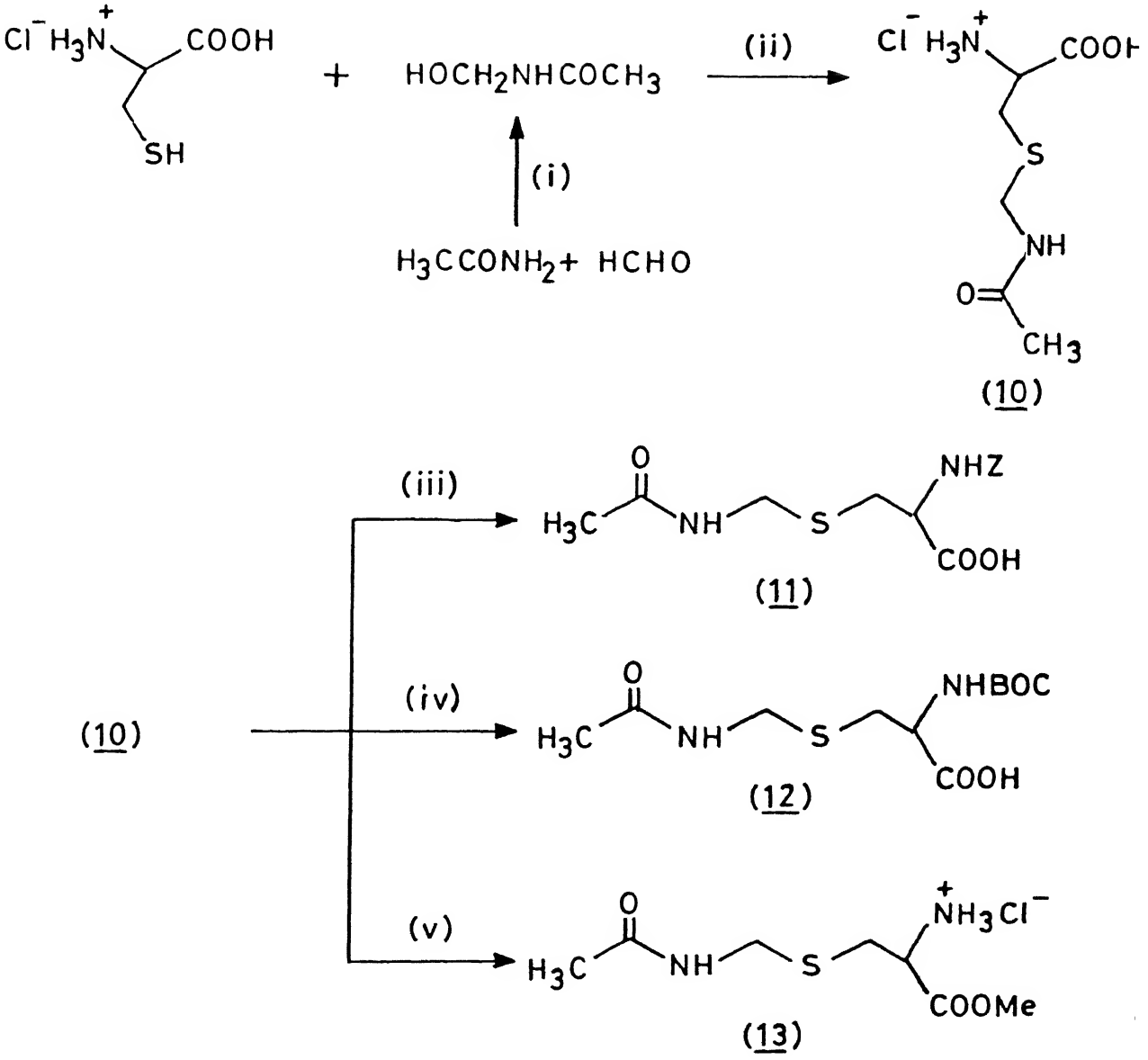

(i) $K_2CO_3 - H_2O$ (ii) $HCl - H_2O$ (iii) $ZCl - NaOH - H_2O$

(iv) $BOCN_3 - TMG - DMF$ (v) $SOCl_2 - MeOH$

α-CH), 4.15(m, 2H, -CH_2NHAc).

Z-S-Acm Cys (11):

ir: ν_{max} (neat) cm^{-1} : 3370, 1748, 1650, 1556.

Boc-S-Acm Cys (12):

mp 104°-106°C (lit.[29] 110°-112°C).

ir: ν_{max} (KBr)cm^{-1}: 3359, 1718, 1700, 1527, 1164.

nmr:δ ($CDCl_3$ (80MHz): 1.43 (s, 9H, $(CH_3)_3$C-), 2.00 (s, 3H, Ac-), 3.07 (2H, m, β-CH_2), 4.46 (b-m, 3H, α-CH-, -S-CH_2-NH-), 5.61 (b, 1H, -O-CO-NH-), 8.82 (b, 1H, -CH_2-NH-CO-).

S-Acm Cys-OMe (13):

ir: ν_{max} (KBr) cm^{-1} : 1732, 1240.

As with the case with cystine (*vide supra*), the required p-nitrophenyl ester for coupling were made by reaction of Z-S-Acm cysteine (11) and Boc-S-Acm cysteine (12) with p-nitrophenol and DCC in EtOAc leading to, respectively, Z-S-Acm Cys ONp (14)(88.4% yield) and Boc-S-Acm Cys ONp (15) (78% yield) (Chart C-5).

Z-S-Acm Cys ONp (14):

mp 102°-105° C.

ir: ν_{max} (KBr) cm^{-1} : 3320, 1720, 1692, 1533, 1347.

Boc-S-Acm Cys ONp (15):

mp 88°-90°C.

ir: ν_{max} (KBr) cm^{-1} : 3338, 1771, 1685, 1534, 1517, 1345,1152, 1064.

L-Histidine . HCl was converted to histidine methyl ester hydrochloride (His-

CHART C.5

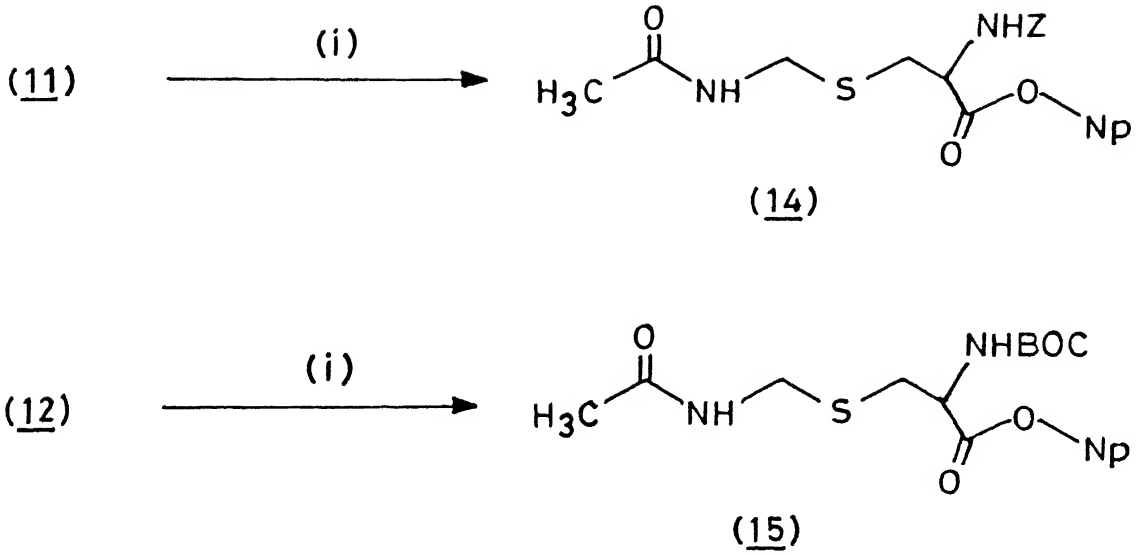

(i) Np-OH-DCC-EtOAc

OMe.HCl) (16) [30] (43% yield) by treatment with HCl-H_2SO_4 in anhydrous MeOH. An aspect noteworthy of mention from practical vantage is that the procedure for (16) by treatment of His.HCl with methanolic HCl alone [31] failed to give any product. Treatment of a CH_2Cl_2 suspension of His-OMe.HCl (16) with dry NH_3 afforded His-OMe (17) (90-95% yield). The latter could also be prepared *in situ* from (16) by addition of Et_3N. Treatment of (17) with di-t-butyl-dicarbonate in pyridine afforded N^{α}-Boc His-OMe (18)[32] (93.43% yield) and N^{α},N^{ω}-di-^{t}butyl His-OMe (19). Interestingly, compound (19) when allowed to stand at room temperature for prolonged periods lost elements of CO_2 and isobutylene leading to (18).

As a starting material for the synthesis of basic 'anti sense' zinc finger template, which was also undertaken in DNA interaction studies, N^{α}-Boc-His-OMe (18) was transformed to the hydrazide by treatment with methanolic $N_2H_4.H_2O$ to afford N^{α}-Boc-His hydrazide (20) (93% yield) (Chart C-6).

HisOMe.2HCl (16):

mp 204°-206°C (lit.[30] 200°-202°C).

ir: ν_{max} (KBr) cm^{-1}: 1760.

nmr: δ (D_2O)(80MHz) : 3.38(d, 2H, β-CH_2), 3.78(s, 3H,

ester), 7.59(s, 1H, im4-H), 8.69(s, 1H, im4-H).

N^{α}-Boc-His-OMe (18):

mp 118°-120°C (lit.[32] 125.5°-126°).

ir:ν_{max} (KBr) cm^{-1}: 3326, 3239, 1675, 1524, 1168, 1052.

nmr: ($CDCl_3$) (80MHz): 1.45 (s, 9H, $(CH_3)_3C$-), 3.14 (d, 2H, β-CH_2), 3.73(s, 3H, ester), 4.53 (q, 1H, α-CH), 5.82 (d, -CONH-, 1H), 6.90(s, 1H, im4-H), 7.61 (s, 1H,

CHART C.6

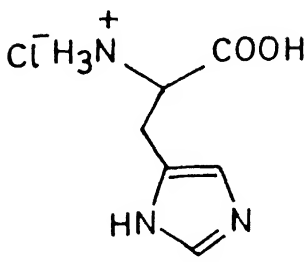

(i)

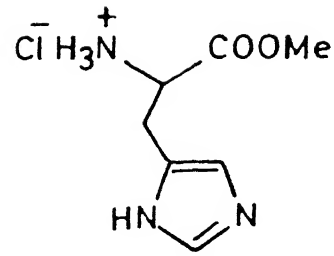

(16)

(ii)

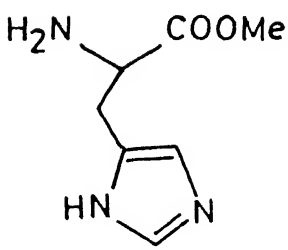

(17)

(iii)

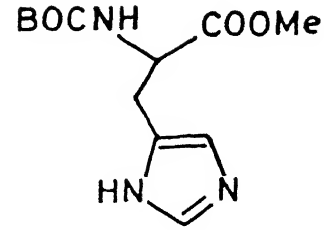

(18)

+

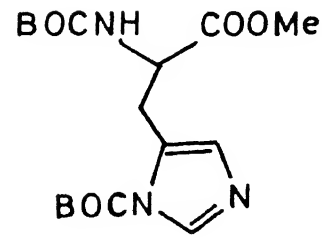

(19)

(18)

(iv)

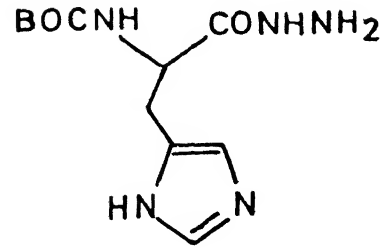

(20)

(i) $HCl-H_2SO_4$ -MeOH

(ii) $Et_3N-CH_2Cl_2$ (iii) $(^tBuO)_2CO$-Pyridine (iv) N_2H_4-MeOH

CHART C 7

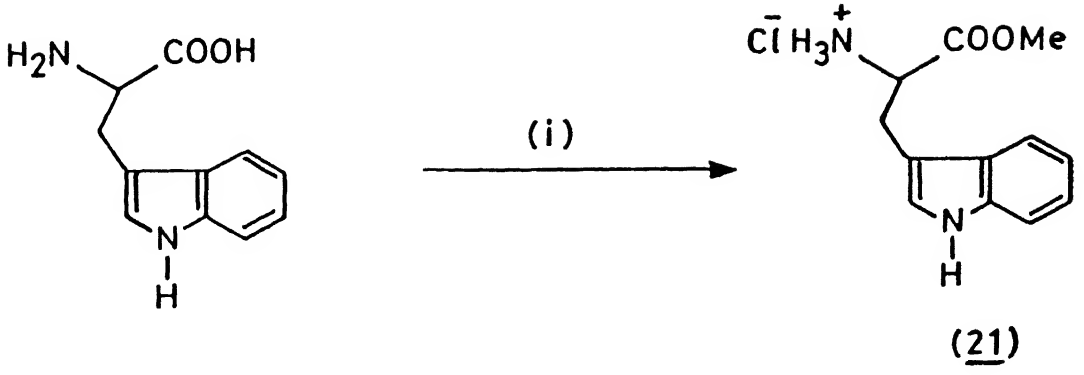

(21)

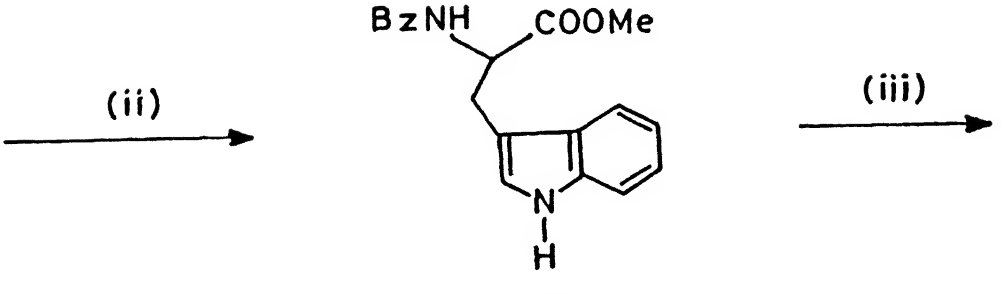

(22)

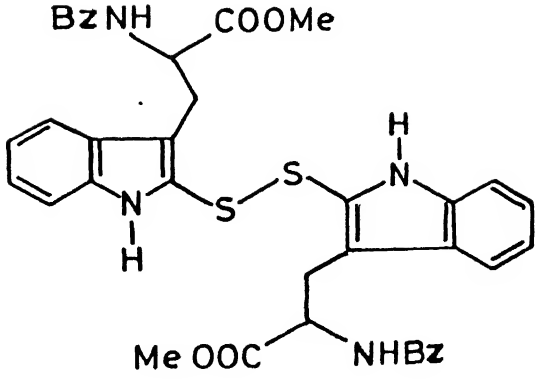

(23)

(i) $SOCl_2$–MeOH (ii) BzCl–$NaHCO_3$–H_2O (iii) S_2Cl_2

afforded the desired tripeptide bis-Z-Cystine di-His-OMe (24) in 89% yields.[35] The Boc protected derivative (9) was similarly transformed to bis-Boc-Cystine di-His-OMe (25) in 67% yields (Chart C-8).

Bis-Z-Cystinyl di-His-OMe (24):

mp 154°-156°C.

ir: ν_{max} (KBr) cm^{-1} : 3307, 1734, 1695,1654, 1540.

nmr: δ (DMSO-d_6) (400MHz): 2.83, 3.08(q,q, 4H, Cystine β-CH_2), 2.93 (m, 4H, His β-CH_2), 3.55(s, 6H, ester), 4.32(q, 2H, Cystine α-CH), 4.47(q, 2H, His α-CH), 5.04(s, 4H, Ar-CH_2), 6.83(s, 2H, His4H), 7.33(m, 10H, Ar), 7.52(s, 2H, His2H), 7.56(d, 2H, Cystine NH), 8.5(d, 2H, HisNH).

ms: (FAB) m/z 811 $(M+H)^+$, 407 (Z-Cys-His-OMe + H)$^+$.

$[\alpha]_D^{25}$ = -78.77 (c = 0.9, MeOH).

Bis-Boc-Cystine di-His-OMe (25):

mp 142°-145°C.

ir: ν_{max} (KBr) cm^{-1} : 3327, 1737, 1691, 1657, 1521, 1171, 1047.

nmr: δ($CDCl_3$ + $DMSO_6$) (80MHz): 1.43 (s, 18H), 3.14 (b, 8H,Cys β-CH_2 , His β-CH_2), 3.69 (s, 6H), 4.65 (b, 4H, Cys α-CH, His α-CH), 6.26 (d, 2H, Cys NH), 6.88 (s, 2H, His 4H), 7.74 (s, 2H, His2H), 8.06(d, 2H, His NH).

ms: (FAB) m/z : 743 $(M+H)^+$, 372 (Boc-Cys His-OMe+ H)$^+$.

$[\alpha]_D^{25}$ = -73.30 (c, 0.232, MeOH).

In addition to data provided above, the structure of the tripeptide (24) was

fully confirmed by detailed nmr studies, including TOCSY (totally correlated spectroscopy). A comparison of 400MHz nmr of (24) and its TOCSY spectrum (section D) would show a complete correlation of peak assignment. Amongst the through bond coupling observed, the important ones are, the cross peaks, histidine(His) peptide NH for both α- and β-CH_2 of His residues, cystine NH for both α and β-CH_2 of cystine residues, of α-CH of cystine and α-CH of His residues to their respective β-CH_2 units. FAB mass spectrum of (24) exhibited strong peak at mass number 811 $(MH)^+$. Fragmentation leading to two halves was also observed. Conventional mass spectrum failed to give satisfactory mass spectral results.[35]

It may be noted that in the usual zinc finger module, the conserved cysteines are towards the amino end and the histidines towards the carboxyl end. This aspect could be clearly seen from compound (25), Chart C-8. Since the minimal zinc finger template should reflect a Zn^{II} placed in a $(thiolate)_2(imidazole)_2$ environment, yet another synthetic alternative exists wherein the histidines are towards the amino end and the cysteines at the carboxyl end. The latter, therefore, would be an 'anti sense' analog of the normal zinc template. It was, therefore, considered logical to prepare this compound as well to monitor its DNA interaction profile.

A retrosynthetic analysis pertaining to the preparation of the 'anti sense' analog is shown in Scheme C-4. Endeavours towards this 'anti sense analog' is based on bis Boc-His Cystine di-OMe (26), which can be easily seen as structurally analogous but directionally opposite to (25) (Chart C-8). Compound (26) was prepared in 21% yields by the coupling of Boc His hydrazide (20) with Cystine-di-OMe, via sequence, azide formation ($NaNO_2$-aqueous HCl) and peptide formation (Et_3N) (Chart C-9).

CHART C.8

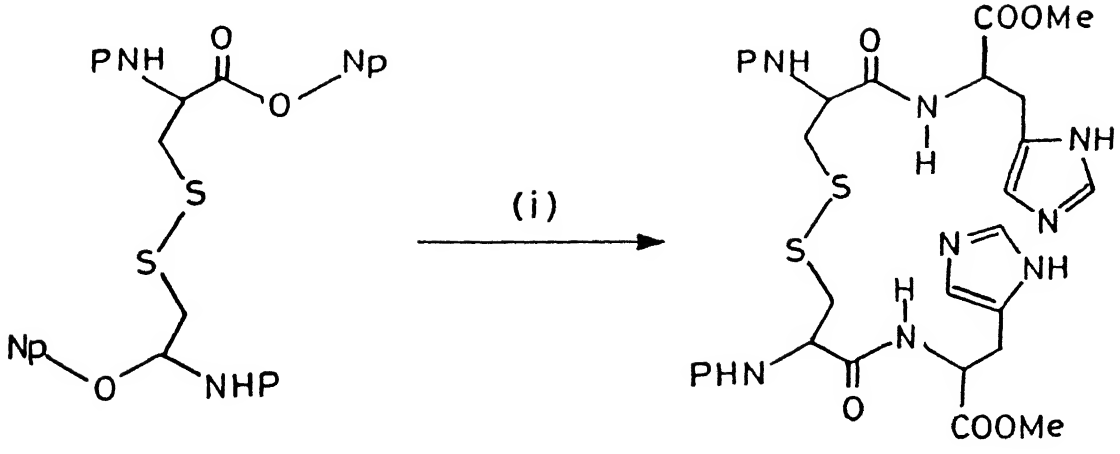

P = Z : (8)
P = BOC: (9)

(i) (17) – CH_2Cl_2

P = Z : (24)
P = BOC: (25)

Scheme C4

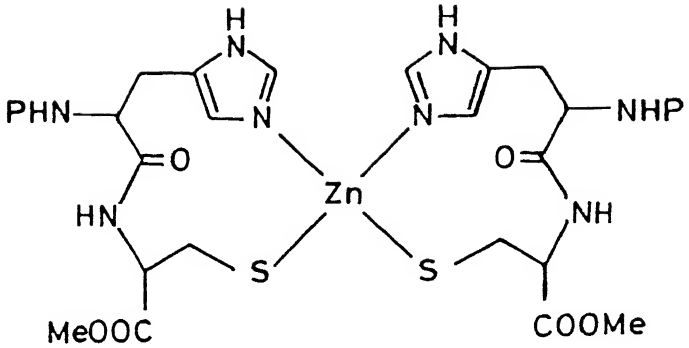

P = $-COOC(CH_3)_3$ (BOC)

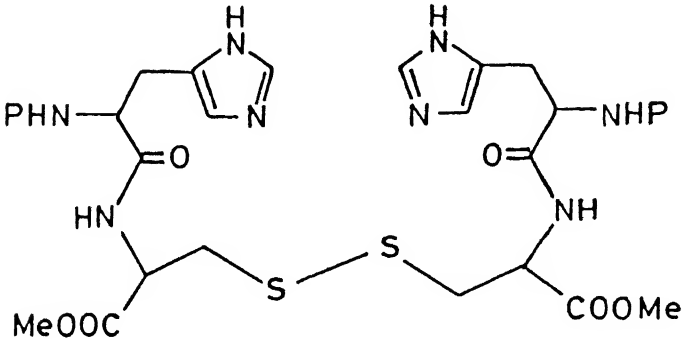

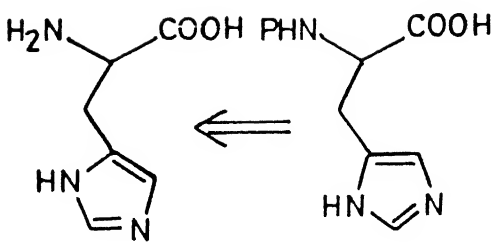

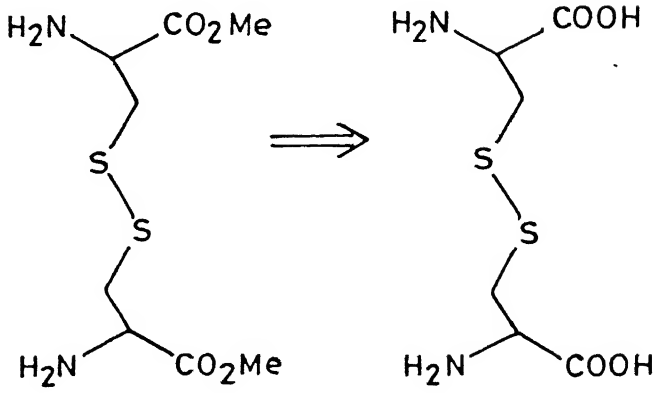

CHART C.9

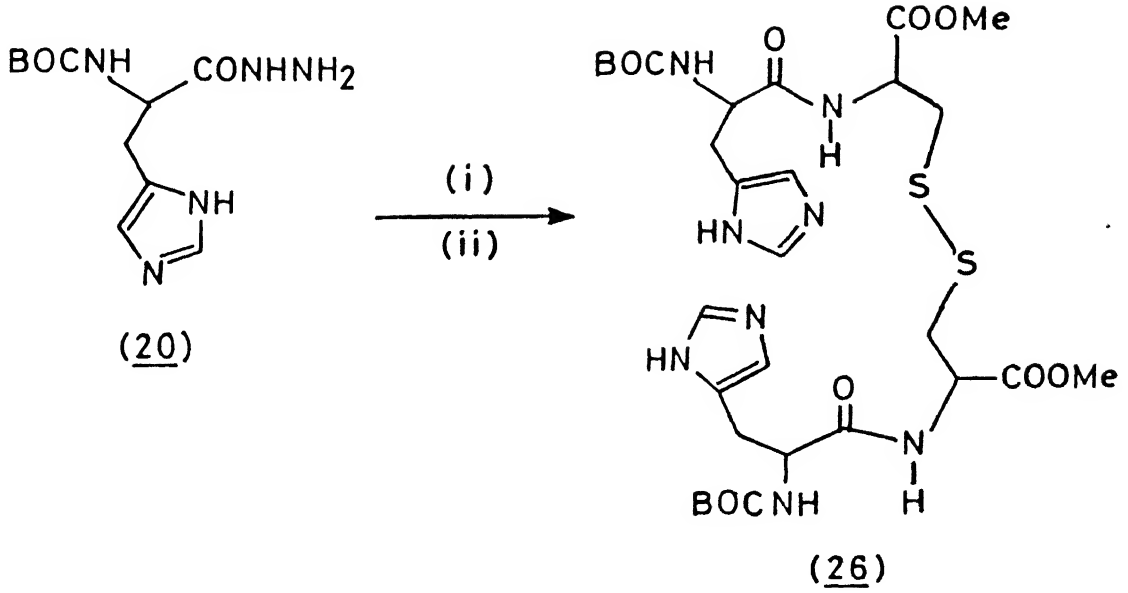

(20)

(26)

(i) $NaNO_2$ – HCl – H_2O (ii) (1) – Et_3N

Bis-Boc-His Cystine di-OMe (26):

mp 125°-128°C.

ir: ν_{max} (KBr) cm^{-1} : 3304, 1746, 1679, 1521, 1167, 1049.

nmr: δ ($CDCl_3$) (80MHz): 1.44(s, 18H, $(CH_3)_3$-), 3.09(b, 8H, Cys β-CH_2 , His β-CH_2), 3.75(s, 6H, ester), 4.64(b, 4H, Cys α-CH, His α-CH), 6.36(d, 2H, HisNH), 6.86(s, 2H, His4H), 7.64(s, 2H, His2H), 7.76(d, 2H, CysNH).

ms: (FAB) m/z : 743 $(M+H)^+$, 372 (Boc-His Cys-OMe+H)$^+$.

$[\alpha]_D^{25}$ = -70.1 (c, 0.291, MeOH).

The second strategy envisaged for the basic zinc finger template, illustrated in Scheme C-1, would lead to a general method for construction of zinc finger modules wherein cysteines, histidines and the recognition are rightly placed. This would necessitate using S-protected precursors and the key compound towards the basic zinc finger template would be N-protected Cys(Acm) His-OMe (Scheme C-5). This objective was realised via condensation of His-OMe (17) with either Z-S-Acm Cys-ONp (14) or Boc-S-Acm Cys-ONp (15) in CH_2Cl_2 leading to, respectively, Z-S-Acm-Cys His-OMe (27) (40.8% yield) and Boc-S-Acm-Cys His-OMe (28) (41% yield)[36] (Chart C-10).

Z-S-Acm-Cys His-OMe (27):

mp 110°-112°C.

ir: ν_{max} (KBr) cm^{-1} : 3309, 1743, 1692, 1644, 1526, 1262,1048.

nmr: δ($CDCl_3$-DMSO-d_6) (80MHz): 1.98(s, 3H, Ac-), 2.88, 3.13 (d,d, 4H, Cys

Scheme C 5

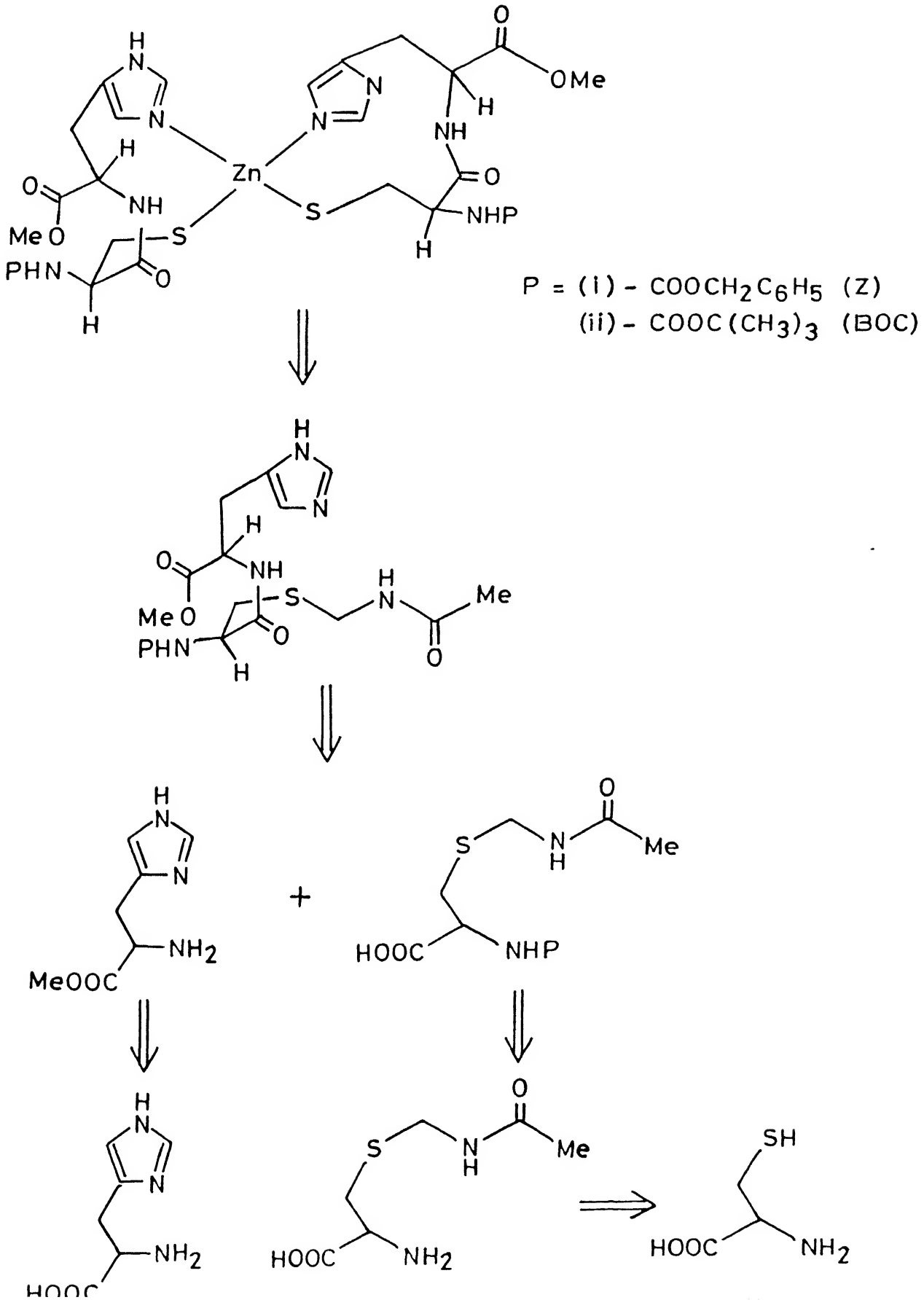

CHART C.10

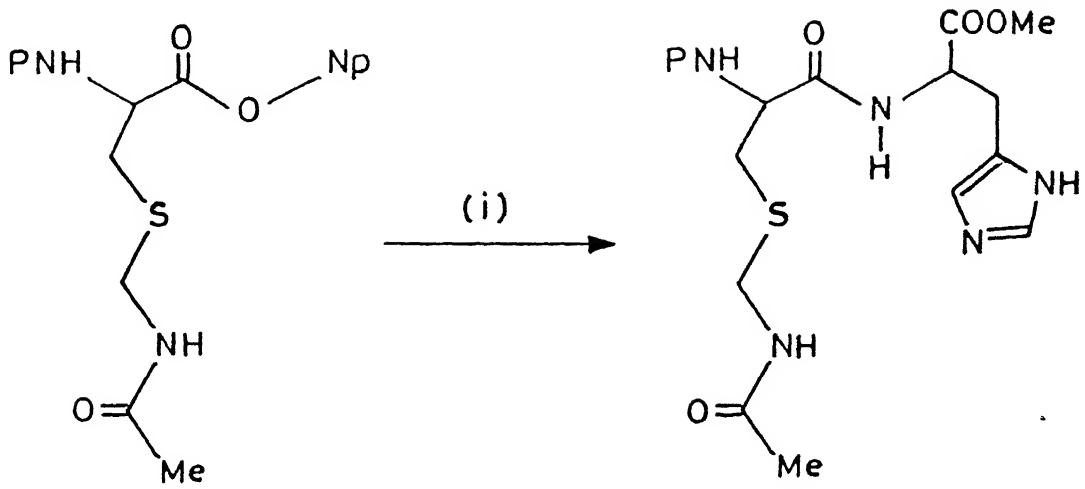

P = Z : (14)

P = BOC : (15)

P = Z : (27)

P = BOC : (28)

(i) (17) - CH_2Cl_2

β-CH_2 , His β-CH_2), 3.75(s, 3H, ester), 4.38, 4.66(m, Cysα-CH, His α-CH), 5.16(s, 2H, $ArCH_2$-), 6.47(d, 1H, CysNH-), 6.84(s, 1H, His4H), 7.41(s, 5H, Ar-), 7.69(s,s, 2H, His2H, HisNH), 8.0(d, 1H, AcNH).

ms: (FAB) m/z: 478 $(M+1)^+$.

$[\alpha]_D^{23}$ = -22.96° (c, 0.527, MeOH).

Boc-S-Acm-Cys His-OMe (28):

mp 128°-130°C

ir: ν_{max} (KBr) cm^{-1}: 3298, 1745, 1662, 1540, 1257, 1168, 1050

nmr: δ ($CDCl_3$) (80MHz): 1.38(s, 9H, t-Butyl), 2.83 (t, 2H, Cys β-CH_2), 3.1(t, 2H, His β-CH_2), 3.66(s, 3H, ester), 4.70(m, 2H, Cys α-CH, His α-CH), 5.78(d, 1H, CysNH), 6.78(s, 1H, His4H), 7.59(b, 2H, His2H, HisNH), 7.77(d, 1H, AcNH).

ms: (FAB) m/z : 444 $(M+1)^+$.

$[\alpha]_D^{23}$ = -14.86° (c, 1.05, MeOH).

The appropriate precursor for the basic template corresponding to gluco-corticoid receptor was discovered in a serendipitous manner.

During endeavours to prepare 'left immobilised' zinc finger template, having the tethered ends in place of the short loop in zinc finger modules, cystine di-OMe was reacted with oxalyl chloride. Simultaneous slow addition of either cystine di-OMe or cystine di-O^{t}Bu and oxalyl chloride under high dilution afforded as the sole isolable product compounds (29) and (30) which were not the expected 10 membered cyclooxalyl cystine, but the 20 membered cyclo [bisoxalylcystine], as was at once evidenced from their FAB mass spectra. Thus, the reaction of either cystine di-OMe or cystine di-^{t}OBu under the above described conditions (oxalyl chloride-

Et_3N-benzene) led to, respectively, cyclo [bisoxalyl cystine di-OMe](29) (30% yield) and cyclo [bisoxalyl cystine di-^{t}OBu] (30) (26% yield)[37] (Chart C-11).

Cyclo [bisoxalyl cystine di-OMe](29):

mp 195°-197°C

ir: ν_{max} (KBr) cm^{-1}: 3288, 1743, 1660, 1510.

nmr: $CDCl_3$, 24°C (400MHz): 3.22, 3.26 (4H, d,d, J = 16Hz, 8Hz); 3.30, 3.34 (4H,d,d, J = 16Hz, 8Hz) (β-CH_2), 3.80 (12H, s) (ester), 4.87(4H, t, J = 8.5Hz) (α-CH), 8.13 (4H, d, J = 8Hz), (NH).

ms: (FAB) m/z : 645.71 $(MH)^+$

$[\alpha]_D^{25}$ = -33.8° (c = 0.142, $CHCl_3$).

Cyclo [bisoxalylcystine di-O^{t}Bu](30):

ir: ν_{max} (KBr) cm^{-1}: 3384, 1737, 1682, 1503, 1154.

nmr: δ $CDCl_3$, (80MHz): 1.5(s, 36H, $(CH_3)_3C$-), 3.23(b-m, 8H, β-CH_2), 4.73(b, 4H, α-CH), 8.09(b, 4H, -CONH-).

ms: (FAB) m/z : 589 (M - ^{t}butyl + H)$^+$.

The 400 MHz ^{1}H NMR profile in $CDCl_3$, DMSO-d_6 and Pyridine-d_5 of (29) were complementary and brought-out diverse structural features. Significant observations are, the pronounced chemical shift separation of the β methylene protons into two sets of double doublets in DMSO-d_6 (a. 2.82, 2.86; b. 3.15, 3.19 δ) and the appearance of, in the NH region, a single doublet centered at 8.13, 9.34 and 10.57δ in, respectively, $CDCl_3$,DMSO-d_6 and pyridine-d_5 , suggesting that all the NH pro-

CHART C.11

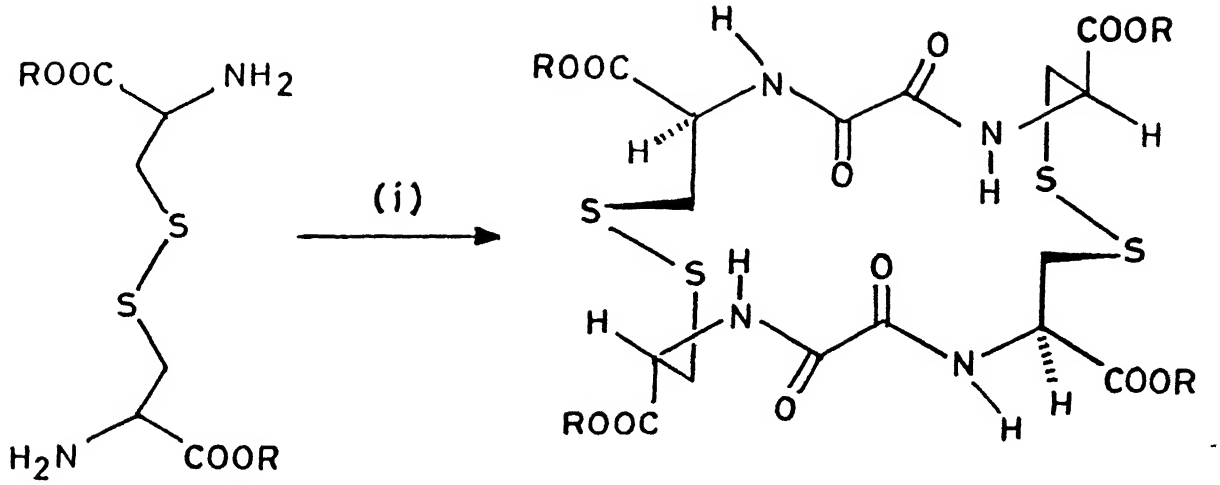

R = Me: (1)
R = Bu^t: (2)

R = Me: (29)
R = Bu^t: (30)

(i) ClCOCOCl – Et_3N – PhH

tons are solvent exposed. This conclusion is supported by NMR solvent titration studies (gradient $CDCl_3$:DMSO-d_6 : 0-40% ; 24° C) and VT studies. VT studies in DMSO-d_6 between 297 K and 343 K yielded a $d\delta/dT$ value of -7.18 ppb/K. All these observations are clearly in agreement with a structure for (29) lacking intra-molecular hydrogen bonding and having solvent exposed NH protons.[37]

Cyclo [bisoxalyl cystine di-OMe](29):

^1H NMR (400 MHz) studies on (29) :

^1H NMR (δ):

i. $CDCl_3$, 24°C: 3.22, 3.26 (4H, d,d, J = 16Hz,8Hz); 3.30, 3.34 (4H,d,d, J = 16Hz, 8Hz) (β-CH_2), 3.80(12H, s) (ester), 4.87(4H, t, J = 8.5Hz) (α-CH), 8.13 (4H, d, J = 8Hz), (NH).

ii. DMSO-d_6, 24°C: 2.82, 2.86 (4H, d,d, J = 16Hz, 8Hz); 3.15, 3.19 (4H, d,d, J = 16Hz, 8Hz) (β-CH_2), 3.65 (12H,s)(ester), 4.59 (4H, d,d,J = 8Hz) (α-CH), 9.34 (4H, d, J = 8.48Hz)(NH).

iii.Pyridine-d_5, 24°C: 3.41 (8H,d,d, J = 8Hz,8Hz) (β-CH_2), 3.60(12H, s)(ester), 5.39 (4H,d,d,J = 8Hz,8Hz) (α-CH), 10.57 (4H, d, J = 8 Hz)(NH).

NH shift from solvent titration (gradient $CDCl_3$:DMSO-d_6): δ (% DMSO-d_6): 8.14 (0), 8.27 (2), 8.40 (4), 8.50 (6), 8.58 (8), 8.64 (10), 8.83 (18), 8.90 (20), 9.08 (40); shift Σ 0.94.

Temperature dependent NH shift in DMSO-d_6, δ (°C): 9.34 (24), 9.28 (30), 9.22 (40), 9.15 (50), 9.08 (60), 9.0 (70); $d\delta/dT$ ppb/K = -7.18.

The proton decoupled ^{13}C NMR in $CDCl_3$ at 50° C revealed the non-equivalence of the C_α as well as the ester carbonyl carbons and the appearance of both the carbons of the ester groups at higher fields ($\sim$ 10 ppm). The upfield shift exhibited by the carbons of the esters coupled with the finding that all the NH protons in (29) are solvent exposed can be rationalised on the basis of the anticipated[38] nearly orthogonal placement of the carbonyls of the oxalamide units.

Cyclo [bisoxalyl cystine di-OMe](29):

^{13}C NMR (100 MHz), $CDCl_3$, 50°C: δ: 29.69 (β-CH_2), 52.85,52.97 (α-CH), 41.38 (OCH_3), 159.16,159.53 (COOMe), 159.64 (NHCO).

The UV spectrum of (27) in EtOH showed λ_{max} at 250nm ($\epsilon = 1360$ M^{-1} cm^{-1}) which indicates an A type of transition pertaining to the disulfide chromophore. The CD spectrum, also recorded in EtOH, exhibited at 265 nm a shallow negative ellipticity (-2800 deg. cm^2 $dmol^{-1}$). Taken in conjunction these results place the CSSC dihedral angle close to + 90° (P helical)[39].

This conclusion is in agreement with an overwhelming body of evidence from crystallographic and solution studies that the most stable disulfide conformation have a CSSC dihedral angle in the neighbourhood of $\pm$ 90° , with preferance for P helical modes[40–42]. Since each of the β-CH_2 protons appear, as a clear set of double doublets (J= 8Hz, 16 Hz), the helicity of both disulfide bridges would be the same with a strong likelihood for the PP helical conformation[43].

A rational structure for (29), presented in Chart C-11, can be derived, taking

into consideration the exposed nature of the NH protons, the likely CSSC dihedral angle $\sim +90^{o}$ and the orthogonal disposition[38] of the oxalamide units.

The above data are in agreement with the proposed structure for the product (29), arising from the reaction of cystine di-OMe with oxalyl chloride, the key features of which are the expected nature of the NH protons, the likely CSSC dihedral angle of $\sim 90^{o}$ and the orthogonal disposition of the oxalamide units.

The most likely reason for the formation of the 20 membered cyclo[bisoxalyl cystine] rather than the expected 10 membered cyclooxalyl cystine is strain considerations, principally arising from the need to place two peptide units in a 10 membered ring and coupled with the natural propensity of the CSSC unit to maintain a dihedral angle close to 90°. Further experiments have shown that this notion is correct.

Thus, the reaction of Cys(Acm)-OMe (13) with oxalyl chloride precisely under conditions described above afforded the expected bis-oxaloCys(Acm)-OMe (31) (15.7% yield) (Chart C-12). Compound (31) is of interest, since the removal of the S-protected groups and coupling could afford either cyclo [bisoxalylcystine di-OMe](29) or cyclooxalyl cystine. The most important feature of (31) would be its transformation to via deprotection and metal complexation to zinc template related to gluco-coritcoid receptor proteins.

Bis-oxalo Cys(Acm)-OMe (31):

mp 154°-156° C.

ir: ν_{max} (KBr) cm^{-1}: 3277, 1744, 1660, 1530, 1020

nmr: δ ($CDCl_3$ (400MHz): 2.02(s, 6H, Ac-), 3.14 (m, 4H, Cys β-CH_2), 3.8(s, 6H,

ester), 4.39(m, 4H, AcNH-CH_2-), 4.85(b-m, 2H, Cys α-CH), 6.58(b, 2H, AcNH-), 8.17(d, 2H, oxamideNH).

ms: (FAB) m/z: 467 $(M+1)^+$.

The control of the bis acid chloride on the nature of the product was dramatically illustrated with succinyl chloride, which under the above conditions, with cystine-di-OMe, afforded exclusively the 12 membered cyclo succinyl cystine [(32), mp 215°-220°C, 20%] (Chart C-13).

400MHz ^{1}H NMR studies with (32), in $CDCl_3$and in DMSO-d_6, show that the NH protons, which appear as a single doublet, are solvent exposed and significantly shielded. The UV profile of (32) is quite similar to that of (29) (Section D).

Cyclo succinyl cystine di-OMe [(32):

mp 215°-220°C

ir: ν_{max} (KBr) cm^{-1} : 3317,3292,1742,1647,1541,1035

^{1}H NMR (400MHz) studies on (32):

^{1}H NMR (δ):

i. $CDCl_3$, 24°C : 2.5 (4H, d,J=11.50Hz) (succinyl), 2.8 (4H, d, J=14.20Hz) (β-CH_2), 3.80 (6H,s) (ester), 4.85 (2H,q) (α-CH), 6.70(2H, d, J=7.8Hz)(NH).

ii. DMSO-d_6,24°C: 2.55(4H, d, J=10.3Hz)(succinyl), 2.89(4H, m) (β-CH_2), 3.63(6H, s) (ester), 4.62(2H, q)(α-CH), 8.20(2H, d)(NH).

NH shift from solvent titration (gradient $CDCl_3$: DMSO-d_6): δ(%DMSO-d_6): 6.65 (0), 6.76(2), 6.85(4), 6.97(10), 7.17(20), 7.35(40); shift Σ 0.70.

CHART C.12

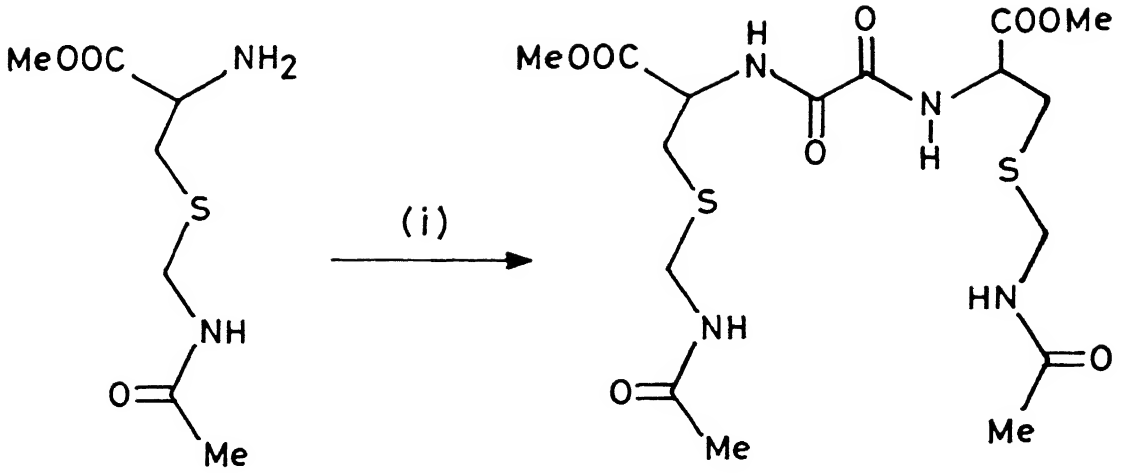

(10) (31)

(i) $ClCOCOCl - Et_3N - PhH$

CHART C.13

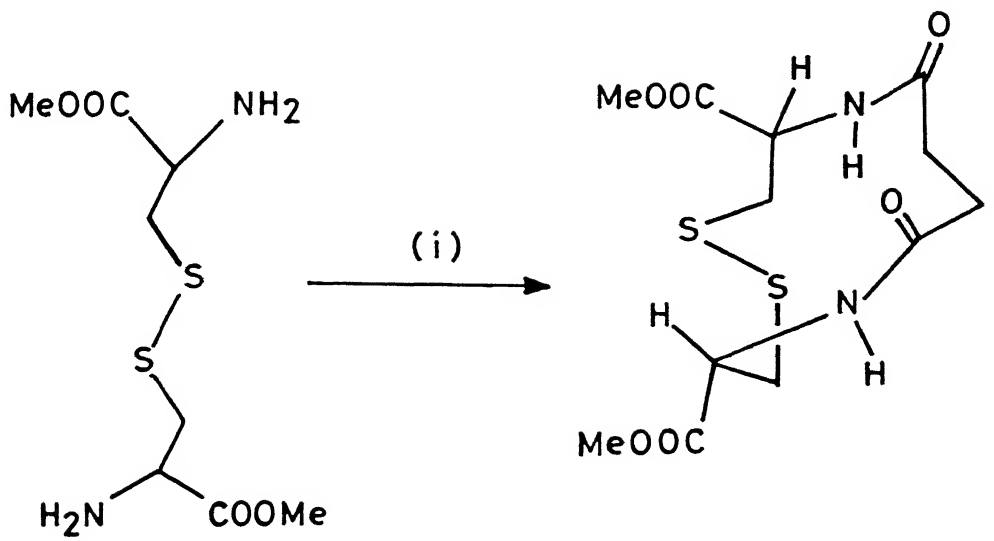

(1) (32)

(i) $ClCO(CH_2)_2COCl - Et_3N - PhH$

Temperature dependent NH shift in DMSO-d_6, δ (°C): 8.196(25), 8.17(30), 8.14(35), 8.11(40), 8.07(45), 8.06(50), 8.03(55); dδ/dT ppb/K = -9.5.

ms: (FAB) m/z : 351.41 $(MH)^+$.

$[\alpha]_D^{28}$ = -62.75° (c = 0.153, $CHCl_3$).

Structure (32) assigned for cyclosuccinyl cystine is in accordance with all observations cited above and accounts for the shielding of the NH protons, which might arise from proximately aligned carbonyls.[37]

The motifs represented by (29) and (30), and (32) offer novel possibilities for protein design. Some of which have been illustrated in the present thesis (*vide infra*).

The orthogonally disposed carbonyls of the oxalamide unit in (29) and (30) represents a ground state geometry, similar to the twisted peptidyl prolyl amide bond, envisaged as the transition state in the cis-trans interconversion, mediated by immunophilins, which seem to stabilise this conformation (Rotamase activity). This activity, linked with T cell activation is potently inhibited by immunosuppressants, such as cyclosporin, FK506 and rapamycin[44]. Recent crystallographic studies have shown that the 1,2-dicarbonyl environment similar to that in (29), present in rapamycin, is deeply buried in the immunophilin[45].

The tripeptides (25) and (26) and the cyclo[bisoxalyl cystine](29) and (30) are designed as precursors to the basic templates corresponding to zinc finger proteins and gluco-corticoid receptors. The templates generated would be used for DNA interaction studies. Since these have to be performed in aqueous conditions, the t-butyl groups have to be removed. Two experimental protocols are required with

(25), (26), and (30), namely, their direct deprotection to afford systems that would be used as controls in DNA interaction studies, as well as deprotection after template formation. The first of these is described below:

Bis-Boc-Cystine di-His-OMe (25) and its 'anti sense' analog bis-Boc-His Cystine di-OMe (26) on treatment with TFAA-H_2O smoothly afforded the N-deprotected products, namely, Cystine di-His-OMe (33) (100% yield) and bis-His Cystine di-OMe (34) (96% yield) as TFA salts.

Carboxyl deprotection of cyclo [bisoxalyl cystine di-^{t}Obu] was also accomplished smoothly on treatment with TFAA-H_2O to afford an unusually interesting tetracarboxlic acid, namely, cyclo [bisoxalylcystine] (35)(89% yield) (Chart C-14).

H_3N^+ Cystine di His-OMe . $2TFA^-$ (33):

nmr (D_2O)(400MHz): 3.04(m, 4H, His β-CH_2), 3.18(m, 4H Cys β-CH_2), 3.56(s, 6H, ester), 4.16(t, 2H, Cys α-CH), 4.68 (t, 2H, His α-CH), 7.14(s, 2H, His 4,4'H), 8.42(s, 2H, His 2,2'H).

ms: (FAB) m/z : 543 $[M\text{-}2Boc\text{-}2TFA^- + 1]^+$, 271 $[(M\text{-}2Boc\text{-}2TFA^-)/2]^+$.

H_3N^+ His Cystine di-OMe . $2TFA^-$ (34):

nmr (D_2O)(400MHz): 2.86(m, 4H, His β-CH_2), 3.04(m, 4H Cys β-CH_2), 3.58(s, 6H, ester), 4.08(t, 2H, Cys α-CH), 4.24 (His α-CH), 7.16(d, 2H, His 4,4'H), 8.30(d, 2H, His 2,2'H).

ms: (FAB) m/z : 543 $[M\text{-}2Boc\text{-}2TFA^- + 1]^+$.

Cyclo[bisoxalyl cystine] (35):

nmr δ (D_2O) (80MHz): 3.8(m-b, 8H, Cystine β-CH_2, 4.56(4H, Cystine α-CH).

CHART C.14

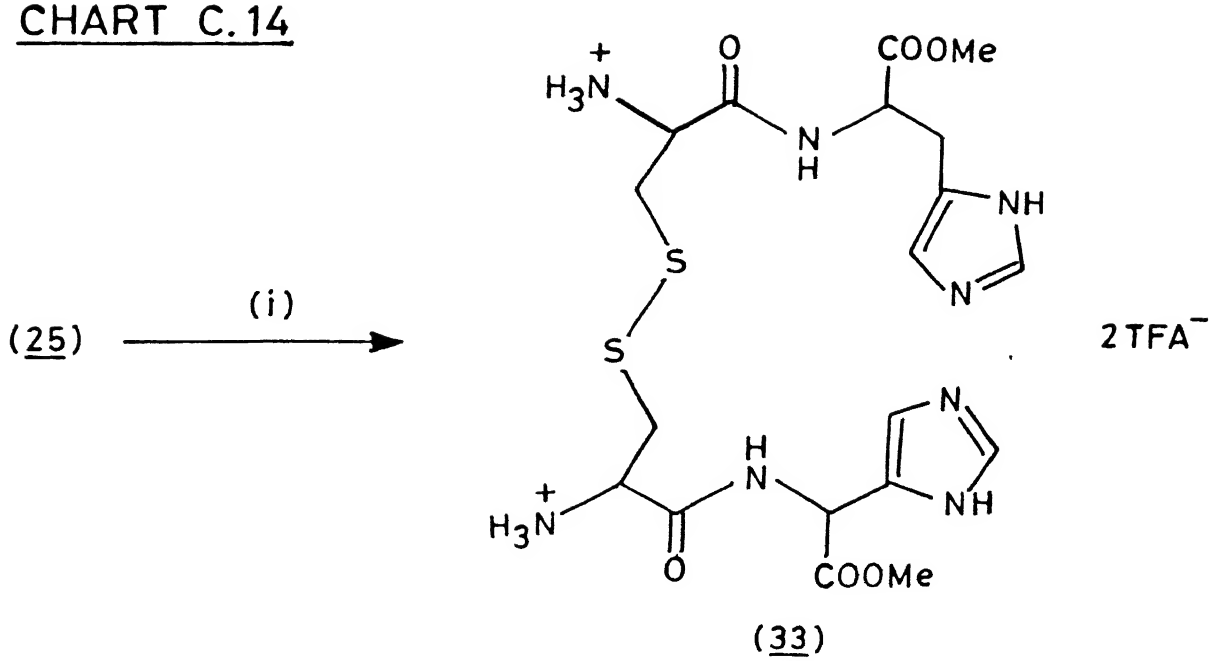

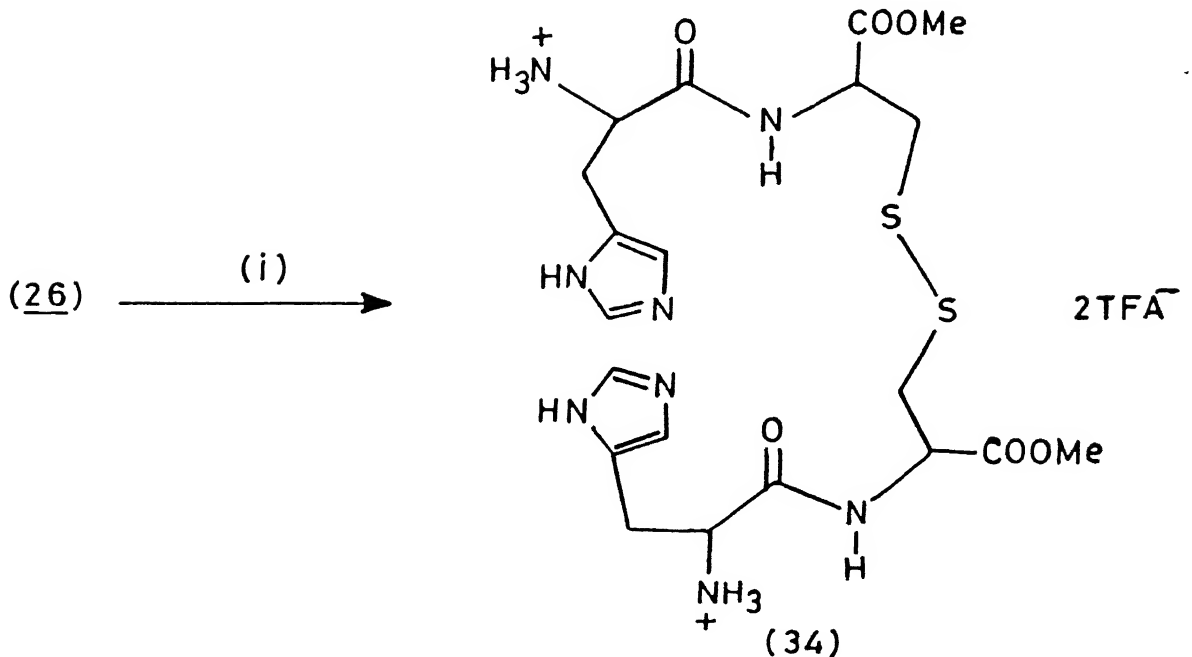

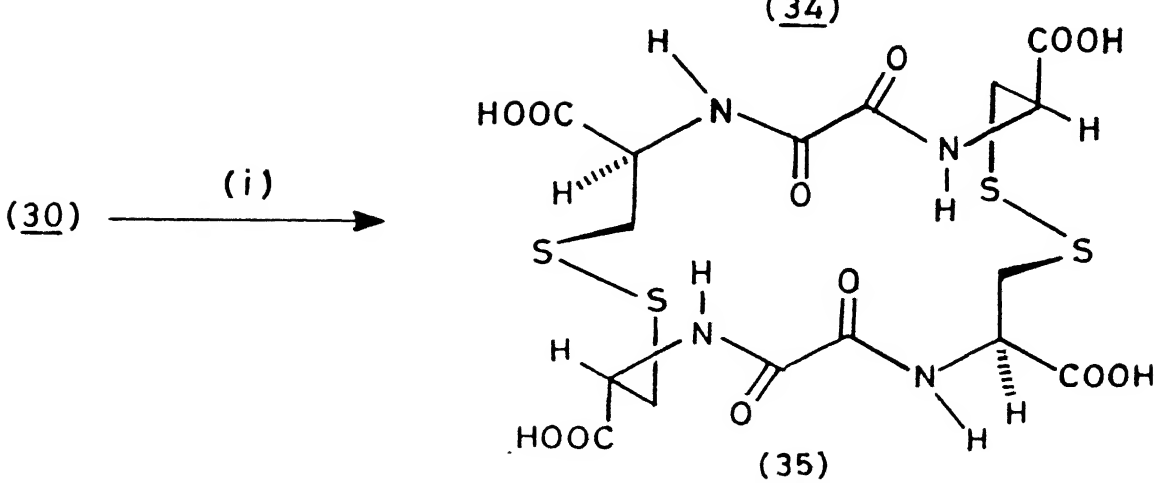

The foregoing account has identified compounds (24), (25) and (30) as precursors to metal templates. The procedure here would involve, in sum, the reduction of the disulphide bond and metal complexation. The options available in this regard are shown in the Scheme C-6.

It was considered, *a priori*, that reductions with $NaBH_4$ or with metal ammonia systems would be unsuitable because of the nature of the substrate involved. The direct transformation of the substrates to zinc finger template prototype with Zn^0, at first , appeared attractive. In the event, the reaction of bis-Z-Cystine di His-OMe (24) with metallic zinc in DME[46] under sonication was found to be sluggish. However, a very small amount of product whose nmr appeared to be in fair agreement with that of metal template was obtained. The choice for reduction therefore narrowed to via thiol - disulphide exchange. Since the substrates were insoluble in water, the exchange reagent had to be effective in non-aqueous media. Additionally, it was essential to use only equivalent amount of the reagent and ensure that the product arising from the thiol - disulphide exchange of the reagent do not interfere with the complexation. However no such reagents were available in the literature, thus necessitating the design of one which would be effective not only in non-aqueous media but also be one of general applicability in peptide and protein domain. The reagent generally used for the reduction of disulphide bond by interchange reaction in proteins is dithiothreitol(DTT). The favourable equilibrium constant $\sim 10^4$ for reduction with DTT has been ascribed to the ready formation of six membered ring containing the disulphide bridge. The reactions are done at pH 7-8 in aqueous medium with excess of DTT[47]. DTT was not suitable to our purposes mainly because removal of excess reagent involves the use of reagents carrying metal ions (e.g. arsenic salts).

Scheme C-6

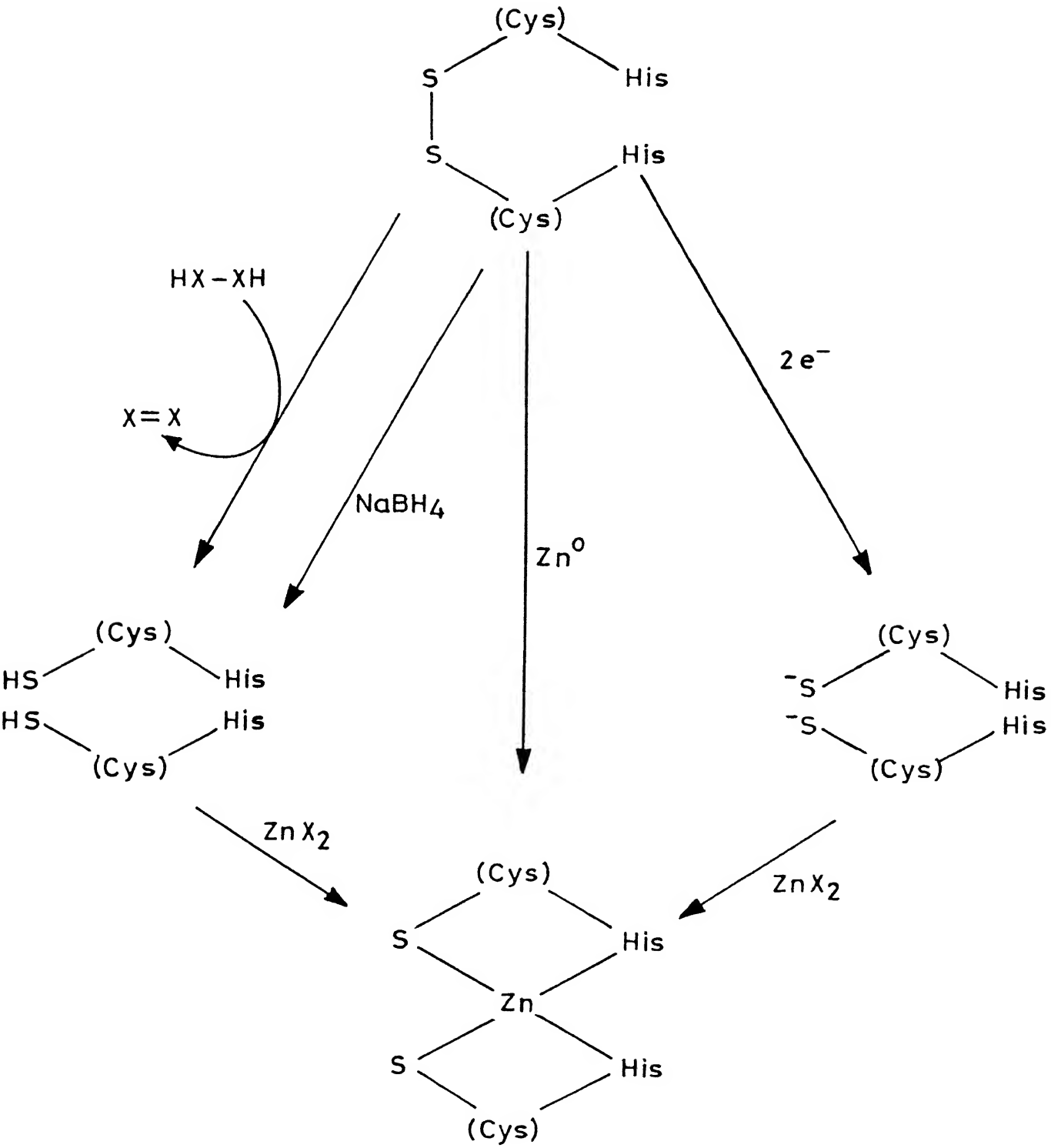
(Cys)
S
His
S
His
(Cys)
HX–XH
X=X
2e⁻
NaBH4
Zn⁰
(Cys)
HS
His
HS
His
(Cys)
(Cys)
⁻S
His
⁻S
His
(Cys)
ZnX2
ZnX2
(Cys)
S
His
Zn
S
His
(Cys)

Fortunately, a perusal of the literature revealed that 1,2-dithiolane, which would be the product of thiol - disulphide interchange from propane-1,3-dithiol (PDT) is rapidly transformed into a methanol insoluble polymer[48]. Indeed, when a 10^{-2} solution of PDT in MeOH was kept aside at room temperature and protected from light for $\sim$ 12 days, in a volumetric flask (10ml) , the dithiolane polymer deposited on the walls.

In view of the above, it was envisaged that methanolic solution of the disulphide precursors when treated with equivalent amounts of readily available PDT would result in thiol - disulfide interchange, particularly since the equilibrium would be shifted favourably in view of ready polymerisation of 1,2-dithiolane. Happily, this turned-out to be true, leading to the identification of the readily available PDT as a very efficient reagent that neatly brings about S-S $\rightarrow$ 2SH change at room temperature and in the absense of any promoter. A common practice, particularly in the protein domain, to assess the S-S $\rightarrow$ 2SH is via isolation and characterisation as acrylonitrile adducts.[49]

At the outset, Z-Cystine di-OMe (6) and the tripeptide bis-Z-Cystinyl di-His-OMe (24) were chosen to assess the efficiency of PDT in bringing about the S-S $\rightarrow$ 2SH change by reduction and to assess the efficiency of PDT in comparison with normally used reagent DTT. It could be seen that the reduction of (24) would lead to appropriate intermediate for the primary zinc template formation when complexed with Zn^{II} species. To gain a quantitative assessment of the extent of reduction, it was planned to transform the product thiols - which are quite air sensitive - to acrylonitrile adducts, which can be fully characterised.

Reaction of Z-Cystine di-OMe (6) with methanolic PDT (1.5 equivalents) in dry MeOH under nitrogen and stirring for 5 hours, as monitered by TLC, led to

the disappearance of the starting material. S-Protection was then carried out, *in situ*, by direct addition of acrylonitrile (4 equivalents). The adduct formation was complete in $\sim$ 5 hours (TLC). Evaporation of MeOH and trituration with hexane - in which the 1,2-dithiolane polymer is freely soluble - afforded 71% yield of Z-S-β-cyanoethyl-Cys-OMe (36).[50] A parallel run using 4 equivalents of DTT, according to literature procedure[51], followed by acrylonitrile addition afforded only 41% yield of (36). Similarly, the reaction of bis-Z-Cystinyl di His-OMe (24) with PDT followed by acrylonitrile addition afforded in 90% overall yield, Z-S-β-cyanoethyl Cys His-OMe (39). In sharp contrast, under similar conditions, DTT afforded a mere 8% of (39). Thus, we feel that particularly in the case of complex substrates, PDT would be very superior. The formation of thiols in these reactions was directly established by treatment of bis-Z-Cystinyl di His-OMe (24) with PDT in dry MeOH followed by work-up involving solvent evaporation and trituration with hexane to remove the 1,2-dithiolane polymer. This reaction afforded a 95% yield of Z-Cys His-OMe (38), which as expected, on reaction with acrylonitrile readily afforded the β-cyanoethyl compound (39).[50] The alternative zinc finger template precursor tripeptide bis-Boc-Cystinyl di His-OMe (25) could be similarly processed in 65% overall yield to Boc-S-β-cyanoethyl Cys His-OMe (40). Finally Bz-Cystine di-OMe (6) afforded, under similar conditions, Bz-S-β-cyanoethyl Cys-OMe (37) in 40% yields (Chart C-15).

Z-S-β-cyanoethyl-Cys-OMe (36):

ir: ν_{max} (neat) cm^{-1} : 3330, 2240, 1745, 1720, 1525, 1220, 1060.

nmr: $\delta(CDCl_3)$ (80MHz): 2.7 (m, 4H, $-SCH_2CH_2CN$, 4H), 3.1 (q, $-CH_2S-$, 2H), 3.85(s, 3H, ester), 4.65 (m, 1H, α-CH), 5.16 (s, 2H, $CH_2C_6H_5-$), 5.60(b, -CONH-,

1H), 7.43 (s, C_6H_5-, 5H).

Bz-S-β-cyanoethyl Cys-OMe (37):

ir: ν_{max} (neat) cm^{-1} : 3320, 2265, 1740, 1650, 1540, 1030.

nmr: $\delta(CDCl_3)$ (80MHz): 2.69 (m, 4H, -SCH_2CH_2-), 3.22 (q, 2H, -CH_2S-), 3.85(s, 3H, ester), 5.0 (m, 1H, α-CH), 7.09 (d, 1H, -CONH-), 7.49, 7.82 (m, 5H, C_6H_5-).

Z-S-β-cyanoethyl Cys His-OMe (39):

ir: ν_{max} (KBr) cm^{-1} : 3300, 2240, 1740, 1690, 1640, 1520.

nmr: $\delta(CDCl_3)$ (80MHz): 3.0(m,8H, Cys β-CH_2, His β-CH_2, -CH_2CH_2S-), 3.75(s,3H, ester), 4.44(m, 1H, Cys α-CH), 4.8(q, 1H, His α-CH), 5.16(s, 2H), 6.00(b-d, 1H, CysNH), 6.81(s, 1H, His4H), 7.44(s, 5H), 7.56(s, 1H, His2H), 7.78(d, 1H CysNH).

$[\alpha]_D^{26}$ = -37.97 (c = 1.33, MeOH).

Boc-S-β-cyanoethyl Cys His-OMe (40):

ir: ν_{max} (KBr) cm^{-1} : 3340, 2254, 1746, 1661, 1516, 1257, 1168, 1047.

nmr: $\delta(CDCl_3)$ (80MHz): 1.43(s, 9H,$(CH_3)_3$-), 2.80(m, 8H, -SCH_2CH_2-, Cys β-CH_2 , His β-CH_2), 3.70 (s, ester), 4.35(q, 1H, Cys α-CH), 4.75(q, 1H, His α-CH), 5.60(d, 1H, CysNH), 6.83(s, 1H, His4H), 7.56(s, 1H, His2H), 7.66(d, 1H, HisNH).

ms: (FAB) m/z : 426 $(M + H)^+$.

$[\alpha]_D^{27}$ = -30.0° (c, 0.41, MeOH).

An interesting observation, having practical implications, is the reversal of (39) on standing , to the thiol (38). This change is possibly brought about by the imidazole promoted S-deprotection, since similar adducts devoid of the His residues were found to be quite stable.

Several experiments involving exchange with PDT and DTT brought out yet

CHART C.15

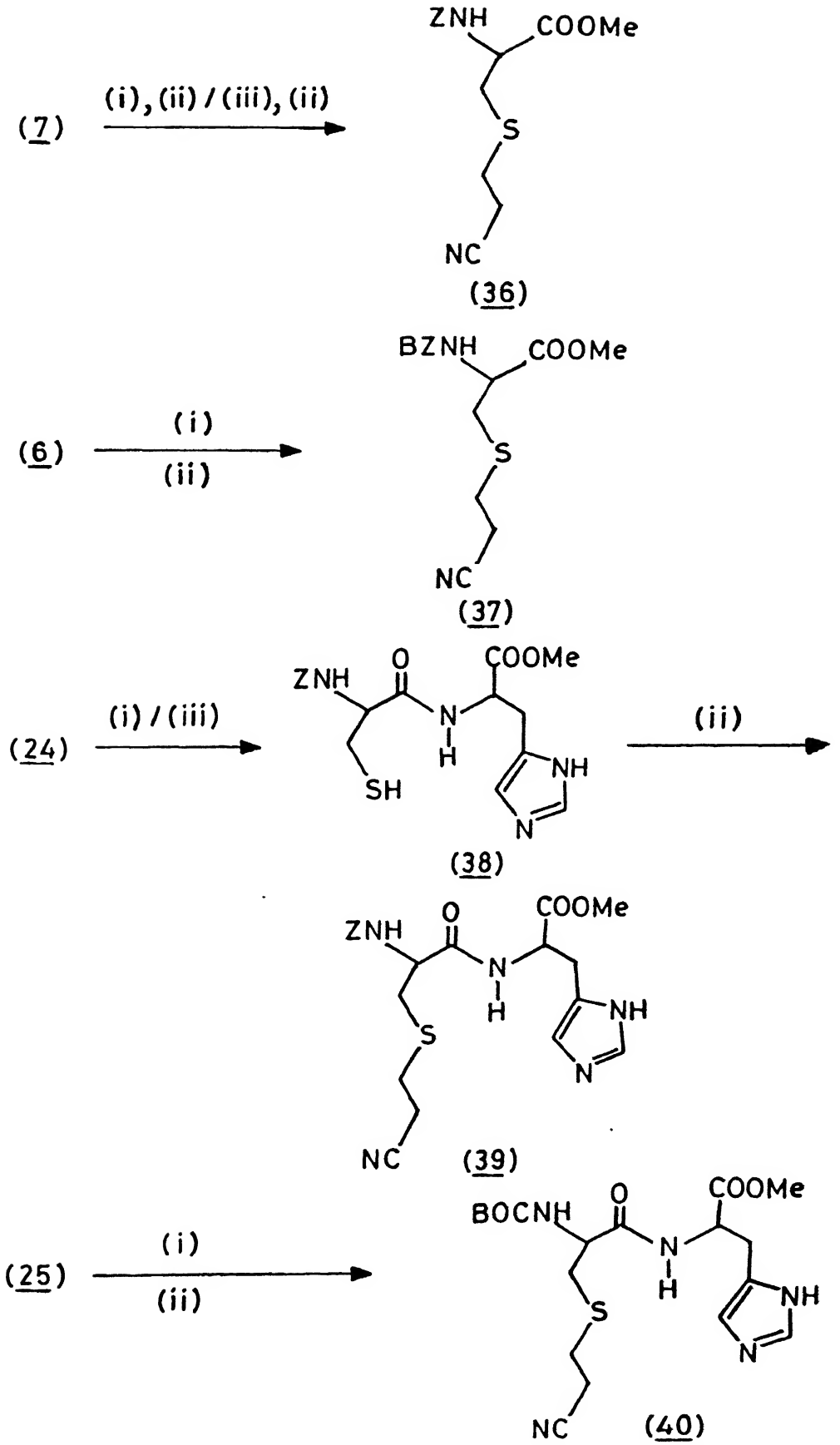

(i) PDT-MeOH (ii) $H_2C=CHCN$ (iii) DTT-MeOH

another attractive aspect of PDT. The reaction in DTT usually carried out at pH 7-8, was found to give rise to small yet detectable amounts of dehydroalanine residues (nmr). This diversion was totally absent when PDT was employed. In large proteins and enzymes (*vide infra*), even formation of small amounts of dehydroalanine would cause complications which could be avoided by using PDT.

In view of the importance of disulphide bond reduction in biologically important compounds, it was considered attractive to assess the utility of PDT for disulphide bond reduction, placed in different environments.

In proteins, the amino acid tryptophan (Trp) is the least abundant. However, because of its highly attractive fluorescence profile, Trp residues have served in the understanding of intricate transformations mediated by enzymes. In ancillary studies, it was considered possible to introduce the Trp residues in enzymes by addition of a cysteine SH moiety to 2-thio tryptophan. It was envisaged that this compound would be readily formed on reduction of 2,2'-dithio bis(Bz-Trp-OMe) (23). In the event, this turned out to be very facile. Thus the reaction of (23) with PDT in MeOH afforded 2-thio-Bz Trp-OMe (41) in 85% yields. A common problem associated with both PDT and DTT is the ready oxidation of the product which takes place, even when all precautions are taken to exclude oxygen. This diversion leading to loss in yields is particularly severe in low molecular weight compounds. This factor, probably accounts for the modest yield of 42% of PhSH on treatment of Ph-S-S-Ph with PDT in MeOH, Chart C-16.

The work described so far has shown that PDT is a very efficient reagent for S-S $\rightarrow$ 2SH change, by interchange. However, it was felt that the real challenge pertaining to the wide application of this reagent would come from similar demonstration involving natural substrates which would necessitate operation under different sol-

CHART C.16

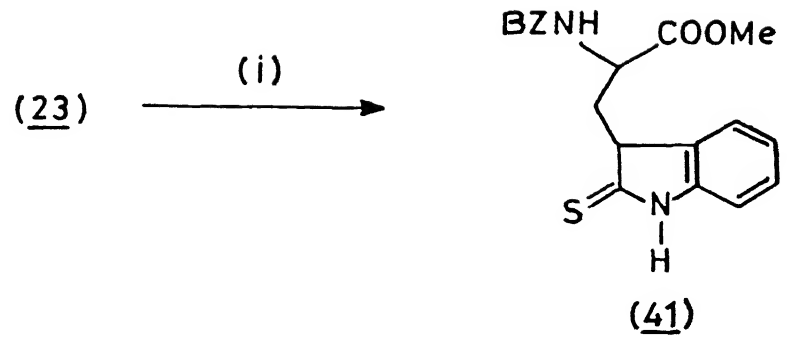

(41)

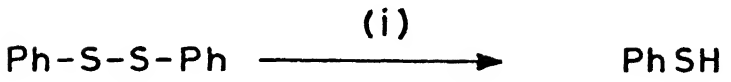

(i) PDT-MeOH

CHART C.17

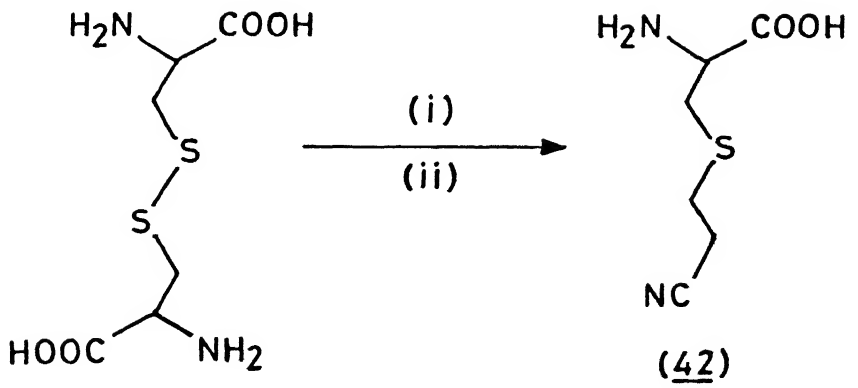

(42)

(i) PDT-MeOH, pH buffer (1:10)

(ii) $H_2C=CHCN$-MeOH

vent environments. From substrates, namely L-cystine, c-lysozyme, bovine insulin and oxytocin were chosen for such a study.

The reaction of cystine with 1.5 equivalents of PDT in MeOH - pH 8 buffer :: 1:10 followed by acrylonitrile addition afforded S-β-cyanoethyl cysteine (42) in 61% yields (Chart C-17).

Preliminary studies has shown that in case of complex proteins where the substrates are used at micromolar levels, the reaction is best carried out with neat PDT. A typical example of this is the reduction of c-Lysozyme.

Under a nitrogen blanket, c-lysozyme, 1 μM, was mixed with PDT (93 μl), after stirring for 0.5 hour, additional PDT (50 μl) was added, stirring continued for 8 hours, the reaction mixture is triturated with dry hexane (3x5ml), to remove PDT polymer, mixed with urea (6M) (0.5ml), follwed by acrylonitrile addition (60 μl), left stirred for 5 hours, evaporated, dried, taken-up in distilled water, dialised, and the clear solution lyophilised. Electrophoresis on dodecyl sulfate polyacrylamide gel, showed no fragment of the enzyme. Further, amino acid analysis showed that two out of the four cystine residues are reduced. This finding is in excellant agreement with DTT, performed in pH 8 (phosphate buffer):8M urea:EDTA[52]. The partially reduced c-lysozyme retains biological activity[53]. The present procedure for c-lysozyme should be applicable to other enzymes.

Bovine insulin on treatment with PDT as described above, followed by acrylonitrile addition, avoiding urea treatment, gave product which on amino acid analysis revealed that 2 of 3 disulphide bridges of the hormone has undergone reduction. Oxytocin acetate salt precisely under the conditions as for insulin gave product in which the only disulfide bridge present was completely reduced (Chart C-18).

The exhaustive studies with PDT particularly those involving bis-Z-Cystinyl di

CHART C.18

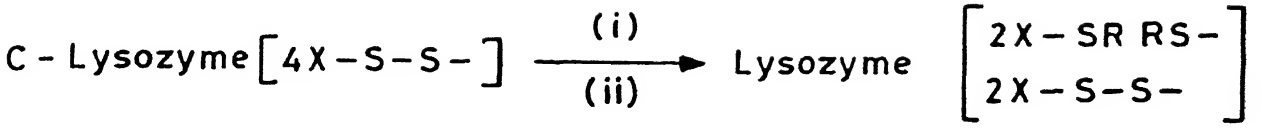

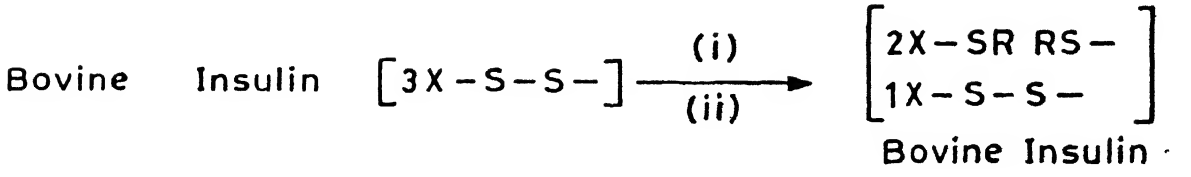

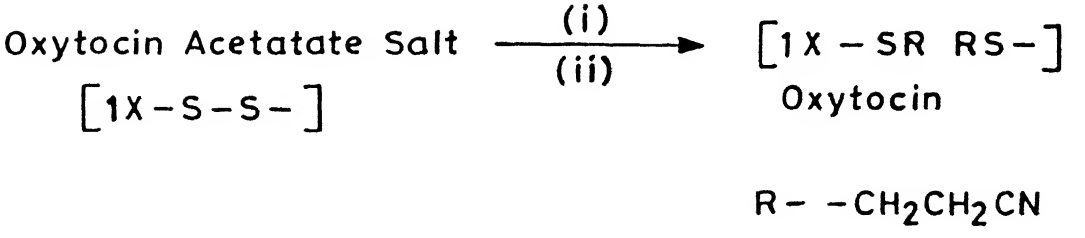

(i) PDT (ii) $H_2C = CHCN$

His-OMe (24) and bis-Boc-Cystinyl di His-OMe (25), clearly showed experimental protocols that would lead to the desired zinc finger template prototypes.

Bis-Z-Cystinyl di His-OMe (24) on treatment with PDT in dry MeOH under total nitrogen blanket, followed by treatment with anhydrous $ZnCl_2$ (99.99%) in dry MeOH afforded zinc finger template (43) in an overall yield of 37% from bis-Z-Cystine.[35]

Template (43) is a white microcrystalline solid, soluble in DMF, DMSO and pyridine. The FAB mass spectrum exhibited strong peak at 874 (M^+) and interestingly one at mass number 911, corresponding to one $2H_2O$. Elemental analysis also lend support to the bonded water. It is likely that the water molecules are coordinated to the His residues.

A comparison of the 400MHz 1D nmr of the precursor peptide, namely, bis-Z-Cystinyl di His-OMe (24) with that of the template (43) (section D) shows close similarities, excepting for the imidazole 2 protons, these are down field shifted and ester comes as two closely positioned peaks. The nmr of template (43) was unchanged at 1, 5, 10, and 20 mmolar concentrations in DMSO-d_6, thus indicating the absence of any association-dissociation phenomena (data not shown). The peak assignment for (43) has been confirmed by its COSY spectrum (Section D) which shows cross peaks, His NH for His α-CH, Cys NH for Cys α-CH, His α-CH for His β-CH_2 and Cys α-CH for Cys β-CH_2. The spatial proximity of the two imidazole ring protons in (43) has been established by NOESY and difference NOE studies. The NOESY spectrum of (43) shows cross peak corresponding to the 4,4' protons. The difference NOE, with respect to the His protons, are particularly revealing, demonstrating clear NOE mutual connections between His4 - His4' and His2 - His2' protons (Section D).

The similarities in the nmr of the basic template (43) to that of the Zn^{II} complex of a consensus zinc finger peptide (CP-1) is very striking. CP-1 has a consensus sequence arrived at by an analysis of data base consisting of 131 zinc fingers. In the 1D nmr of zinc finger, generated from CP-1 and Zn^{II}, the His 4H protons appeared at 6.82 and 6.53 ppm and the His 2H protons appeared at 7.82 and 7.91 ppm. The corresponding values for the template (43) are, 6.78 and 6.85 ppm for the His 4H protons and 7.85 and 7.98 ppm for the His 2H protons. The close similarities observed here support the view that the Zn^{II} environments in (43) and the CP-1 - Zn^{II} complex are similar[12].

An energy minimised DTMM profile of (43) is presented in Chart C-20 spatial configuration for (43) presented in Chart C-19 is based on this model. As could be seen either from Chart C-19 or from Chart C-20, the ligand environments around the two imidazoles in (43) are different. This conclusion is also in agreement with nmr results which show a chemical shift separation for the ester groups as well as for the imidazole 2 and imidazole 4 protons (*vide supra*). Such differences would not be present for a symmetrical representation for (43) arising from 180° in-plane rotation of one of the imidazole rings. Molecular models tend to show that steric crowding is more pronounced in a symmetrical structure.

The tetrahedral nature of Zn^{II} in (43) has been demonstrated by Co^{II} substitution. Thus, compound bis-Z-Cystine di His-OMe (24) was transformed to (44), the cobalt analog, by procedure delineated above, and the use of $CoCl_2.6H_2O$ in place of $ZnCl_2$. The resulting bluish-green solid (44), exihibited UV maximum at 595 nm (Section.D), with a profile similar to that observed for several Co^{II} analogs of natural and synthetic zinc finger proteins and clearly showing an envelope of intensity definitive of a tetrahedral site and fully in agreement with a metal coordination in

CHART C.19

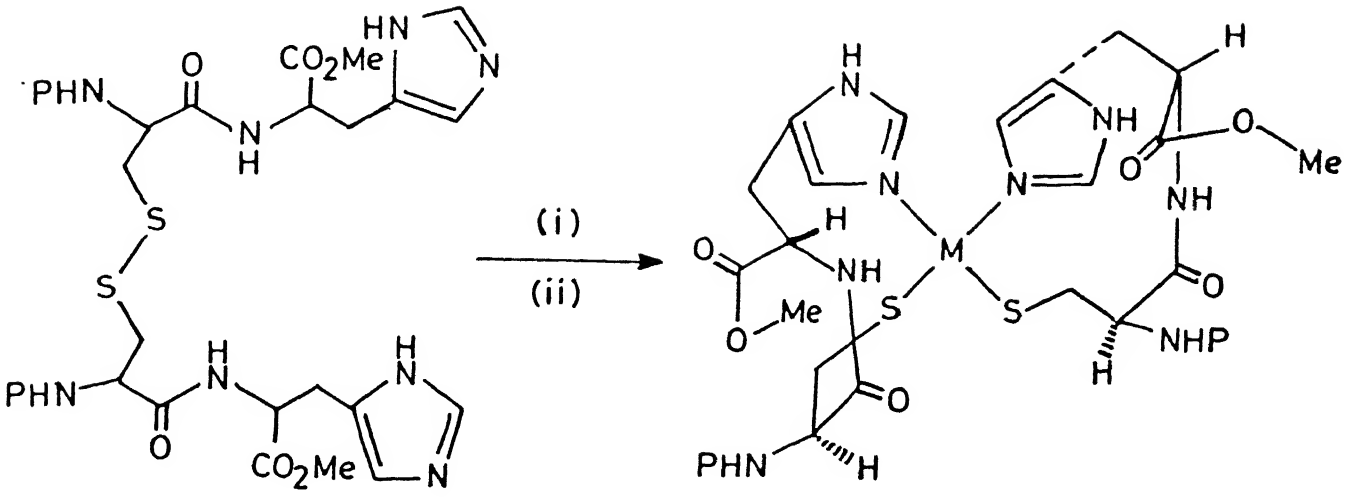

PRECURSOR	TEMPLATE	P	M
(24)	(43)	Z	Zn
(24)	(44)	Z	Co
(24)	(45)	Z	Cd
(25)	(46)	BOC	Zn
(25)	(47)	BOC	Co
(25)	(48)	BOC	Cd

(i) PDT (ii) Et_3N, $ZnCl_2$ / $CoCl_2 \cdot 6H_2O$ / $CdCl_2 \cdot 2H_2O$

Chart C.20

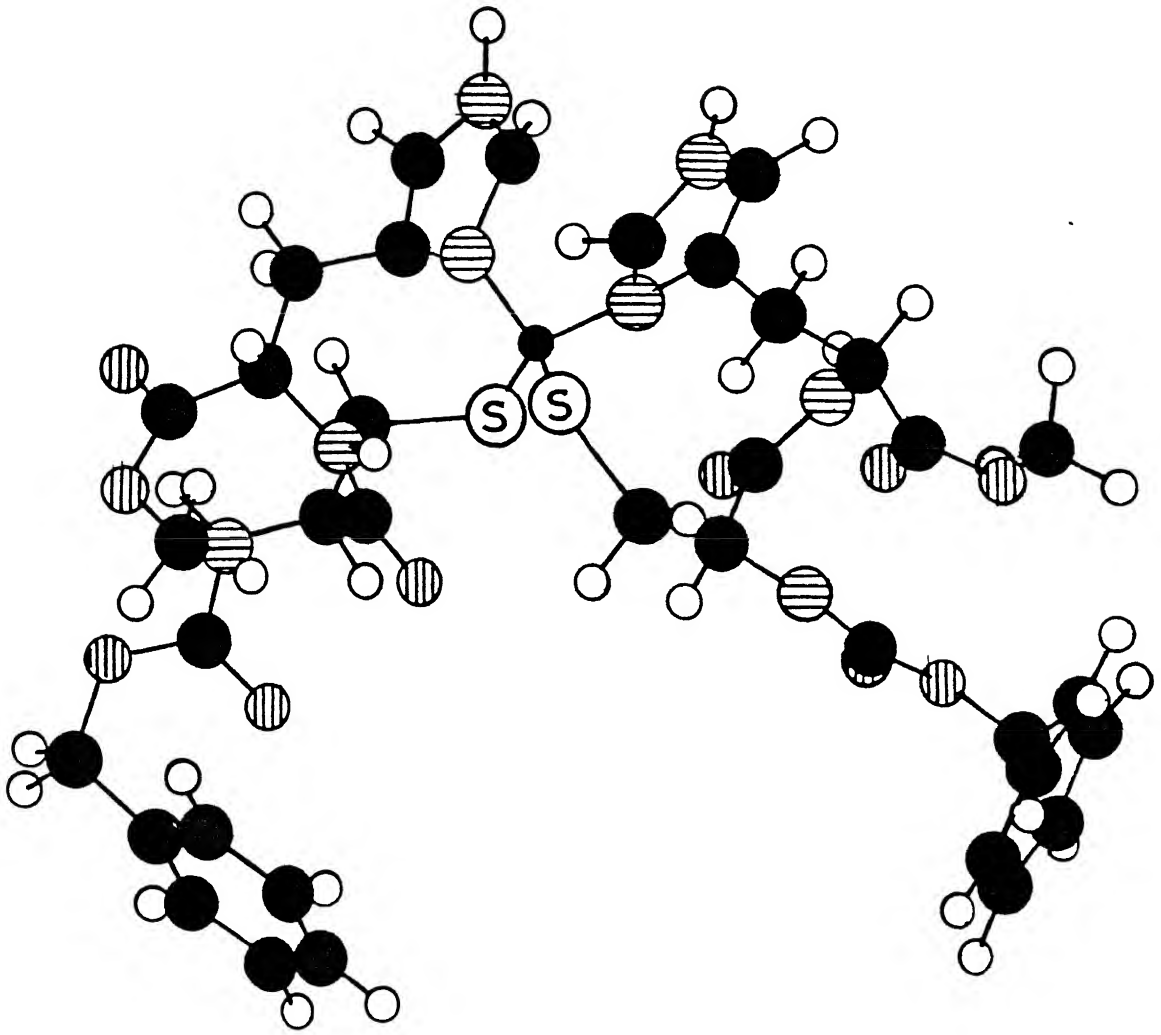

DTMM profile of (Z-Cys-His-OMe)$_2$Zn^{II} complex (43)

●-Carbon ; ○-Hydrogen ; ⊜-Oxygen ; ⊜-Nitrogen

Ⓢ-Sulfur ; ●-Zinc

a $(thiolate)_2(imidazole)_2$ environment[54]

The protocol delineated here, namely, reduction with PDT followed by metal complexation should enable the preparation of templates having different metal ions in place of zinc. This has been illustrated by the formation of basic cadmium template prototype (45) (61% yield) by procedures, delineated above and with the use of $CdCl_2.2H_2O$. Numerous experiments have shown that the methodology presented above is quite general. Thus bis-Boc-Cystinyl di His-OMe (25) was readily transformed to its zinc template (46) (36% yield), cobalt template (47) (45% yield) and cadmium template (48) (27% yield) (Chart C-19). The DTMM profile of (46) is shown in page Chart C-21

(Z-Cys His-OMe)$_2$Zn^{II} complex (43):

mp 188°-192°C (dec.).

ir:ν_{max} (KBr) cm^{-1} : 3308, 1718, 1674, 1508.

nmr: δ (DMSO-d_6) (400MHz): 2.75,3.05(m, 4H, His β-CH_2), 2.83, 3.10(m, 4H, Cys β-CH_2), 3.55, 3.63(s,s,6H, ester), 4.08, 4.35(b-d, 2H, Cys α-CH), 4.40,4.52(b-d, 2H, His α-CH), 5.05(s, 4H, $ArCH_2$-), 6.78(s)6.85 (s)(2H, His 4,4'H), 7.38(s, 10H, Ar), 7.6(b, 2H, Cys NH), 7.85(s) 7.98(s) (2H, His 2,2'H), 8.45(m, 2H, His NH).

ms: (FAB) m/z: 874 $(M+H)^+$,911 $(M+2H_2O+H)^+$

$[\alpha]_D^{25}$ = -21.15 (c=1.04, DMF).

ms: (FAB) m/z : 874 $(M-1)^+$, 911$(M+2H_2O+H)^+$.

(Z-Cys His-OMe)$_2$Co^{II} complex (44):

mp 175°-180°C (dec).

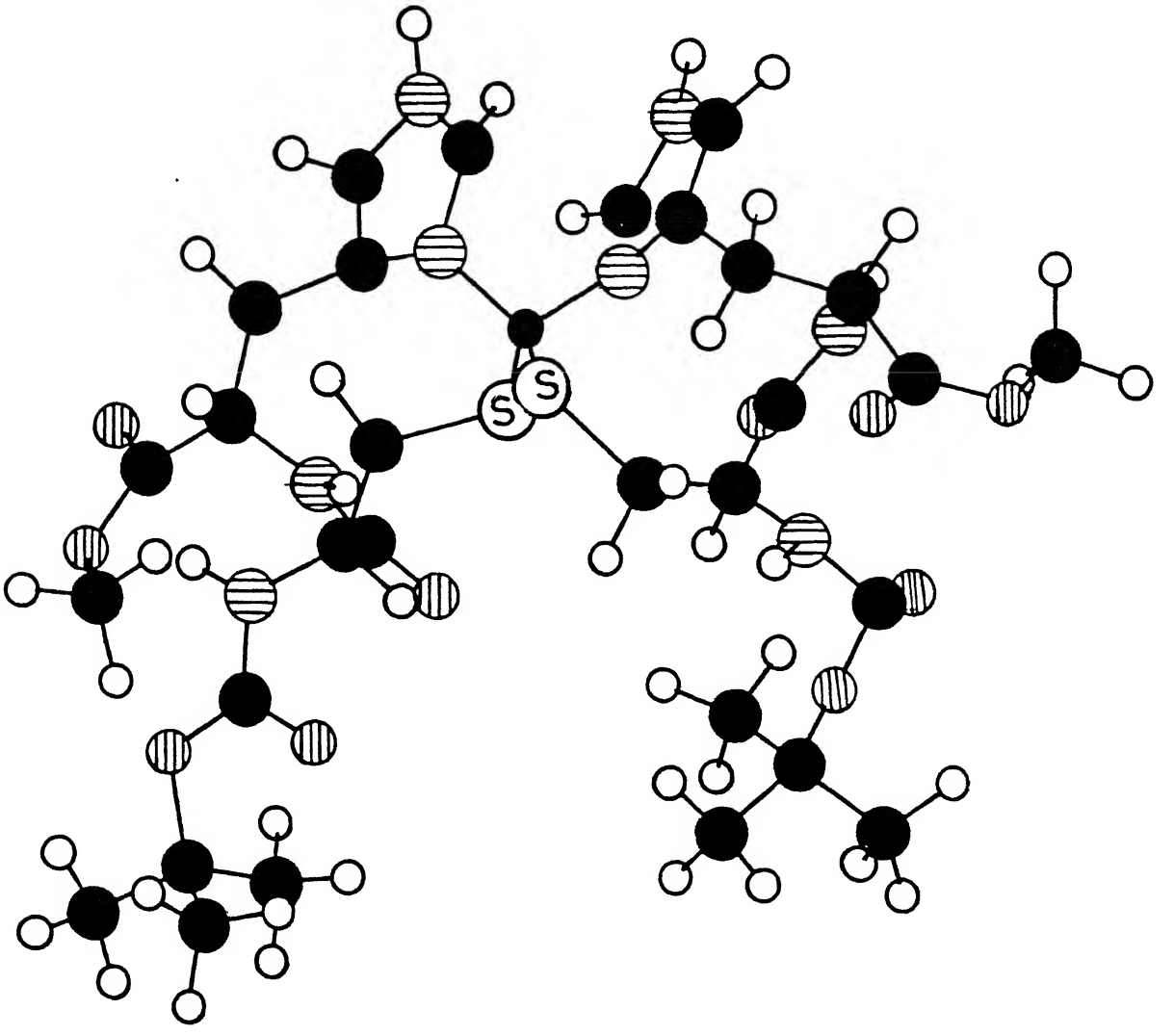

DTMM profile of $(Boc\text{-}Cys\text{-}His\text{-}OMe)_2Zn^{II}$ complex (46)

●-Carbon ; ○-Hydrogen ; ▤-Oxygen ; ▥-Nitrogen

Ⓢ-Sulfur ; ●-Zinc

UV: λ_{max} nm (c, 2x10^{-4} M, DMF): 595 (sh)(ϵ = 225$M^{-1}cm^{-1}$), 280 (sh)(ϵ = 3400 $M^{-1}cm^{-1}$).

ms: (FAB) m/z: 867 $(M-1)^+$.

(Z-Cys His-OMe)$_2$Cd^{II} complex (45):

mp 170°-172°C.

ir: ν_{max} (KBr) cm^{-1}: 3311, 1730, 1681, 1518.

nmr: ($CDCl_3$ + DMSO-d_6) (80MHz) : 3.33(b-m, 8H, Cys β-CH_2, His β-CH_2), 3.68(s, ester), 4.35(b-m, 2H, Cys α-CH), 4.73(b-m, 2H, His α-CH), 5.01(s, 2H, -CH_2Ar), 6.9(b, 2H, His 4,4'H), 7.38(b, 12H, Ar- & CysNH), 7.75(b-m, 4H, His 2,2'H & HisNH).

(Boc-Cys His-OMe)$_2$Zn^{II} complex (46):

mp 255°-265°C (dec.).

ir: ν_{max} (KBr) cm^{-1} : 3368, 1740, 1676, 1508, 1167, 1250, 1049.

nmr: δ(DMSO-d_6) (400MHz): 1.5 (s, 18H, $(CH_3)_3$-), 2.74 (b, 4H, His β-CH_2), 3.0 (b, 4H, Cys β-CH_2), 3.59 (b-d, 6H, ester), 4.38 (b, 4H, Cys α-CH, His α-CH), 6.28(b, 2H, Cys NH), 6.72(b-d, 2H, His4,4'H), 7.92 (b-d, 2H, His2,2'H), 8.40(b, 2H, HisNH).

ms: (FAB) m/z: 807 $(M)^+$, 843 $(M + 2H_2O)^+$.

$[\alpha]_D^{23}$ = -21° (c, 0.250, DMF).

(Boc-Cys His-OMe)$_2$Co^{II} complex (47):

CHART C.22

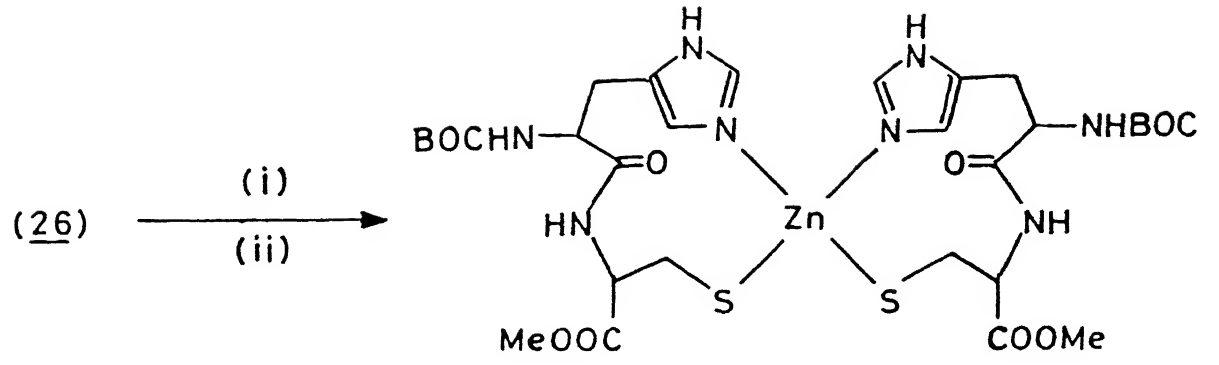

M = Zn : (49)
M = Co : (50)
M = Cd : (51)

(i) PDT (ii) Et_3N $ZnCl_2$ / $CoCl_2 \cdot 6H_2O$ / $CdCl_2 \cdot 2H_2O$

ms: (FAB) m/z : 807 $(M)^+$, 843(M^++2H_2O).

(Boc-His Cys-OMe)$_2$Co^{II} complex (50):

mp 220°-225° C

ir: ν_{max} (KBr) cm^{-1} : 3382, 1728, 1674, 1507, 1166, 1049.

UV: λ_{max}(nm) (c, 7.65 x 10^{-3} M, DMF): 608.5(sh) (ϵ = 282 $M^{-1}cm^{-1}$, 583 (ϵ = 272 $M^{-1}cm^{-1}$).

ms: (FAB) m/z : 801 (M^+).

As stated previously, it was necessary to transform the templates to one which is soluble in aqueous media. This was readily achieved taking advantage of the Boc- protecting group precursor present in the normal zinc finger template (46) as its analog (49). Both of these on treatment with aqueous TFA anhydride afforded from (46), the bis-N-deprotected zinc finger template (52) (~ 100% yield)and from (49), the 'anti sense' analog of the basic template, namely, (53) (~ 100% yield). As anticipated, compounds (52) and (53) were soluble in water and was used in DNA interaction studies (*vide infra*) (Chart C-23). An energy minimised DTMM profile of (52) is shown (Chart C-24)

(H_3N^+-Cys His-OMe)$_2$Zn^{II} TFA^- complex (52):

mp. 235°-240°C.

nmr: δ(D_2O) (400MHz): 2.81 (m, 4H, His β-CH_2), 3.08(m, 4H, Cys β-CH_2), 3.68(d, 6H, ester), 4.42(m , 2H, Cys α-CH), 4.75(m, 2H, His α-CH), 7.17(d, 2H, His4,4'H), 8.49 (d, 2H, His2,2'H).

CHART C.23

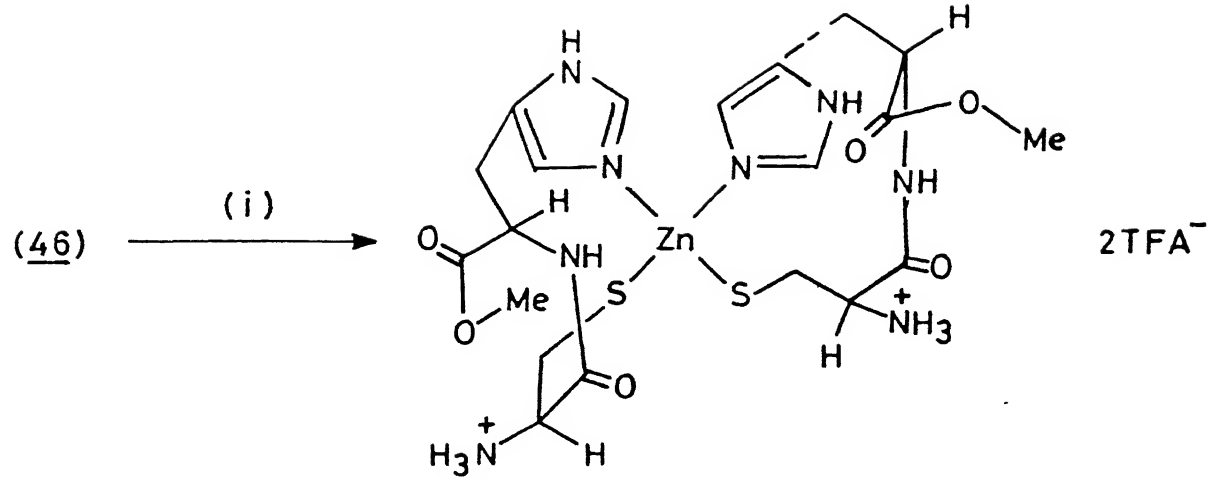

(52)

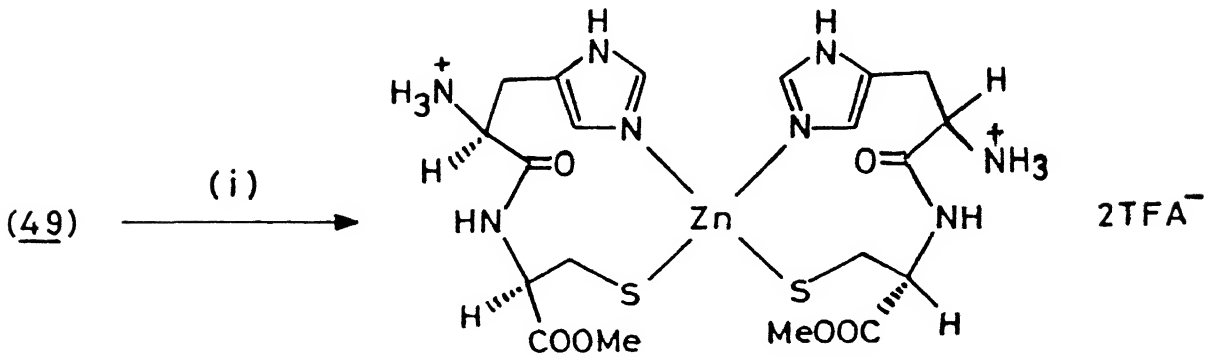

(53)

(i) TFAA–H_2O

CHART C-24

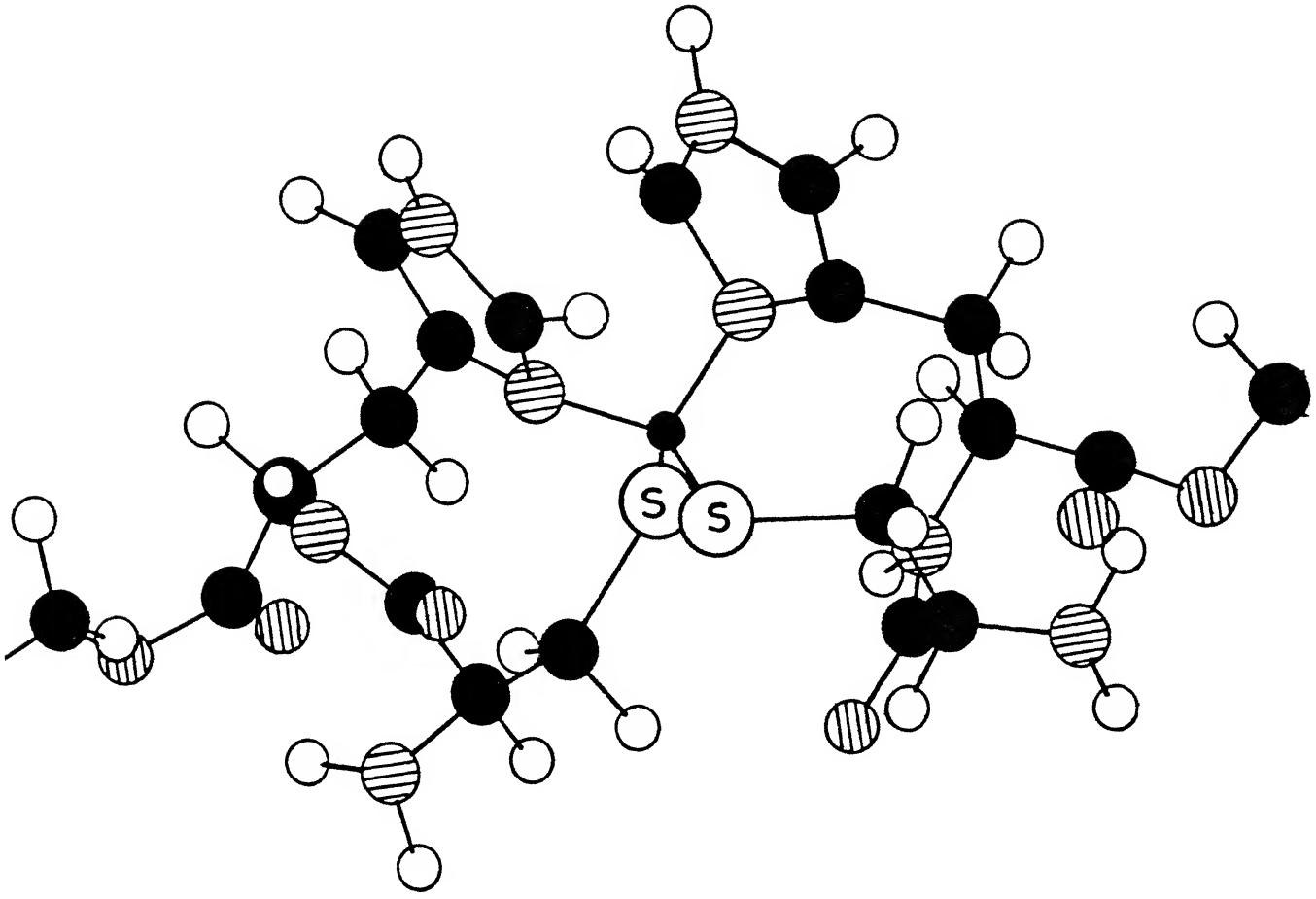

DTMM profile of $(NH_2\text{–Cys-His-OMe})_2Zn^{II}$ complex (52)

●-Carbon; ○-Hydrogen; ▨-Oxygen; ▨-Nitrogen

Ⓢ-Sulfur; ●-Zinc

ms: (FAB) m/z : 762 [M-2Boc+TFA$^-$+2]$^+$, 648 [M-2Boc-2TFA$^-$+2H_2O]$^+$, 605[M-2BOc-2]$^+$, 325 [M+2H_2O/2-2Boc-2TFA$^-$]$^+$.

(H_3N^+-His Cys-OMe)$_2Zn^{II}$ TFA$^-$ complex (53):

nmr: δ(D_2O) (400MHz): 2.90(b, 4H, His β-CH_2), 3.40(b, 4H, Cys β-CH_2), 3.72(d, 6H, ester), 4.32(b,2H, Cys α-CH), 4.66 (b, 2H, His α-CH), 7.40(d, 2H, His 4,4'H), 8.60(m, 2H, His 2,2'H).

ms: (FAB) m/z : 606[M-2Boc-1]$^+$, 301[(M-2Boc)/2 - 2]$^+$.

The next phase of synthetic endeavours, pertaining to the zinc finger motif was protocols that would enable the construction of actual zinc finger modules from precursors having carefully designed $\sim$ 30 residue peptide wherein, the cysteines and histidines are appropriately positioned. Obviously, the strategy for zinc finger template prototype, involving the reduction of disulphide bond as a key step should be difficult towards attaining this objective. What would be needed here is a methodology wherein distally placed cysteine SH groups can be, at appropriate opportunity, be brought together to form zinc finger template, thus the strategy here called for making in the beginning zinc finger templates (43) and (46) by this procedure. The preparation of S-Acm-Cys His-OMe has been described earlier. Thus, both Z-S-Acm-Cys His-OMe (27) and Boc-S-Acm-Cys His-OMe (28) were available for this approach. As could be seen from Chart C-23, the transformation of these to the zinc finger templates would involve Acm group deprotection and complexation with Zn^{II} species. In our hands, the recommended methodologies for S-Acm deprotection, namely, treatment with silver acetate followed by treating with H_2S gas [55] to get the deprotected -SH group gave very poor yields, if at all, of

the desired products. Eventually success came about in a most pleasant manner by reagent that not only led to smooth deprotection, but also to the desired zinc finger template prototype.

Thus, when methanolic solutions of either (27) or (28) when treated with 0.2M methanolic anhydrous $ZnCl_2$ under argon for 10 hours, S-deprotection as well as metal complexation ensued.

This approach to zinc finger template prototype is not only versatile but also involves fewer number of steps with comparable yields. For example, Z-S-Acm Cys His-OMe (27) afforded in a single step and in 92% yields, on treatment with anhydrous $ZnCl_2$, the template (43) which was identical in all respects to samples prepared by the PDT reduction - metal complexation strategy. The overall yield from cysteine here, involving five steps, is estimated to be an impressive 10%. Boc-S-Acm Cys His-OMe, when processed similarly afforded template (46) (yield 80%) which on treatment with TFAA-H_2O gave the TFA salt described earlier (52).

The direct transformation of S-Acm compounds to zinc dithiolates with methanolic $ZnCl_2$ is rationalised in Chart C-26 on the basis of a tandem complexation - deprotection sequence.

The strategy to the zinc finger template presented in Chart C-25 will find application, since it permits, *inter alia*, the incorporation of peptide linker and recognition elements between the N-terminal cysteines and the C-terminal histidines as illustrated in Chart C-27.

Fortuitous formation of cyclo [bisoxalylcystine di-OMe](29) afforded a gratuitous substrate for the preparation of zinc template motif present in gluco-corticoid receptors. Thus the treatment of (29) with PDT in MeOH, followed by metal complexation using $ZnCl_2$-Et_3N-$(Et_4N)^+$ Br^- in MeOH afforded in 28% yields, the

CHART C.25

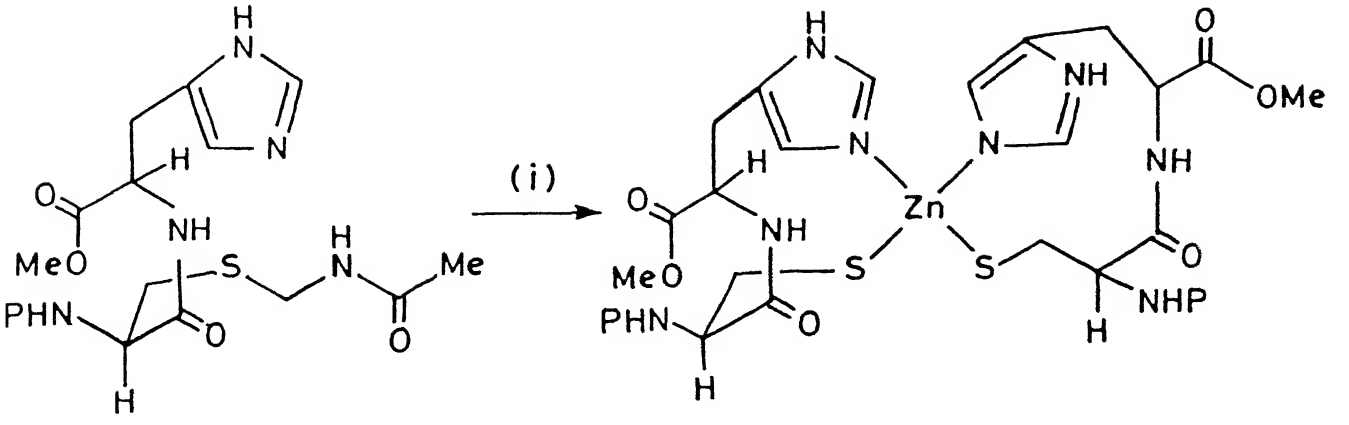

P = Z : (27)

P = BOC : (28)

P = Z : (43)

P = BOC : (46)

(i) $ZnCl_2$ - MeOH

CHART C.26

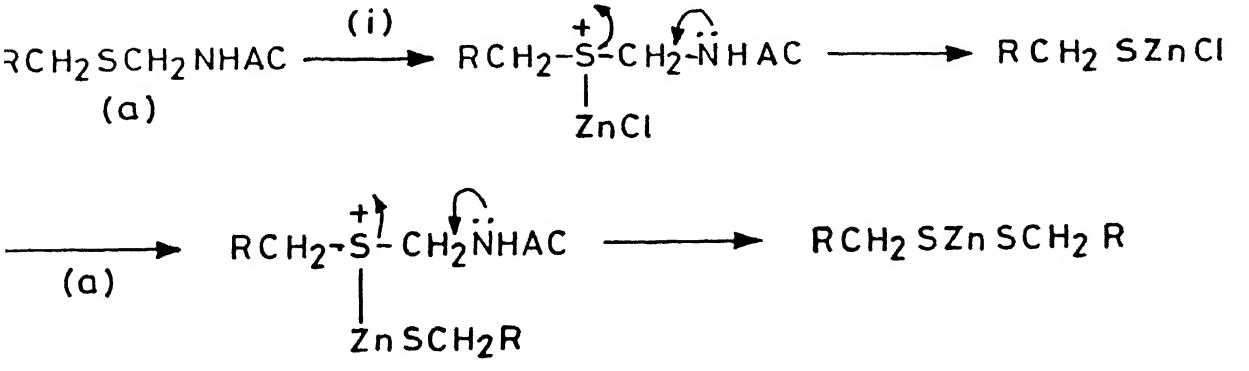

(i) $ZnCl_2$

CHART C.27

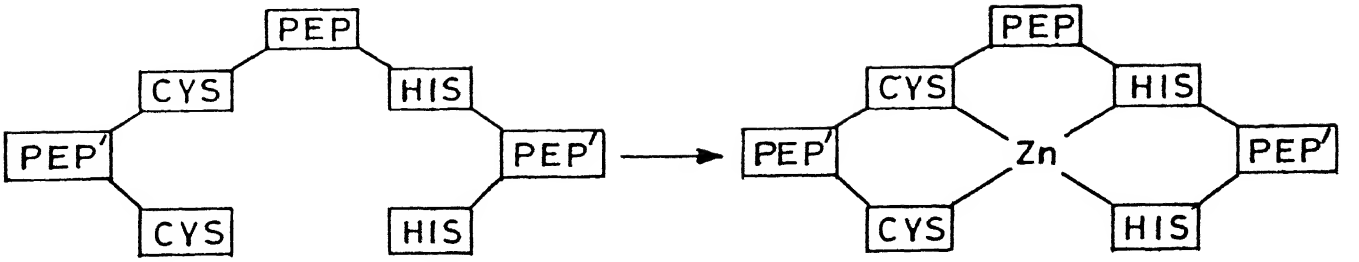

CYS: CYSTEINE HIS : HISTIDINE PEP′: LINKER (~3 RESIDUES)

PEP; RECOGNITION ELEMENT (~12 RESIDUES)

CHART C.28

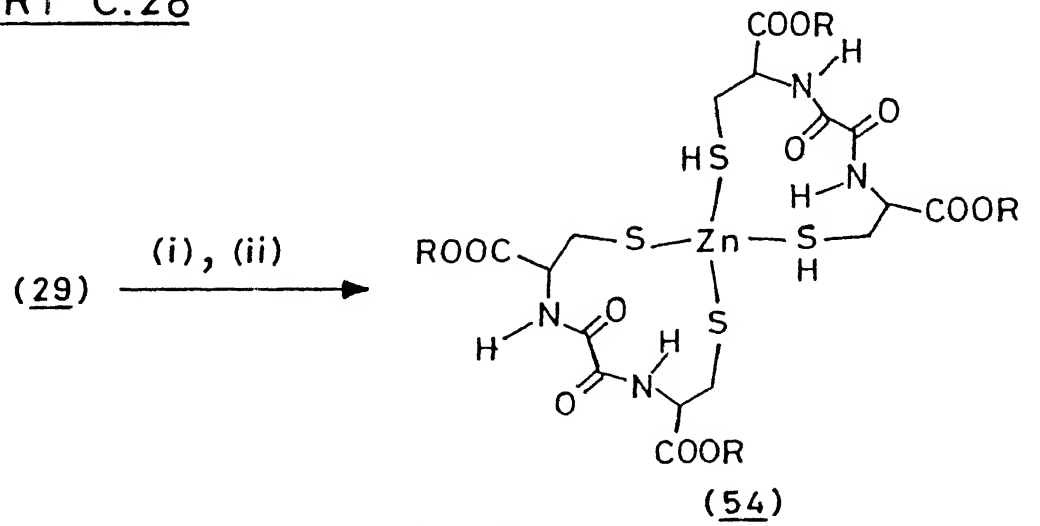

(54)

R = Me

(i) PDT - MeOH (ii) $ZnCl_2$ - Et_3N - $Et_4\overset{+}{N}Br^-$ - MeOH

neutral and aesthetically pleasing motif (54). An amusing instance of the proclivity for reaction to proceed in an unexpected manner is reflected in this transformation. In natural gluco-corticoid receptor systems, as stated previously, the Zn^{II} could be represented by $(Zn(SR)_4)^{2-}$. It was felt that the transformation of (29) to the template would offer the product of the same profile, and it was for this reason, that $(Et_4N)^+ Br^-$ was used to provide the counter ion. Conductivity measurements has shown that the compound (54) is neutral molecule, wherein, the Zn^{II} is of the type $(Zn(SR)_2.2RSH)$ (Chart C-28).

(Bisoxalyl-Cys-OMe)$_2$Zn (54):

mp 275°-280° C.

ir: ν_{max} (KBr) cm^{-1} : 3376, 1740, 1683, 1575, 1506.

nmr: δ (DMSO-d_6) (400MHz): 1.01 (b, 2H, -SH), 2.82 (m, 4H) 3.17 (m, 4H, β-CH_2), 3.64 (s, 12H, ester), 4.58 (m, 4H, α-CH), 9.28 (d, J=8Hz, 4H, -NH-).

ms: (FAB) m/z: 712 $(MH)^+$.

In addition to the understanding of the nature of the interaction of the minimal zinc finger template with DNA, the endeavours described above should find application in the domain of protein engineering to create novel proteins which will adopt predetermined structures, bind specific ligands and exhibit novel catalytic profiles. This notion finds much support from recent studies which clearly show that Zn^{II} ions exhibit great propensity to form well delineated tetrahedral structures, whenever possibilities for the formation such motifs are favourable. This aspect can be

illustrated with numerous instances where the zinc finger protein were constituted from metal-free precursors, the dimerisation of the human growth hormone (HGH)[20] and the introduction of a tetrahedral metal binding site into a designed protein[54].

With this objective, a search was made of protein crystallographic studies, wherein a disulphide bridge is proximately aligned to the histidines. Happily, such a constellation was readily seen in insulin (Chart C-29), whose partial X-ray crystal structure profile[56] is presented in Chart C-30. It could be seen from this chart that intramolecular disulphide bridge A6 - A11, is in close proximity with two histidines located, respectively, 5 and 10 positions in the B-chain. Molecular modelling showed that reduction of the relatively strained intramolecular disulphide bridge would afford an opportunity for the formation of a zinc finger template prototype, which would involve the swinging of B 5 histidine inwards, with little alteration in the remaining structure. This could be seen in Chart C-31 and Chart C-32.

Commercial human insulin (Sigma), comes as stabilised by zinc[57]. As a first step, zinc-free insulin was prepared[58], and was converted to its hexa methyl ester[59]. Treatment of zinc-free insulin hexa methyl ester with PDT in MeOH followed by reaction with anhydrous $ZnCl_2$ (99.99%) afforded compound with incorporation of the zinc. The gel picture of this (Section-D)) clearly showed that no fragmentation has taken place. 400MHz nmr comparison of the insulin hexa methyl ester with product of this reaction showed that the expected features from the incorporation of zinc template. Detailed studies are to be undertaken to clearly establish the

nature of the product. The transformation of insulin to one in which the zinc finger template is inscribed, could be considered as an example of protein engineering wherein a peptide hormone is putatively transformed to a DNA recognition system!

CHART C-29

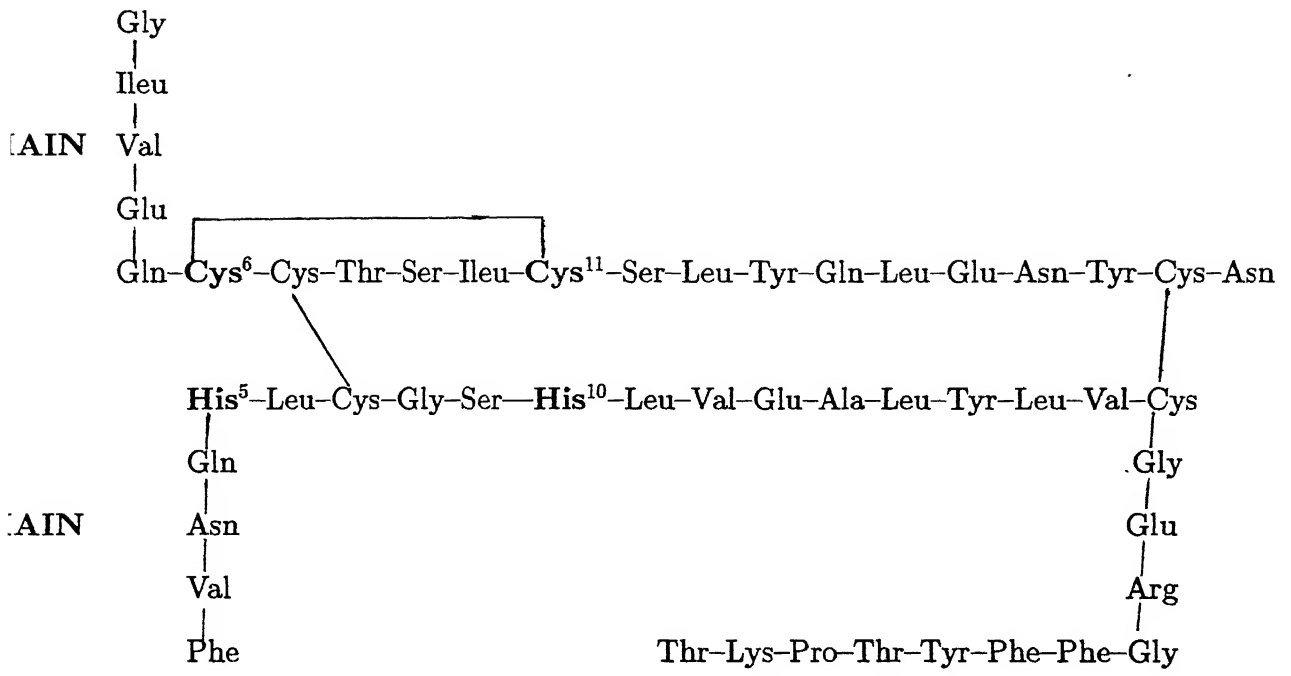

Amino Acid Sequence of Human Insulin

CHART C-30

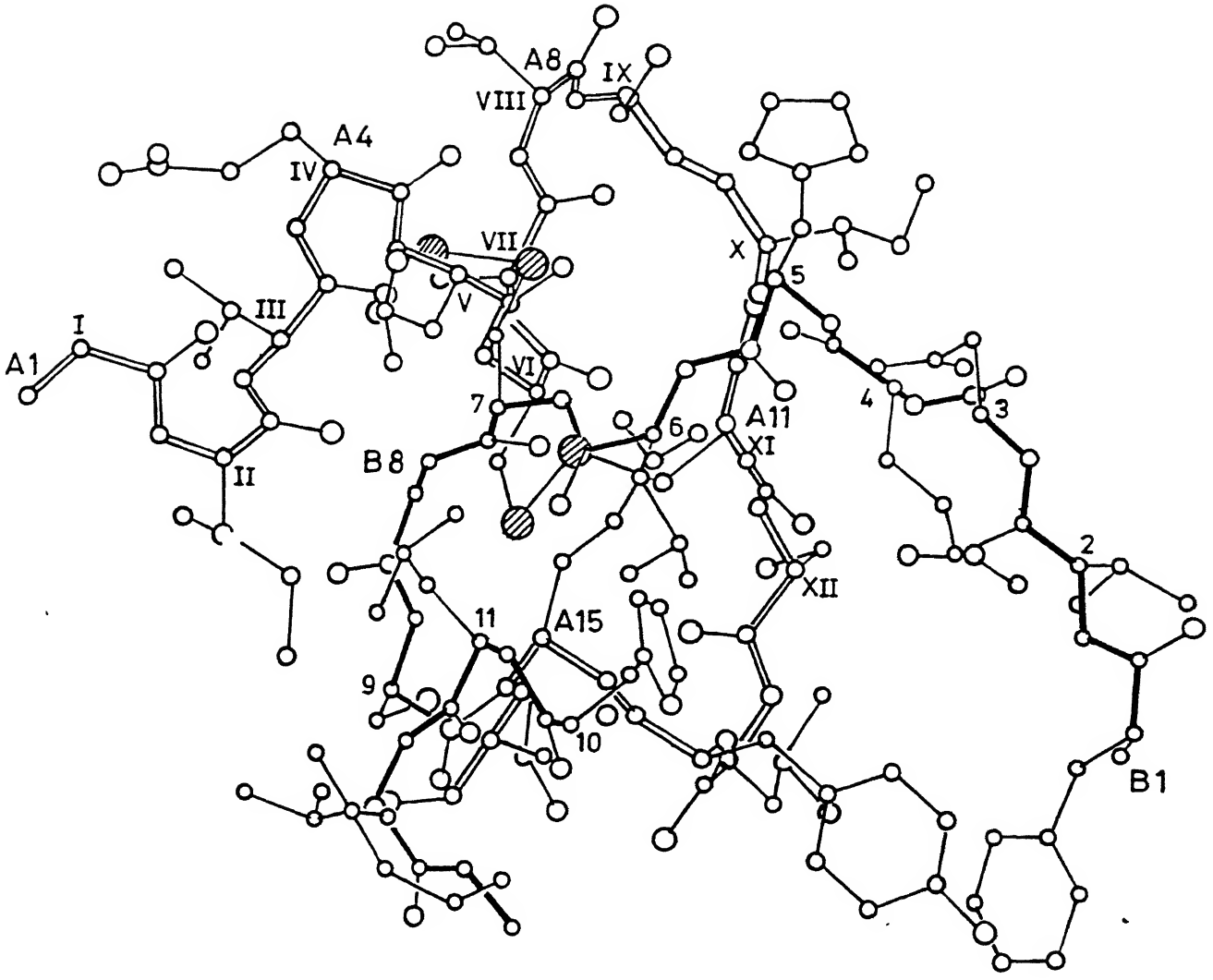

Partial X-ray crystal structure of insulin[50a]

CHART C-31

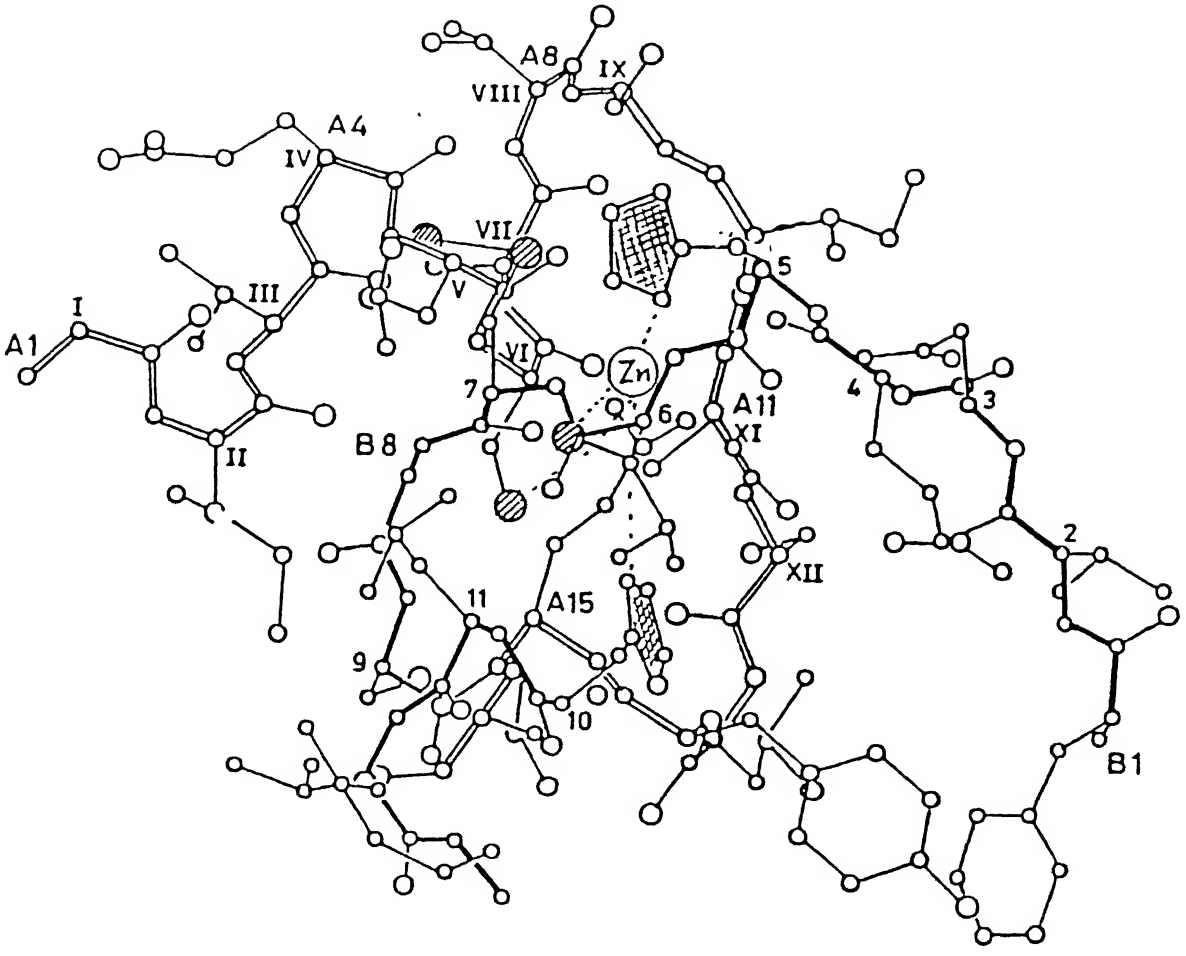

Proposed location and structure of the Zn^{2+} binding site in insulin-zi
finger complex

CHART C-32

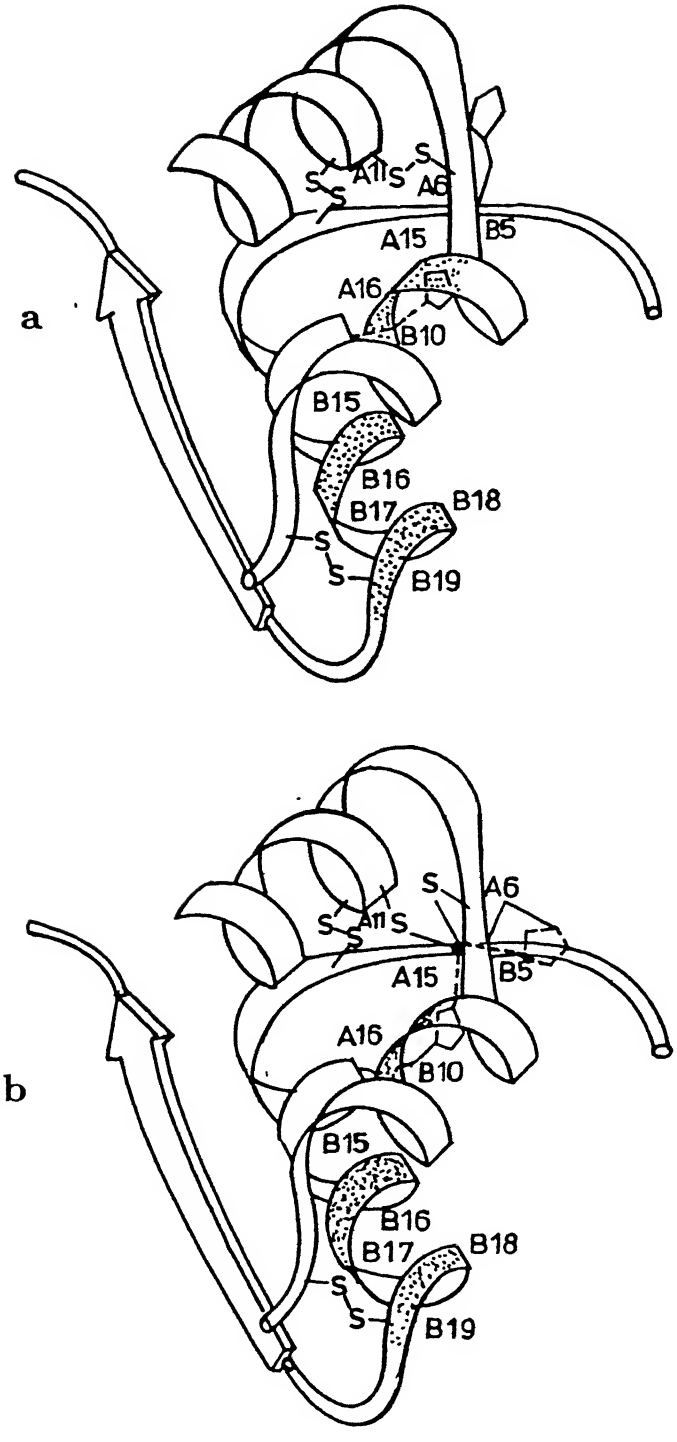

a. Ribbon drawing of the insulin based on X-ray Model b. Ribbon drawing for the insulin-zinc finger complex

C. PRESENT WORK: DNA INTERACTION STUDIES

DNA INTERACTION STUDIES WITH ZINC FINGER TEMPLATE (52) [$(CH)_2Zn^{II}$ (A)] AND ITS ANTISENSE ANALOG (53) [$(HC)_2$ Zn^{II} (B)]

As stated previously, the DNA interaction studies of a minimal zinc finger structural motif is essential not only with respect to the the understanding of the structural interactions involved with DNA, but also to provide the corner stone for construction of finger modules so designed as to recognise specific DNA triplet sequences. Thus, the major objective of the study of the interaction of zinc finger template prototypes with DNA were to determine whether a chemically synthesised zinc finger template prototype is enough for sequence specific recognition of DNA. More importantly, such a study could reveal, with respect to the templates themselves, the nature of the order and the conformational changes brought about by interaction of the templates, which, in turn, would enable the further understanding of the role of the basic templates. Thus, it became necessary to determine whether the basic templates are involved in simple orientation or in addition bringing about a notable change in the structure of DNA.

Analysis of large data set of zinc finger - DNA recognition domain sequences showed that there lies a preference for guanine-rich sequences and thus three recognition templates, namely, poly d(G-C), poly dG and 5' AGCGTGGGCGTT 3' (oligo-1) were used in this study with appropriate controls. Poly d(A-T) was also studied for comparison (Chart C-33)(Please see abbreviations, p xvi).Substrates used in the DNA binding studies are, the zinc finger motifs [$(CH)_2Zn^{II}$] (A) (52), its "antisense"

CHART C-33

STRUCTURES OF DNA USED FOR DNA INTERACTION STUDIES

1. .....→ -G-C-G-C-G-C-G-C-G-C-G-C- →
← -C-G-C-G-C-G-C-G-C-G-C-G-C-G- ←

.....Poly d(G-C)

2. → -G-G-G-G-G-G-G-G-G-G-G-G- →
← -C-C-C–C-C–C-C–C-C–C-C-C- ←

.....Poly dG

3. → -A-T-A-T-A-T-A-T-A-T-A-T- →
← -T-A-T-A-T-A-T-A-T-A-T-A-T- ←

.....Poly d(A-T)

4. → A-G-C-G-T-G-G-G-C-G-T →
← T-C-G-C-A-C-C-C-G-C-A ←

Synthetic Oligonucleotide
.....(Oligo-1)

analog [$(HC)_2Zn^{II}$] (B)(53) and as blanks, the tripeptides $(CH)_2$(33) and $(HC)_2$(34) devoid of Zn^{II}, co-valent $Zn^{II}(acac)_2$ and the ionic $Zn^{II}(NO_3)_2$ (Chart C-30).

The methodologies employed are tabulated below:

Methodology	.Nature of interaction monitered
1. UV Hypochromism	Binding and Stacking and determination of binding constants.
2. CD Studies	Secondary Structural Changes in DNA Back bone.
3. Thermal Denaturation	Specificity and Binding
4. Gel Retardation Studies	DNA complexation
5. Competitive Binding Assay Through Ethidium Bromide Fluorescence Quenching	Competitive DNA binding

Methods of DNA Interaction Studies

1. UV Titrations:

Ultraviolet spectra were recorded on a Hitachi 150-20 spectrophotometer at ambient room temperature (17° - 19° C), using a 1cm path length quartz cells. Each spectrum was corrected by background subtraction. Stock solutions of the DNA and the metal template complexes were prepared with water (Millipore) and these stan-

dard solutions could be used for about 3 weeks without much change in the profile. The concentration of the DNA was measured from its optical density (O.D) (1 O.D = 50 μg of DNA =150 μM of DNA phosphates) and are expressed as molar phosphates (DNA(phosphates)). An accurately known weight of metal template complexes was used to prepare standard solutions and this served to calculte the concentrations of metal template complexes in total volume of test solutions. Titrations were carried out using a constant volume of DNA stock solutions and adding varying amounts of metal templates with vigorous mixing. The spectra were then measured from 320 nm to 220 nm. The titrations were continued until the ratio of metal template complexes to DNA were about 1. The metal template complexes alone showed negligible absorbance at wavelength greater than 240 nm. The concentration of various DNA(phosphate) used in the experiments were as follows: Poly d(G-C): 69 μM; Poly d(A-T): 43 μM - 63 μM; Poly dG: 62 μM - 70 μM.

2. CD Titrations:

Circular dichroism spectra were measured at ambient room temperature (17^o - 19^o C), using a 1 cm pathlength quartz cells, on a Jasco J-20 automatic recording spectropolarimeter between 220 nm to 325 nm. Each spectrum was corrected by background subtraction. Samples were prepared using Millipore water. CD values were expressed in molar ellipticity: $[\theta] = (\theta_{obs} \text{ x } 100)/(\text{c X l})$, where θ_{obs}, c and l represent the observed ellipticity (in millidegrees), the molar concentration of the absorbing species and the pathlength respectively[60]. CD titrations were performed in the same way as UV titrations. Dry nitrogen gas (9 L/min.) was flushed over the cuvette windows to prevent condensation of dust particles. The CD pattern of the metal template complexes alone were negligible above 225 nm. The concentrations of

dard solutions could be used for about 3 weeks without much change in the profile. The concentration of the DNA was measured from its optical density (O.D) (1 O.D = 50 μg of DNA =150 μM of DNA phosphates) and are expressed as molar phosphates (DNA(phosphates)). An accurately known weight of metal template complexes was used to prepare standard solutions and this served to calculte the concentrations of metal template complexes in total volume of test solutions. Titrations were carried out using a constant volume of DNA stock solutions and adding varying amounts of metal templates with vigorous mixing. The spectra were then measured from 320 nm to 220 nm. The titrations were continued until the ratio of metal template complexes to DNA were about 1. The metal template complexes alone showed negligible absorbance at wavelength greater than 240 nm. The concentration of various DNA(phosphate) used in the experiments were as follows: Poly d(G-C): 69 μM; Poly d(A-T): 43 μM - 63 μM; Poly dG: 62 μM - 70 μM.

2. CD Titrations:

Circular dichroism spectra were measured at ambient room temperature (17° - 19° C), using a 1 cm pathlength quartz cells, on a Jasco J-20 automatic recording spectropolarimeter between 220 nm to 325 nm. Each spectrum was corrected by background subtraction. Samples were prepared using Millipore water. CD values were expressed in molar ellipticity: $[\theta] = (\theta_{obs} \text{ x } 100)/(\text{c X l})$, where θ_{obs}, c and l represent the observed ellipticity (in millidegrees), the molar concentration of the absorbing species and the pathlength respectively[60]. CD titrations were performed in the same way as UV titrations. Dry nitrogen gas (9 L/min.) was flushed over the cuvette windows to prevent condensation of dust particles. The CD pattern of the metal template complexes alone were negligible above 225 nm. The concentrations of

various DNA used in these experiments were as follows: Poly d(G-C): 38 μM (av.); Poly d(A-T): 57 μM - 60 μM (av.); Synthetic oligonucleotide (Oligo 1): 60 μM (av.) and Poly dG : 74 μM (av.).

3. Thermal Melting Experiments:

Absorbance - temperature transitions were performed on a Hitachi 330 spectrophotometer, fitted with a thermostated cell compartment. The temperature of the cell compartment was regulated by a programmable constant temperature circulating bath (Julabo). The temperature of the DNA - metal template complex solutions were monitered by a linear thermal sensor. The temperature of the cell compartment was raised approximately 1° C/3 to 4 min. in the region of the optical density transition; absorbance measurements were made repeatedly at a given temperature to ensure that the equilibrium has reached. The values were not corrected for the thermal expansion of the solution. Stoppered quartz cuvettes with 1 cm pathlength ($\sim$ 0.65 ml capacity) were used. Melting curves were monitored at the λ_{max} for the DNA. For poly d(G-C) in addition to its λ_{max} at 256 nm, λ_{max} at 275 nm, were greater percentage of hyperchromicity could be observed, was also monitered. The width of the absorbance vs. temperature curve for a DNA, at a given ionic strength, is defined as the change in temperature required to bring the absorbance transition from 25% to 75% completion. This definition was adopted here to express the T_m values. The concentration of DNA(phosphates) were as follows: Poly d(G-C): 117 μM and Poly d(A-T): 57 μM DNA(phosphates)

4. a-1 Oligonucleotide Synthesis:

Each of the single strand 11-mer DNA, (i) d(A G C G T G G G C G T) and (ii) d(A T C G C A C C C G C) were synthesised by phosphoramidate method on an automated gene assembler (Pharmacia), attached with facility to programme the sequential addition of 'active nucleotide' addition onto the nucleotide attached to solid support, solvent washings after the coupling step, deprotection etc.. The synthesised sequence were fully deprotected using aqueous ammonia (25%) in a sealed tube for 2-3 h at 80°-90° C, centrifuged and the supernatant were lyophilised. These were then spun column purified on a pre-equilibrated Sephadex G-25 column using MilliQ water for elution. The fractions were pooled and taken for annealing.

4. a-2 Annealing of single strands to double strand:

Equivalent concentration of each of the single strands were mixed in an eppendorf tube, heated at 80°-90° C on a water bath and were left at room temperature overnight. A stock solution of this double strand oligonucleotide (Oligo-1) was prepared in MilliQ water and it had a concentration of 38.91U.

4. a-3 Radiolabeling of 5'-end of Oligo-1:

The 5'-end labeling was accomplished using enzyme, polynucleotide kinase, and γ-^{32}P-ATP, according to the procedure[61]. The following were mixed in an eppendorf tube:

Oligo-1 (38.91U)(15 μl), 10 X kinase buffer* (3 μl), T4 polynucleotide kinase (10 - 20 units)(1 μl), γ-^{32}P-ATP (1 μml) (incubated at 37° for 30 min., and kept in a Lead vial at -20° C. The concentration of this end labeled synthetic oligomer was 29.8U.

---

* 10 X kinase buffer: A stock solution of kinase buffer was prepared:

Tris.Cl (pH 7.6)(0.5M), $MgCl_2$(0.1M), dithiothreitol (50mM), spermidine (1mM) and EDTA (1mM).

---

4. a-4 20% Non-denaturing polyacrylamide gel electrophoresis to observe complex formation of (52) with γ-^{32}P - 5'-end labeled Oligo-1:

The following reagents were prepared:

(i). Acrylamide monomer solution (30%): An aqueous solution (100 ml) containing acrylamide (29 g) and methylene bisacrylamide (1 g) was prepared and was used as a stock solution.

(ii). Gel running buffer: TBE: 10 X stock solution*: 45mM Tris base; 45mM boric acid and 0.2mM EDTA.

---

* 10 X stock solution of TBE was prepared:

Tris base (54 g), boric acid (27.5 g) and EDTA (0.5M)(pH 8.0)(2ml)

EDTA concentration was kept low in order to minimise the possibility of metal ion exchange with EDTA.

(iii). The loading buffer: It was the same buffer solution as above but without the addition of EDTA.

(iv). Ammonium persulfate (initiator)(10% w/v): Ammonium persulfate (0.5g) and water to 5.0ml.

Gel preparation:

The following procedure was adopted for a single 1.00mm polyacrylamide gel of 16 cm height.

Twenty percent acrylamide/methylene bis acrylamide was prepared from 30% stock solution and was made upto 50ml using Trisborate buffer, added ammonium persulfate (0.5ml) and TAMED (50 μl), swirled gently to mix well and transferred to the gel sandwich using a plastic syringe with blunt end and filled to the top. Care was taken to avoid polymerisation and bubble formation during this process, inserted a comb. The gel polymerised in about 10 -15 min., and was aged for about 4h and was preelectrophoresced for about 3h before using it.

Sample preparation:

The samples for the experiment were prepared in two sets: In the first set, unlabeled Oligo-1 was mixed with varying amounts of (52) such that the final concentration of unlabeled Oligo-1 were (i) 162.5 μM; (ii) 139 μM; (iii) 132 μM and (iv) 116.3 μM and the ratio of (52)/Oligo-1 were, respectively, (i) Oligo-1 alone; (ii) 0.69; (iii) 12.3 and (iv) 25.11. To each of the above solution were added γ-^{32}P- 5'-end labeled Oligo-1 (1 μl, 450ng) and glycerol (2 μl). Finally the solutions were made upto exactly known volume, nearing 20 μl, with water.

The second set of solutions were prepared exactly as above excepting the addition of 2 μl of labeled Oligo-1.

As the control set, solutions were prepared with $(CH)_2$ (33) as above with 2 μl of labeled Oligo-1.

The above samples were incubated at 37° C for 10min., and cooled to room temperature before loading onto the gel.

Gel electrophoresis:

Before loading the samples, the comb was removed from the gel sandwich and the wells were rinsed with gel running buffer. Samples were loaded carefully, avoiding air

bubbles setting in the wells. As indicator, bromophenol blue, which run along with 10-nucleotide long fragments, was loaded separately.

After the samples were loaded, the upper buffer chamber was fitted to the top of the gel sandwich and safely placed inside the electrophoresis chamber. The upper and lower chambers were filled with gel running buffer ($\sim$ 250ml - 350ml each), the leads were connected to the power supply. The gel was run at a constant current of 1mA and an applied voltage of 90V for about 5h. At the end of the run, the gel layer was carefully taken out from the gel sandwich, rinsed with water, dried covered with saren wrap and placed inside a Kodak X-ray film cassette (with the DNA side up) fitted with an intensifier. Inside a dark room, an X-ray film was placed above the gel layer and closed the cassette and left at -70° C for about 2 days. The film was then developed for about 2min., in Kodak developer/replenisher and was fixed in Kodak fixer/replenisher, washed in running water for $\sim$ 10min., and dried the film and the resulting film was photographed.

5. Fluorescence Experiments:

The fluorescence measurements were carried out using a Hitachi F-4000 Fluorescence spectrophotometer at the ambient room temperature (17° - 19° C). The fluorescence excitation wavelength was set at 540 nm and the emission maximum was observed at 590 nm. DNA, ethidium bromide and metal template complexes alone did not show any fluorescence at these wavelengths. The concentration of various test solutions, prepared in Millipore water, were as follows: ethidium bromide: 10 μM - 50 μM; metal template complexes: 2.7 μM - 54 μM; DNA: 37.5 μM.

RESULTS

In Figure C-1 is shown, the effect of addition of $(CH)_2Zn^{II}$ (A) (52) on poly d(G-C). As could be seen, increasing addition of the template, a hypochromicitry as well as a red shift ($\sim$ 8 nm) occurs which is characteristic of DNA binding and stabilisation. As could be seen from Figure C-2, although hypochromicity effects were of the same order in the case of the antisense template $(HC)_2Zn^{II}$ (B) (53) on the same DNA substrate, there was hardly any red shift thus indicating the predominant effect here is binding. Whereas the templates showed nearly equivalent hypochromicity corresponding to ΔO.D of $\sim$ 0.3, the precursor peptides $(CH)_2$ (33) and $(HC)_2$ (34), as shown respectively, in Figure C-3 and Figure C-4 showed little influence on DNA compared to the templates.

Both the effects observed with (A) (Figure C-1), namely, hypochromicity and red shift, were virtually absent, as could be seen from Figure C-5 and Figure C-6, on addition of respectively, the ionic $Zn(NO_3)_2$ or the covalent $Zn(acac)_2$.

The hypochromicity profile presented in Figures C-1 to C-4 at 256 nm is summarised in Figure C-7 and that pertaining to the blanks, namely, Figure C-5 and Figure C-6 is presented in Figure C-8.

Similar studies with poly d(A-T) is presented in Figures C-9 to C-16. A noteworthy observation is that the hypochromicity profile on addition of (A)(52) (Figure C-9) and (B)(53) (Figure C-10) are very close to that observed on addition of $Zn(NO_3)_2$ (Figure C-13) and $Zn(acac)_2$ (Figure C-14), thus demonstrating that unlike in the case of poly d(G-C) (vide supra),the zinc environments, do not play any additional role with respect to interaction with poly d(A-T). The precursor peptides $(CH)_2$(33) and $(HC)_2$(34) showed no effect on poly d(A-T) (Figure C-11 and Figure C-12). The UV interaction studies at 261 nm with respect to poly d(A-T) and (A), (B), (33)

and (34) are shown in Figure C-15 and that pertaining to $Zn(NO_3)_2$ and $Zn(acac)_2$ in Figure C-16. A noteworthy feature pertaining to studies with poly d(A-T) is that in all cases the initial addition brings about a marked order. This is because, unlike poly d(G-C), poly d(A-T) has a flexible profile.

The above findings clearly show that with poly d(G-C) both $(CH)_2Zn^{II}$ (A) and its antisense analog $(HC)_2Zn^{II}$ (B) exhibit remarkable co-operative transition in the UV absorption profile with the mid-point of transition close to a molar ratio of 1:1 between DNA and the ligands.

These findings are of considerable interest, since a large conformational change in DNA structure which might occur as a consequence of DNA-template complex formation is reflected as a spectral change in this region. It was shown earlier[62] that such a hypochromic effect is suggestive of orderliness induced upon the DNA secondary structure on binding of ligands to it. The co-operative nature of transition in the UV profile, which occurs with a mid-point of transition close to a molar ratio of 1:1 between poly d(G-C) and templates is consistent with a notion that there exists a strong interaction between poly d(G-C) and the templates and that the interaction contributes positively to the helix stabilisation and to the structural rigidity.

Upon Scatchard analysis of the data of Figure C-1 (Figure C-17), pertaining to $(CH)_2Zn^{II}$ (A)(52) and poly d(G-C), a binding curve was obtained with two distinct types of binding. The first phase of binding had more number of binding sites (n) ($\sim$ 14-15 DNA(phosphates)/(A)) and perhaps is due to the phosphate binding. The second phase was characterised by a binding constant having a value of $\sim 1.80 \times 10^7 M^{-1}$ (n = $\sim$ 2-3 DNA(phosphates)/(A)), strongly suggestive of specific interaction with DNA base. All additional probes (*vide infra*) support the notion.

The conformational changes induced upon DNA as a consequence of binding is further demonstrated by CD studies which are extremely sensitive even to small changes in mutual orientation of neighbouring bases in a polynucleotide. The pattern is shown in Figure C-18. The progressive increase in ordering of bases in poly d(G-C) is indicated by decreasing magnitude of the positive long wavelength band. The most dramatic one is reflected at approximately 1:1 ratio of ligand and DNA, where seemingly a reversal of conformation occurs. Poly d(G-C) is prone to undergo such conformatioanl reversals at a variety of conditions[63,64].

In contrast to $(CH)_2Zn^{II}$ (A)(52), addition of the anti sense template $(HC)_2Zn^{II}$ (B)(53) produced only marginal changes in the magnitude of the positive long wavelength band which were quite comparable to that observed on addition of the precursor tripeptide (34) (Figure C-19 to C-21).

Parallel CD interaction studies with poly d(A-T) is presented in Figures C-22 to C-25. It could be seen from this that no noteworthy effects are seen and that the templates and their precursor peptides (33) and (34) show nearly identical profiles.

The most significant of CD interaction studies is the profound effect shown on poly d(G-C) on addition of $(CH)_2Zn^{II}$ (A)(52). All indications are that this interaction eventually gives rise to the transformation of right handed B-form to the left handed Z-form of DNA. It is noteworthy that in the present case the fact that such a reversal was seen with the template $(CH)_2Zn^{II}$ (A) strongly supports increased propensity for binding to poly d(G-C) which can be accomodated by its B $\rightarrow$ Z transition. The possibility that such a change can arise from Zn^{II} contribution alone appears unlikely, since the UV profile of either $Zn(NO_3)_2$ or $Zn(acac)_2$ hardly reflected any kind of interaction in terms of hypochromicity and red shift.

The oligonucleotide (oligo 1) (Chart C-29), the sequence used to make complex with 96 amino acid residue peptide in the crystal struture studies by Pavletich and Pabo[10], strongly interacts with $(CH)_2Zn^{II}$ (A) (52) and considerable ellipticity decrease is observed (Figure C-26). Similar profile can also be seen in $(HC)_2Zn^{II}$ (B) (Figure C-27). In contrast, $(CH)_2$ (33) and $(HC)_2$ (34) devoid of zinc did not show any significant change (Figure C-28 and Figure C-29). Blank experiments with $Zn(NO_3)_2$ showed that it had no effect on oligo 1 (Figure C-30). These spectral changes in oligo 1 are delightful, as these results reflect the pronounced ordering induced on DNA. In conjunction with the results of Pavletich and Pabo[10], it is possible that the model we propose here further asserts the preference for guanine bases by zinc finger templates.

Gel retardation studies were carried out in order to observe complex formation between oligo-1 and $(CH)_2Zn^{II}$(A)(52). The oligonucleotide was specifically end labeled with γ ^{32}P-ATP using standard protocols. The complex formation was examined by electrophoresis in 20% polyacrylamide gel and autoradiography. The results clearly showed marked retardation for oligo-1 adducted with template compared to the control (Figure 31).

Thermal denaturation studies have provided significant insight pertaining to the role of $(CH)_2Zn^{II}$(A)(52) in DNA re-structuring. The addition of (A)(52) resulted in a marked stabilisation of DNA structure. The T_m, which represent helix→Coil transition, of poly d(G-C) was enhanced from 62.5^o to 70.5^o at a (A)/DNA ratio of 0.04. A unique property of this interaction is that it is cooperative and reversible, with an ideal profile, changing to the native state on cooling. Here the heating and cooling curves are nearly superimposible (Figure C-32, Figure C-33). This finding is in sharp contrast to the early report of T_m studies of DNA with Zn ions where the cooling profile was out of phase , the likely reason being that in this type of transition

the complementary base pair in the strands are out of register[65]. It is clear therefore that template A not only binds to poly d(G-C) but also maintain the complementary base in register in the denatured state enabling ideal reversal upon cooling. The T_m was independent of the concentration of A suggesting specific binding to poly d(G-C) (Figures C-32 to C-34). This property is responsible for the fact that when the A/DNA ratio increases towards unity, whilst the T_m is hardly affected, the reversibility is completely lost. In comparison, poly d(A-T) showed a concentration dependent denaturation behaviour. At the lowest concentration the T_m is somewhat lowered, with increasing ratio the T_m gradually shifts along the temperature axis (Figure C-35). Thus T_m studies with poly d(G-C) and $(CH)_2Zn^{II}$ (A) are fairly consistent with a model for interaction having characteristics of reversibility, fairly well-defined stochiometry, cooperativeness, and selectivity[66].

Studies mentioned above have clearly brought out the fact that the template $(CH)_2Zn^{II}$ (A)(53) interacts with guanine residues in DNA in specific manner. This notion is strongly supported from parallel studies with poly dG. Upon addition of increasing amounts of $(CH)_2ZnII$ (A)(52) to poly dG, an effect almost identical to that for poly d(G-C) (vide supra), namely increasing hypochromicity and stability (Figure C-36). Interestingly, precisely, as in the case of poly d(G-C), addition of increasing amounts of $(HC)_2Zn^{II}$ (B) showed increasing hypochromicity, but hardly any red-shift indicating DNA binding (Figure C-37). Finally, similar experiments with precursor peptides $(CH)_2$ (33) and $(HC)_2$ (34) showed no hypochromicity (Figure C-38 and Figure C-39). These results are summarised and presented in Figure C-40.

The CD profile of poly dG on addition of $(CH)_2Zn^{II}$ (A) (52) clearly showed binding (Figure C-41). However, these were not as dramatic as poly d(G-C), where a reversal of structural profile was observed. This can be rationalised on the basis

of the fact that poly dG has a relatively more rigid conformation. Remarkably similar effects were observed on addition of $(HC)_2Zn^{II}$ (B) to poly dG (Figure C-42). Interestingly, the precursor peptide $(CH)_2$ (33), also showed binding in the CD titration studies, although the effect was less here (Figure C-43). In sharp contrast, the precursor peptide $(HC)_2$ (34) did not show any appreciable binding to poly dG (Figure C-44).

Perhaps the most direct experimental evidence for the interaction of template $(CH)_2Zn^{II}$ (A)(52) with guanine residues was secured by competitive binding assay through ethidium bromide fluorescence quenching (Figure C-45 to C-48). From the changes in the ethidium bromide bound to poly dG, on addition of increasing amounts of $(CH)_2Zn^{II}$ (A)(52), it is clear that initial addition of (A) brings about an order on poly dG, arising from non-specific interaction as shown by fluorescence enhancement. Subsequent additions quenches the ethidium bromide fluorescence, eventually effectively quenching the induced fluorescence of ethidium bromide, thus strongly suggesting that the specific interaction of templates with guanine residues that leads to displacement of ethidium bromide. Similar profile was seen on increasing ethidium bromide/DNA ratio from 0.3 (Figure C-45) to 1.1 (Figure C-46 to C-48). It could be seen from Figure C-46 to C-48 that ethidium bromide fluorescence is quenched by (A) but with increasing amounts of fluorophore complete displacement does not take place.

From the studies outlined above and based on the known interaction of zinc finger template with major groove of DNA[10], we propose a model for (A) - DNA interaction involving two types of binding. First of these is the recognition of the sugar-phosphate backbone by one of the imidazoles present and the second a specific

interaction involving the appropriately positioned amino group with guanine of the DNA (Figure C-49).[67]

Although it is known that zinc finger protein bind DNA in tandem giving rise to remarkable specificity in interaction, this study shows that even the simple monomeric unit $(CH)_2Zn$ (A) binds to DNA specifically with appreciable stability.

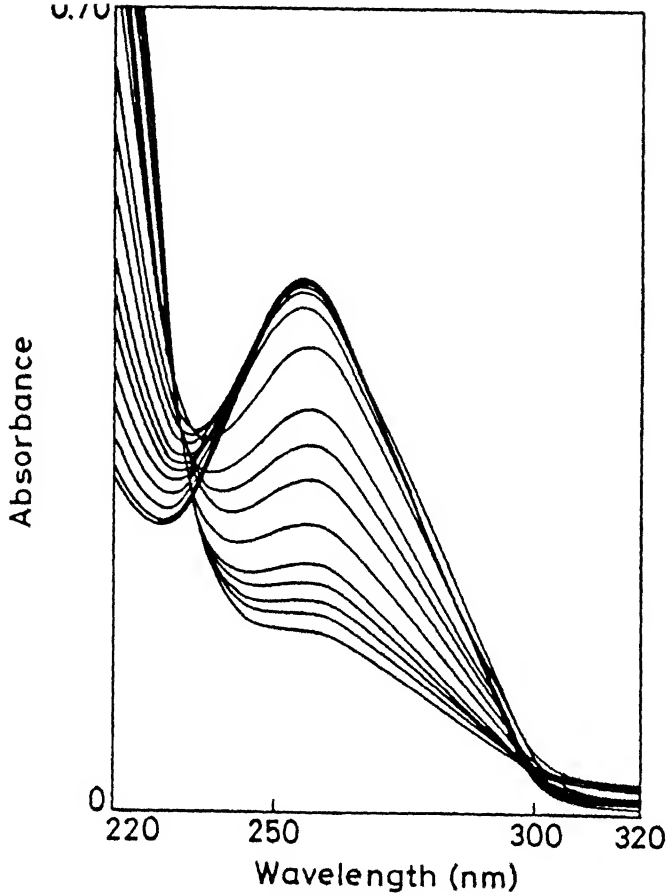

Figure C-1. UV profile of poly d(G-C) (DNA) titrated with (A) [A = $(CH)_2Zn^{II}$. (52)] in H_2O. Concentration of DNA : 69μM DNA (phosphates)

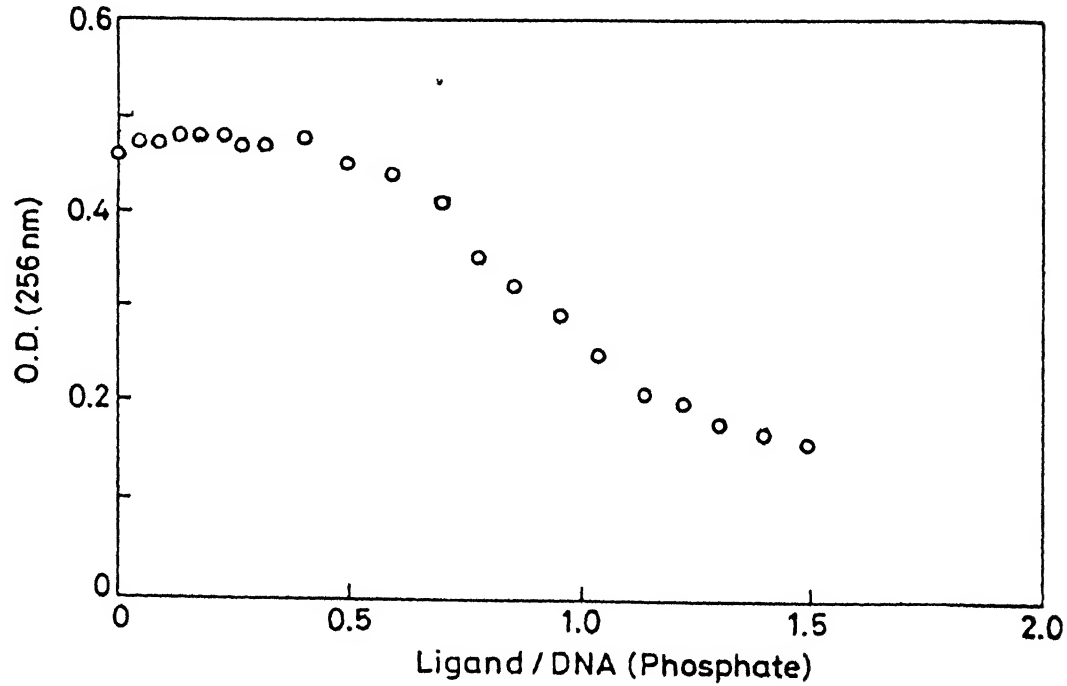

Plot of UV hypochromicity of poly d(G-C) (DNA) (at 256 nm) vs Ligand/DNA (phosphate) Ligand = (A)

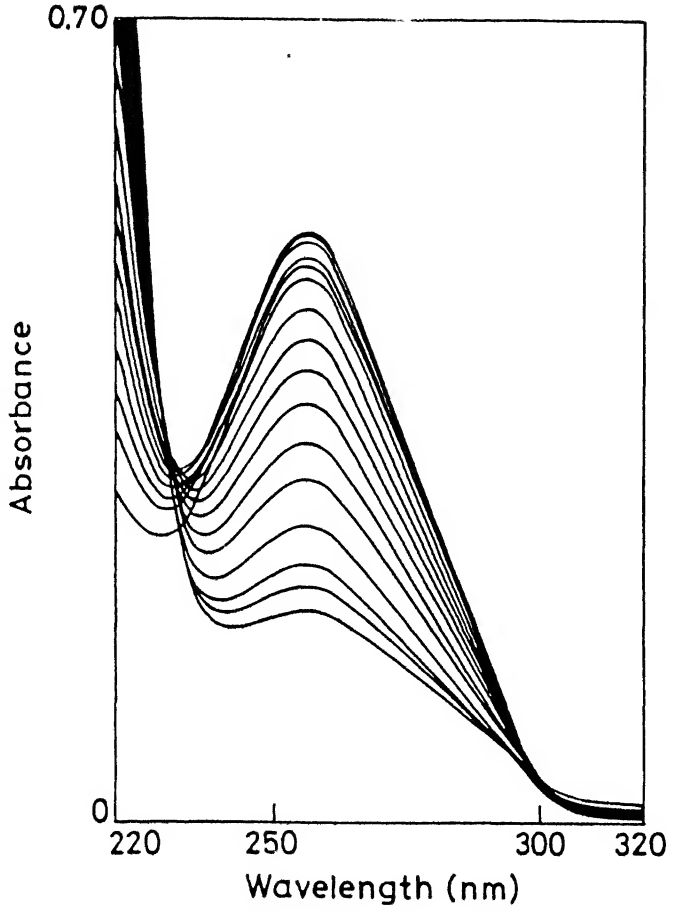

Figure C-2. UV profile of poly d(G-C) (DNA) titrated with (B) [B = $(HC)_2Zn^{II}$, (53)] in H_2O. Concentration of DNA :73.4μM DNA (phosphates)

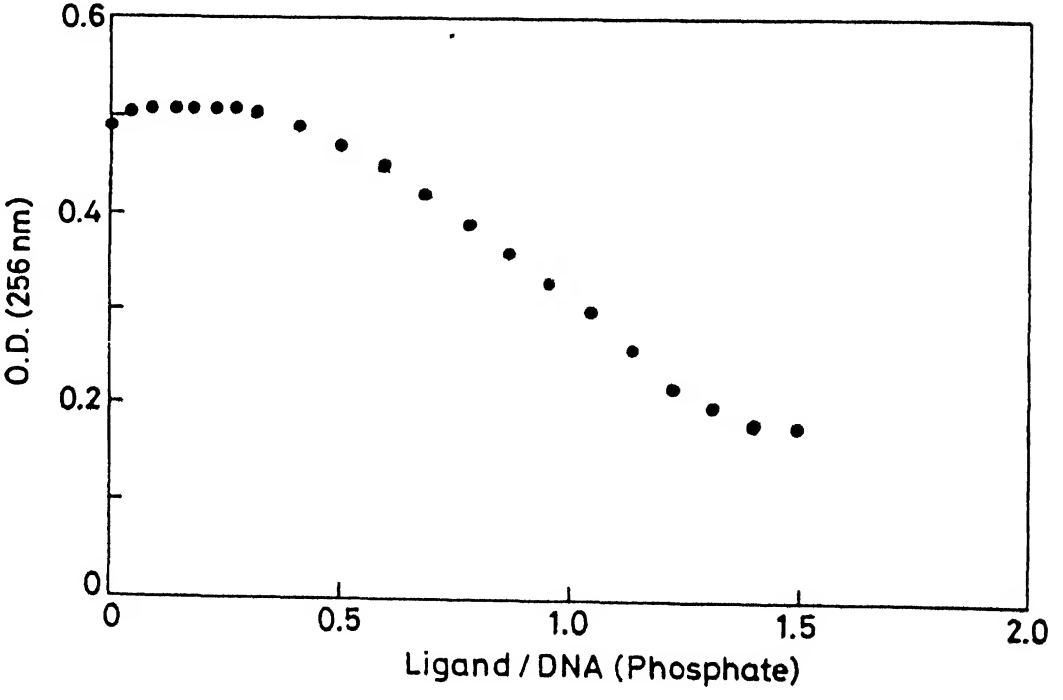

Plot of UV hypochromicity of poly d(G-C) (DNA) (at 256 nm) vs B/DNA (phosphate) Ligand = (B)

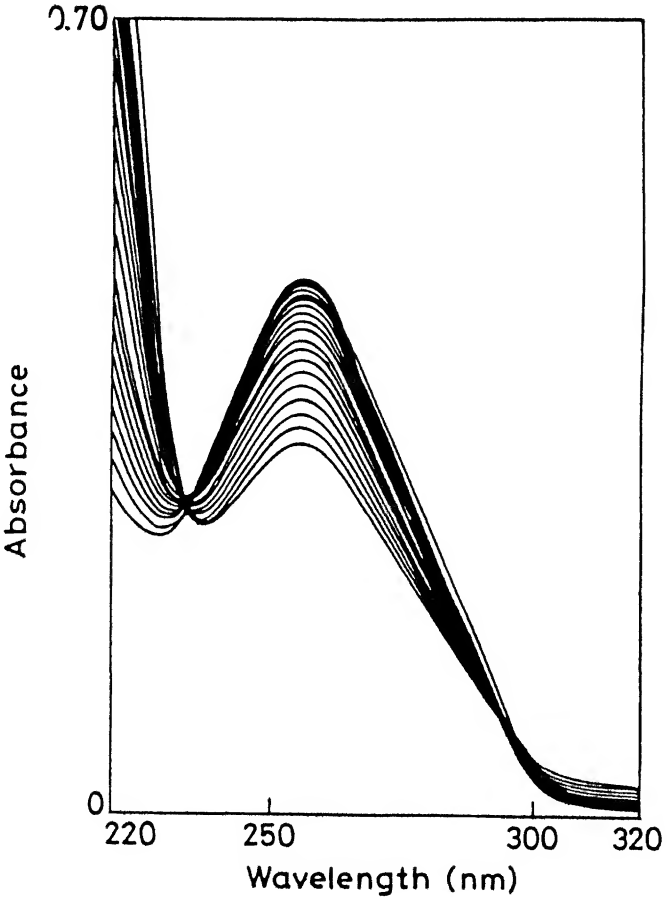

Figure C-3. UV profile of poly d(G-C) (DNA) titrated with precursor peptide $(CH)_2$, (33) in H_2O. Concentration of DNA : 65μM DNA (phosphates)

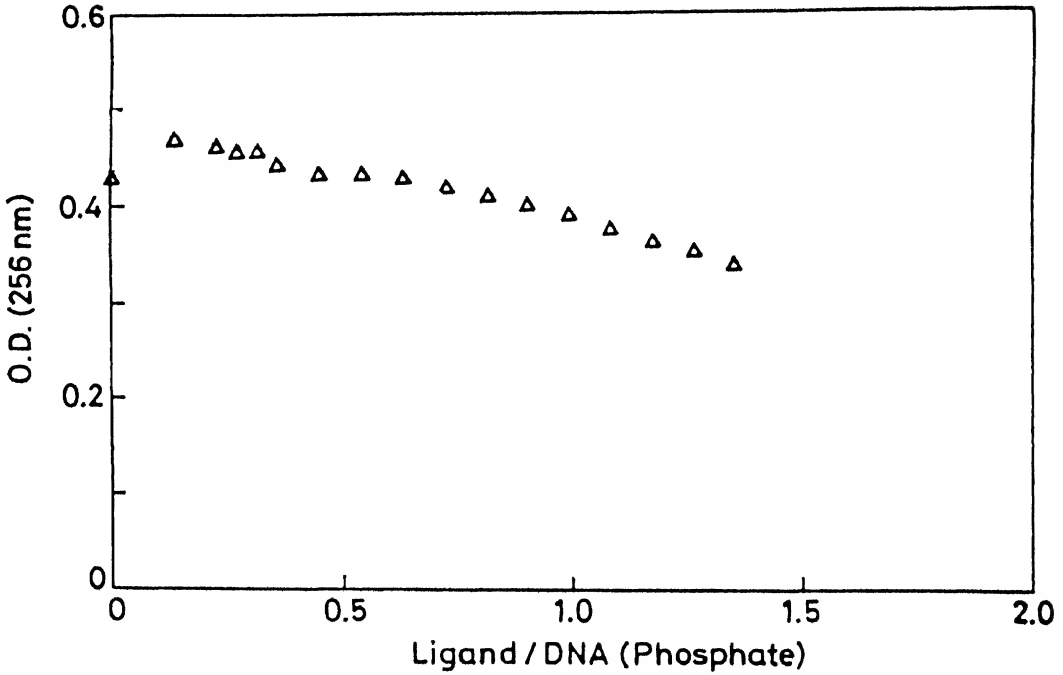

Plot of UV hypochromicity of poly d(G-C) (DNA) (at 256 nm) vs Ligand/DNA (phosphate) Ligand = $(CH)_2$ (33)

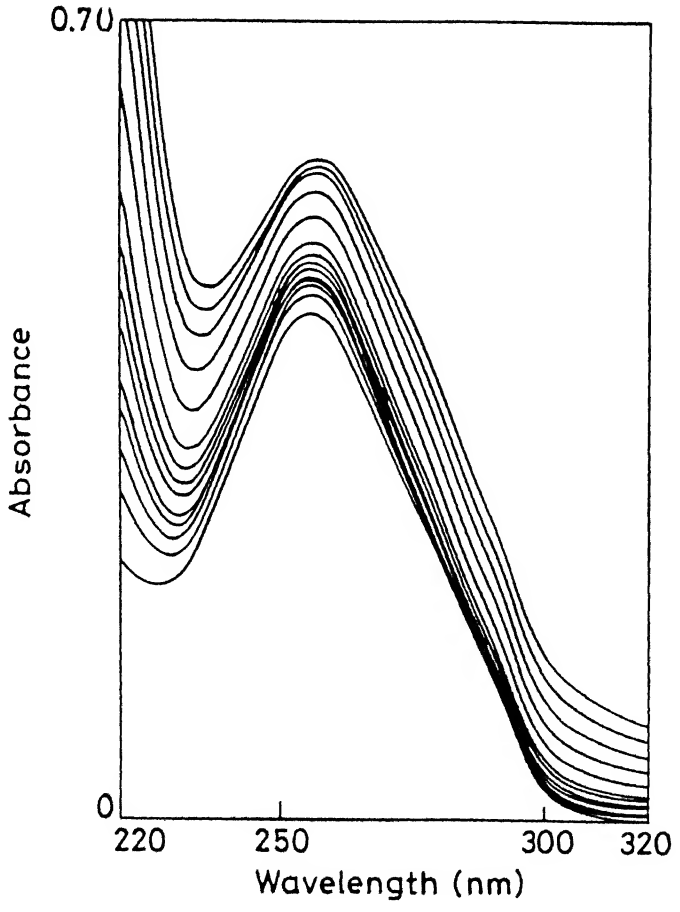

Figure C-4. UV profile of poly d(G-C) (DNA) titrated with precursor peptide $(HC)_2$, (34) in H_2O. Concentration of DNA : 66.50μM DNA (phosphates)

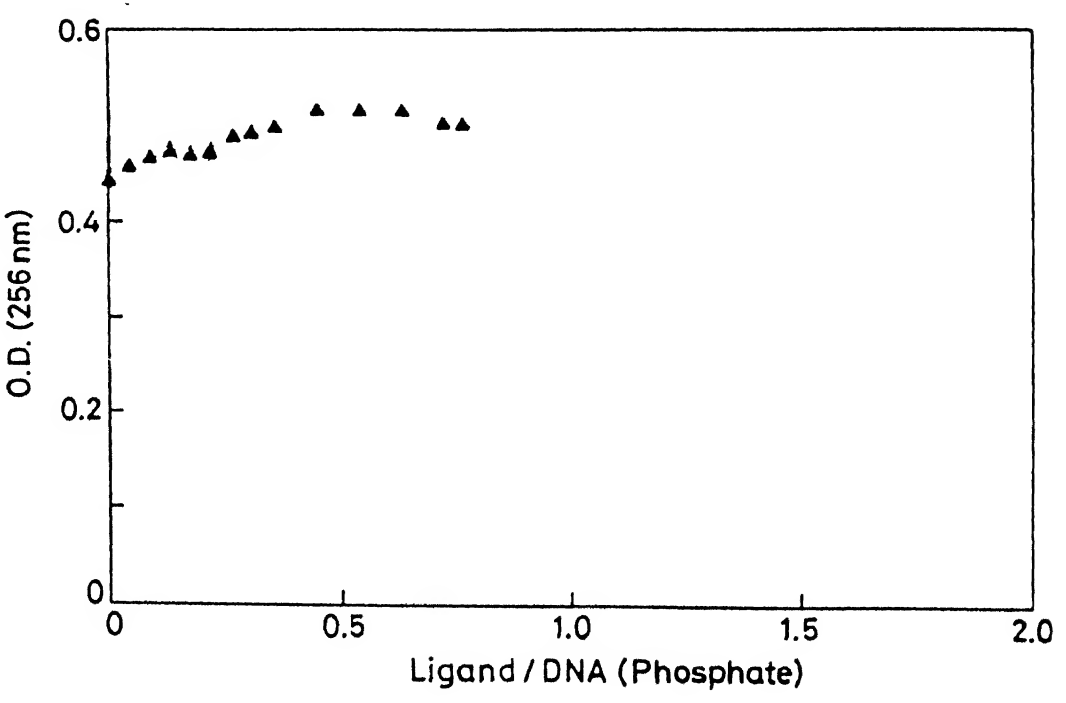

Plot of UV hypochromicity of poly d(G-C) (DNA) (at 256 nm) vs Ligand/DNA (phosphate) Ligand = $HC)_2$ (34)

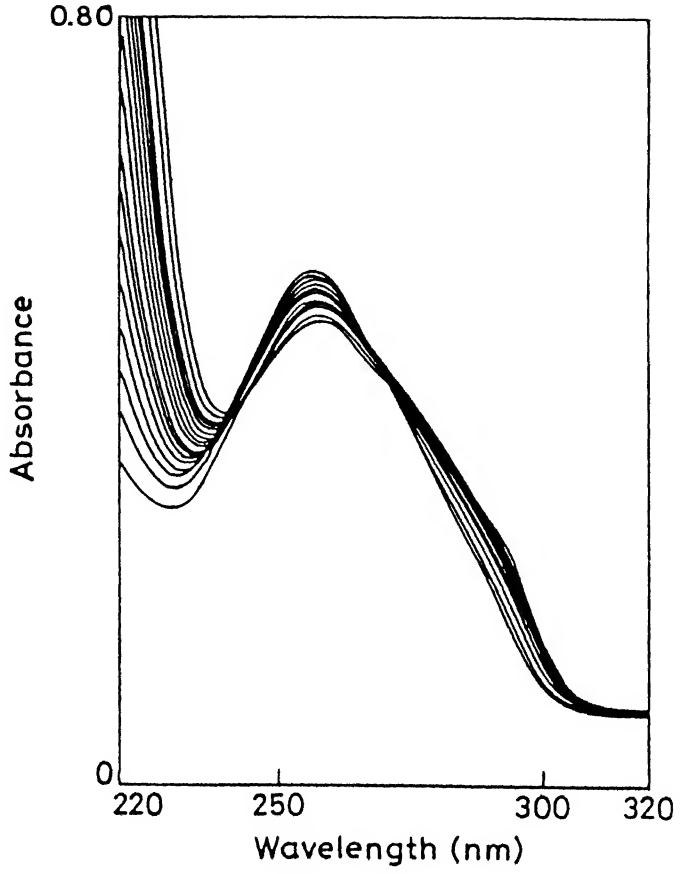

Figure C-5. UV profile of poly d(G-C) (DNA) titrated with $Zn(NO_3)_2$ in H_2O. Concentration of DNA : 38.5μM DNA (phosphates)

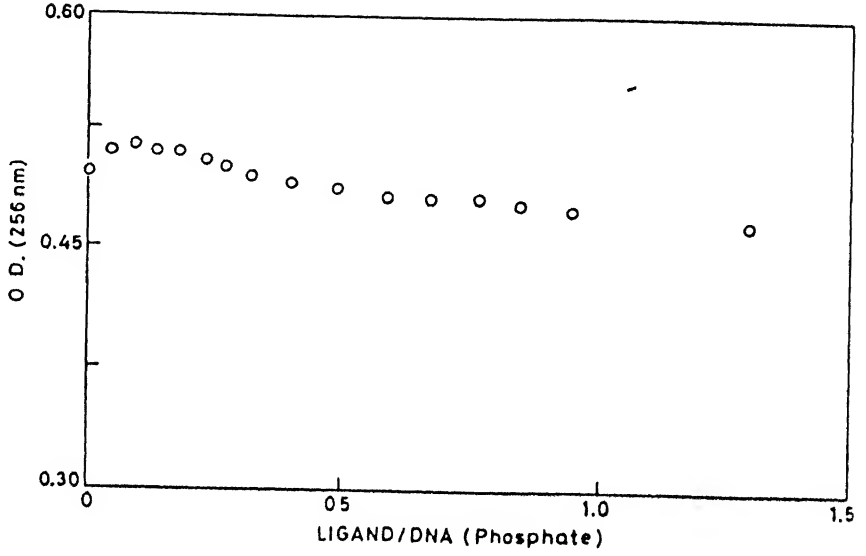

Plot of UV hypochromicity of poly d(G-C) (DNA) (at 256 nm) vs Ligand/DNA (phosphate) ; Ligand = $Zn(NO_3)_2$

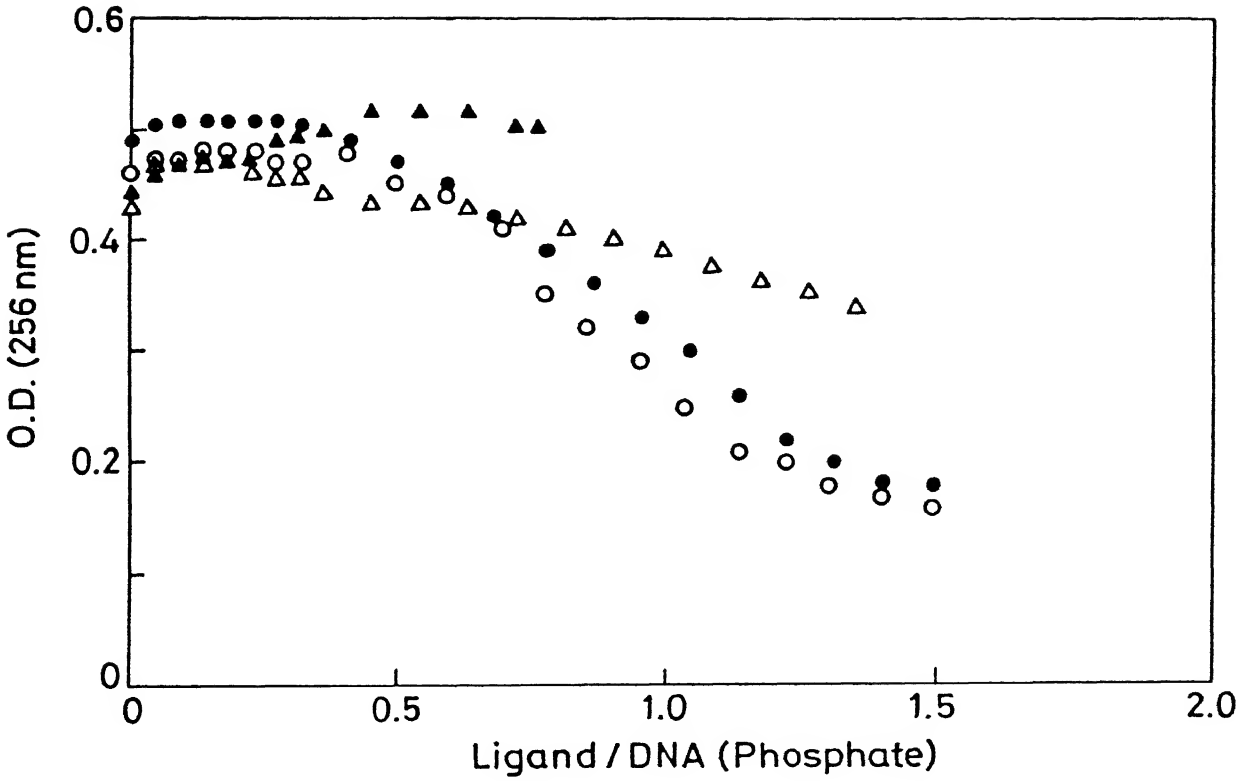

Figure C-7. Comparison plot of UV hypochromicity of poly d(G-C) (DNA) (at 256 nm) vs. Ligand/DNA (phosphate) ; Ligand : o = $(CH)_2Zn^{II}$ (52), (A) (Figure C-1); • = $(HC)_2Zn^{II}$ (53), (B) (Figure C-2); △= precursor peptide $(CH)_2$ (33) (Figure C-3); ▲ = precursor peptide $(HC)_2$ (34) (Figure C-4)

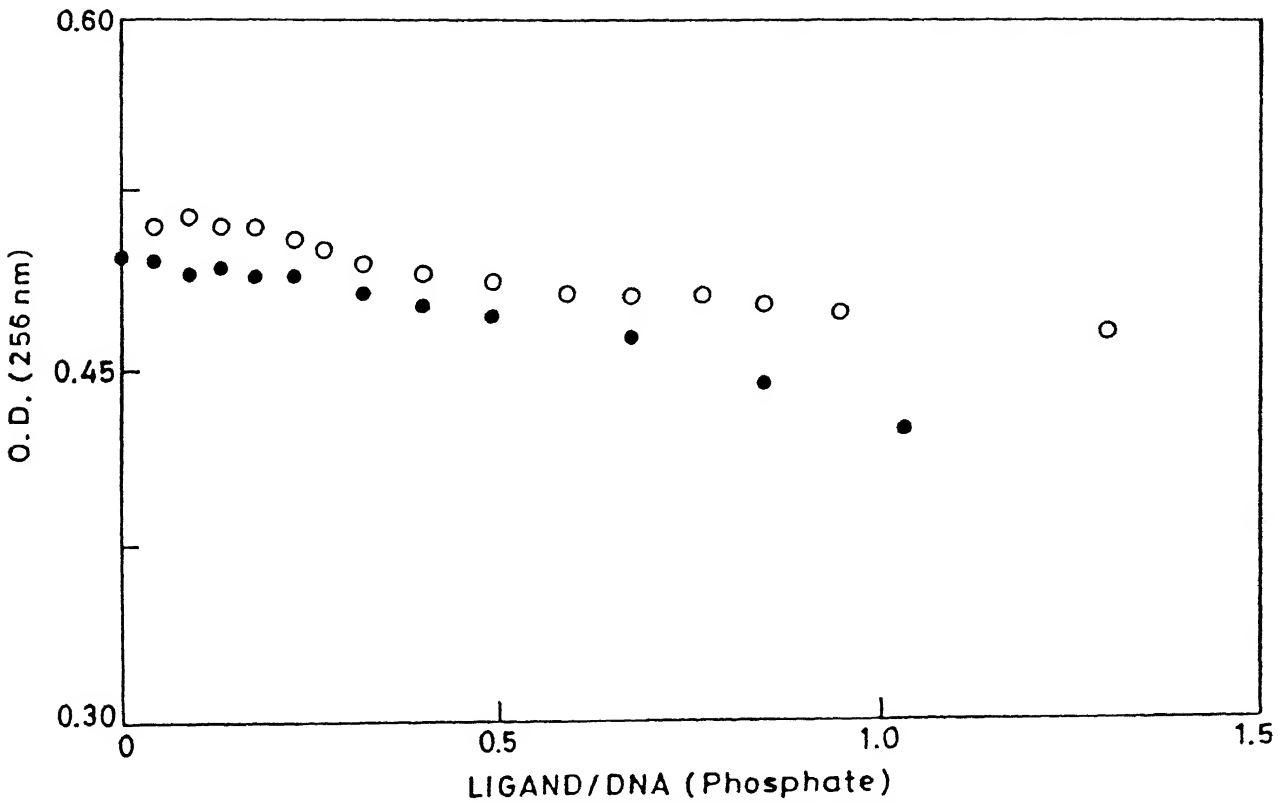

Figure C-8. Comparison plot of UV hypochromicity of poly d(G-C) (DNA) (at 256 nm) vs. Ligand/DNA (phosphate) ; Ligand : ● = $Zn(NO_3)_2$ (Figure C-5) ; O = $Zn(acac)_2$ (Figure C-6)

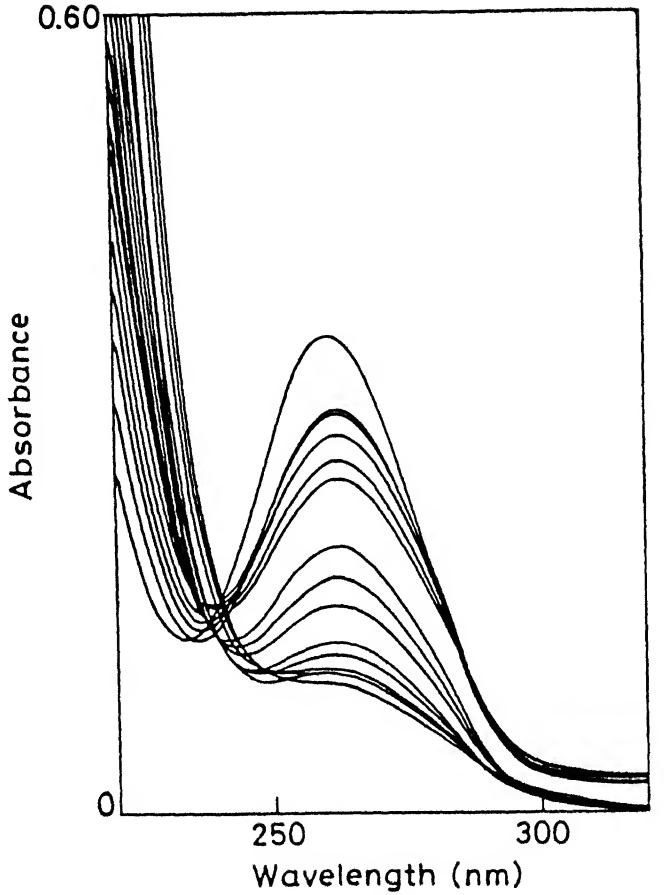

Figure C-9. UV profile of poly d(A-T) (DNA) titrated with (A) [A = $(CH)_2Zn^{II}$, (52)] in H_2O. Concentration of DNA : 54μM DNA (phosphates)

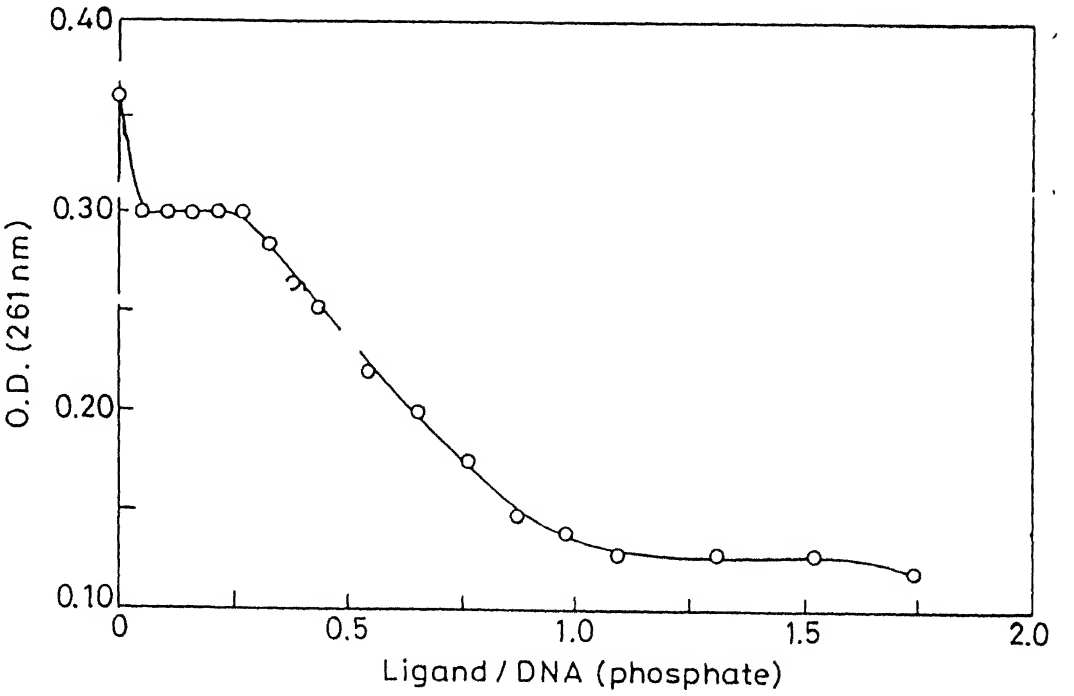

Plot of UV hypochromicity of poly d(A-T) (DNA) (at 261 nm) vs Ligand/DNA (phosphate) Ligand = (A)

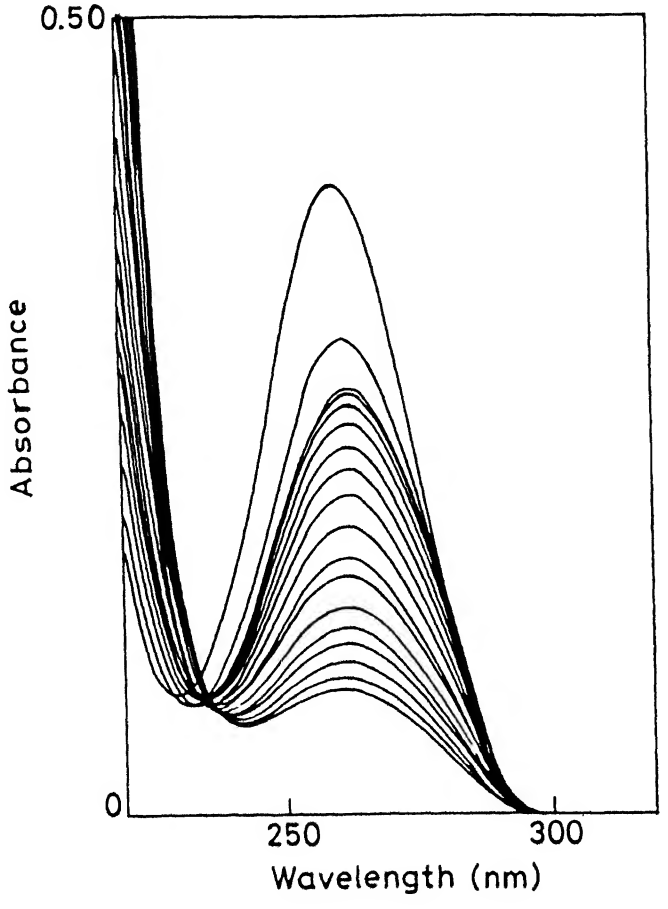

Figure C-10. UV profile of poly d(A-T) (DNA) titrated with (B) [B = $(HC)_2Zn^{II}$, (53)] in H_2O. Concentration of DNA : 63μM DNA (phosphates)

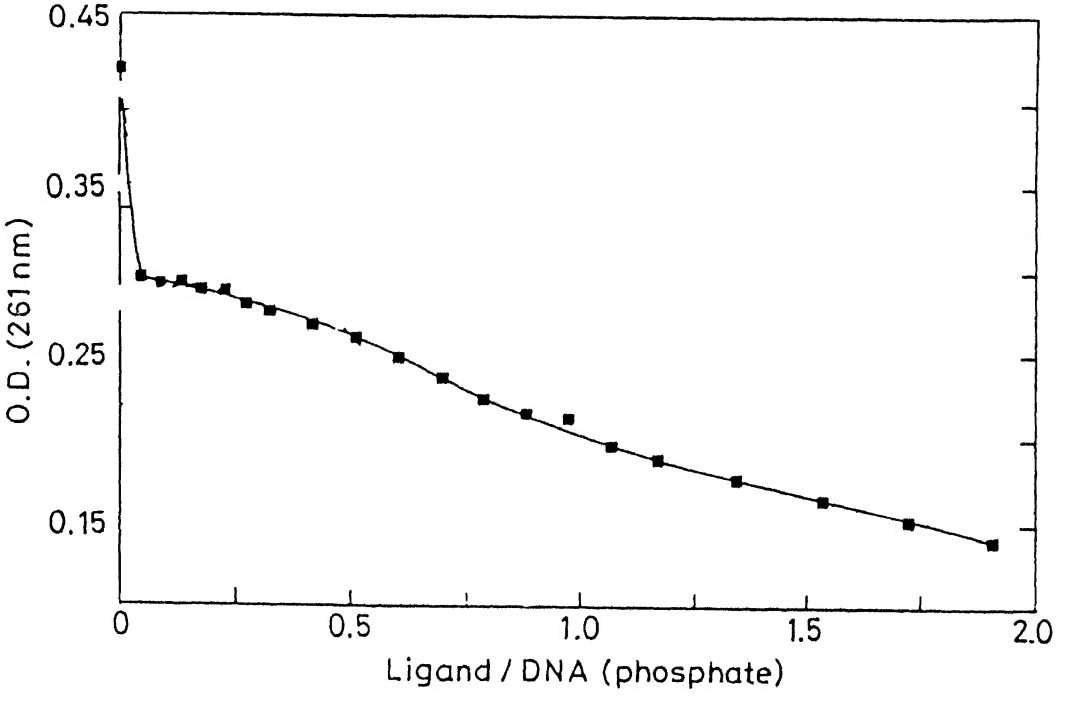

Plot of UV hypochromicity of poly d(A-T) (DNA) (at 261 nm) vs B/DNA (phosphate) Ligand = (B)

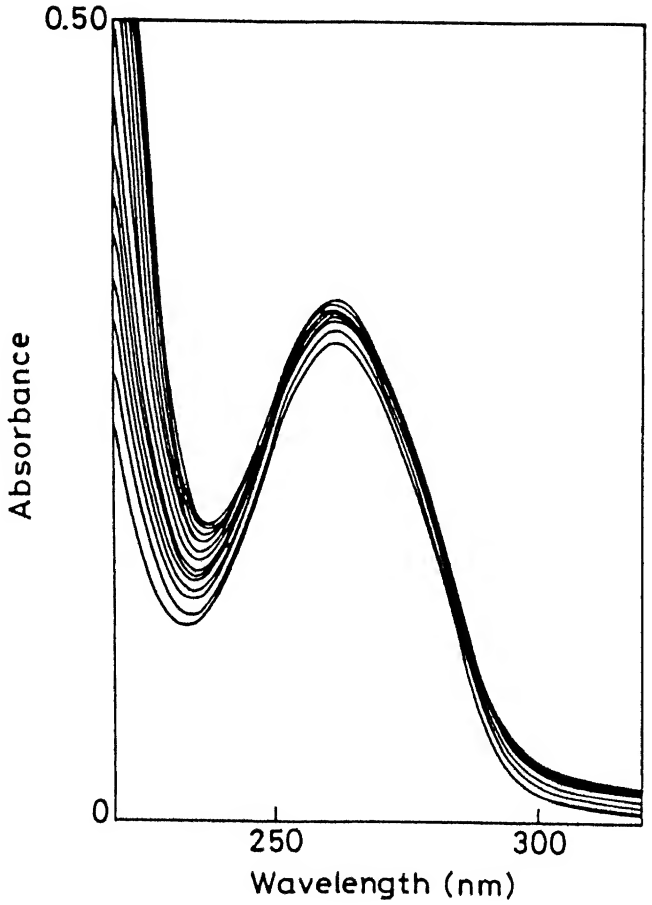

Figure C-11. UV profile of poly d(A-T) (DNA) titrated with precursor peptide $(CH)_2$, (33) in H_2O. Concentration of DNA : 46.5μM DNA (phosphates)

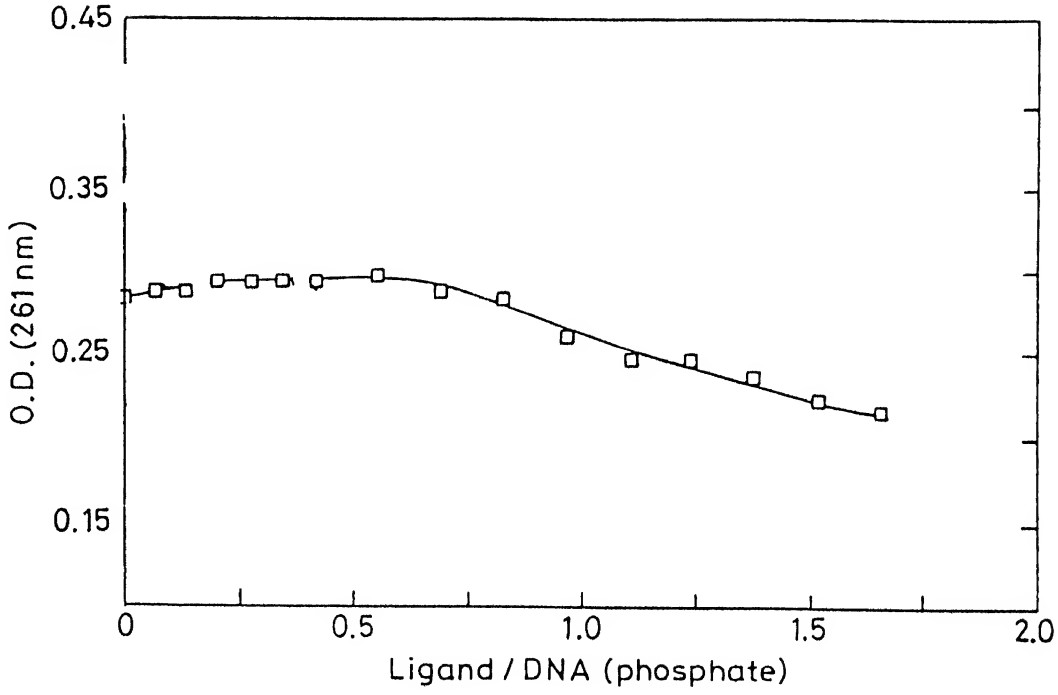

Plot of UV hypochromicity of poly d(A-T) (DNA) (at 256 nm) vs Ligand/DNA (phosphate) Ligand = $(CH)_2$ (33)

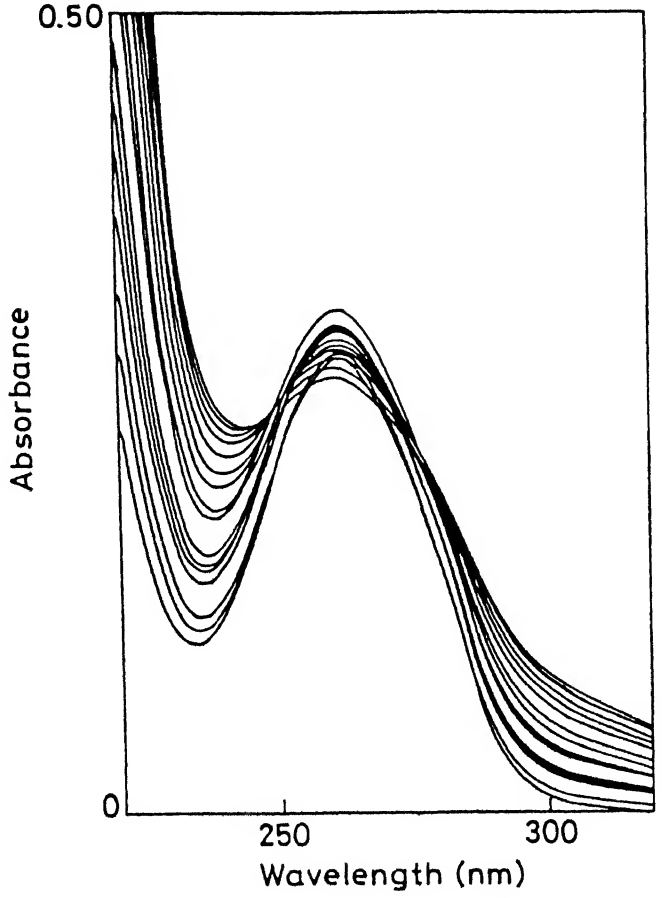

Figure C-12. UV profile of poly d(A-T) (DNA) titrated with precursor peptide $(HC)_2$, (34) in H_2O. Concentration of DNA : 42.5μM DNA (phosphates)

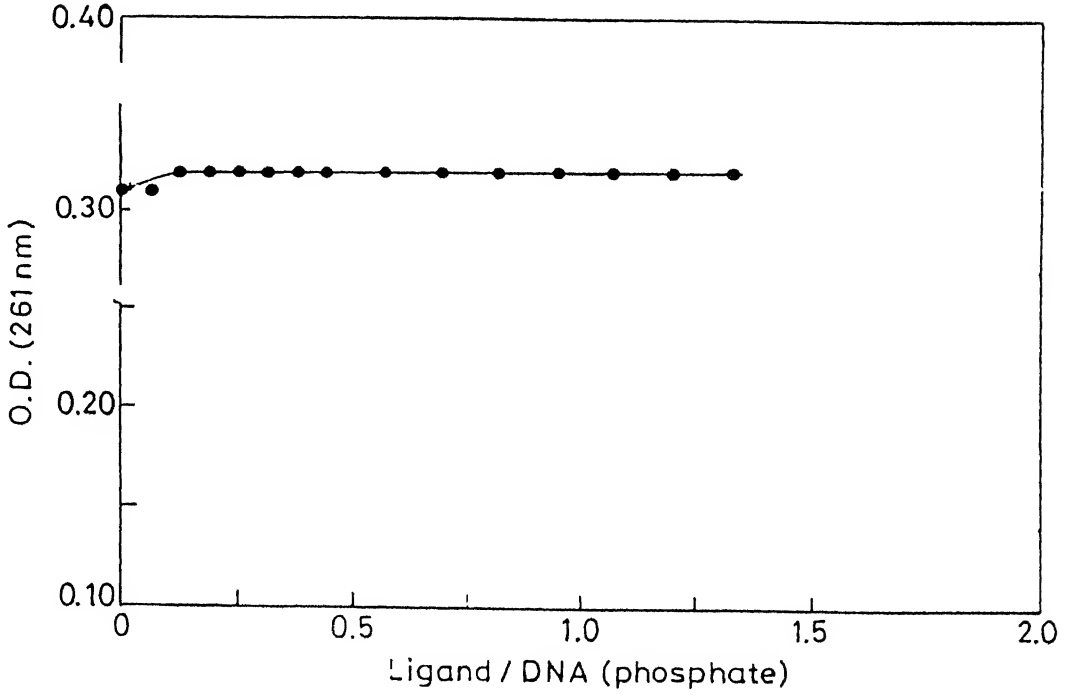

Plot of UV hypochromicity of poly d(A-T) (DNA) (at 256 nm) vs Ligand/DNA (phosphate) Ligand = $(HC)_2$ (34)

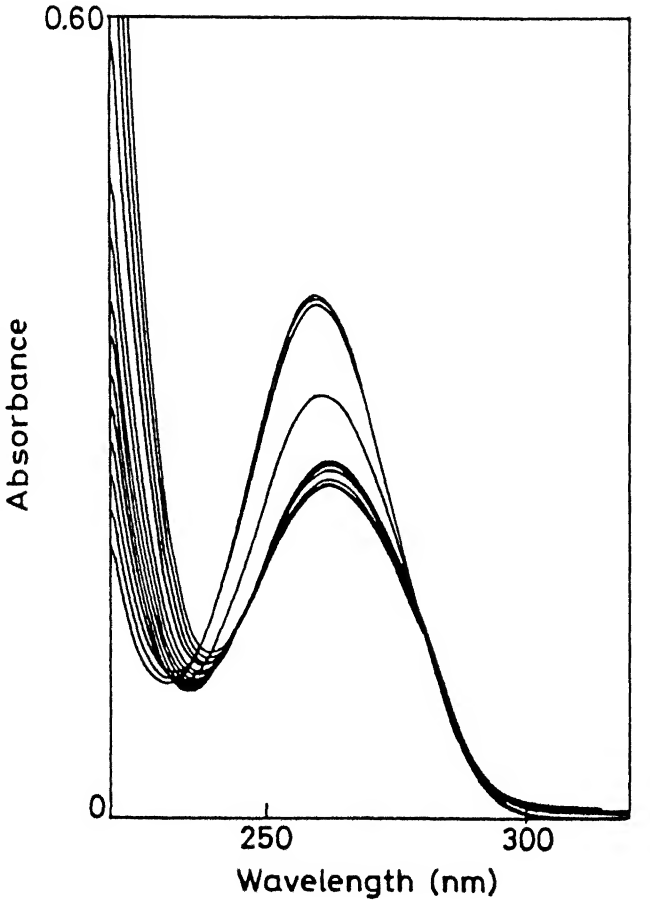

Figure C-13. UV profile of poly d(A-T) (DNA) titrated with $Zn(NO_3)_2$ in H_2O . Concentration of DNA : 63μM DNA (phosphates)

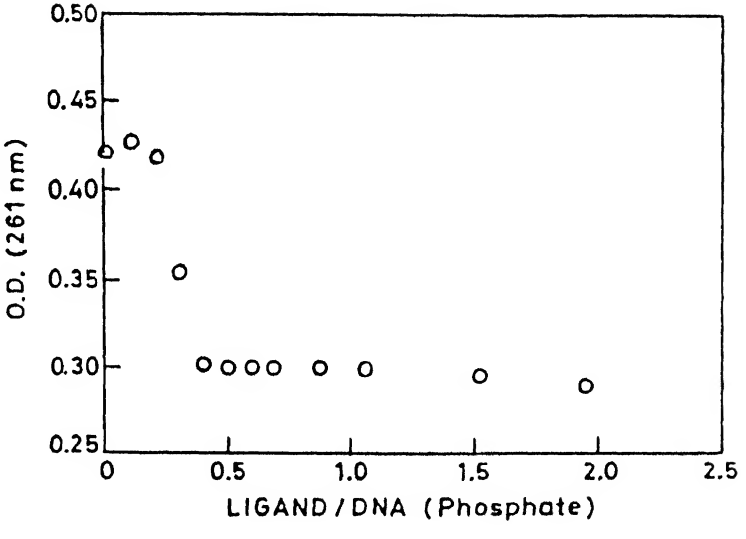

Plot of UV hypochromicity of poly d(A-T) (DNA) (at 256 nm) vs Ligand/DNA (phosphate) ; Ligand = $Zn(NO_3)_2$

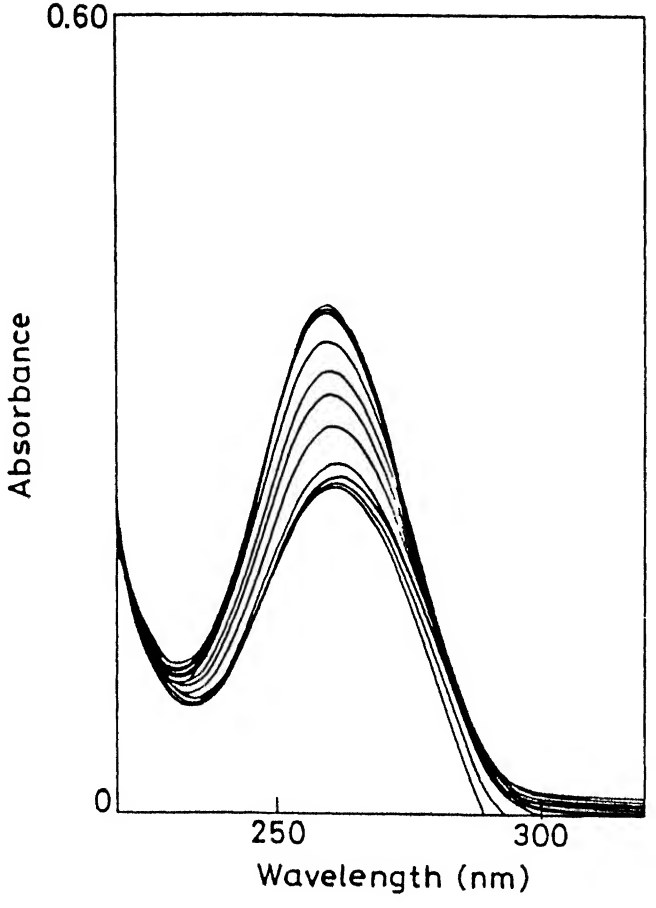

Figure C-14. UV profile of poly d(A-T) (DNA) titrated with $Zn(acac)_2$ in H_2O . Concentration of DNA : 62.5μM DNA (phosphates)

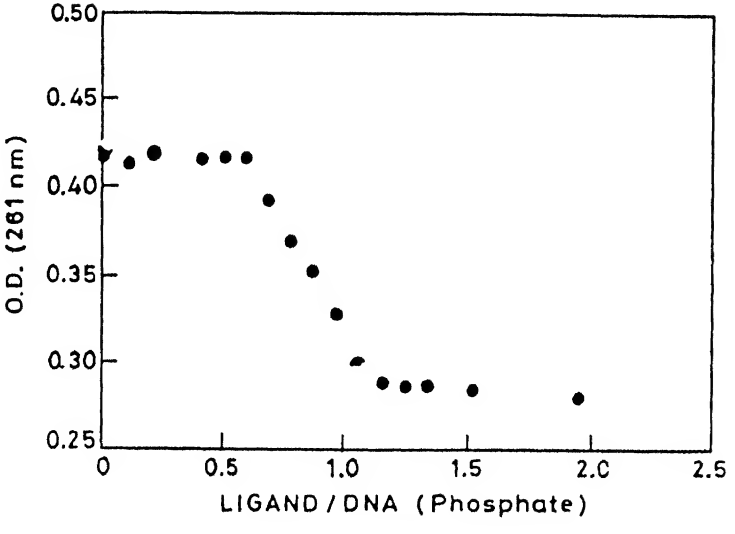

Plot of UV hypochromicity of poly d(A-T (DNA) (at 256 nm) vs Ligand/DNA (phosphate) : Ligand = $Zn(acac)_2$

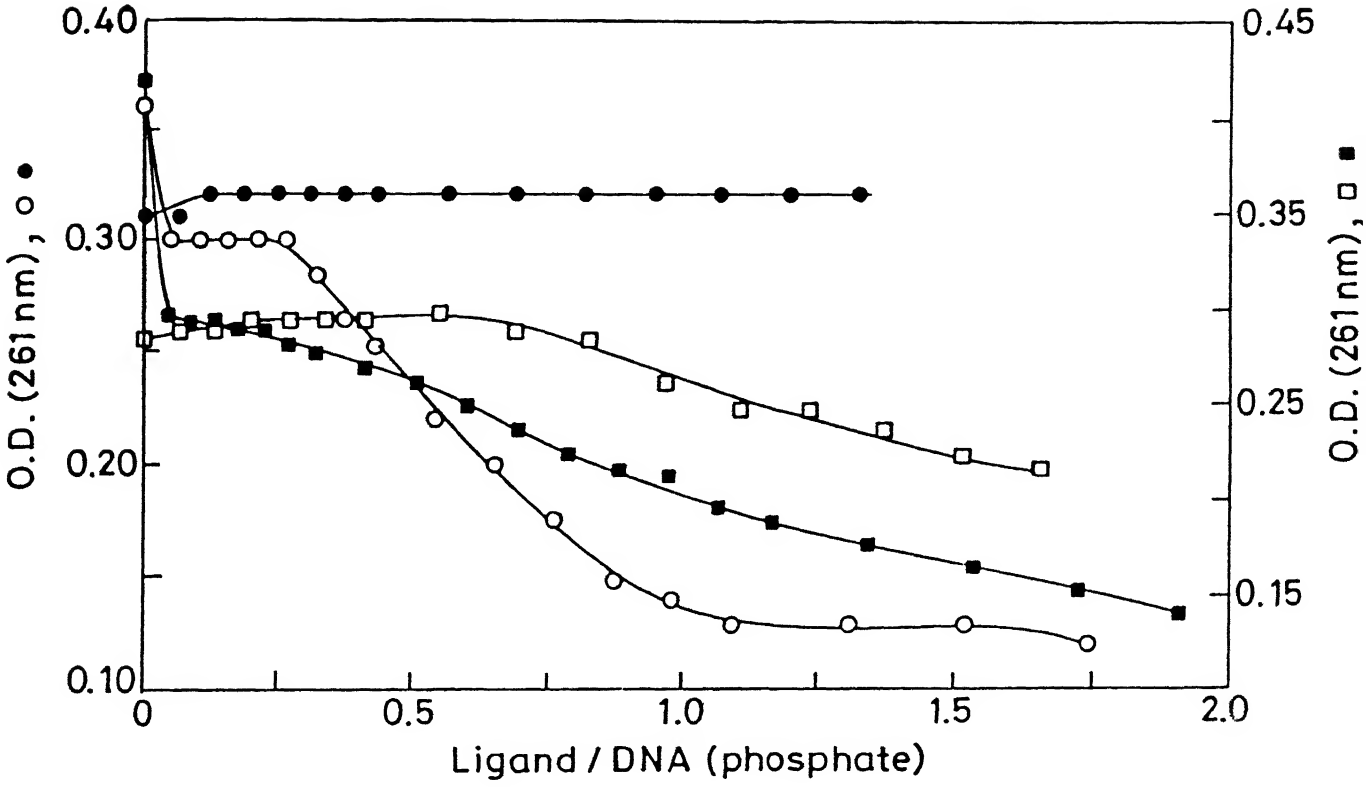

Figure C-15. Comparison plot of UV hypochromicity of poly d(A-T) (DNA) (at 261 nm) vs. Ligand/DNA (phosphate) ; Ligand : a = $(CH)_2Zn^{II}$ (52), (A) (Figure C-9); b = $(HC)_2Zn^{II}$ (53), (B) (Figure C-10); c = precursor peptide $(CH)_2$ (33) (Figure C-11); d = precusor peptide $(HC)_2$ (34) (Figure C-12)

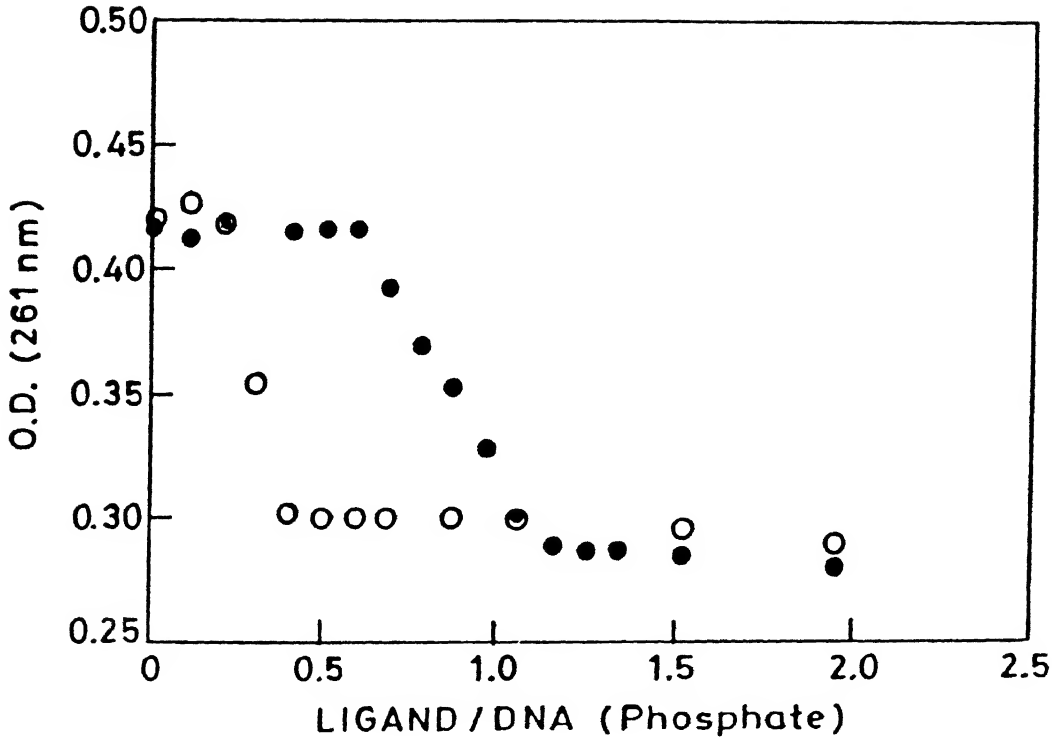

Figure C-16. Comparison plot of hypochromicity of poly d(A-T) (DNA) at O.D (261 nm) vs. Ligand/DNA (phosphate) ; Ligand : o = $Zn(NO_3)_2$ (Figure C-13) ; • = $Zn(acac)_2$ (Figure C-14)

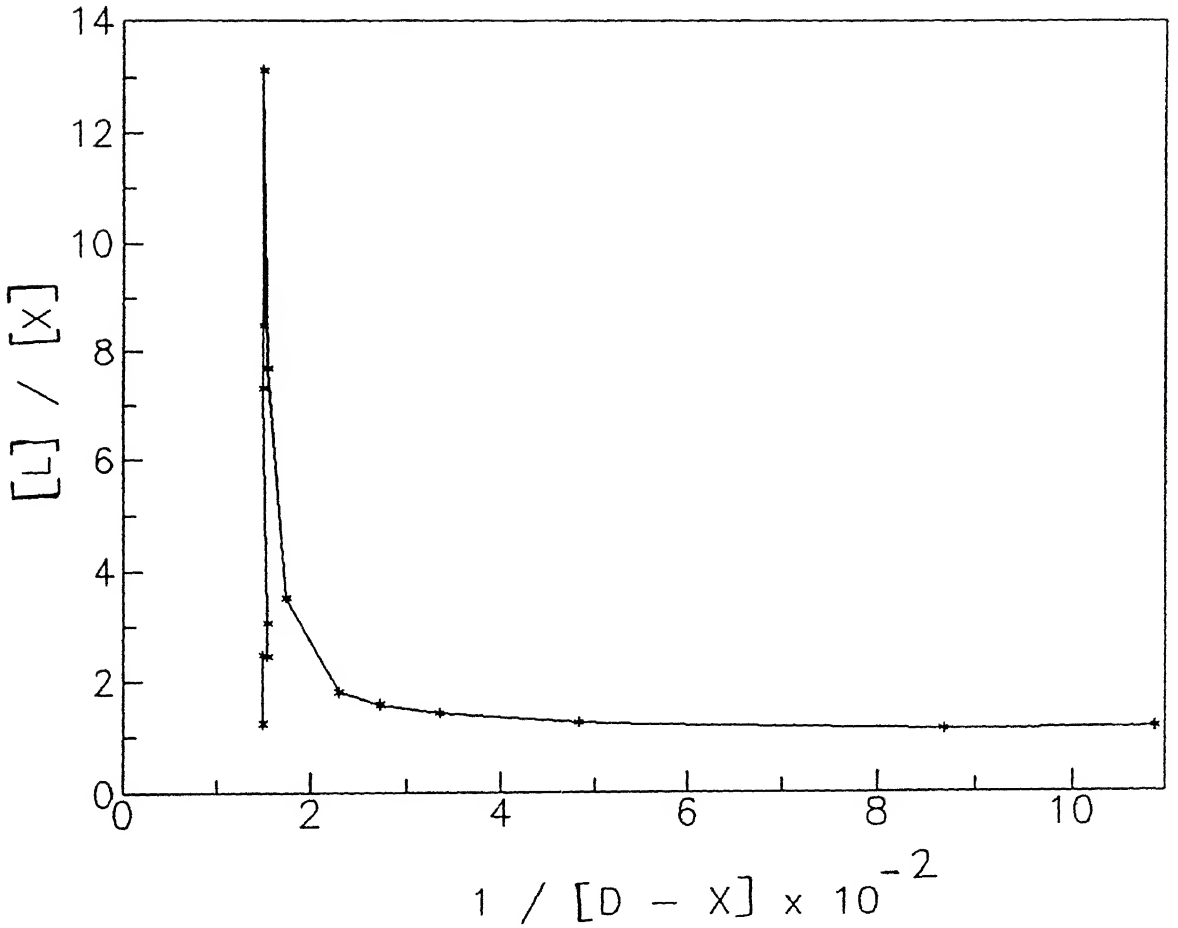

Figure C-17. Scatchard plot from UV hypochromicity profile of interaction between poly d(G-C) and $(CH)_2Zn^{II}$ (A) (52)

Association Constant Calculation (Scatchard Analysis):

For the equilibrium reaction

$$L + D \rightleftharpoons \text{LD}$$

with n number of binding sites on D,

$$K_d = \frac{[L - nX][D - X]}{[X]} \ldots\ldots \Longrightarrow \ldots\ldots \frac{[L]}{[X]} = K_d[D - X] + n$$

where K_d : dissociation constant; [L] : concentration of the Ligand [$(CH)_2Zn^{II}$ (52, (A)); [D] : concentration of the DNA (poly d(G-C)); [X] : concentration of the bound DNA ; [D-X] : concentration of the free DNA and n : number of binding sites on DNA. The concentration of the bound DNA was obtained from its hypochromicity profile, keeping the initial absorbance corresponding to that of totally free DNA concentration and the final absorbance corresponding to that of totally bound DNA concentration. The final addition of ligand to DNA corresponded to a [L]/[D] ratio of $\sim$ 1.2. The DNA [poly d(G-C)] concentration used in this study was 69 μM. The following table gives the details of the calculation.

A plot was derived from the above data (Figure C-17). Evidently, the plot shows quite different affinities, identifying weaker and stronger binding sites. The weaker binding site corresponds to the initial portion of the curve. The calculated values (from the intercept) for n is $\sim$ 14 and the corresponding association constant (K_a) is 3.30 x 10^3 M^{-1}, whereas the final composite portion denotes strong binding with n $\sim$ 2 and K_a 1.786 x 10^7 M^{-1}.

S.No.	[L]	$\frac{1}{[D-X]}$ x 10^{-2}	[X]	$\frac{[L]}{[X]}$
1.	0	1.45	0	-
2.	2.86	1.50	2.30	1.24
3.	5.70	1.50	2.30	2.48
4.	11.29	1.55	4.60	2.45
5.	14.06	1.55	4.60	3.06
6.	16.81	1.50	2.30	7.31
7.	19.52	1.50	2.30	8.49
8.	30.18	1.50	2.30	13.12
9.	35.38	1.55	4.60	7.69
10.	40.5	1.74	11.52	3.52
11.	45.54	2.29	25.32	1.80
12.	50.49	2.72	32.32	1.57
13.	55.37	3.35	39.12	1.42
14.	60.17	4.83	48.30	1.25
15.	64.90	8.68	57.48	1.13
16.	69.56	10.89	59.82	1.16
17.	74.17	21.65	64.38	1.15
18.	78.66	43.86	66.72	1.18

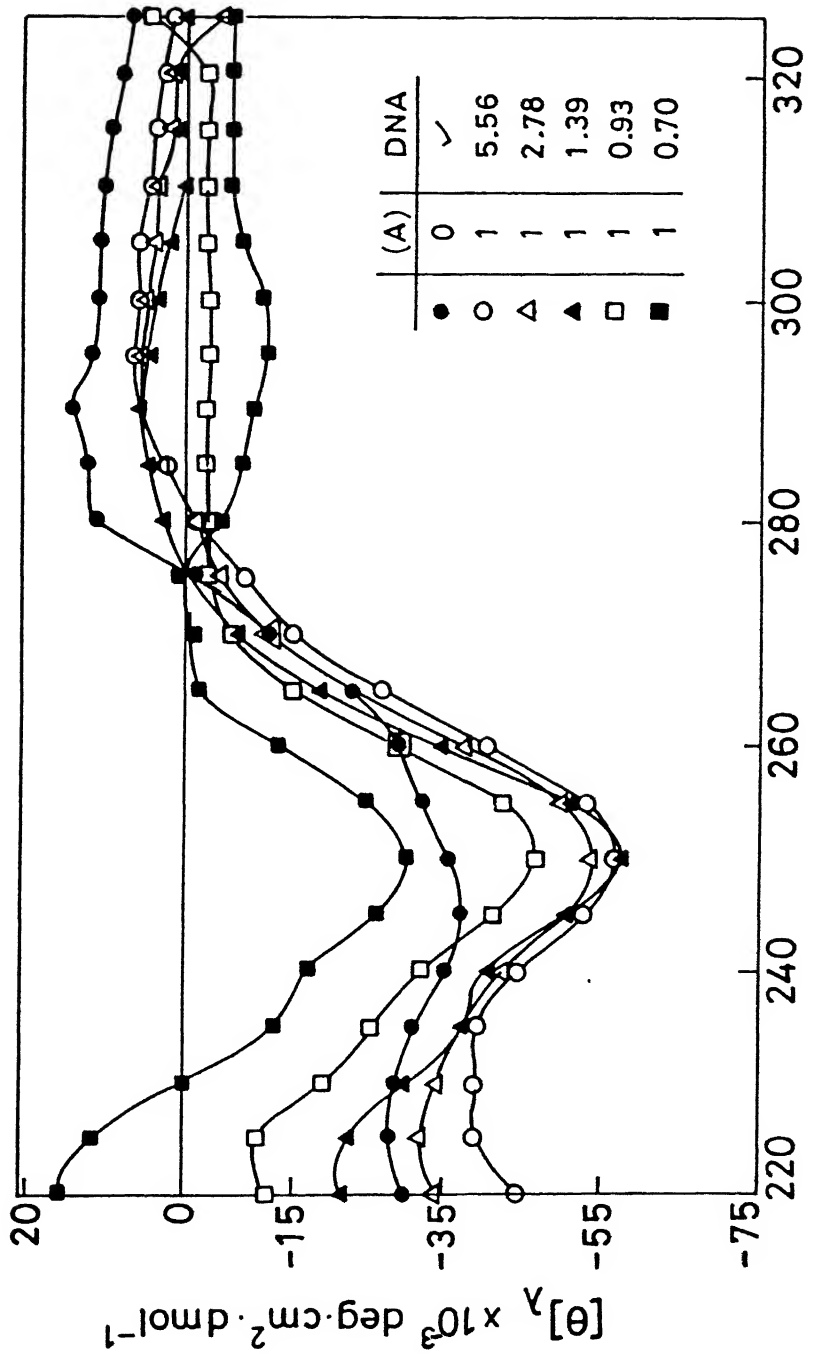

Figure C-18. CD spectra of poly d(G-C) (DNA) titrated with (52) [$(CH)_2Zn^{II}$, (A)] in H_2O. Concentration of DNA : ~ 38μM DNA (phosphates); Inset : Molar ratio of DNA (phosphates) per (A)

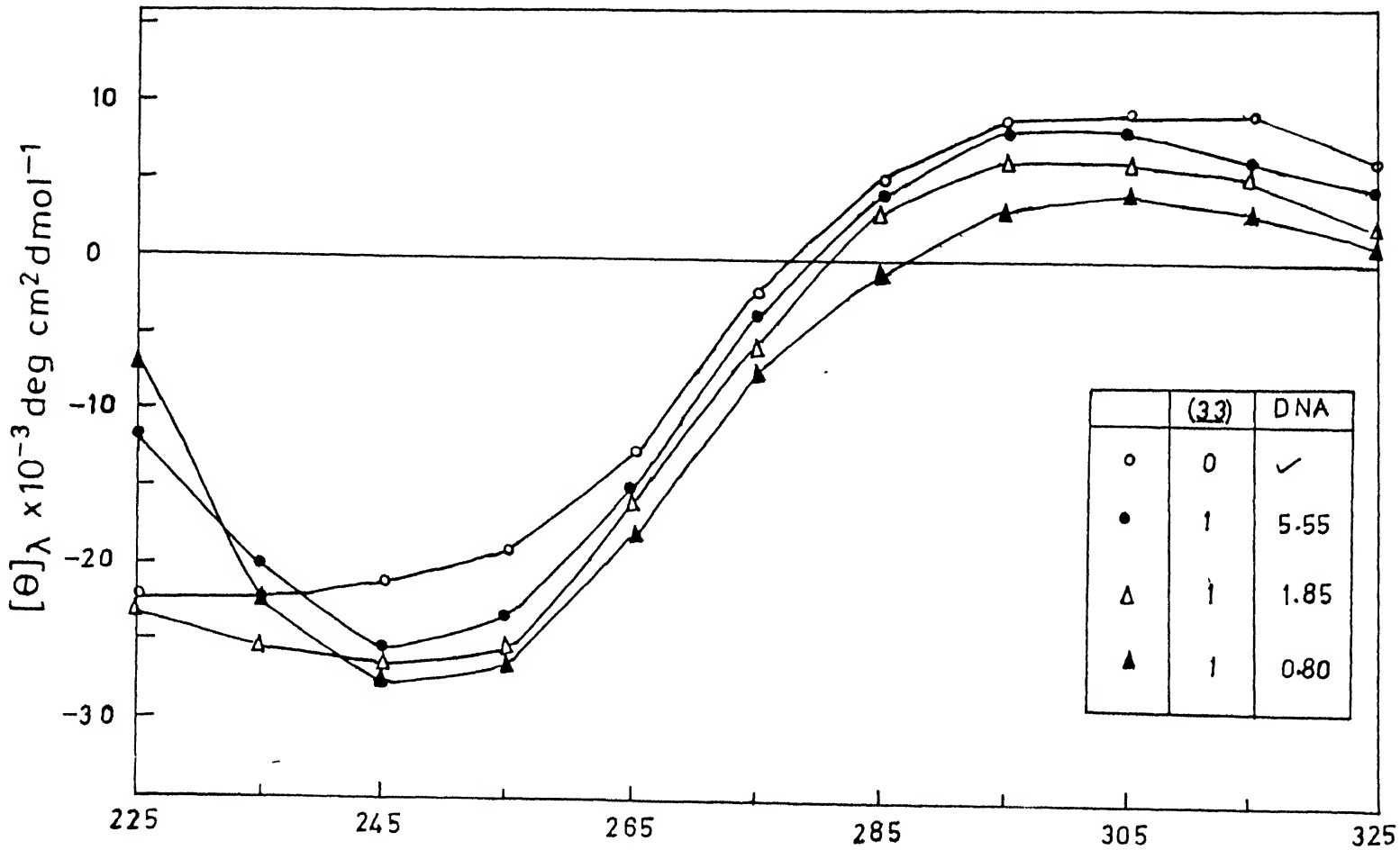

Figure C-19. CD spectra of poly d(G-C) (DNA) titrated with (33) [$(CH)_2$] in H_2O. Concentration of DNA : $\sim 38\mu$M DNA (phosphates); Inset : Molar ratio of DNA (phosphates) per (33)

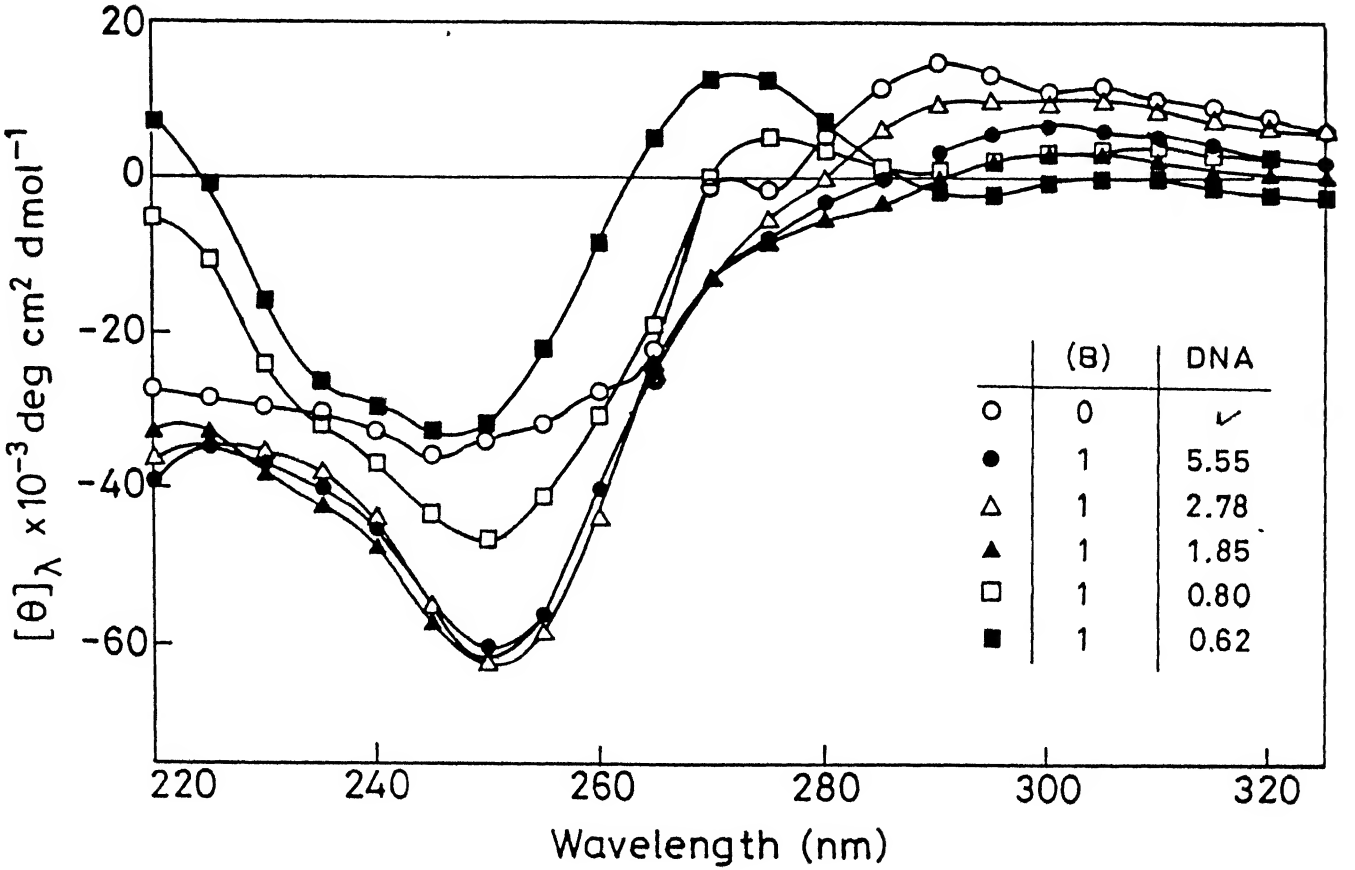

Figure C-20. CD spectra of poly d(G-C) (DNA) titrated with (53) [$(HC)_2Zn^{II}$, (B)] in H_2O. Concentration of DNA : $\sim 38\mu$M DNA (phosphates); Inset : Molar ratio of DNA (phosphates) per (B)

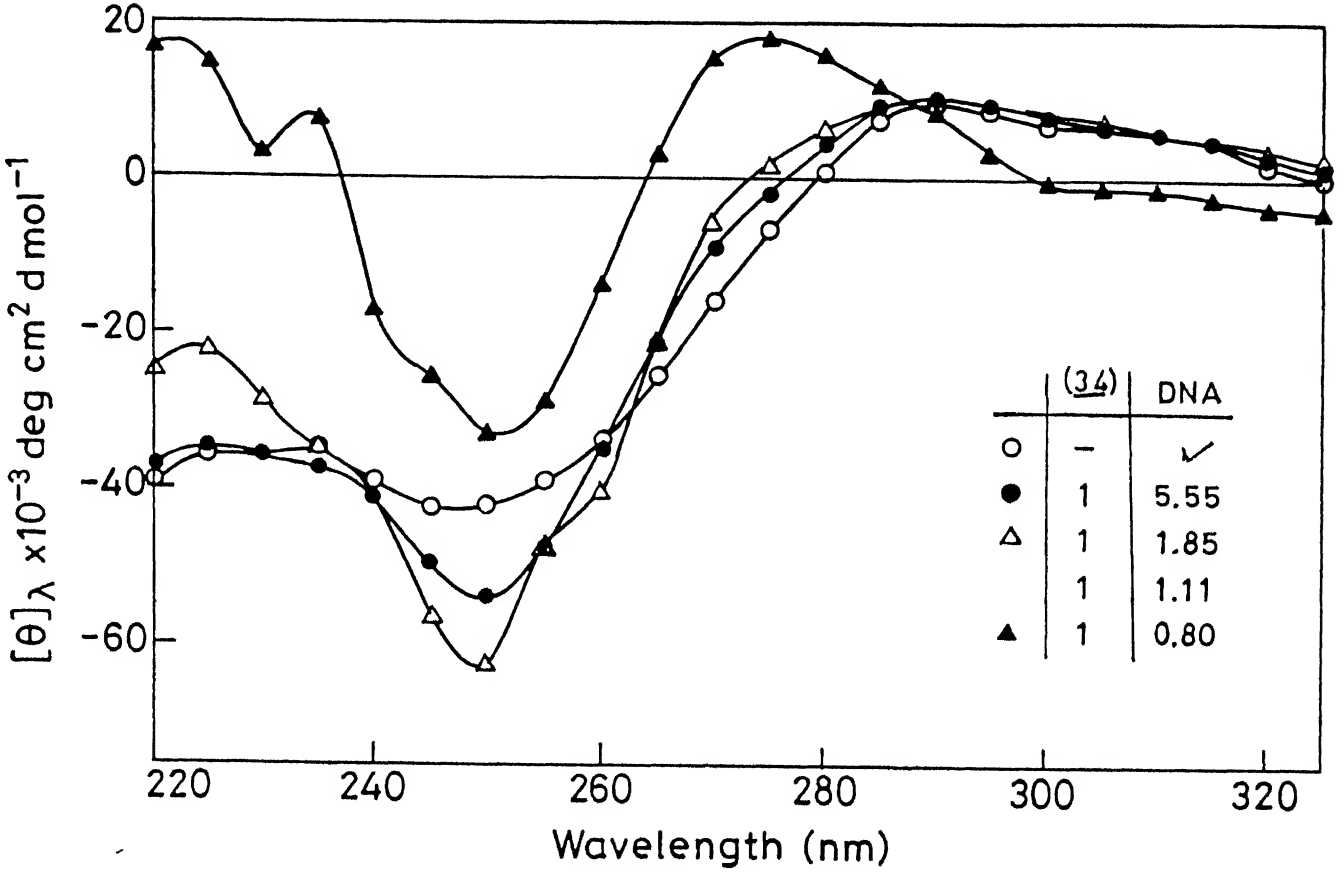

Figure C-21. CD spectra of poly d(G-C) (DNA) titrated with (34) [$(HC)_2$] in H_2O. Concentration of DNA : ~ 38μM DNA (phosphates); Inset : Molar ratio of DNA (phosphates) per (34)

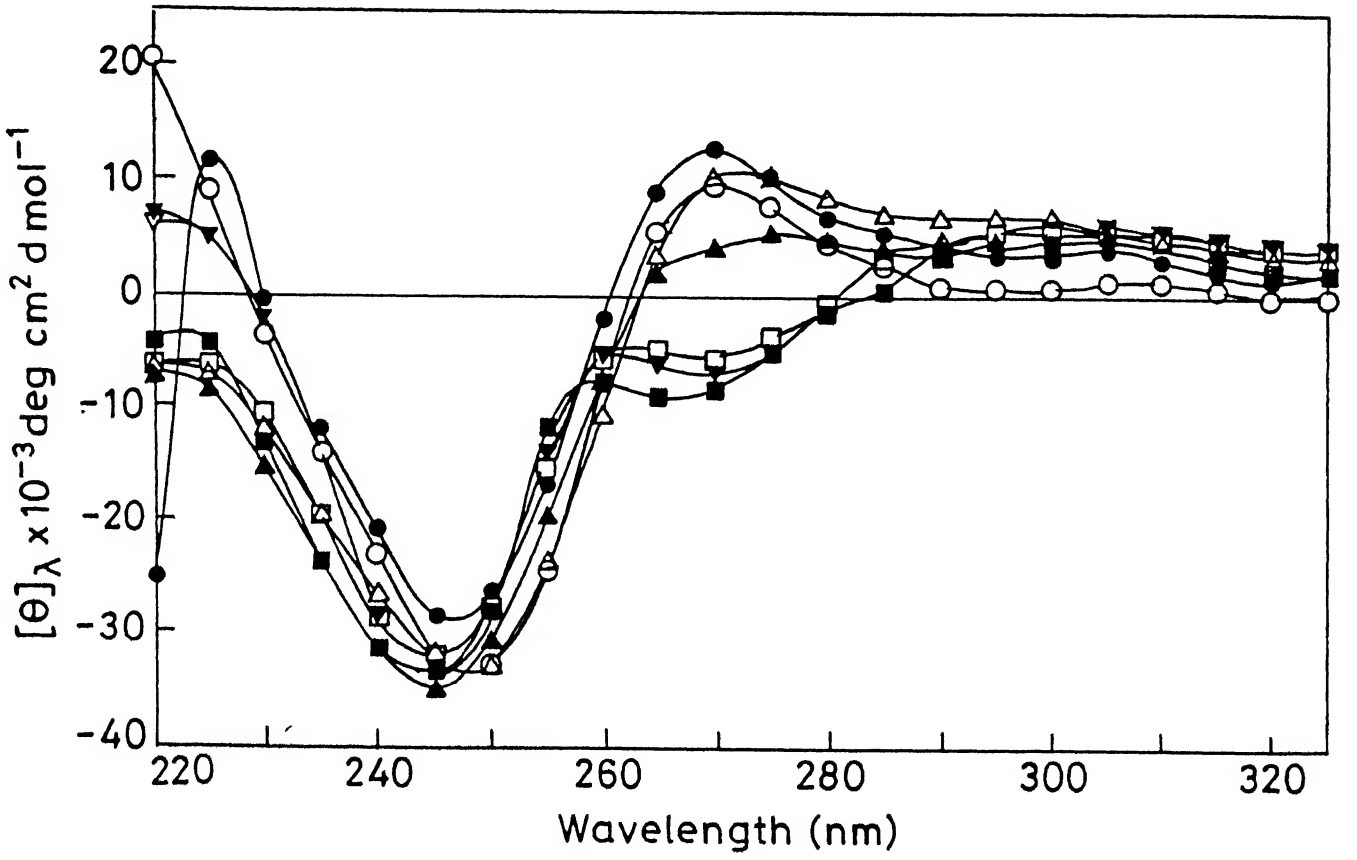

Figure C-22. CD spectra of poly d(A-T) (DNA) titrated with (52) [$(CH)_2Zn^{II}$, (A)] in H_2O. Concentration of DNA : $\sim 57\mu$M DNA (phosphates): Inset : Molar ratio of DNA (phosphates) per (A)

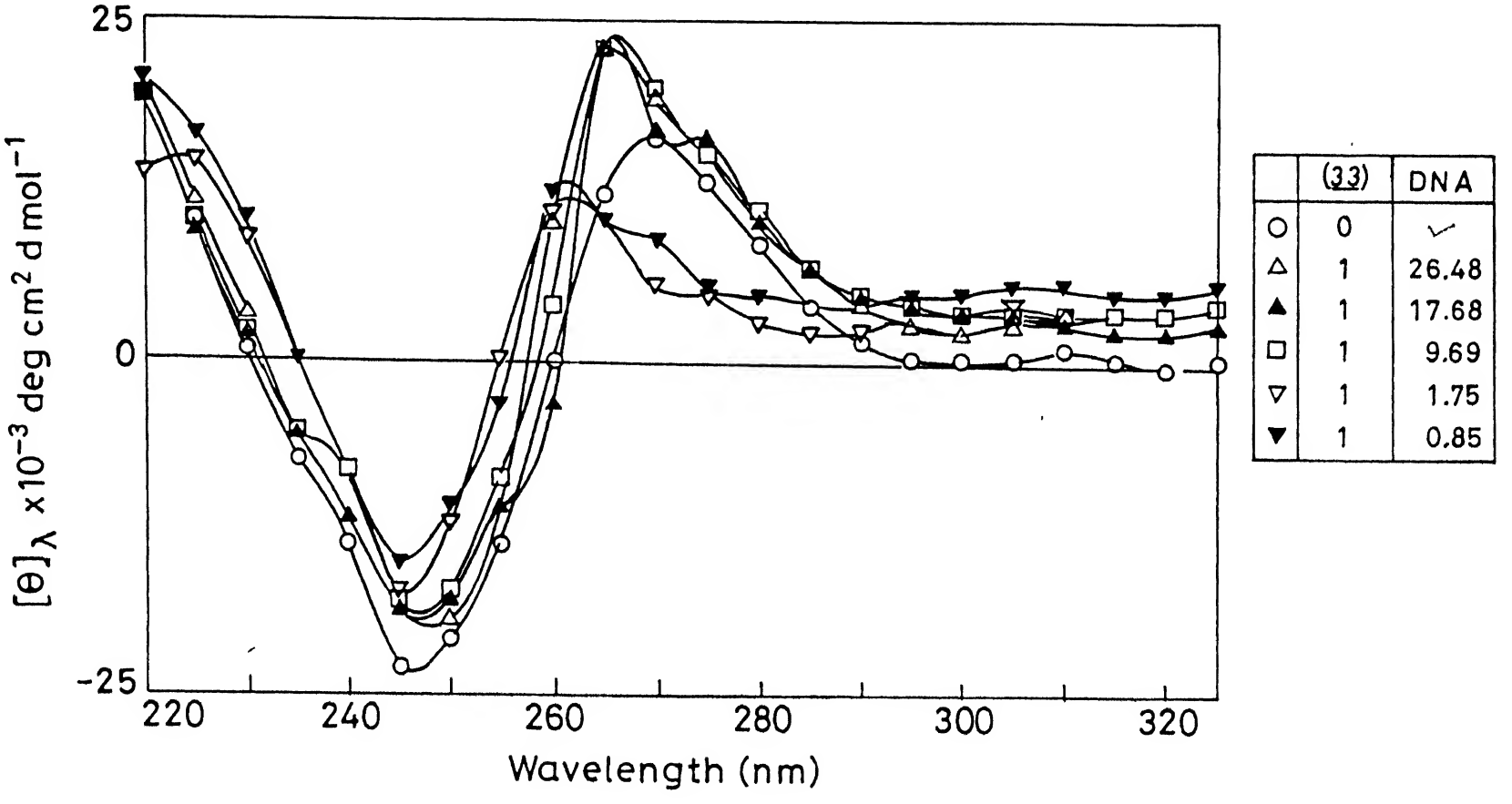

Figure C-23. CD spectra of poly d(A-T) (DNA) titrated with (33) [$(CH)_2$] in H_2O. Concentration of DNA : $\sim 57\mu$M DNA (phosphates); Inset : Molar ratio of DNA (phosphates) per (33)

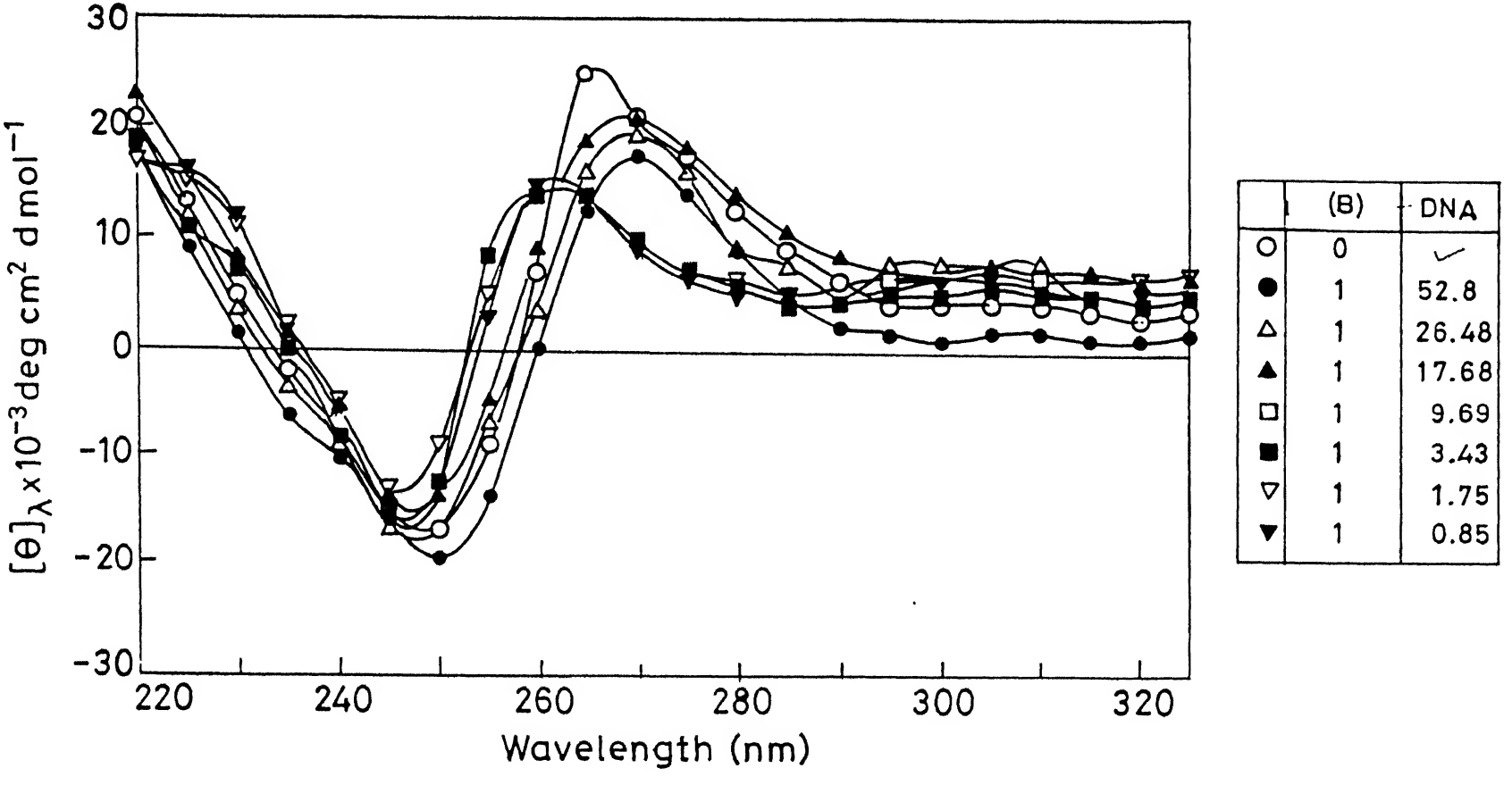

Figure C-24. CD spectra of poly d(A-T) (DNA) titrated with (53) [$(HC)_2Zn^{II}$, (B)] in H_2O. Concentration of DNA : $\sim 57\mu$M DNA (phosphates); Inset : Molar ratio of DNA (phosphates) per (B)

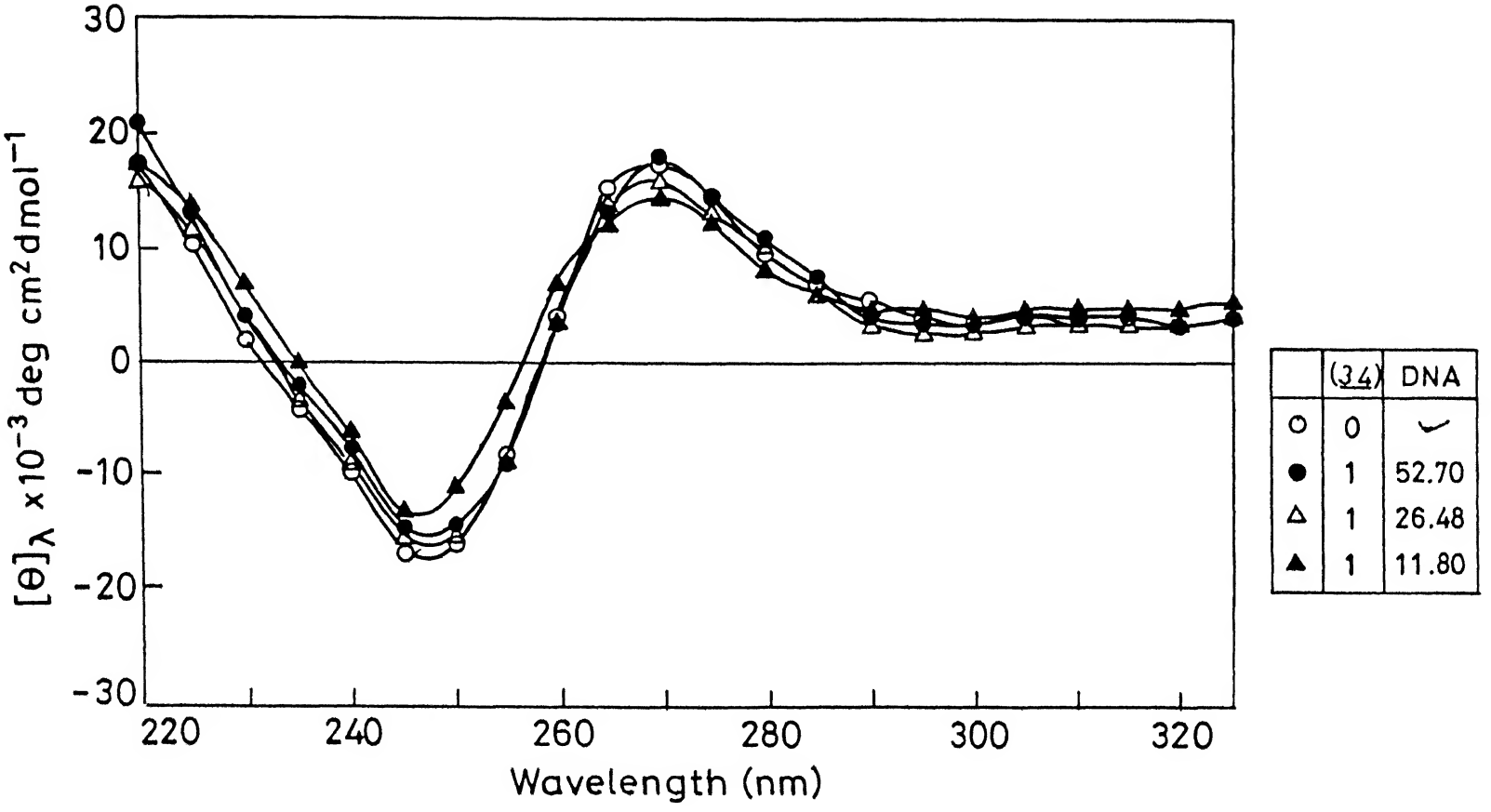

Figure C-25. CD spectra of poly d(A-T) (DNA) titrated with (34) [$(HC)_2$] in H_2O. Concentration of DNA : $\sim$ 57μM DNA (phosphates); Inset : Molar ratio of DNA (phosphates) per (34)

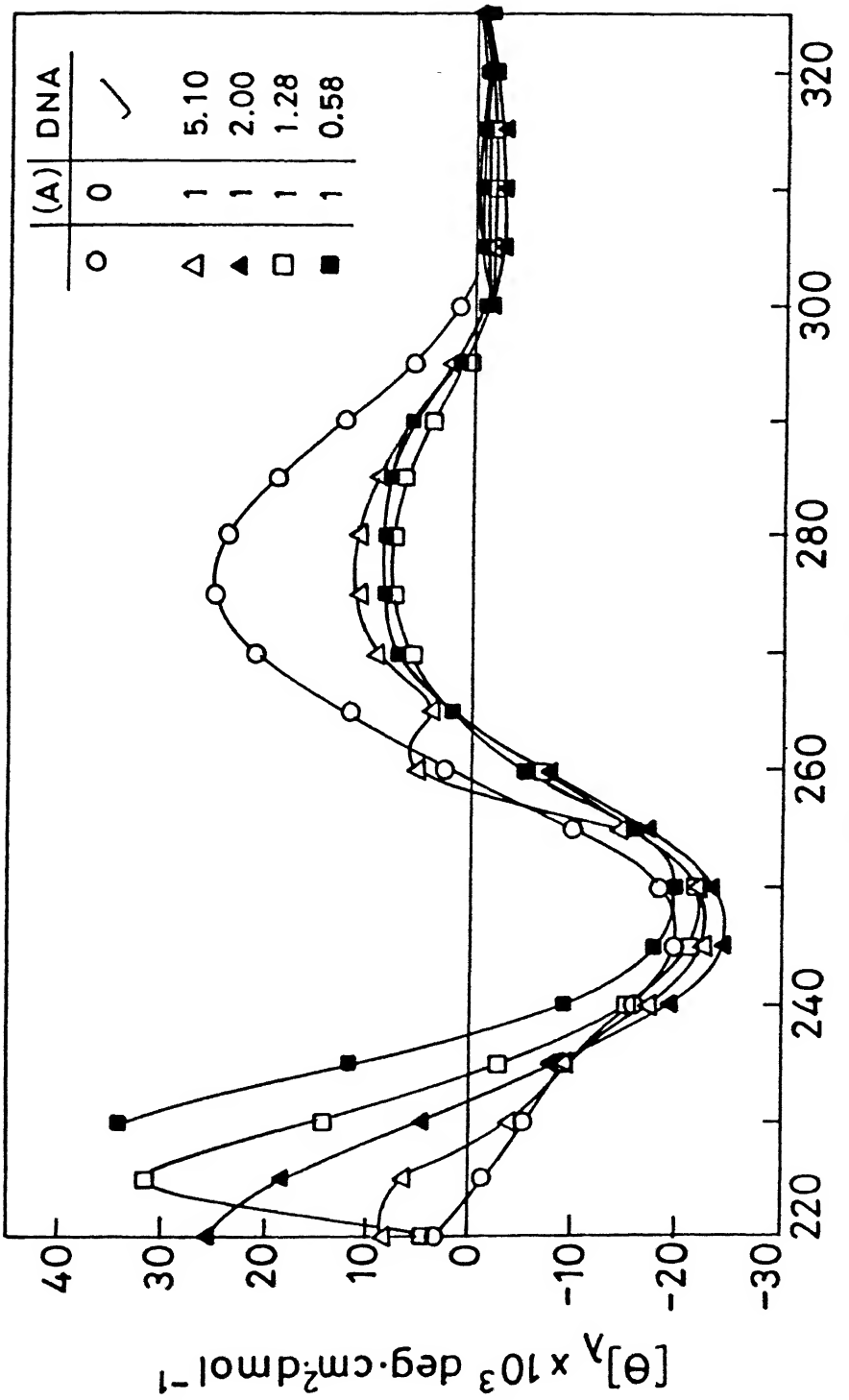

Figure C-26. CD spectra of synthetic oligonucleotide (oligo 1) (DNA) titrated with (52) $[(CH)_2Zn^{II}, (A_i)]$. Concentration of DNA : ~ 60μM DNA (phosphates); Inset : Molar ratio of DNA (phosphates) per (A)

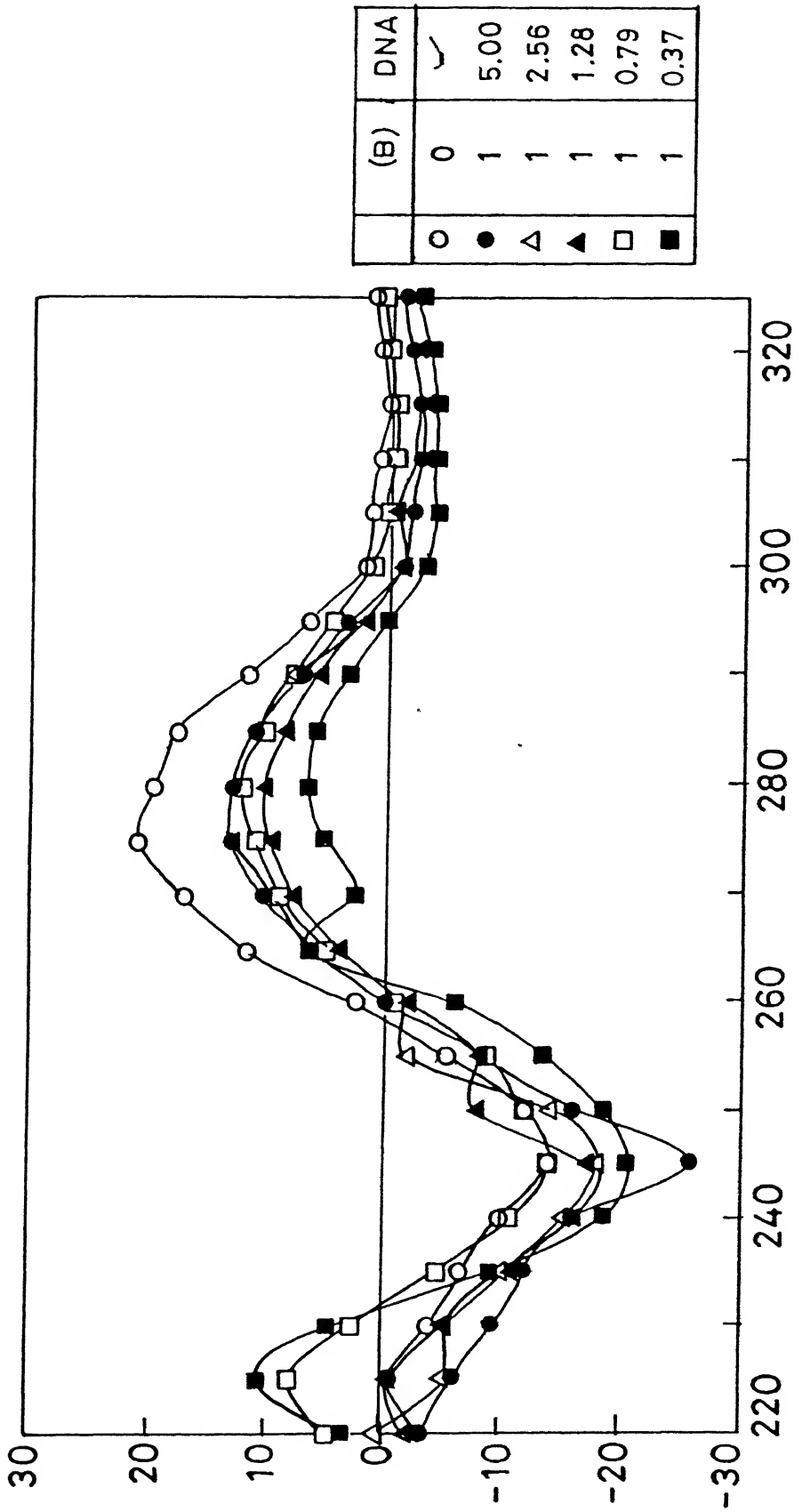

Figure C-27. CD spectra of synthetic oligonucleotide (oligo 1) (DNA) titrated with (53) [$(HC)_2Zn^{II}$, (B)]. Concentration of DNA : ~ 60μM DNA (phosphates); Inset : Molar ratio of DNA (phosphates) per (B)

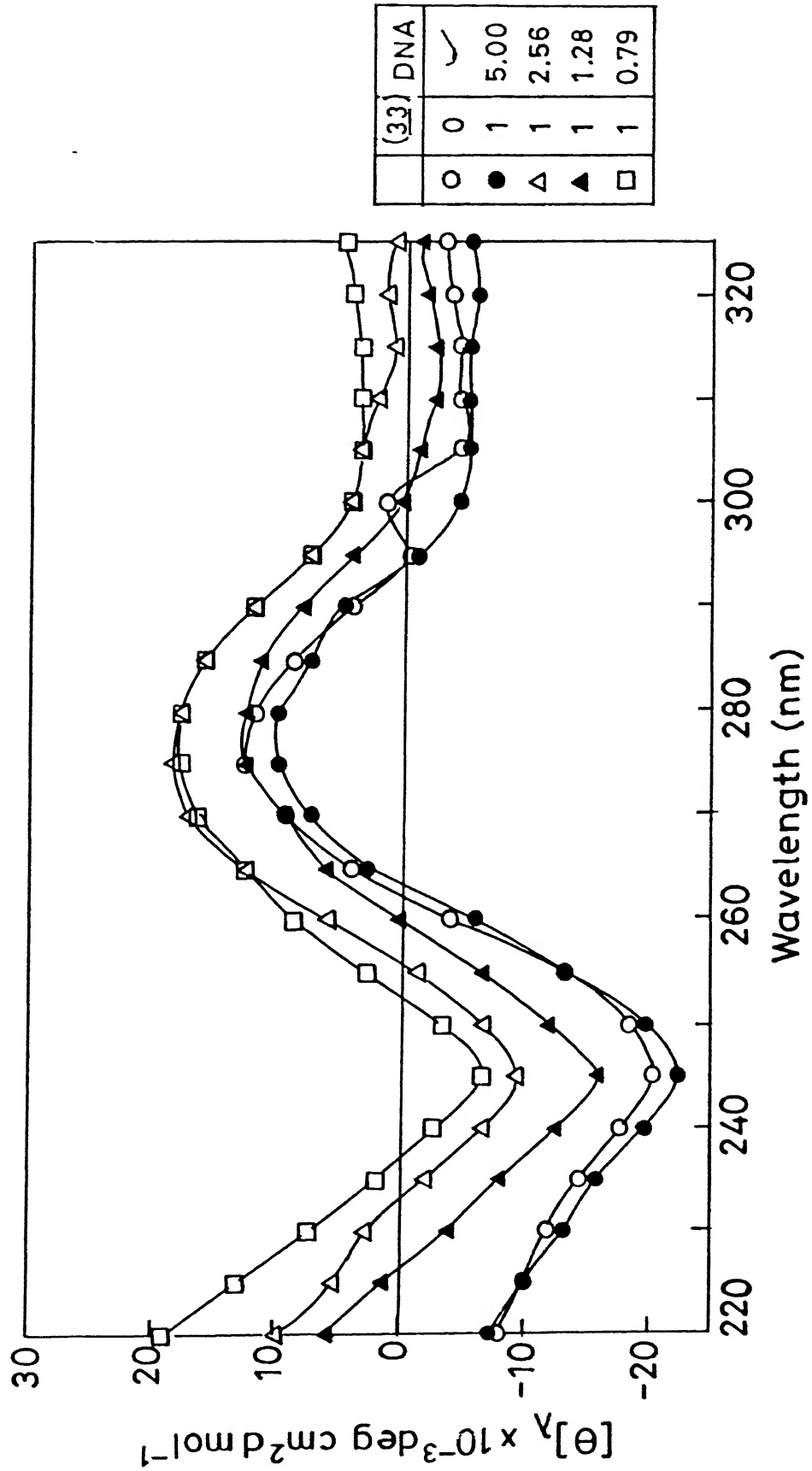

Figure C-28. CD spectra of synthetic oligonucleotide (DNA) titrated with (33) $[(CH)_2]$ in H_2O at Concentration of DNA : ~ 60μM DNA (phosphates); Inset : Molar ratio of DNA (phosphates) per (33)

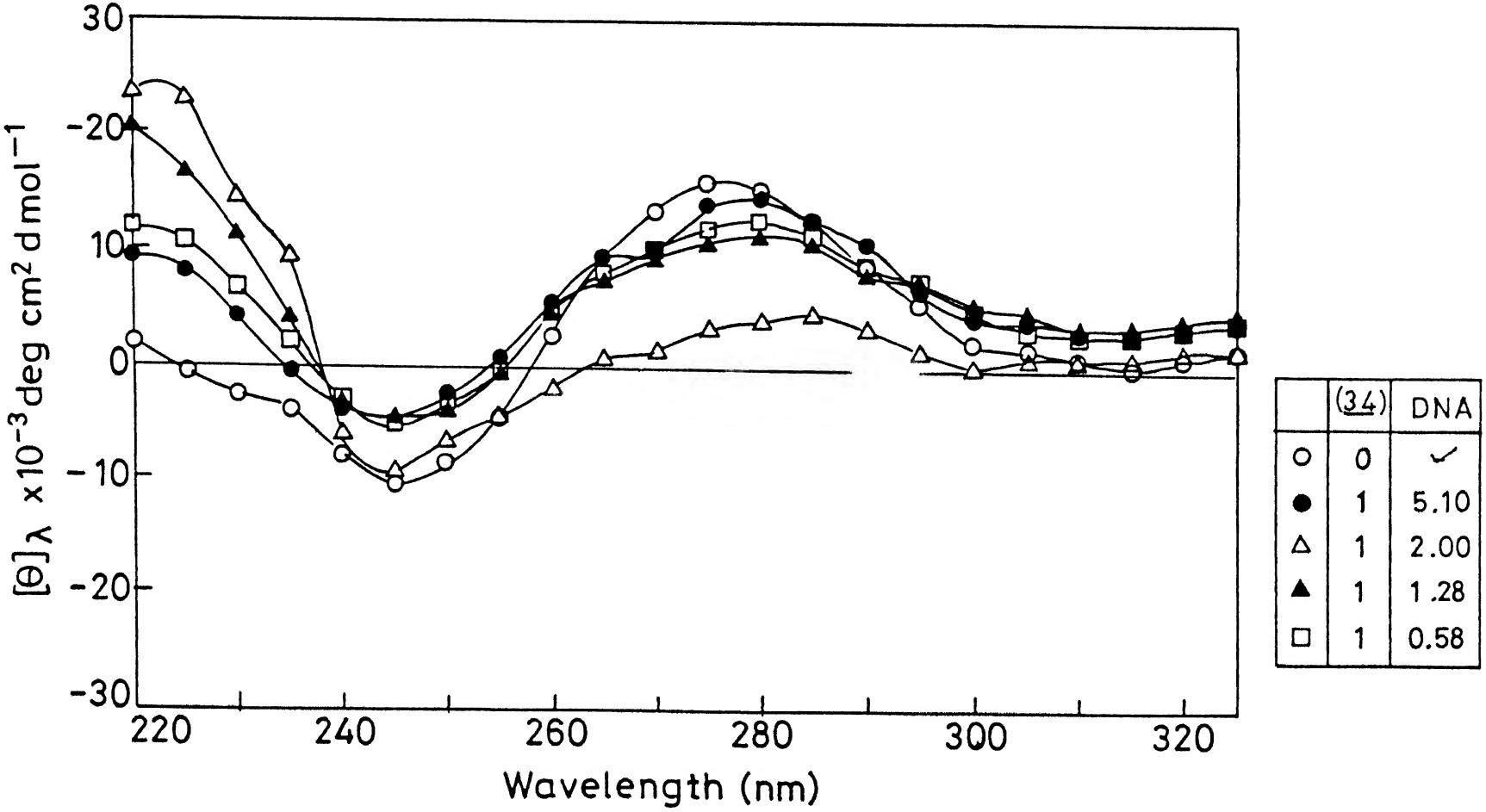

Figure C-29. CD spectra of synthetic oligonucleotide (DNA) titrated with (34) [(HCl.] in H_2O. Concentration of DNA : ~ 60μM DNA (phosphates); Inset : Mol [illegible]o of DNA (phosphates) per (34)

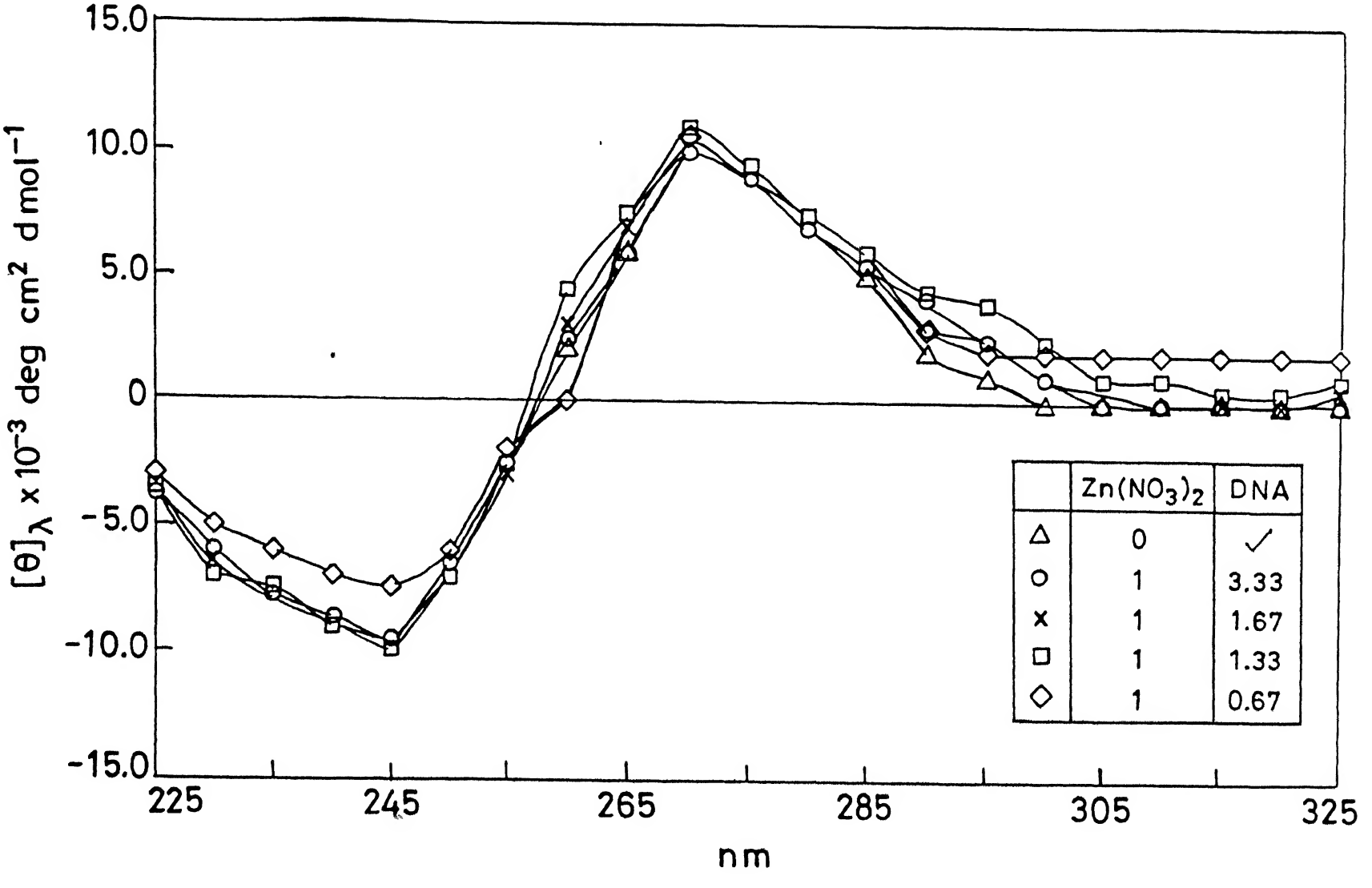

Figure C-30. CD spectra of synthetic oligonucleotide (DNA) titrated with $Zn(NO_3)_2$ in H_2O at Concentration of DNA : $\sim 40\mu$M DNA (phosphates); Inset : Molar ratio of DNA (phosphates) per $ZnNO_3$

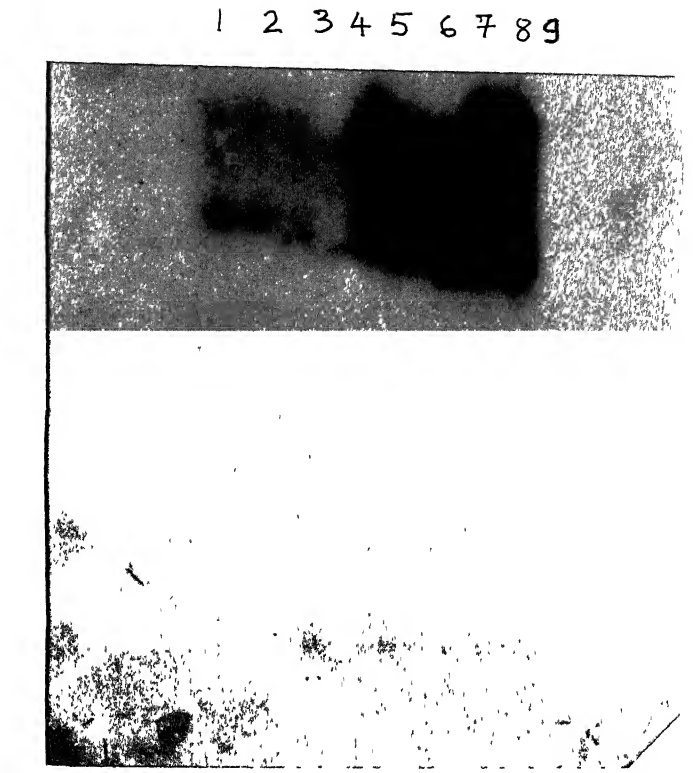

Figure C-31. Gel picture of γ-^{32}P-labeled oligonucleotide (Oligo-1*) complexed with $(CH)_2Zn$, (52). Spot 1 corresponds to Oligo-1 alone, 2 to 7 correspond to Oligo-1 complexed varying ratios of (52) to Oligo-1 (Please refer Methods of DNA Interaction Studies, p. 112). Spots 8 and 9 correspond to that of $(CH)_2$ (33), as control set.

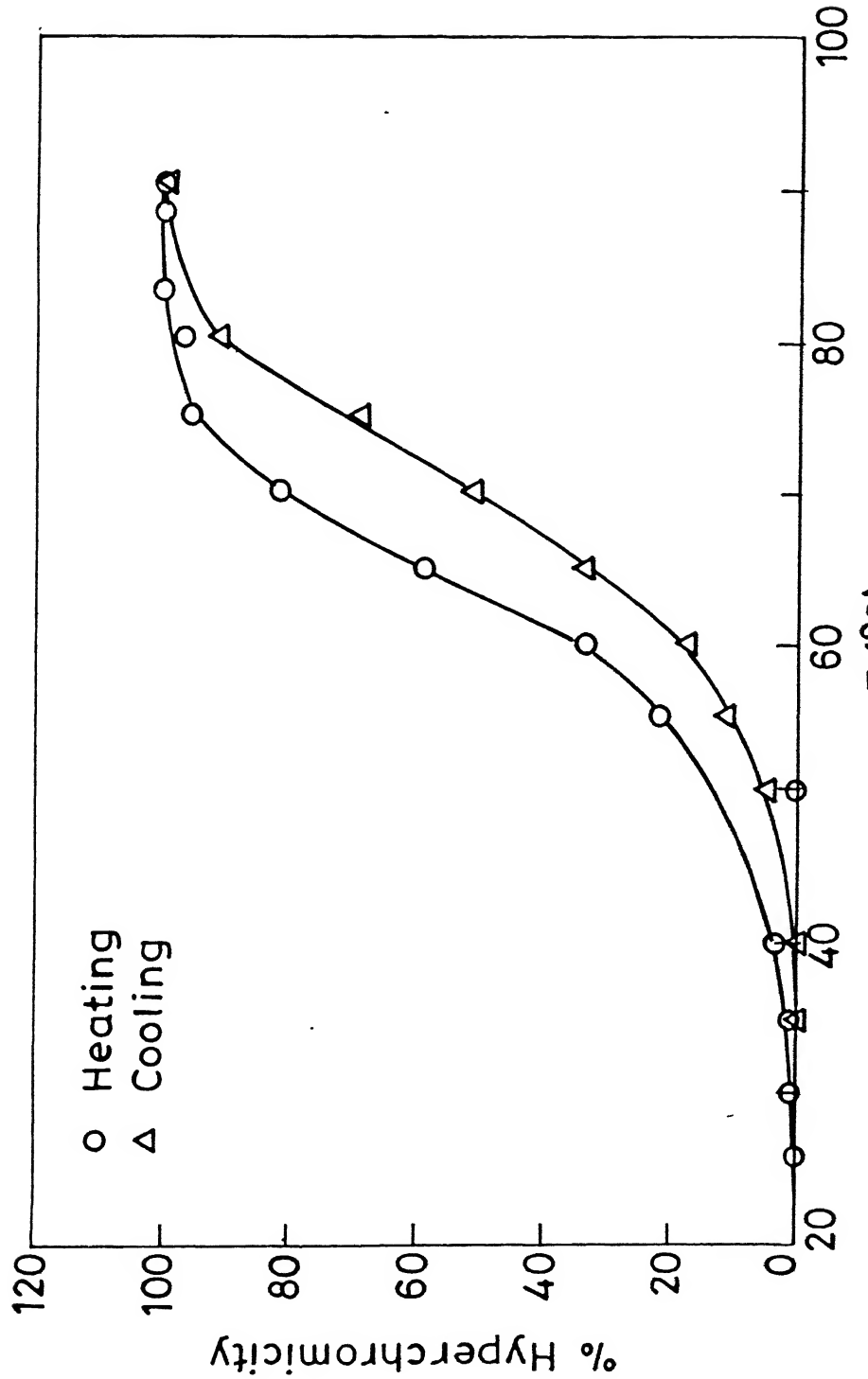

Figure C-32 Absorbance vs. temperature (T_m) profile of poly d(G-C) (DNA)

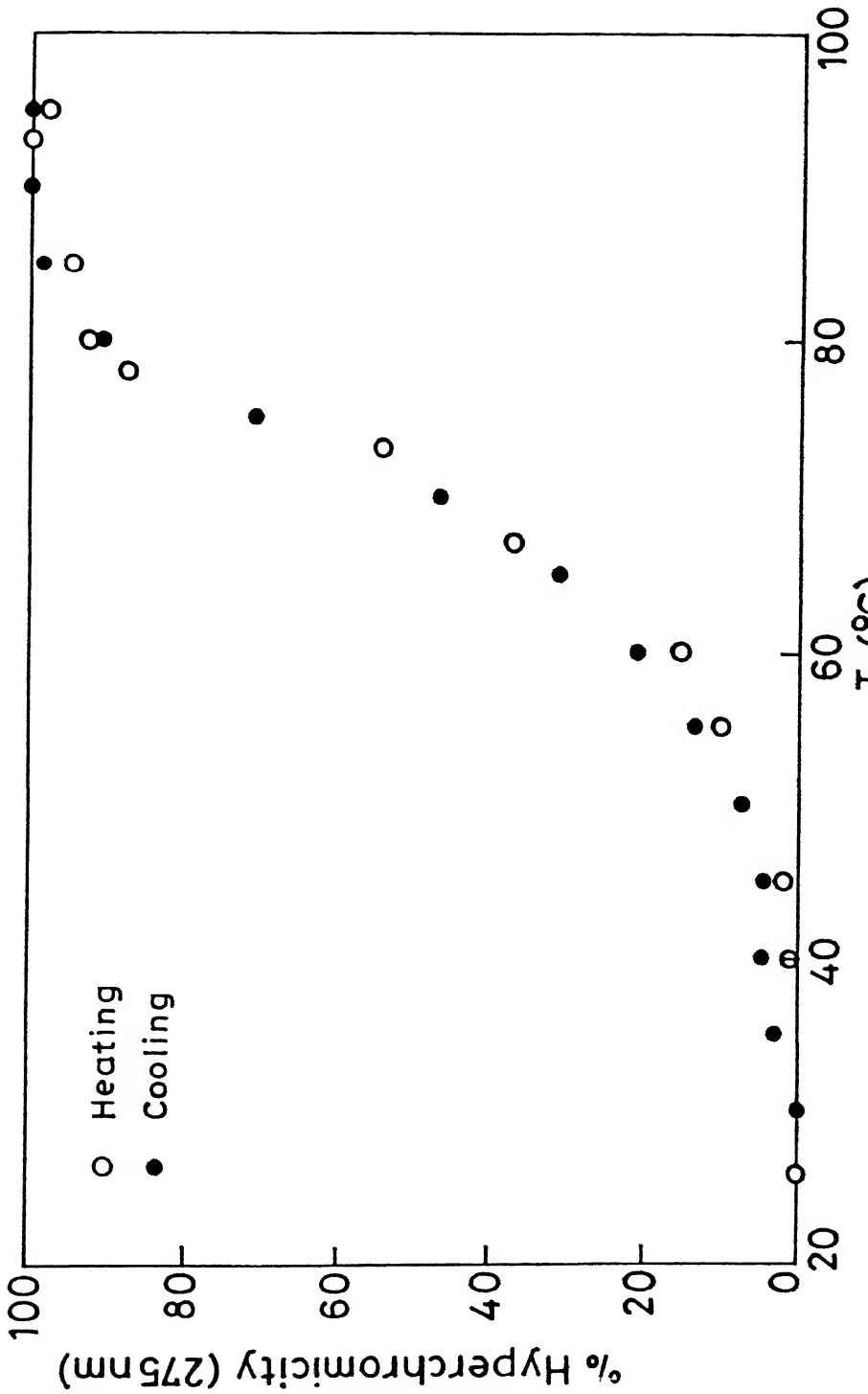

Figure C-33 Absorbance vs. temperature (T_m) profile of a solution of poly d(G-C) (DNA) and (A) [$(CH)_2Zn^{II}$, (52)] at (A)/DNA = 0.04; Concentration of DNA : 81μM DNA (phosphates)

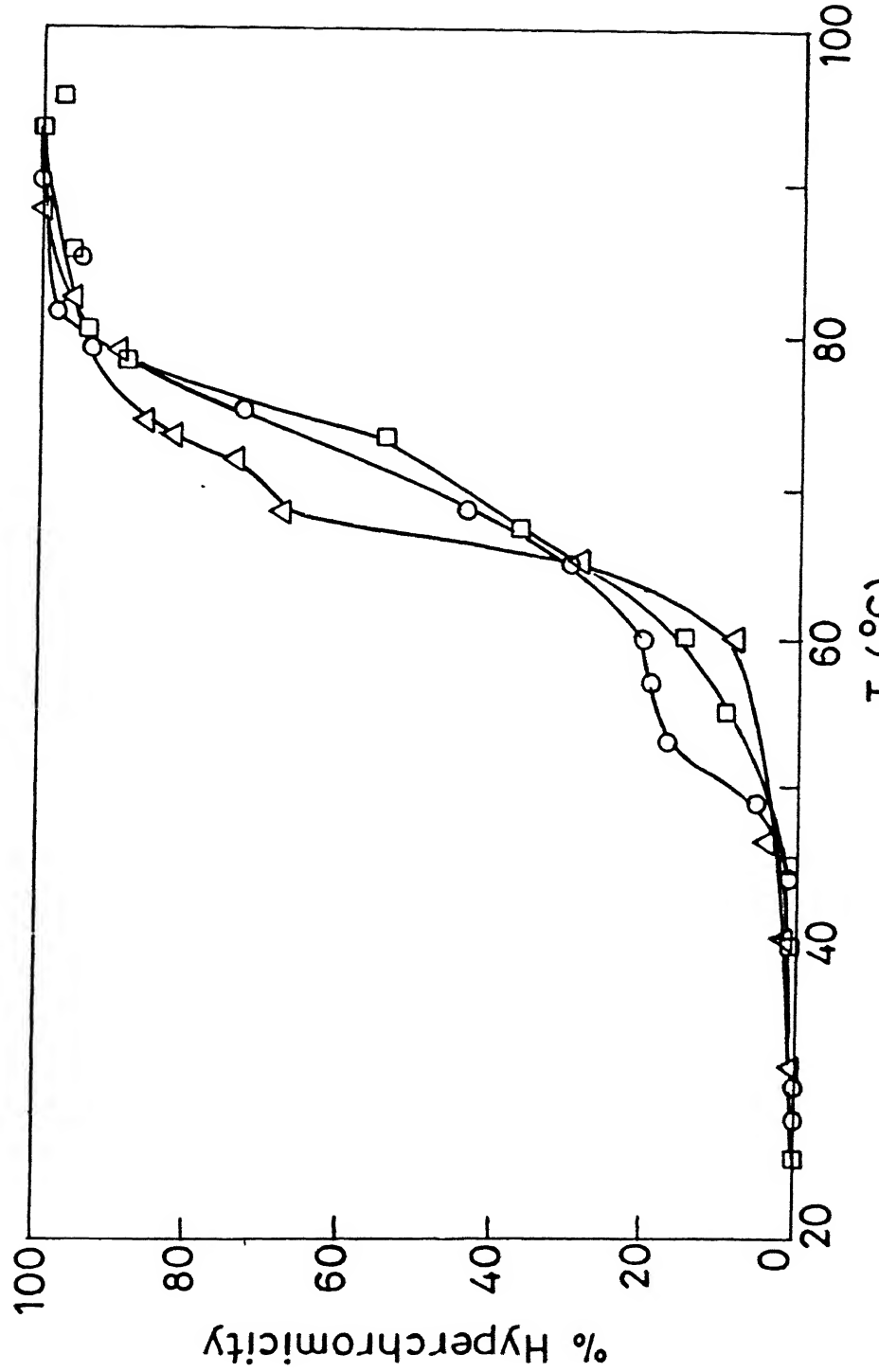

Figure C-34 Absorbance vs. temperature (T_m) profile of a solution of poly d(G-C) (DNA) and (A) [$(CH)_2Zn^{II}$, (52)]; a. DNA alone b. A/DNA = 0.04 c. A/DNA = 0.13 d. A/DNA = 0.33; Concentration of DNA : ~ 81μM DNA (phosphates)

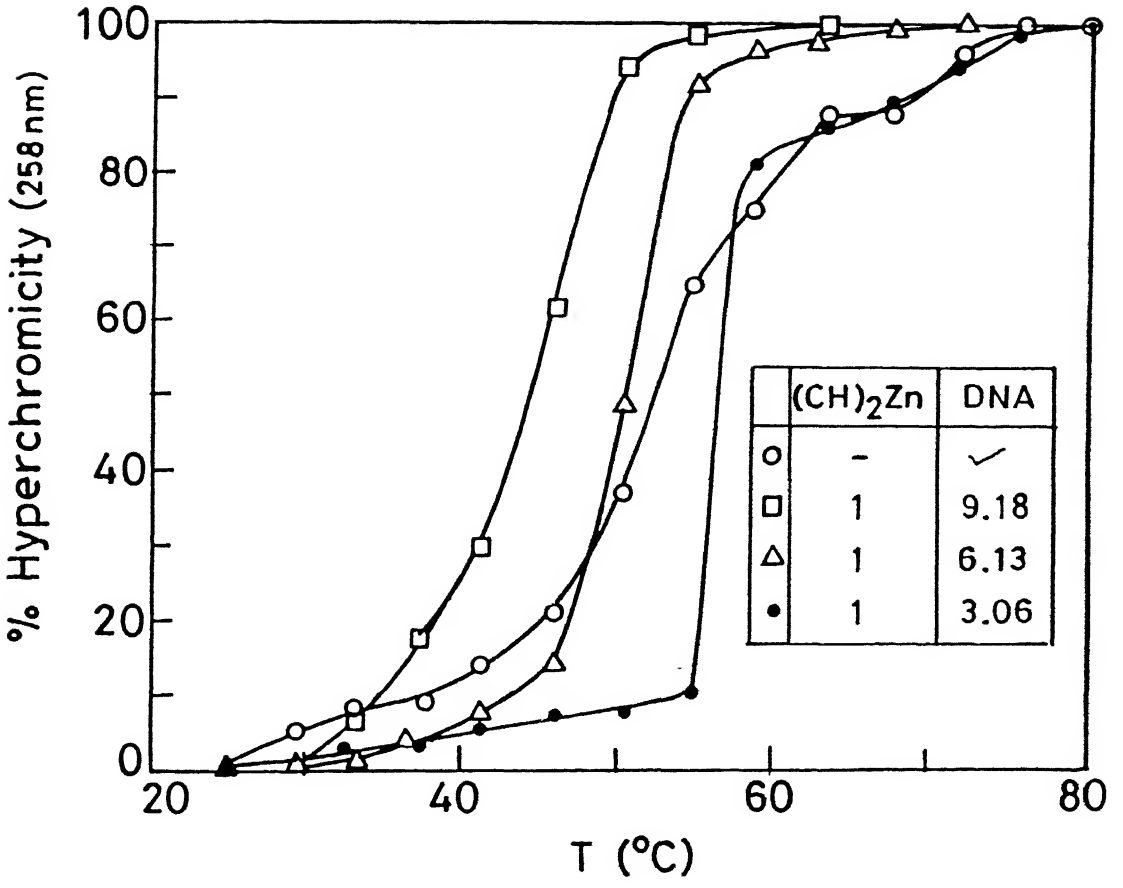

Figure C-35 Absorbance vs. temperature profile of a solution of poly d(A-T) (DNA) and A[$(CH)_2Zn^{II}$, (52)] a. DNA alone b. A/DNA = 0.11 c. A/DNA = 0.16 d. A/DNA = 0.33

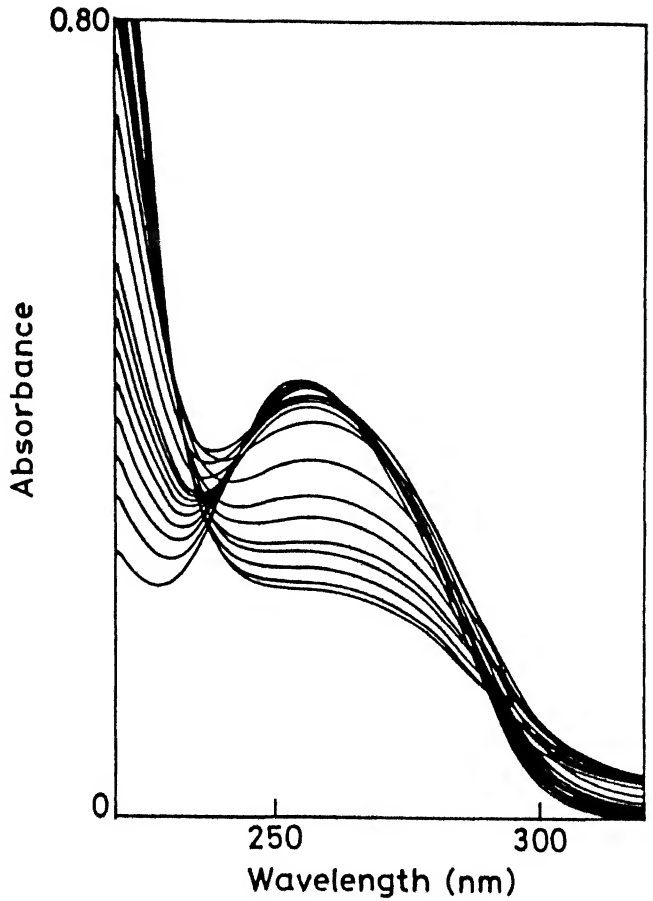

Figure C-36. UV profile of poly d(G) (DNA) titrated with (A) [A = $(CH)_2Zn^{II}$, (52)] in H_2O. Concentration of DNA : 77.5μM DNA (phosphates)

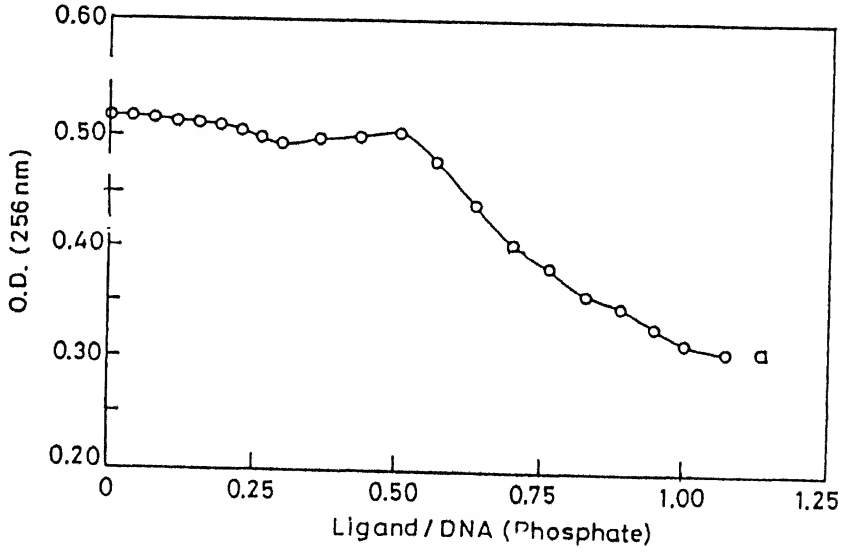

Plot of UV hypochromicity of poly d(G) (DNA) (at 256 nm) vs. (A)/DNA (phosphate) Ligand = (A)

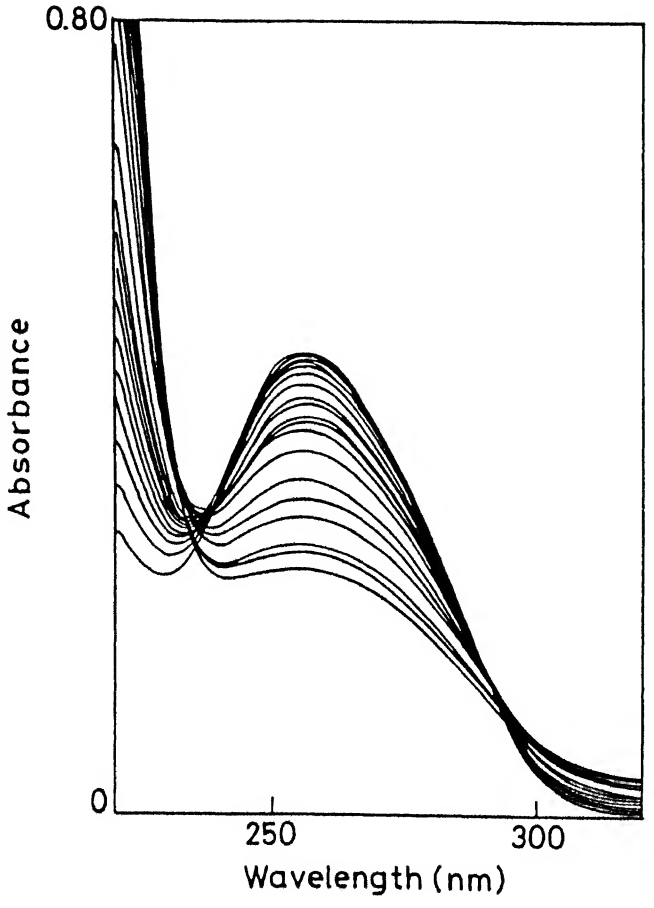

Figure C-37. UV profile of poly d(G) (DNA) titrated with B [B = $(HC)_2Zn^{II}$, (53)] in H_2O. Concentration of DNA : 71μM DNA (phosphates)

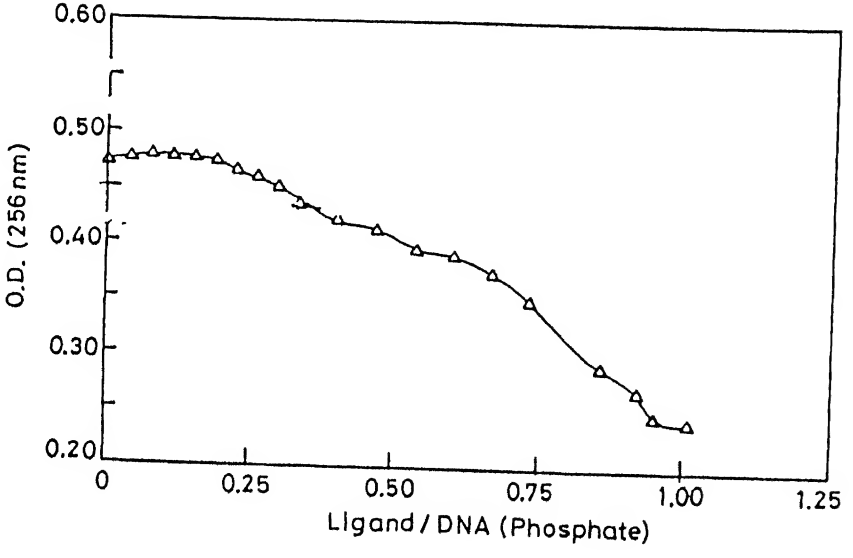

Plot of UV hypochromicity of poly d(G) (DNA) (at 256 nm) vs. (B)/DNA (phosphate) Ligand = (B)

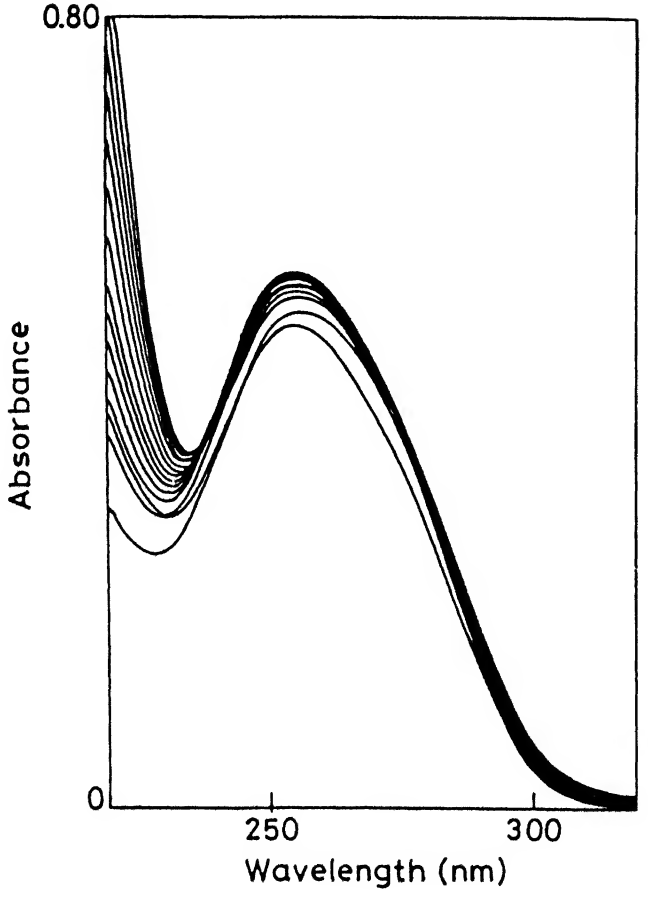

Figure C-38. UV profile of poly d(G) (DNA) titrated with precursor peptide $(CH)_2$, (33) in H_2O. Concentration of DNA : 78μM DNA (phosphates)

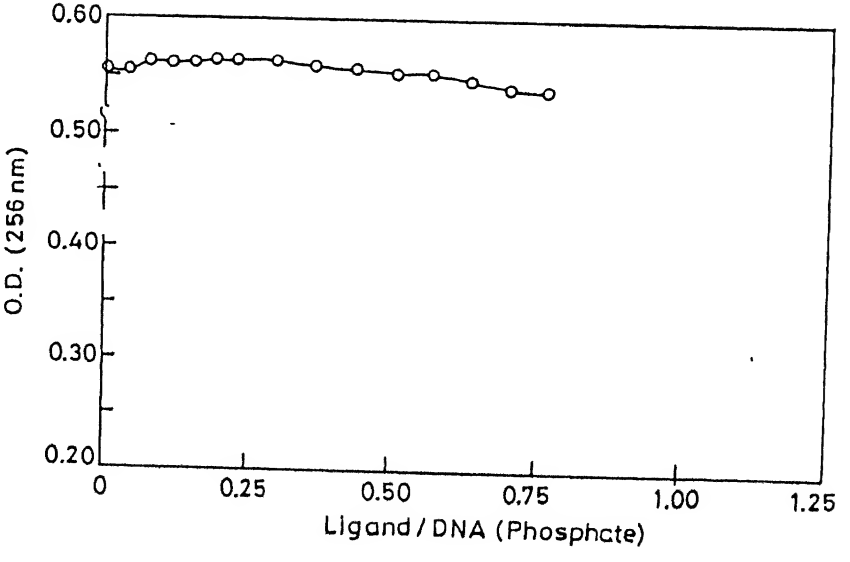

Plot of UV hypochromicity of poly d(G) (DNA) (at 256 nm) vs. Ligand/DNA (phosphate) Ligand = $(CH)_2$ (33)

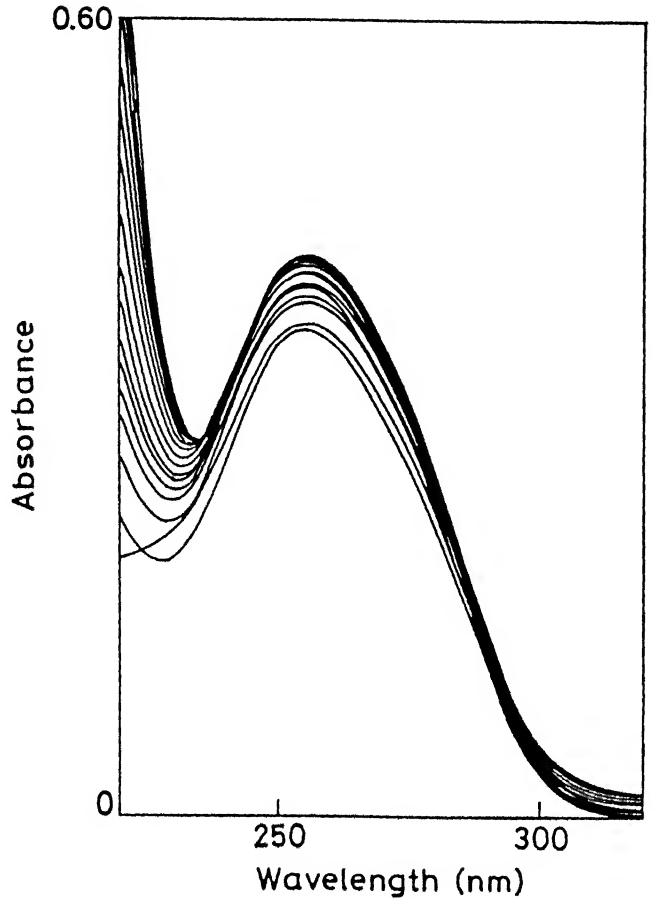

Figure C-39. UV profile of poly d(G) (DNA) titrated with precursor peptide $(HC)_2$, (53) in H_2O. Concentration of DNA : 64μM DNA (phosphates)

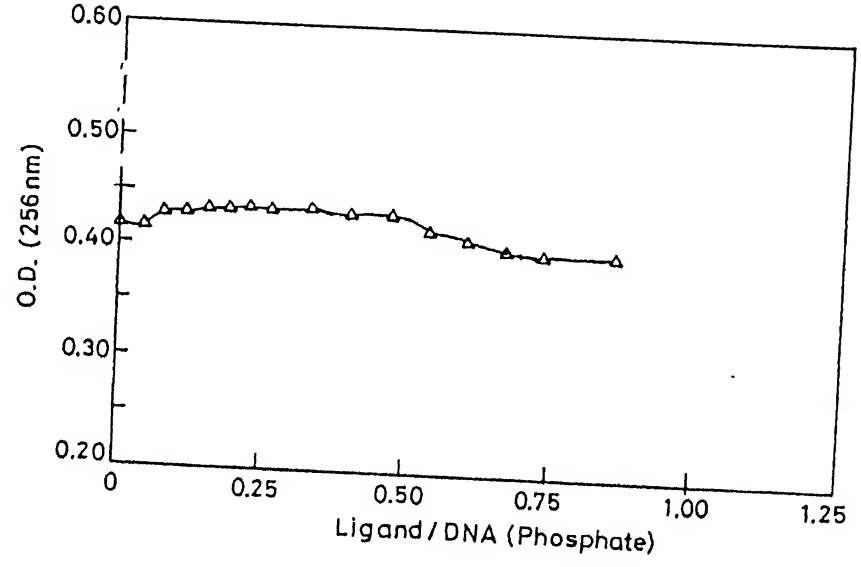

Plot of UV hypochromicity of poly d(G) (DNA) (at 256 nm) vs. Ligand/DNA (phosphate) Ligand = $(HC)_2$ (34)

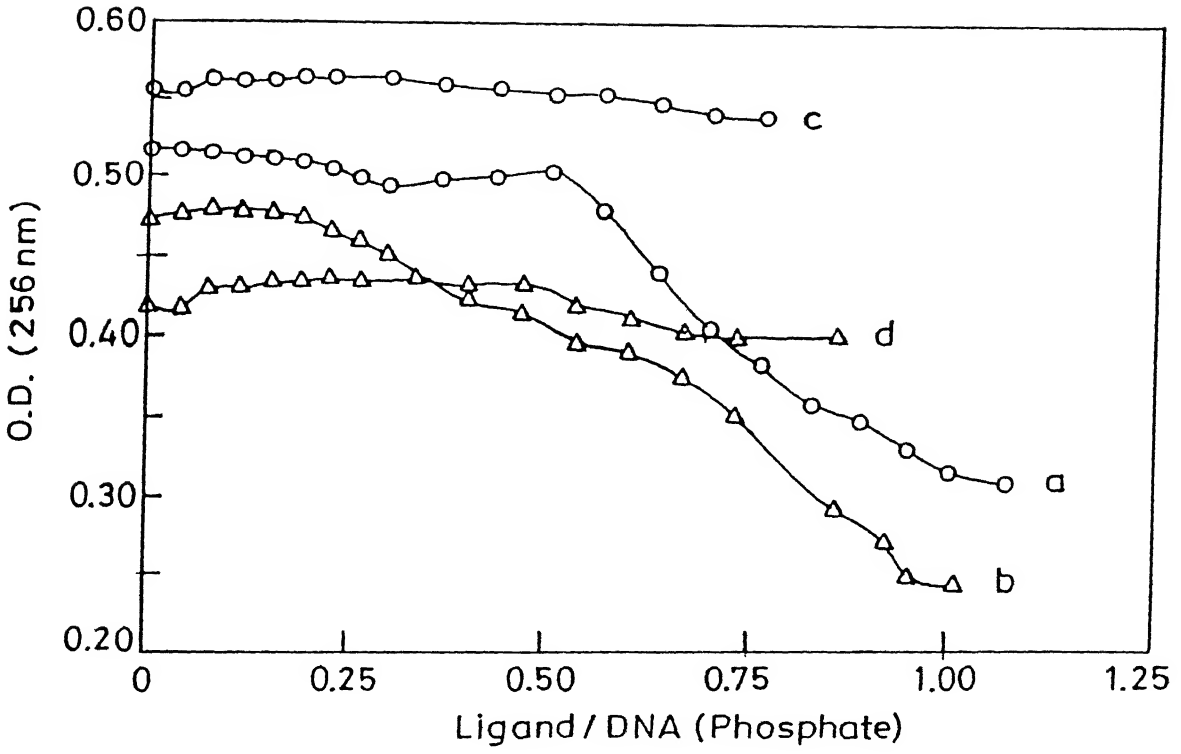

Figure C-40. Comparison plot of UV hypochromicity of poly d(G) (DNA) (at 256 nm) vs. Ligand/DNA (phosphate) ; Ligand : a = $(CH)_2Zn^{II}$ (52), (A) (Figure C-36); b = $(HC)_2Zn^{II}$ (53), (B) (Figure C-37); c = precursor peptide $(CH)_2$ (32) (Figure C-38); d = precursor peptide $(HC)_2$ (33) (Figure C-39)

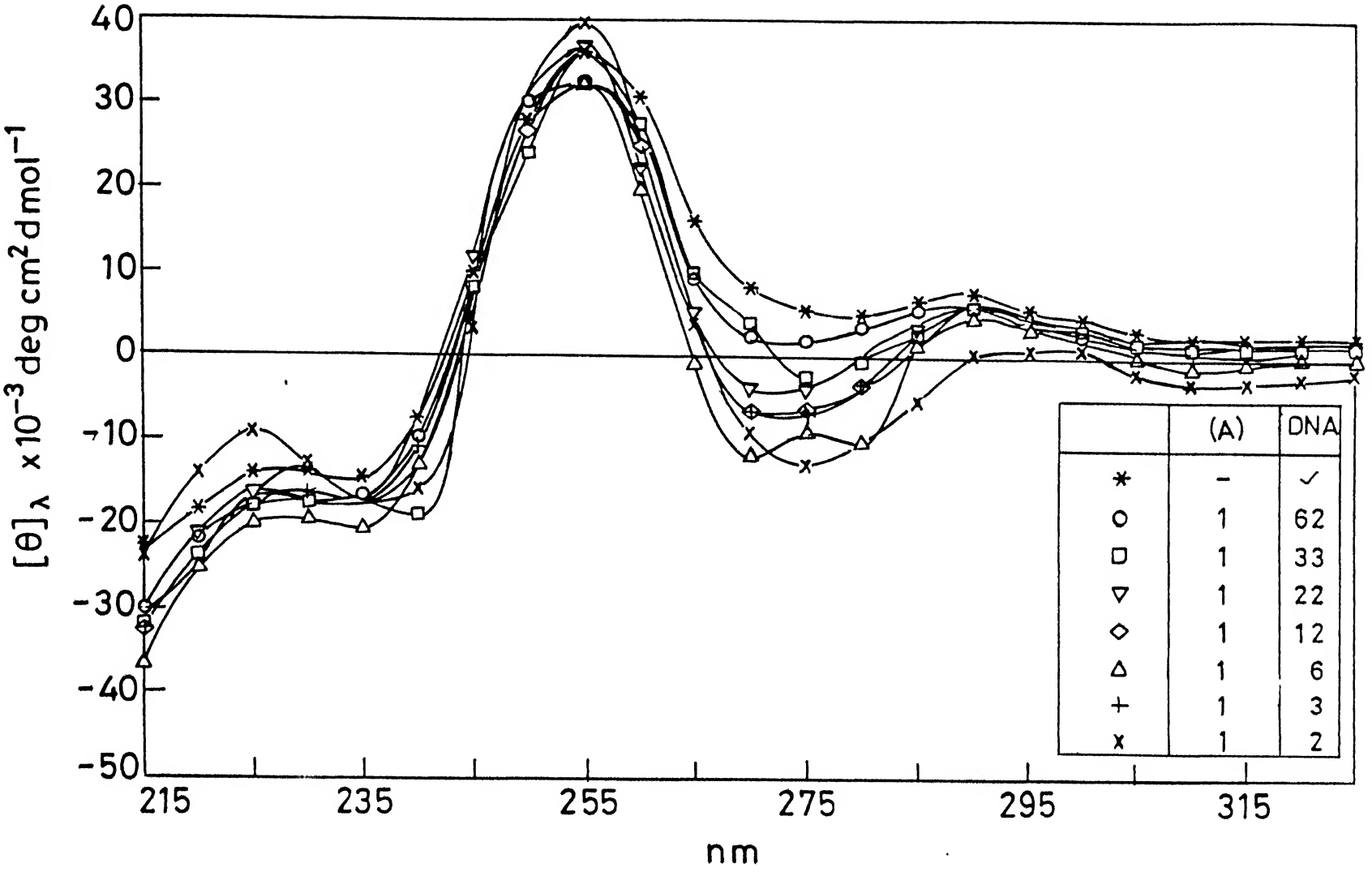

Figure C-41. CD spectra of poly d(G) (DNA) titrated with (52) [$(CH)_2Zn^{II}$, (A)] in H_2O. Concentration of DNA : $\sim$ 74μM DNA (phosphates); Inset : Molar ratio of DNA (phosphates) per (A)

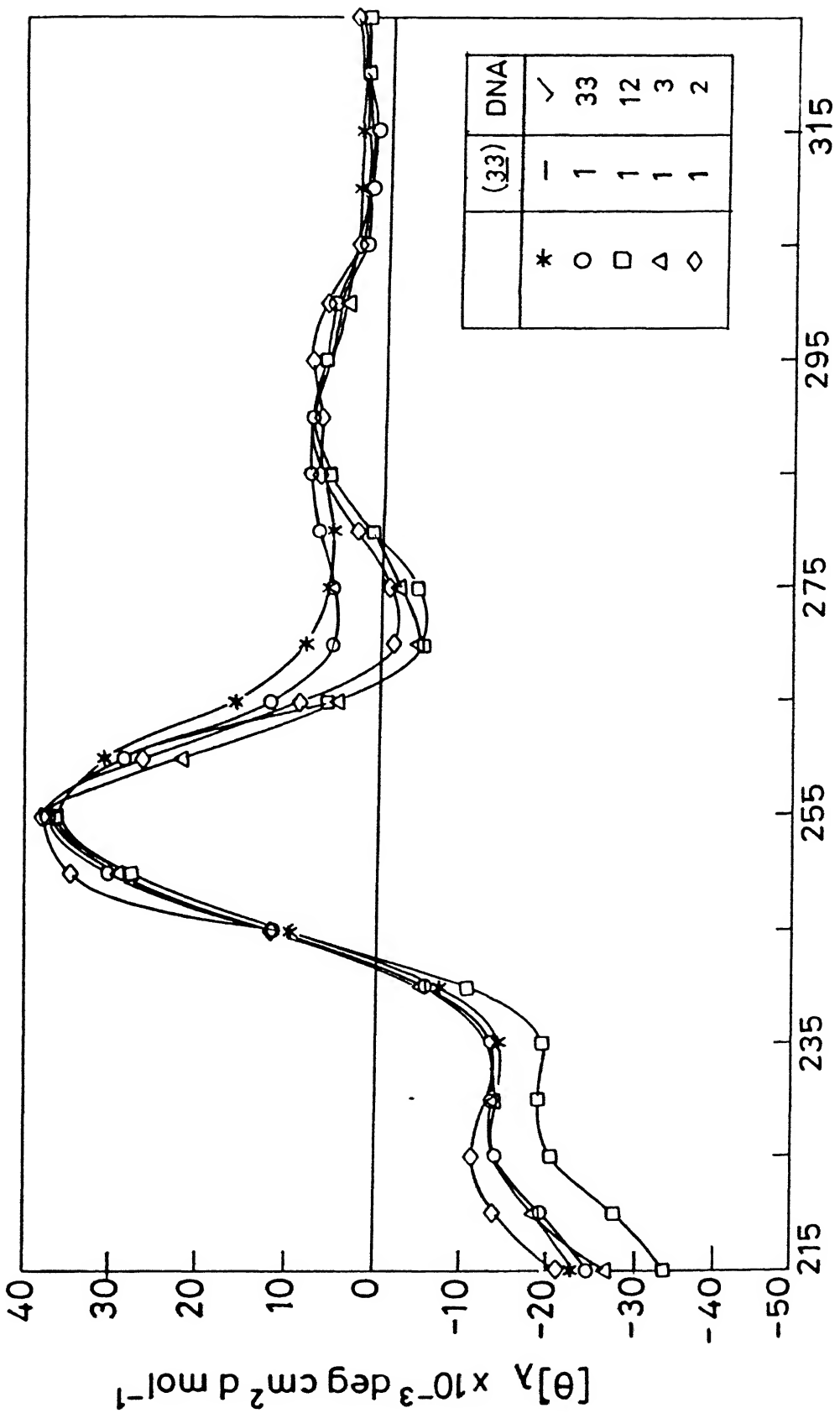

Figure C-43. CD spectra of poly d(G) (DNA) titrated with (33) $[(CH)_2]$ in H_2O. Concentration of DNA : ~ 74μM DNA (phosphates); Inset : Molar ratio of DNA (phosphates) per (33)

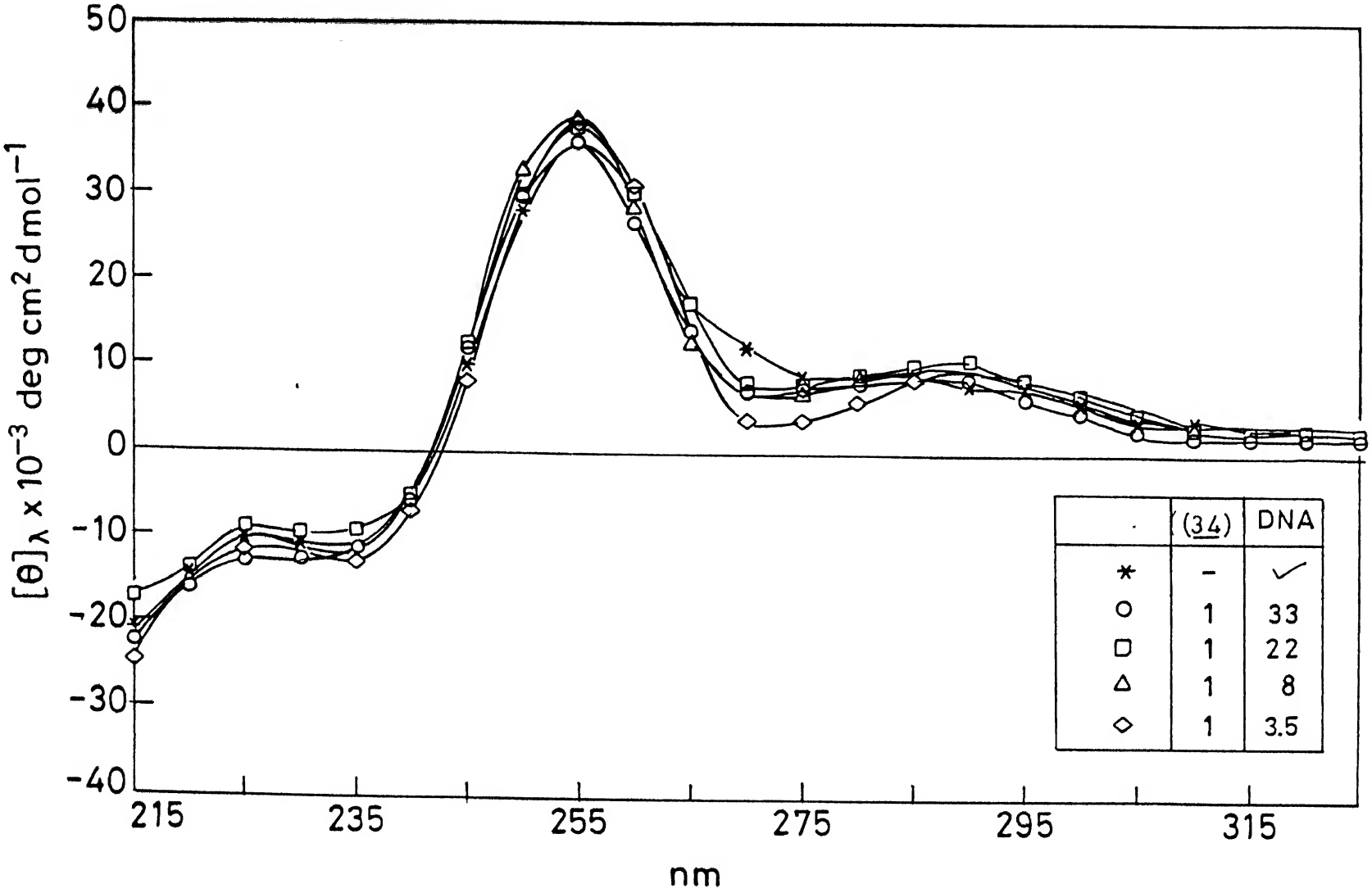

Figure C-44. CD spectra of poly d(G) (DNA) titrated with (34) [$(HC)_2$] in H_2O. Concentration of DNA : $\sim$ 74μM DNA (phosphates); Inset : Molar ratio of DNA (phosphates) per (34)

Figure C-45

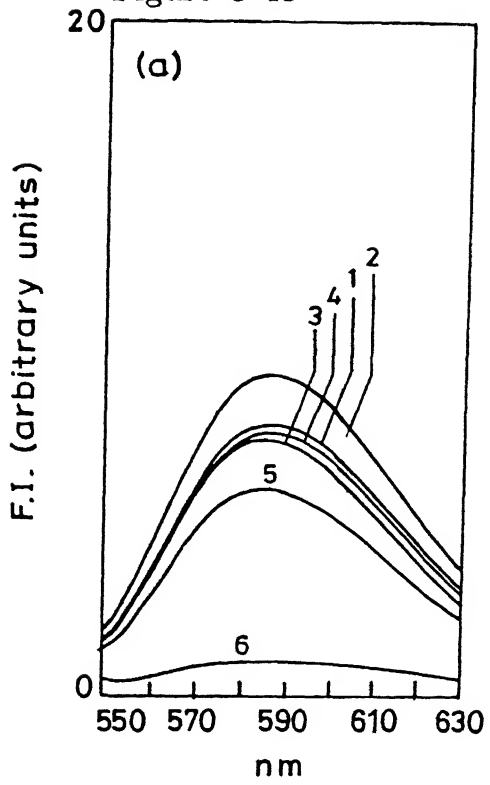

Figure C-46

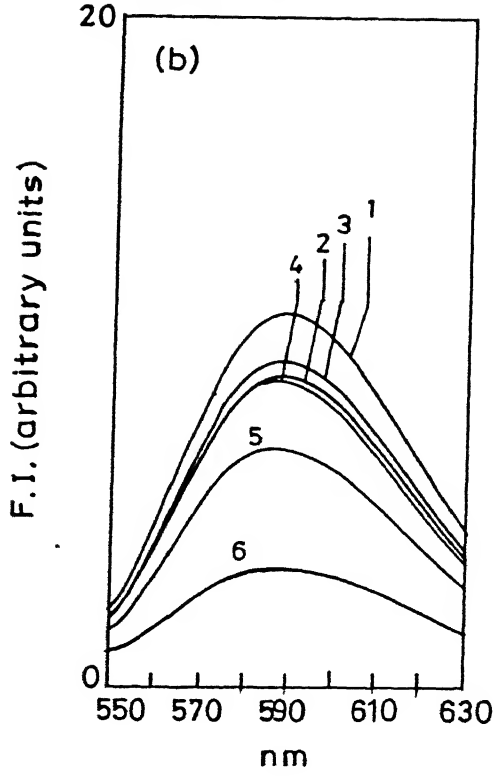

Figure C-47

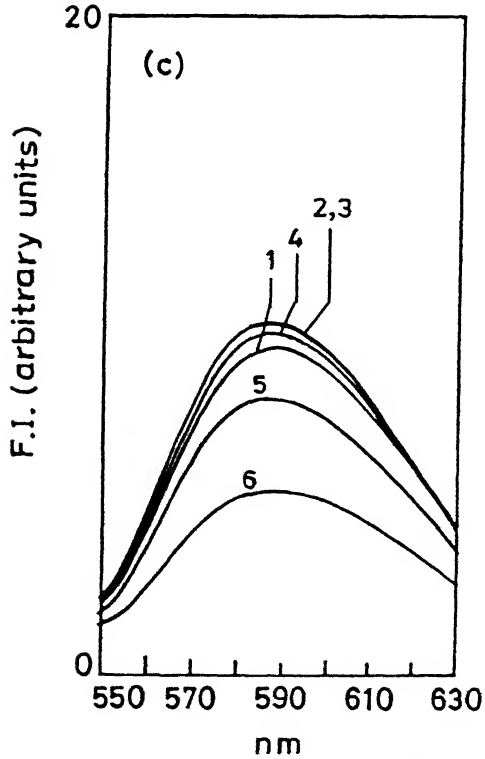

Figure C-48

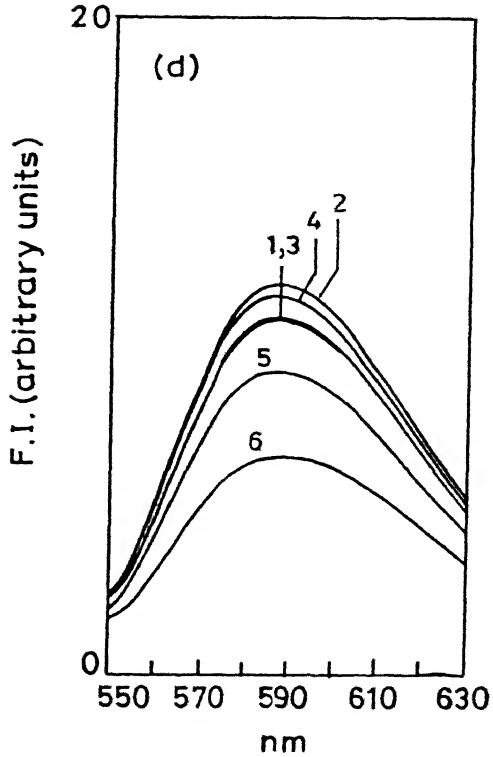

Fluorescence quenching of poly dG (DNA) bound ethidium bromide (ETB) at different ratios of ETB/DNA: Figure C-45. 0.30 ; Figure C-46. 0.53 ; Figure C-47. 0.8 ; Figure C-48. 1.11, and at different ratios of A [A=$(CH)_2Zn^{II}$, (52)] : 1. DNA alone ; 2. 0.071 ; 3. 0.145; 4. 0.286 ; 5. 0.588 ; 6. 1.429.

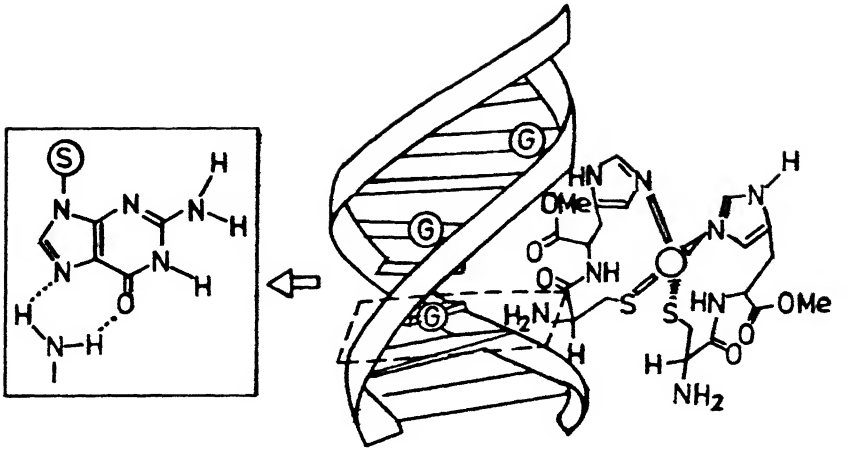

Figure C-49. Model of interaction of (A) [$(CH)_2Zn^{II}$; (53)] with poly d(G-C)
Inset : Molecular interaction of A with guanine

D. SPECTRA

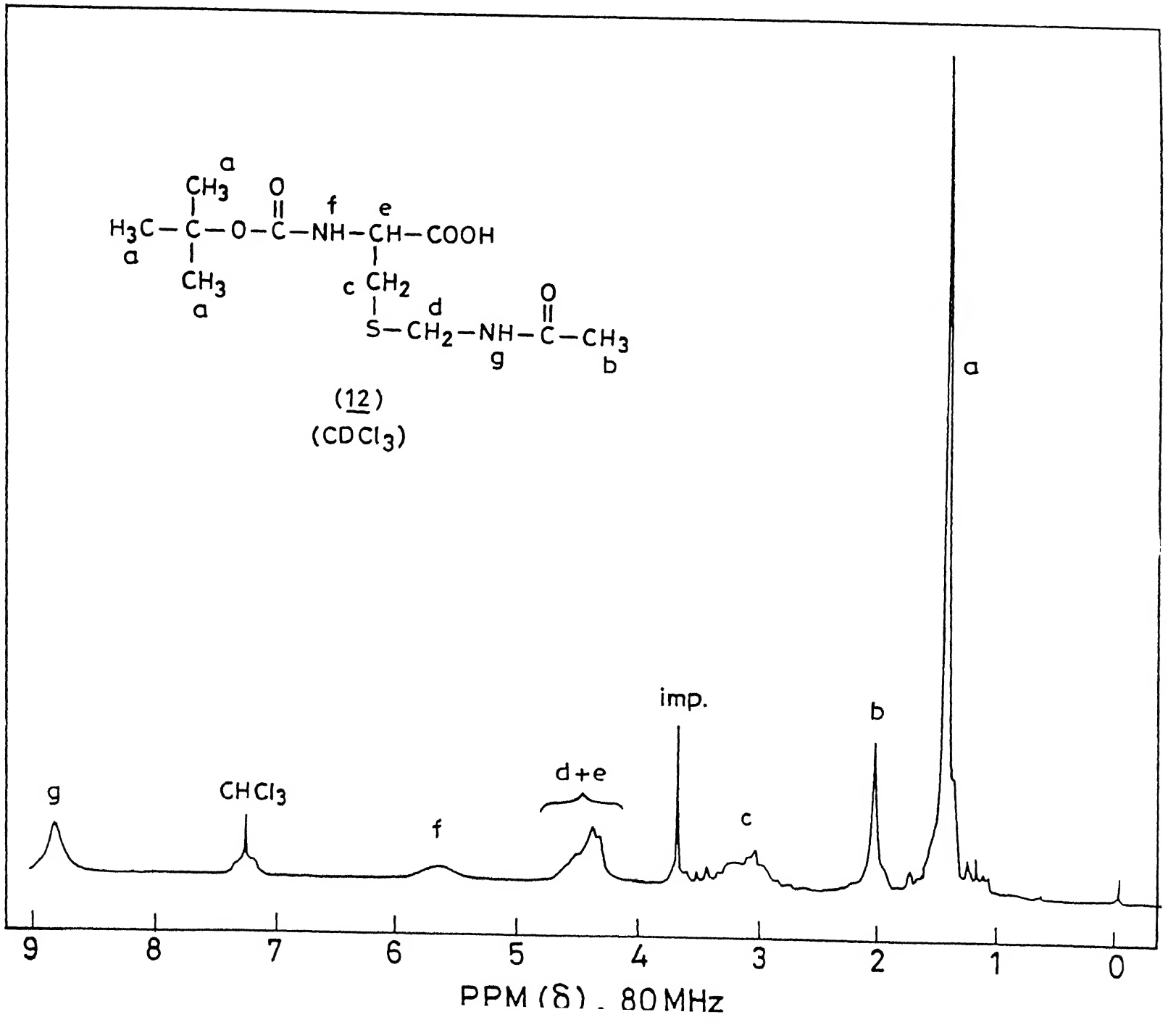
a
CH3
O
f
e
H3C – C – O – C – NH – CH – COOH
a
CH3
a
c CH2
d
O
S – CH2 – NH – C – CH3
g
b
(12)
(CDCl3)
a
imp.
b
d+e
g
CHCl3
f
c
9
8
7
6
5
4
3
2
1
0
PPM (δ), 80 MHz

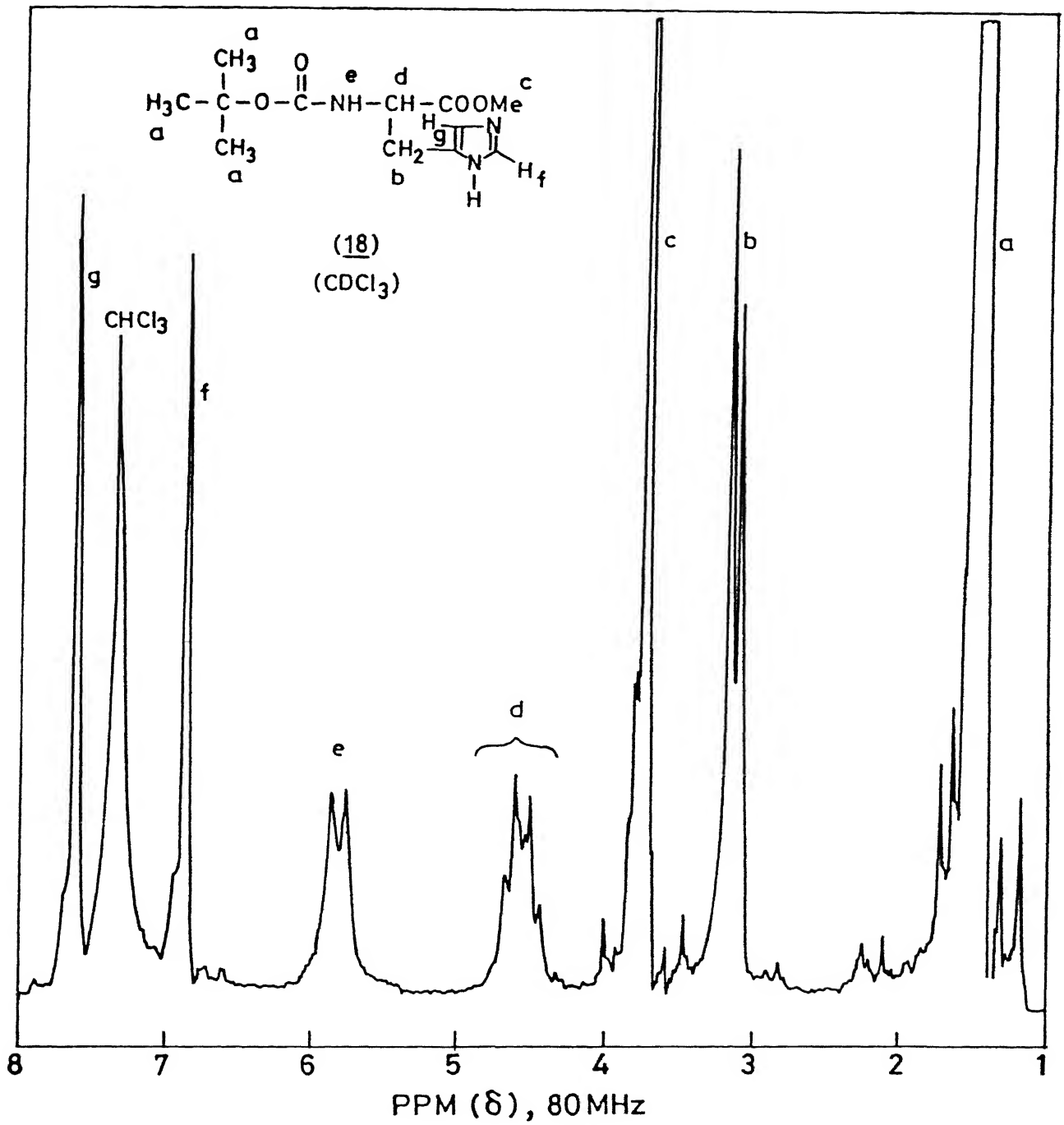
a
CH3
O
e
d
c
H3C-C-O-C-NH-CH-COOMe
a
H
g
N
CH3
CH2
N
Hf
a
b
H
(18)
(CDCl3)
g
CHCl3
f
c
b
a
d
e
8
7
6
5
4
3
2
1
PPM (δ), 80 MHz

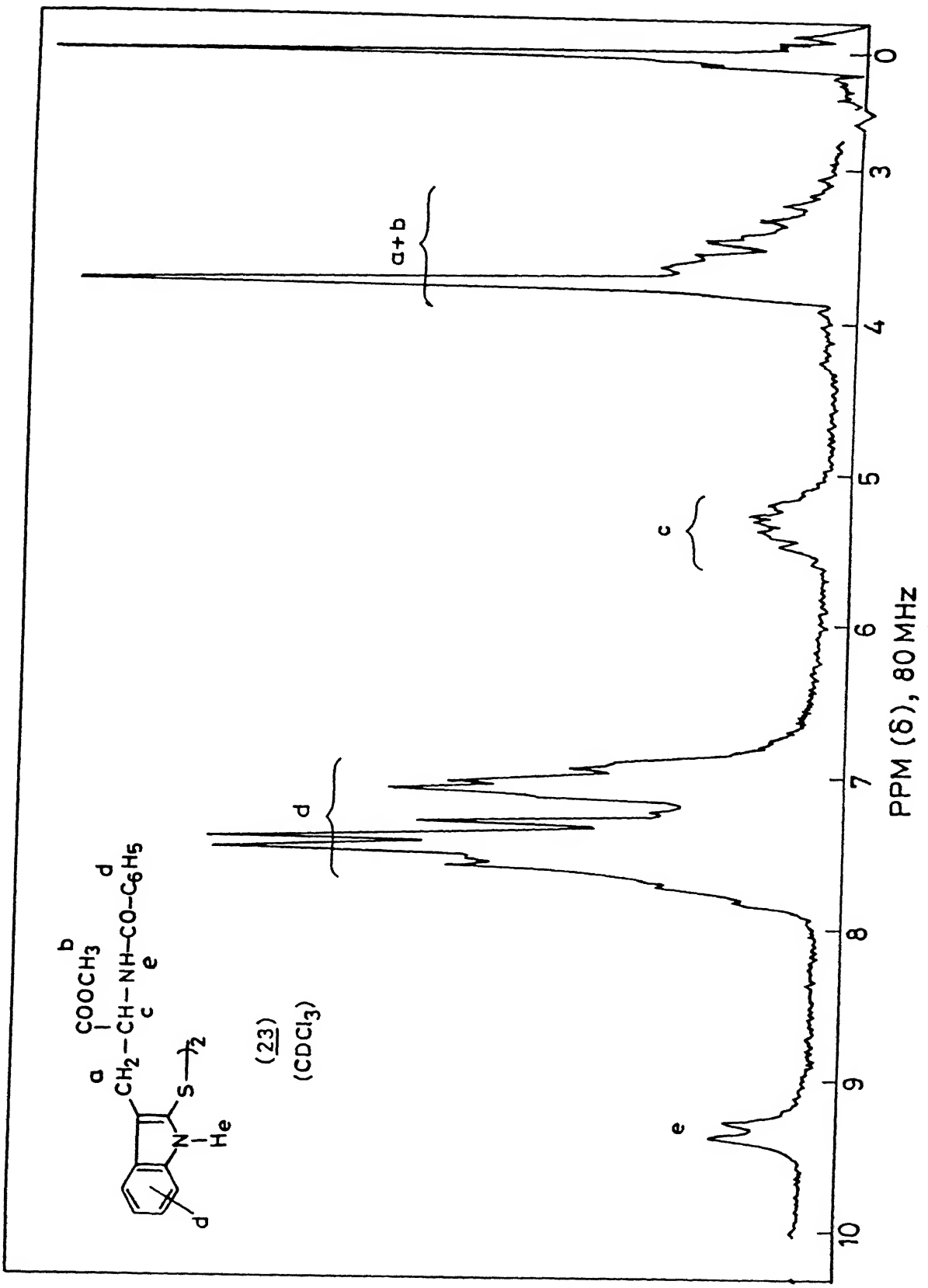
a
b
c
d
e
COOCH3
CH2–CH–NH–CO–C6H5
S
N
He
d
(23)
(CDCl3)
a+b
c
d
e
0
3
4
5
6
7
8
9
10
PPM (δ), 80 MHz

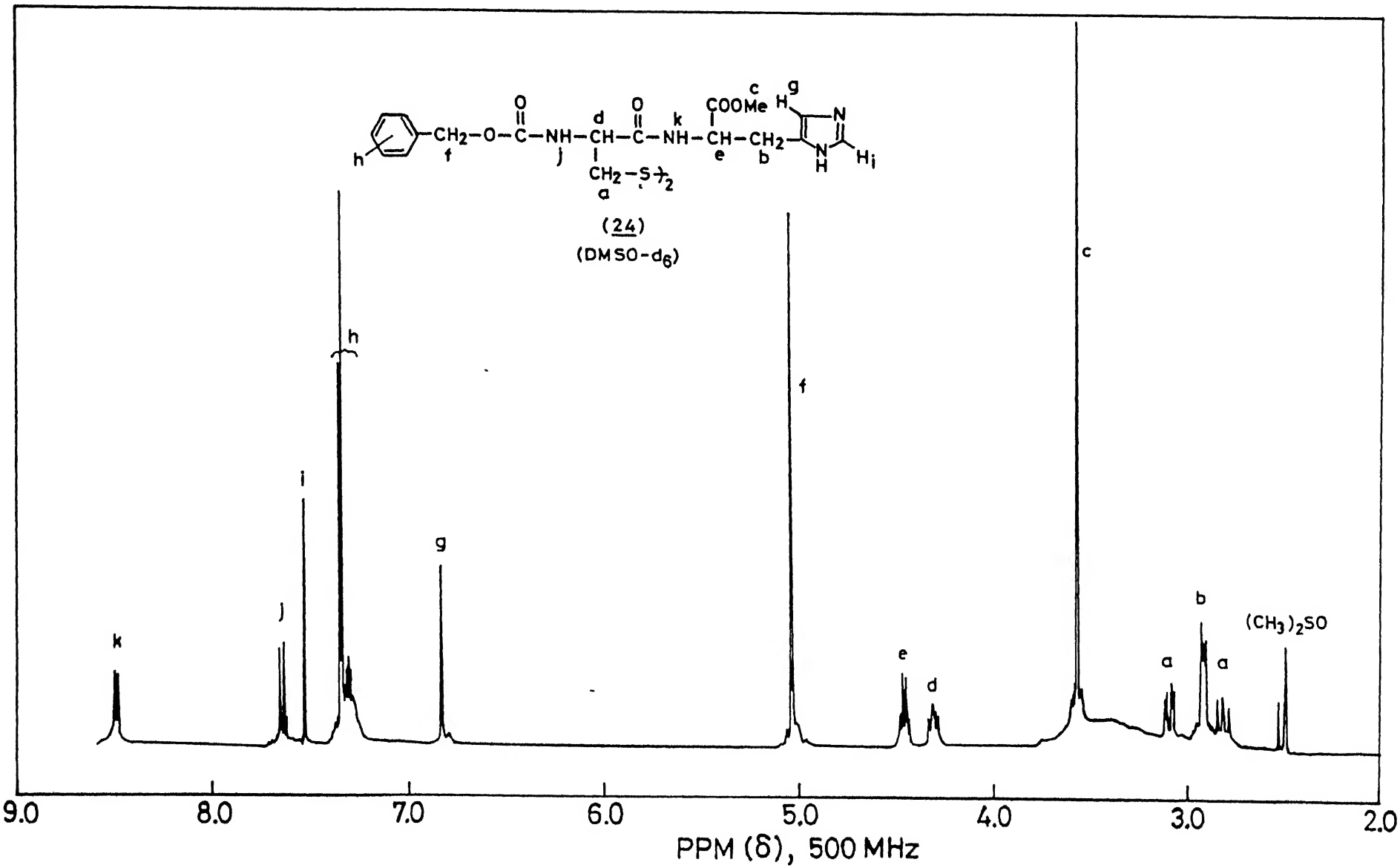
(24)
(DMSO-d6)
k
j
i
h
g
f
e
d
c
a
b
a
(CH3)2SO
9.0
8.0
7.0
6.0
5.0
4.0
3.0
2.0
PPM (δ), 500 MHz

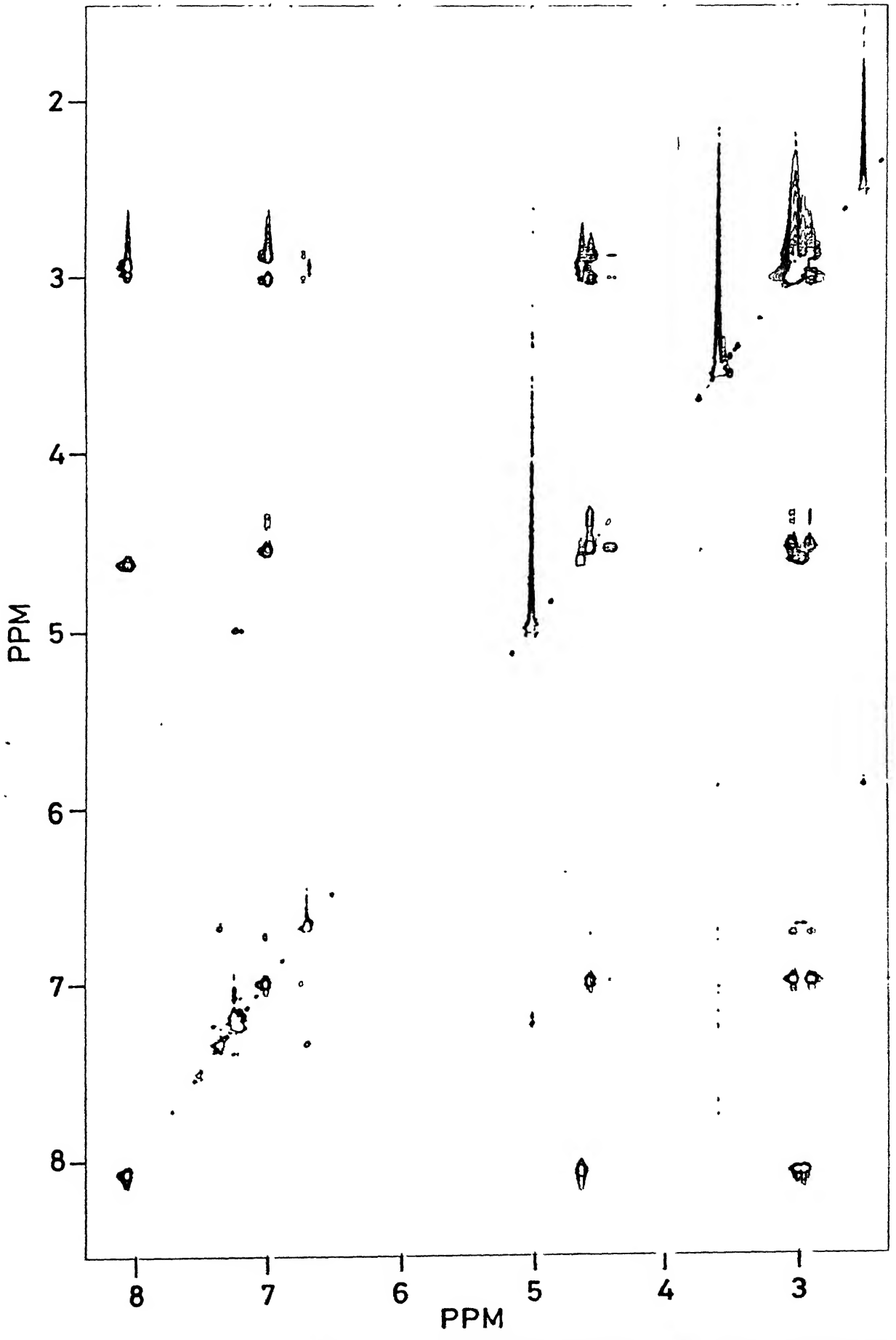

TOCSY Spectrum (500MHz) of Bis-Z-Cystinyl-di-His-OMe (24) in DMSO-d_6

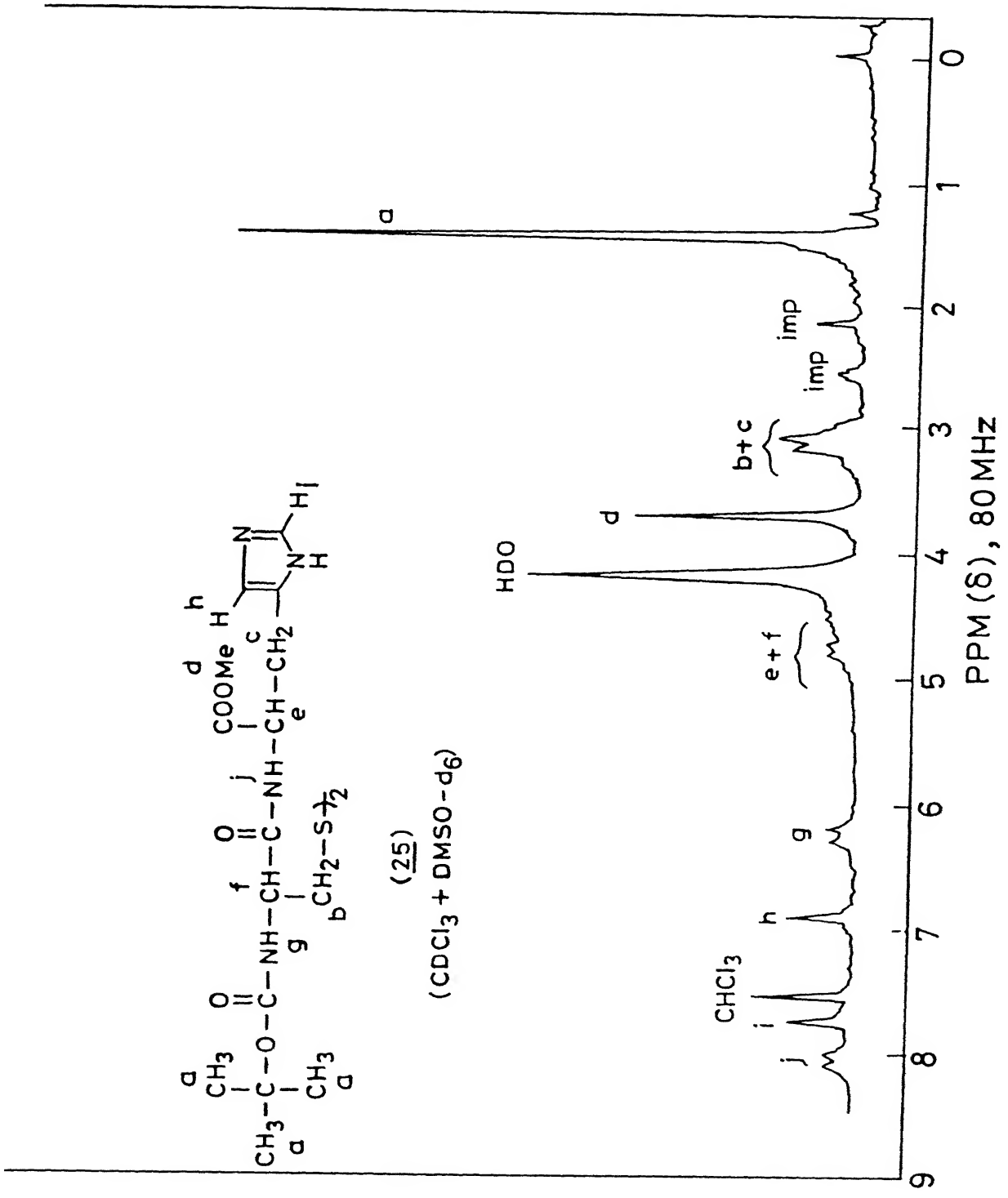
a
CH3
CH3-C-O-C-NH-CH-C-NH-CH-CH2
CH3
COOMe H
bCH2-S
(25)
(CDCl3 + DMSO-d6)
HDO
d
b+c
imp
imp
e+f
g
h
i
j
CHCl3
PPM (δ), 80 MHz
0
1
2
3
4
5
6
7
8
9

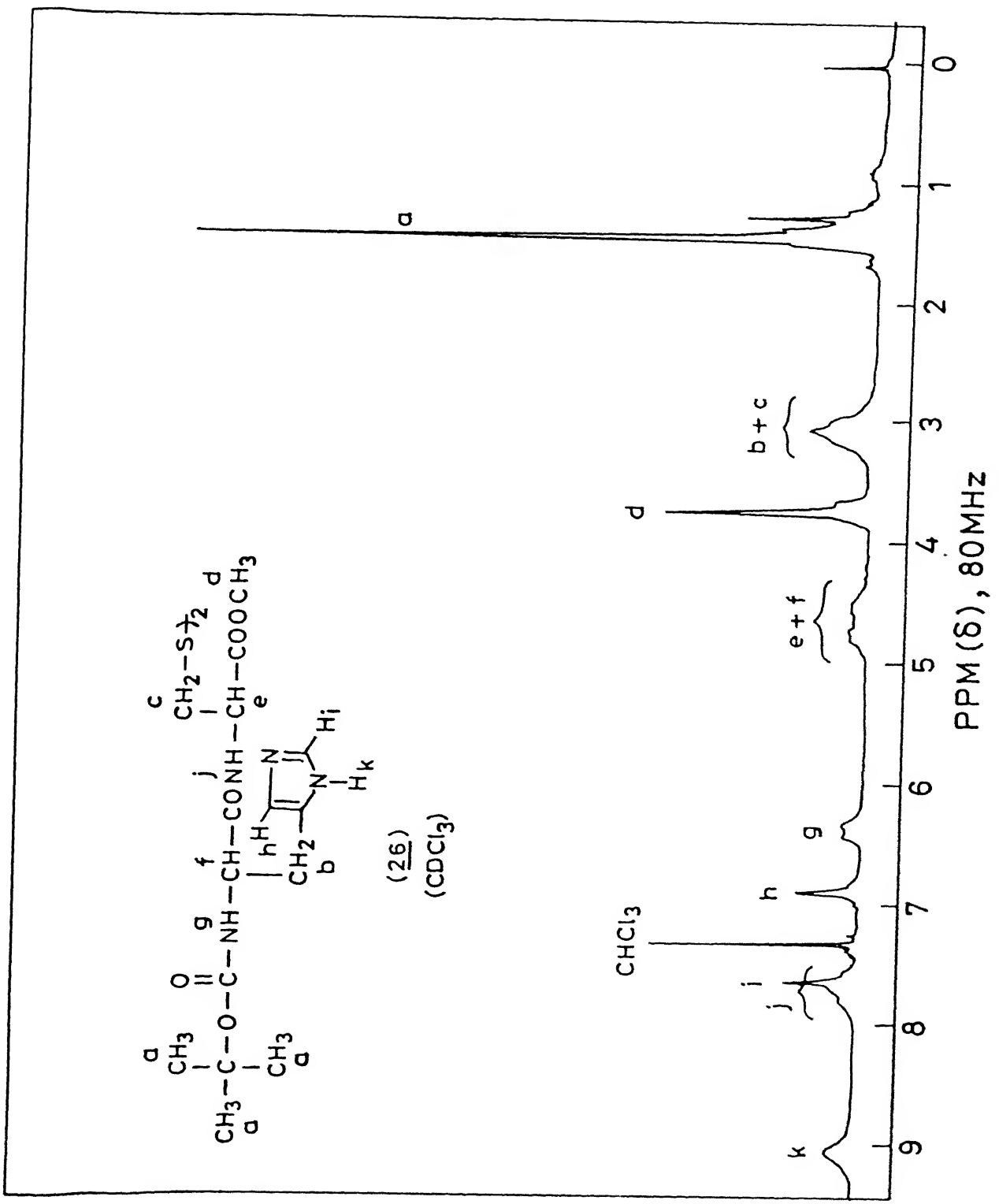
a
CH3
CH3–C–O–C–NH–CH–CONH–CH–COOCH3
CH3
CH2–S–S–CH2
CH2
(26)
(CDCl3)
CHCl3
PPM(δ), 80MHz
0
1
2
3
4
5
6
7
8
9
b+c
d
e+f
g
h
i
j
k

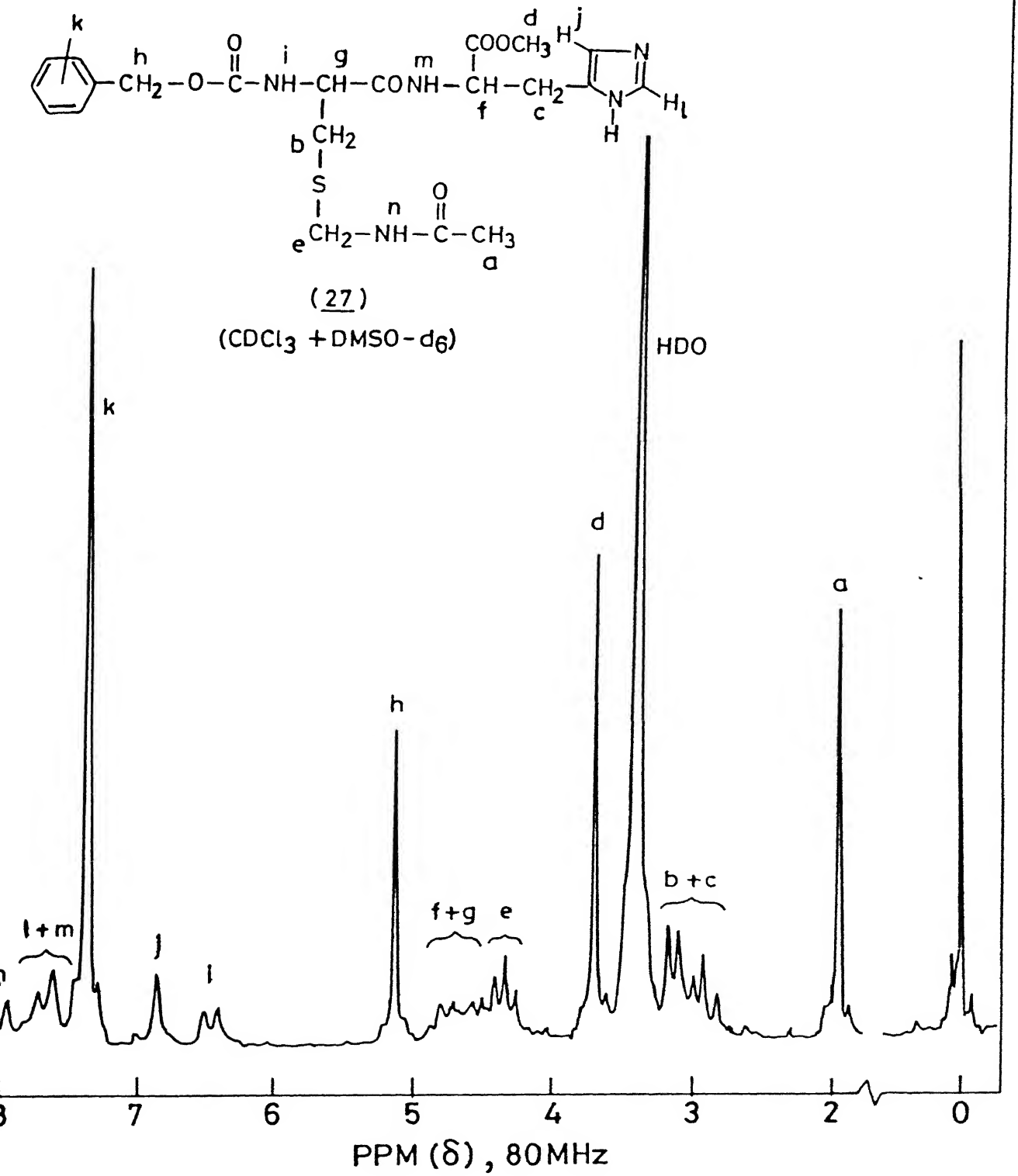
k
h
i
g
m
d
j
COOCH3
CH2–O–C–NH–CH–CONH–CH–CH2
b CH2
S
n
e CH2–NH–C–CH3
a
f
c
N
H
Hl
(27)
(CDCl3 + DMSO-d6)
HDO
k
d
a
h
b + c
f + g
e
l + m
j
l
n
8
7
6
5
4
3
2
0
PPM (δ), 80MHz

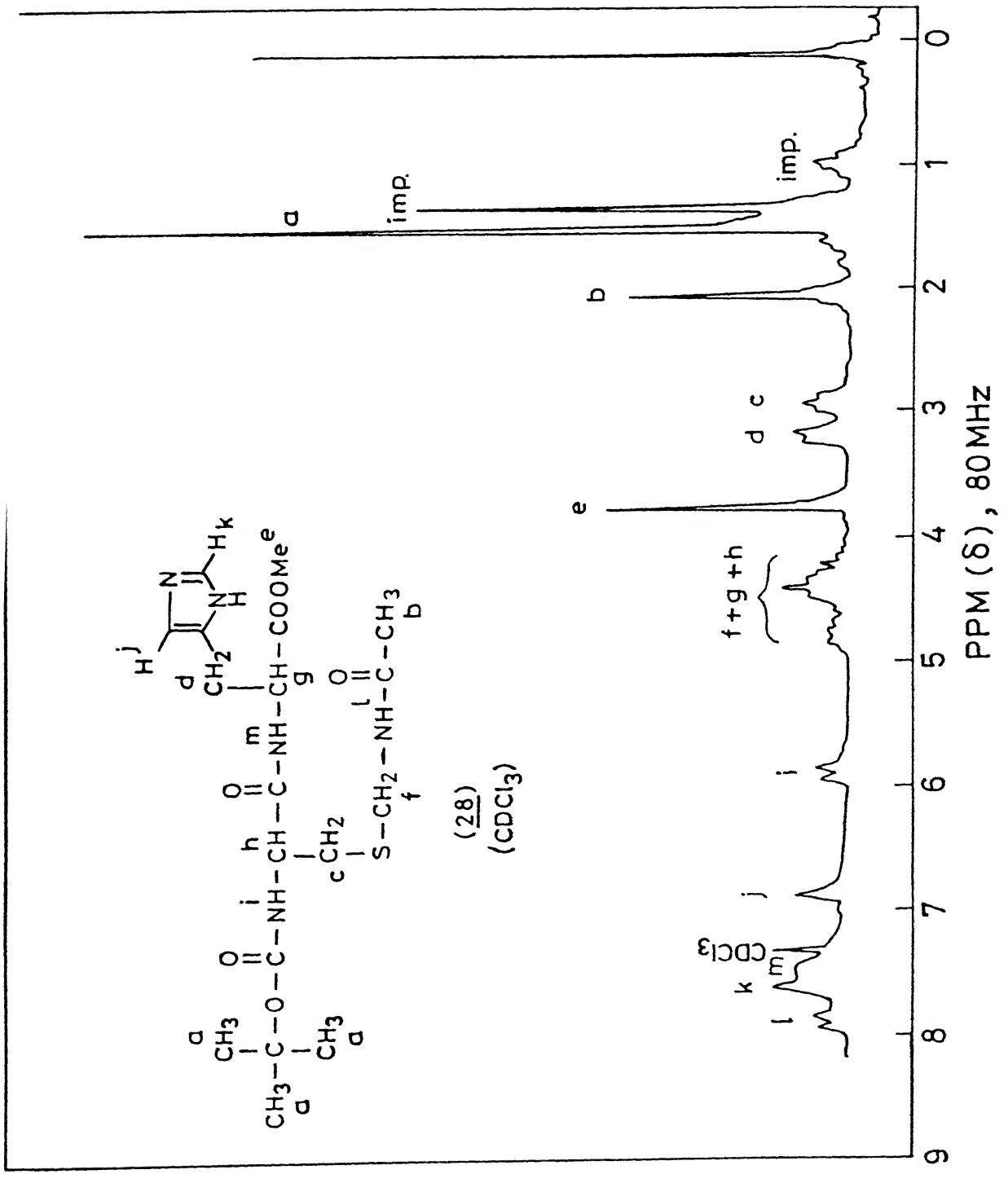
(28)
(CDCl3)
PPM (δ), 80 MHz
imp.
imp.
CDCl3
f+g+h

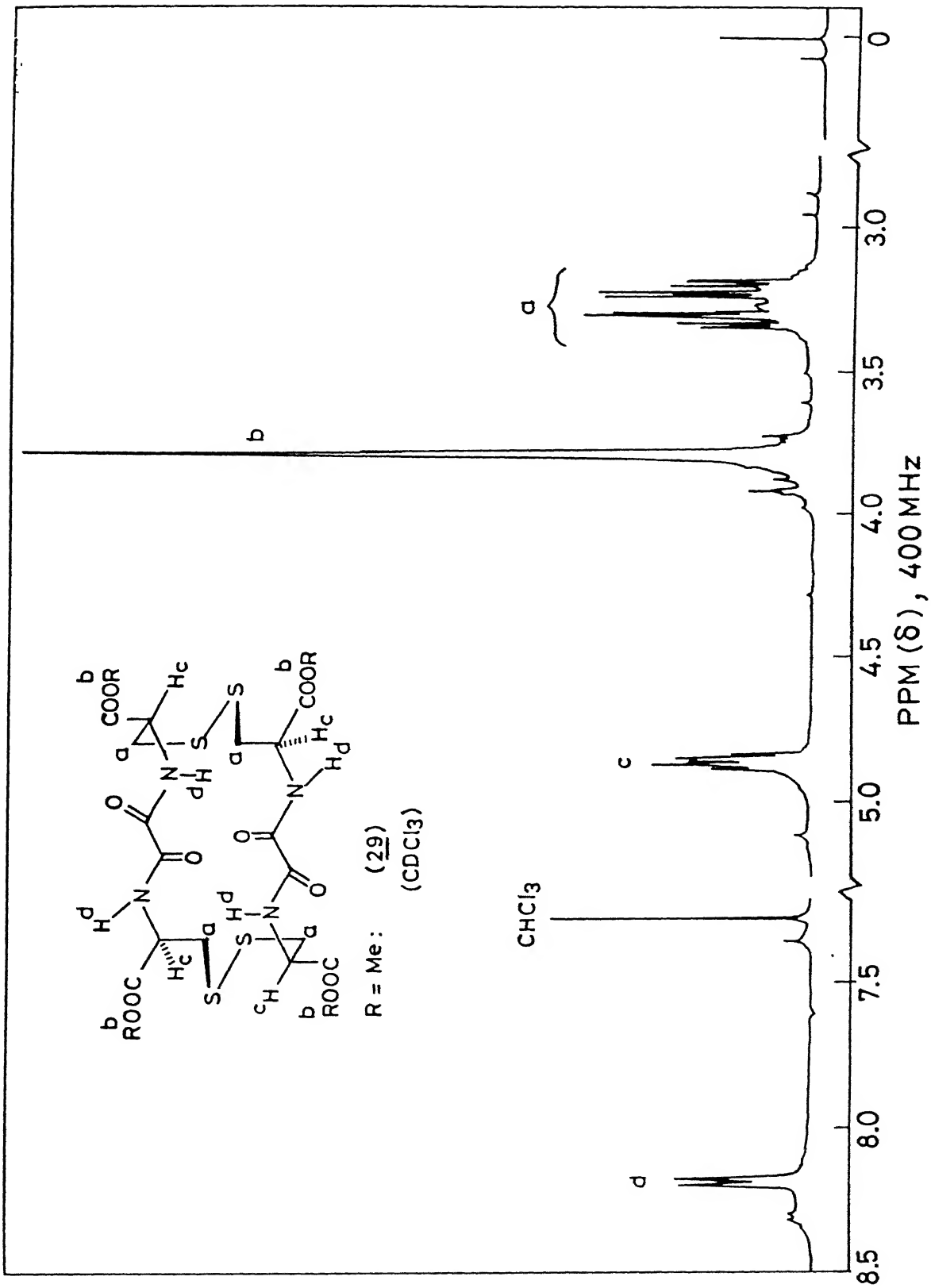
R = Me: (29)
(CDCl3)
CHCl3
PPM (δ), 400 MHz
0
3.0
3.5
4.0
4.5
5.0
7.5
8.0
8.5
a
b
c
d

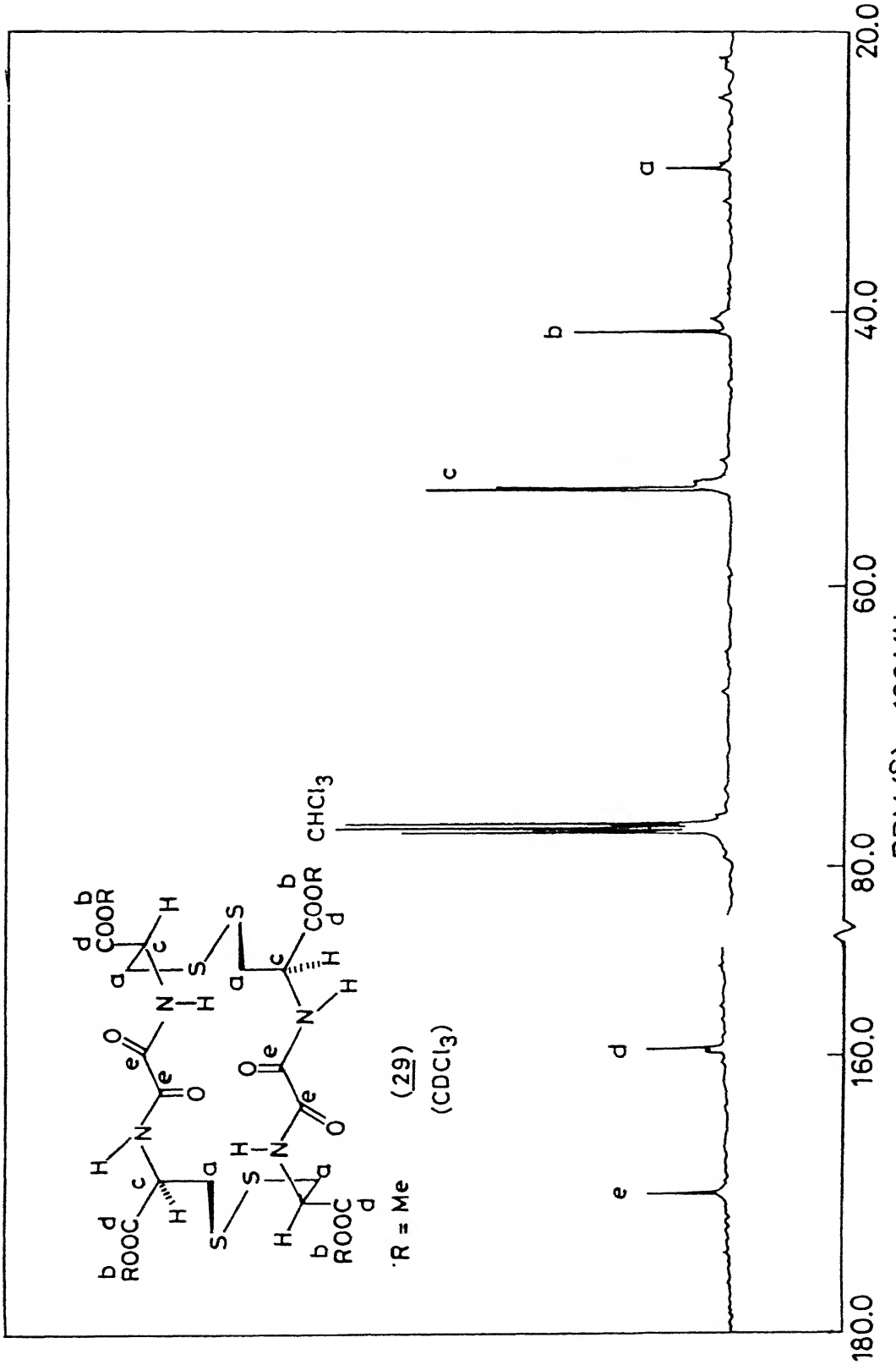
R = Me
(29)
(CDCl3)
CHCl3
a
b
c
d
e
20.0
40.0
60.0
80.0
160.0
180.0
PPM (δ), 100MHz

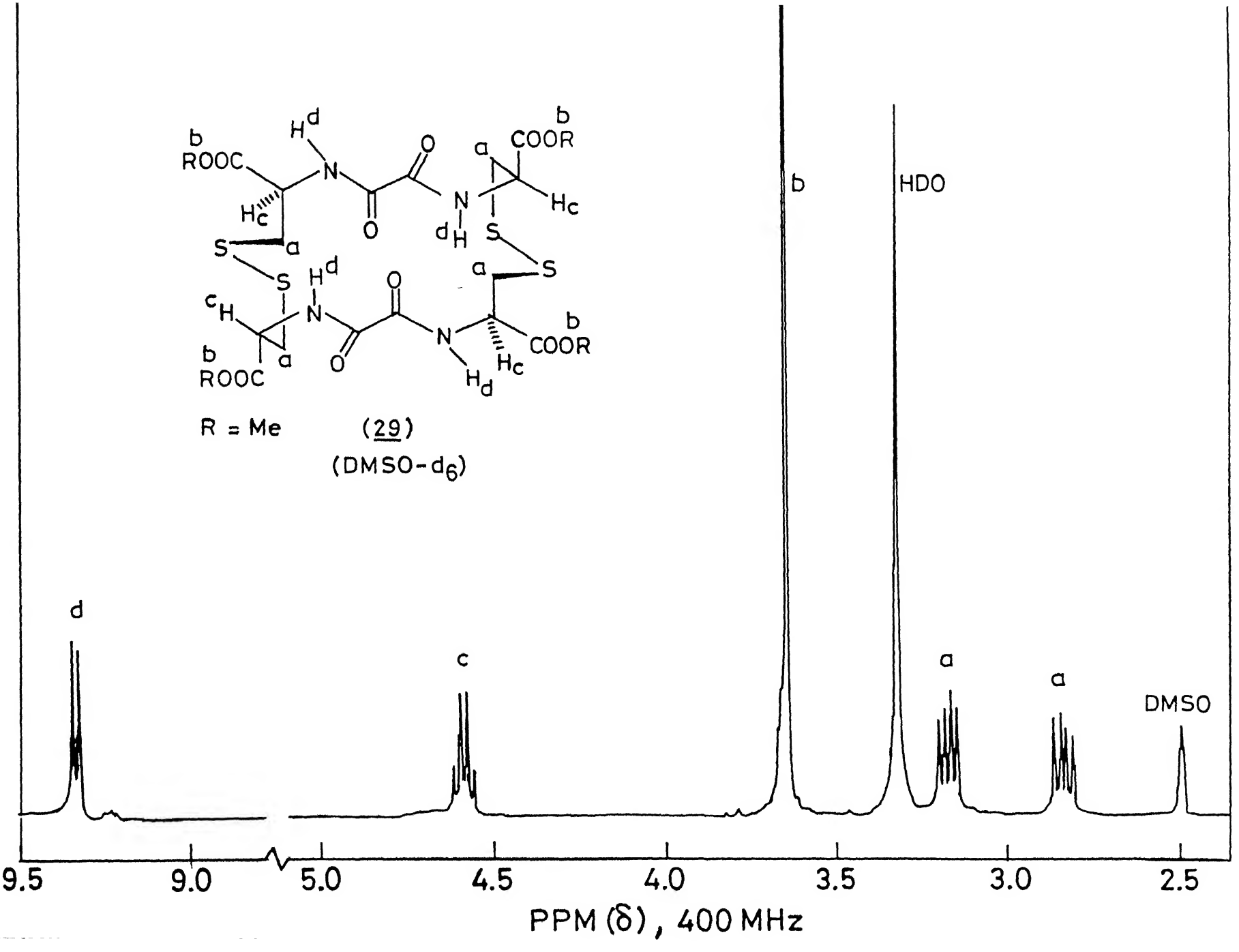
R = Me
(29)
(DMSO-d6)
d
c
b
HDO
a
a
DMSO
9.5
9.0
5.0
4.5
4.0
3.5
3.0
2.5
PPM (δ), 400 MHz

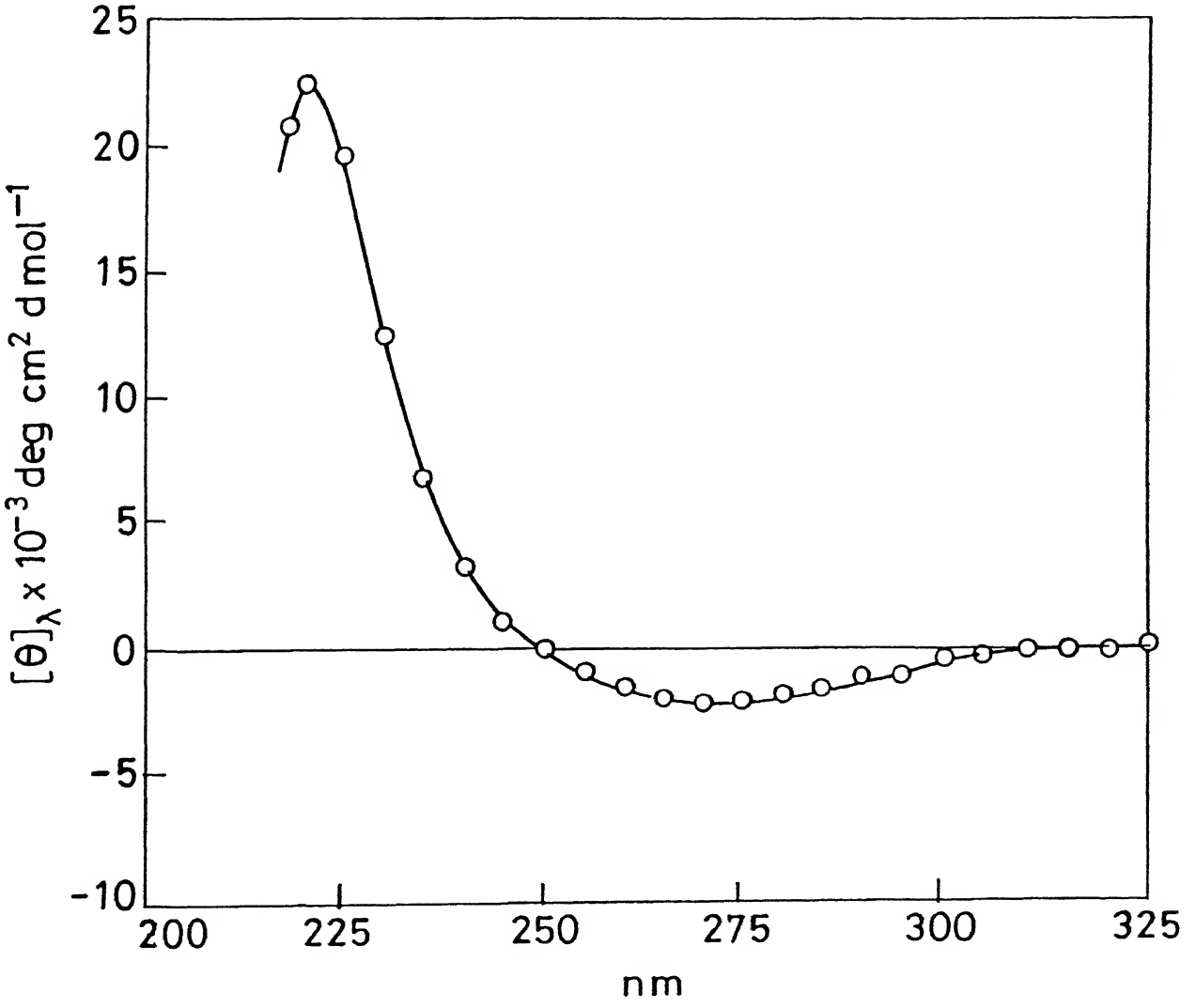

CD spectra of cyclo[bisoxalyl cystine-di-OMe](29) in EtOH

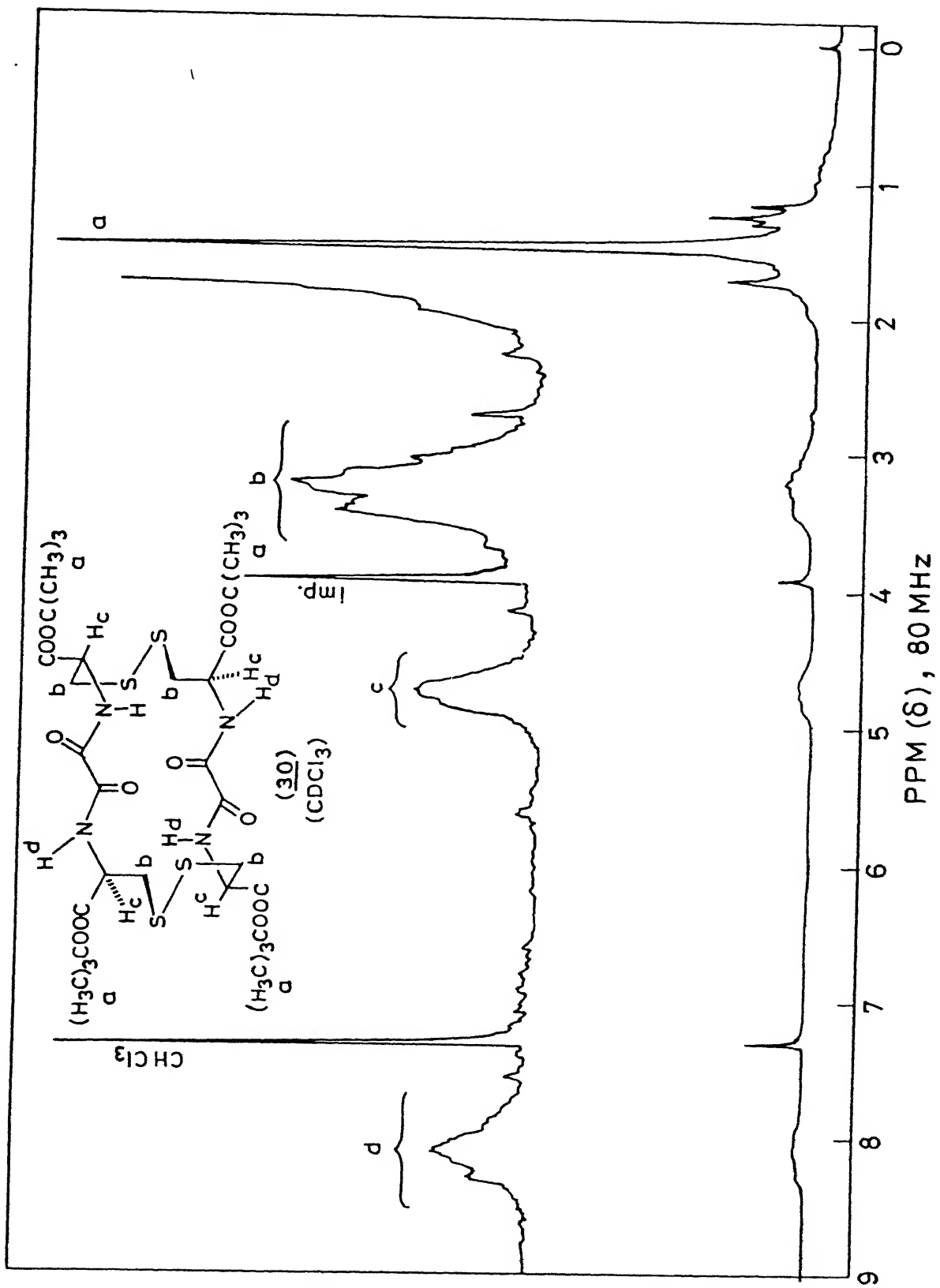
PPM (δ), 80 MHz
0
1
2
3
4
5
6
7
8
9
a
b
c
d
imp.
CHCl3
(30)
(CDCl3)
(H3C)3COOC
COOC(CH3)3
Hc
Hd
N
S
O

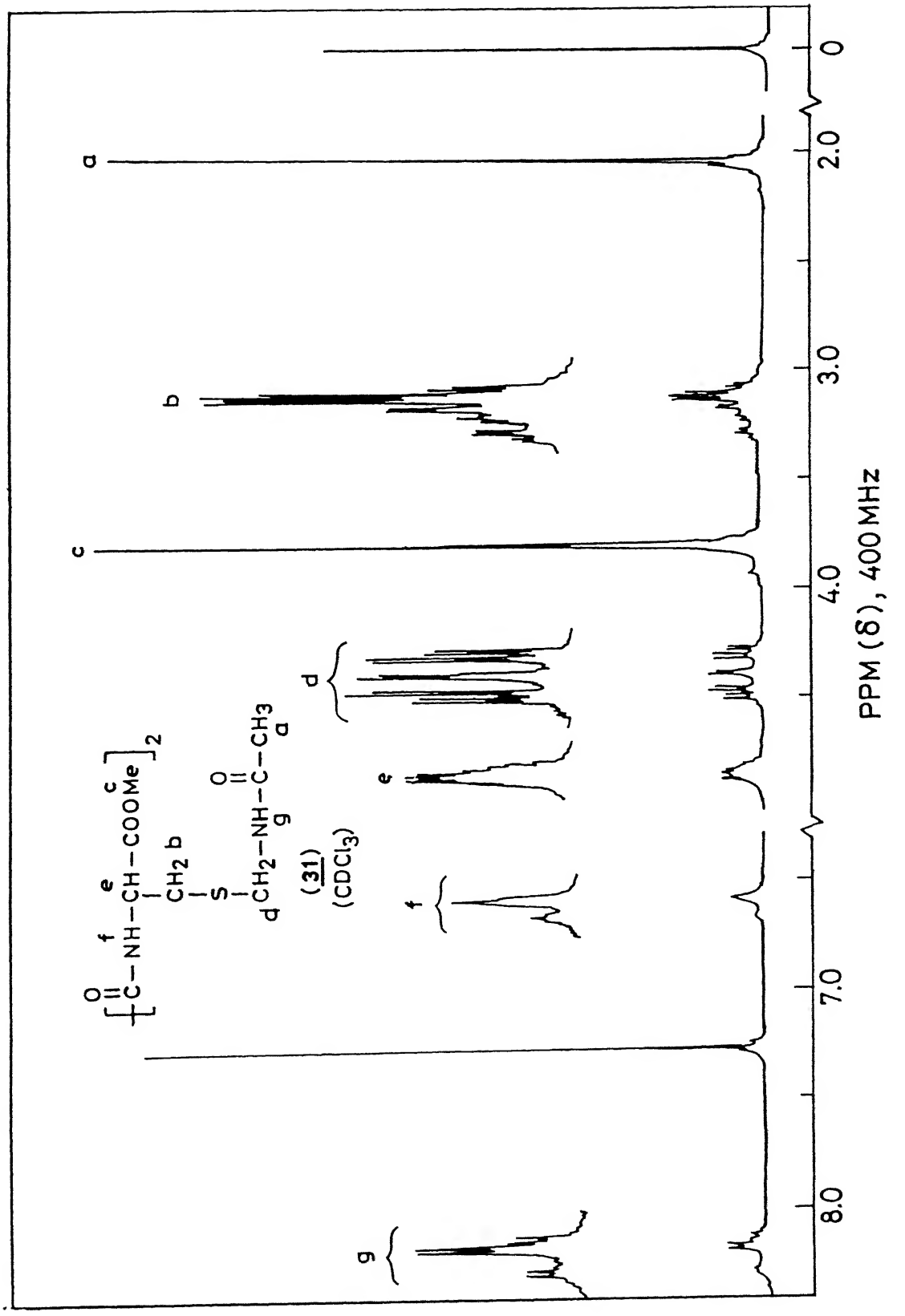
(31)
(CDCl3)
PPM (δ), 400 MHz
8.0
7.0
4.0
3.0
2.0
0

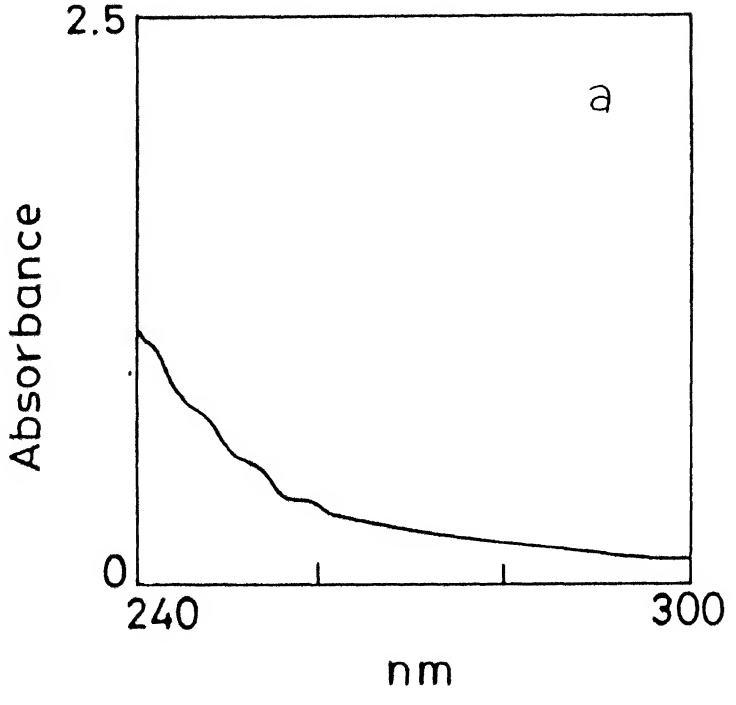

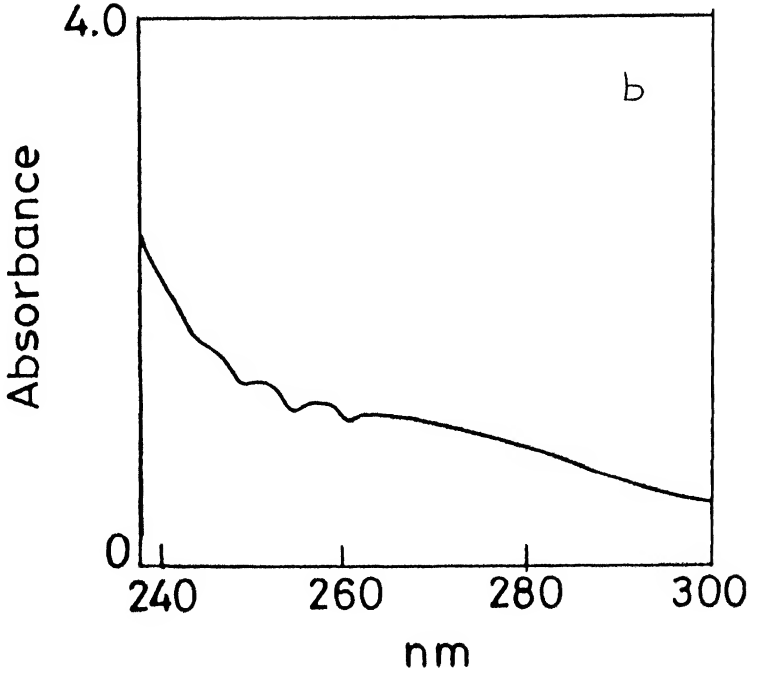

UV Spectrum of : a. Cyclo[bisoxalyl cystine-di-OMe] (29) in EtOH; b. Cyclo succinyl cystine-di-OMe (32)in EtOH

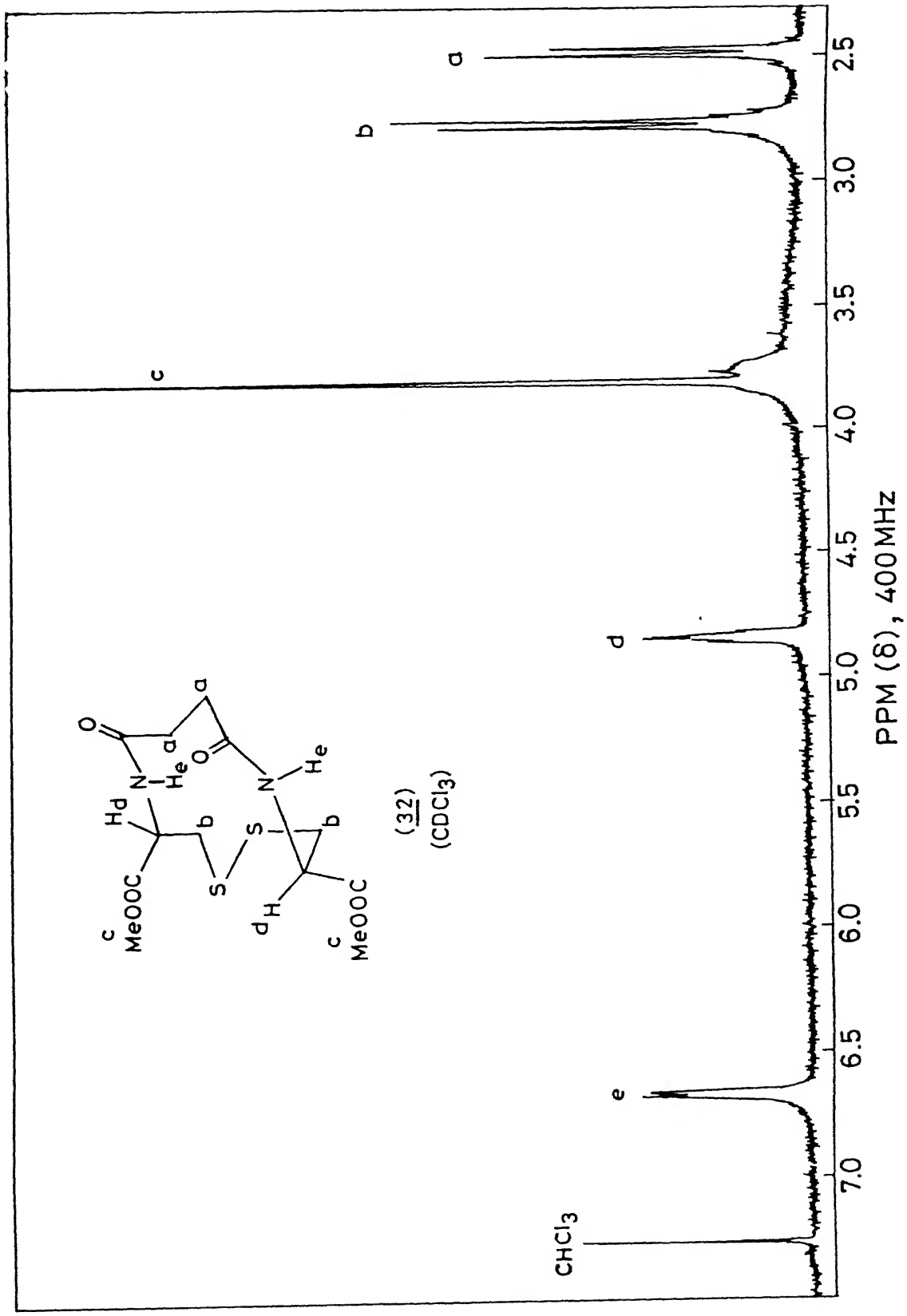
CHCl3
e
d
c
b
a
7.0
6.5
6.0
5.5
5.0
4.5
4.0
3.5
3.0
2.5
PPM (δ), 400MHz
(32)
(CDCl3)
MeOOC
MeOOC
Hd
Hd
He
He
O
O
N
N
S
S

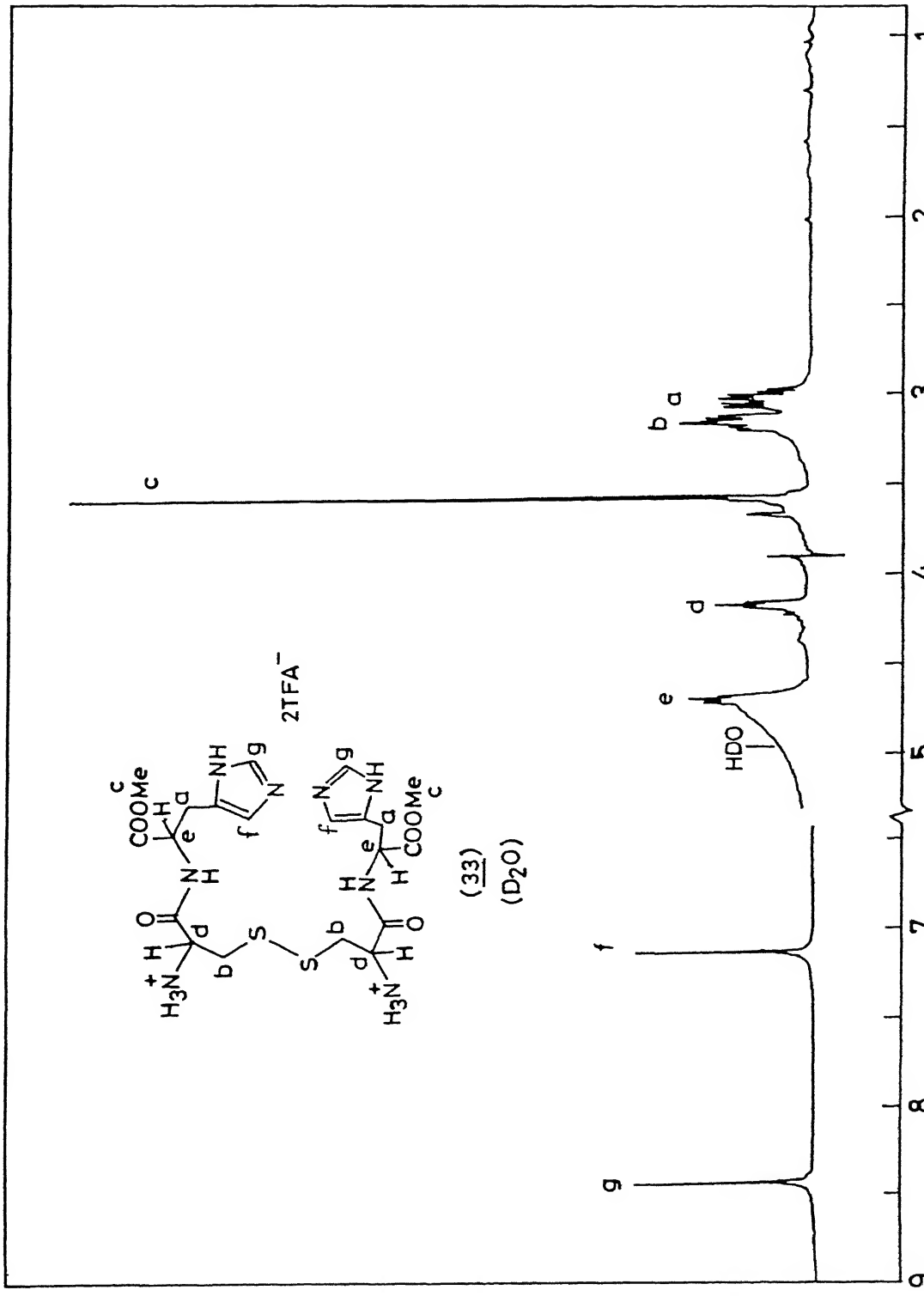
c
b a
e
d
HDO
f
g
9
8
7
6
5
4
3
2
1
PPM (δ), 400 MHz
2TFA⁻
(33)
(D2O)

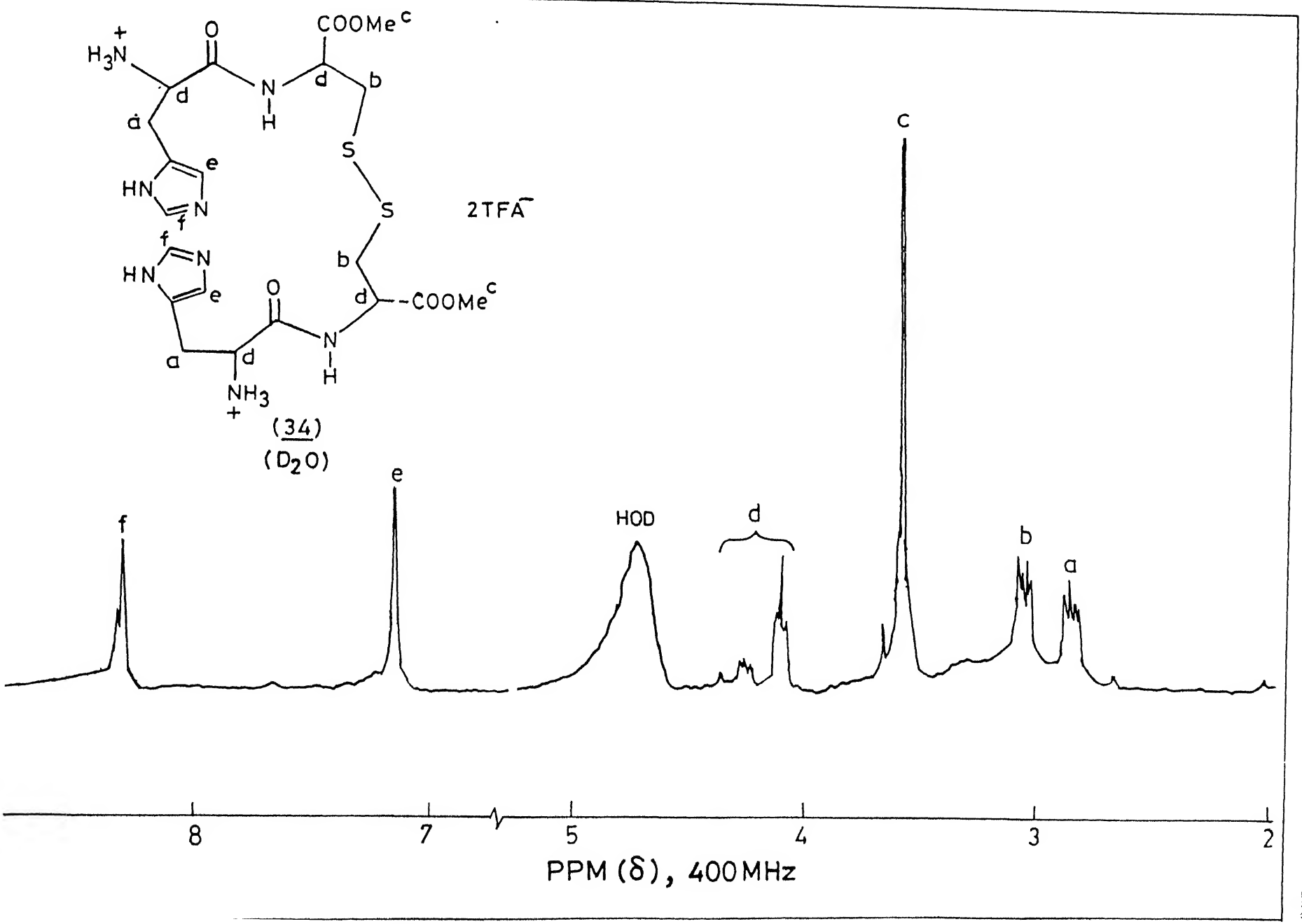
COOMe
2TFA⁻
(34)
(D2O)
c
e
HOD
d
b
a
f
8
7
5
4
3
2
PPM (δ), 400MHz

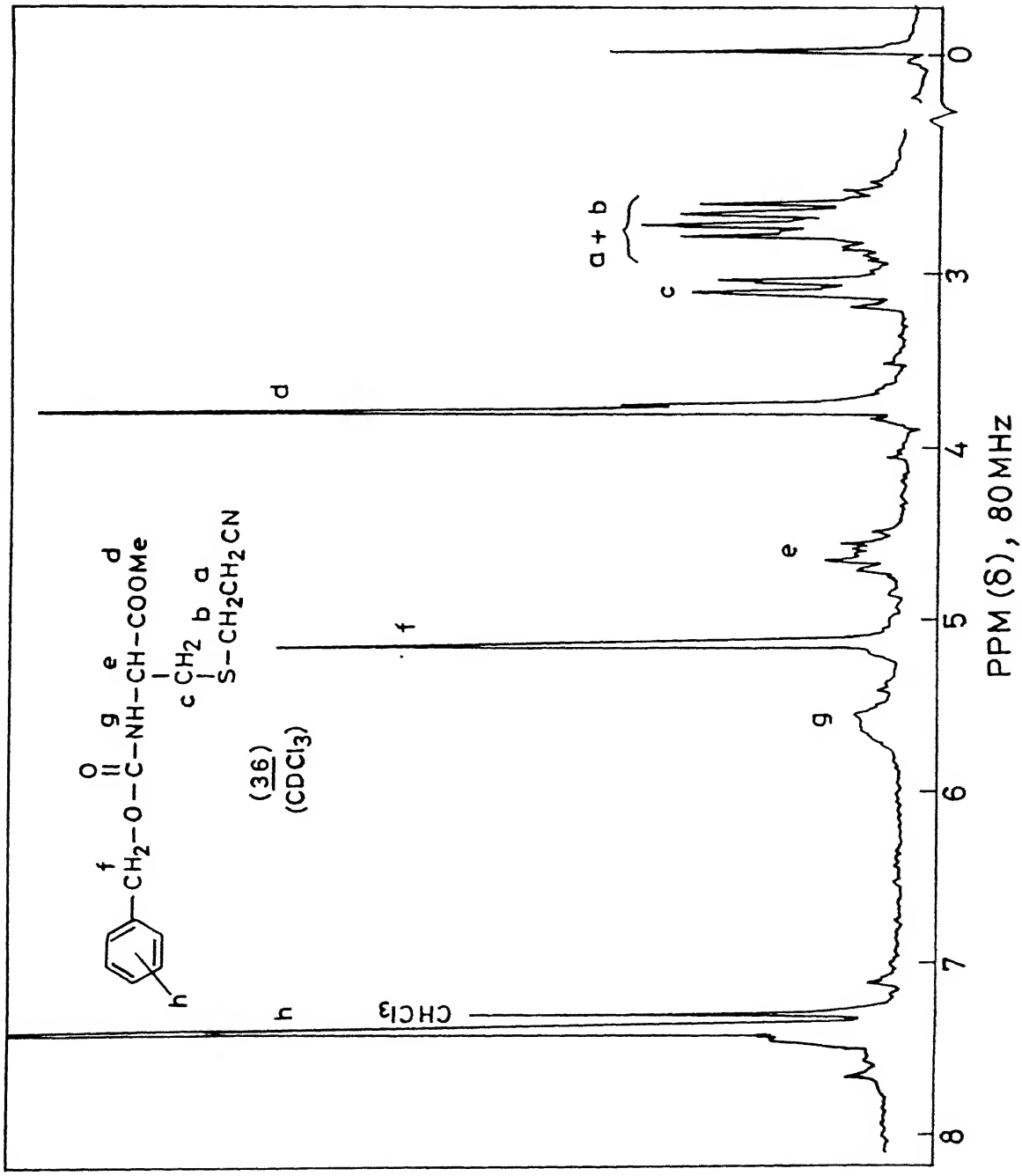
(36)
(CDCl3)
CHCl3
PPM (δ), 80 MHz
a + b
c
d
e
f
g
h

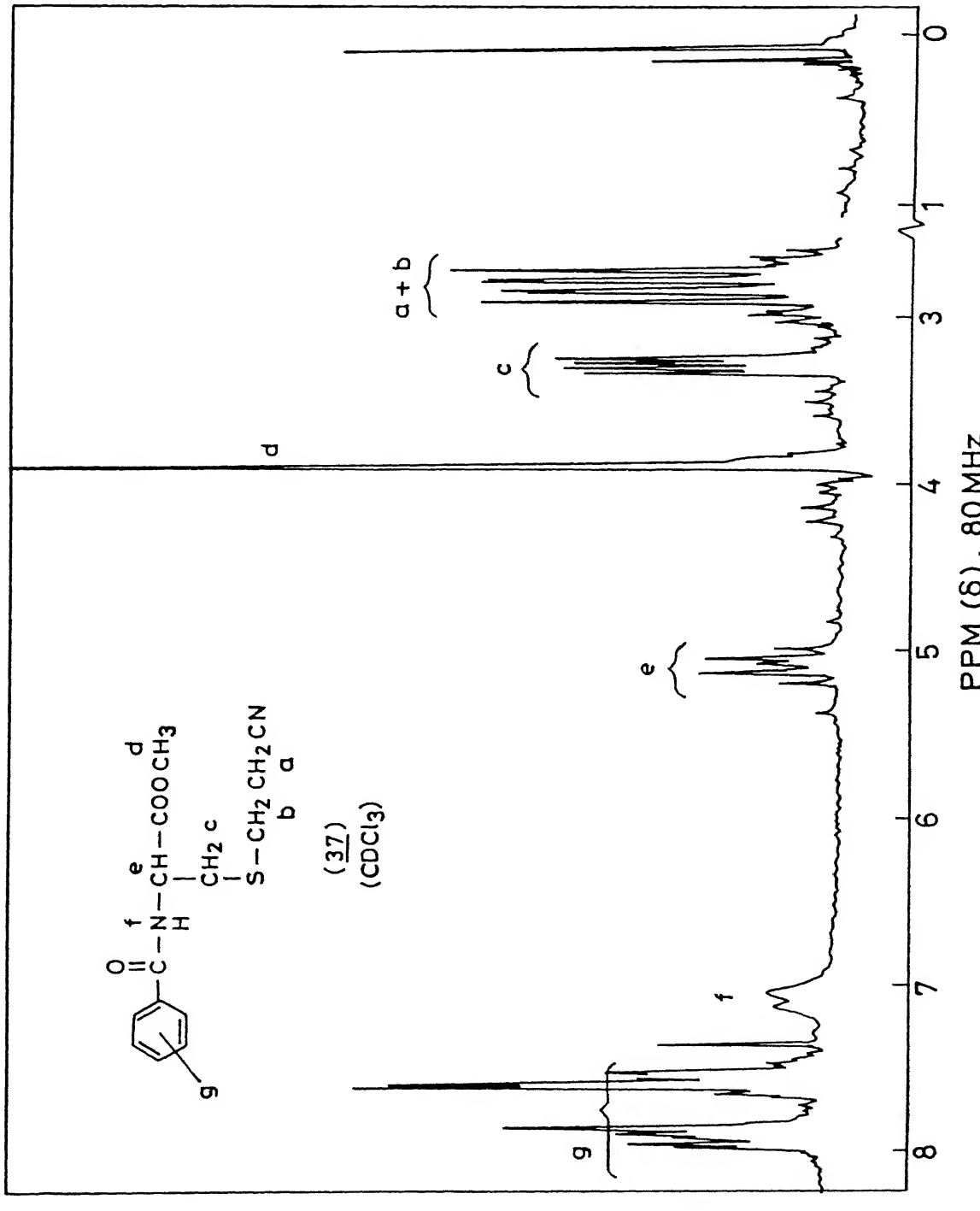
(37)
(CDCl3)
S—CH2 CH2 CN
b a
CH2 c
H
C—N—CH—COOCH3
O
f e d
g
d
a + b
c
e
f
g
0
1
3
4
5
6
7
8
PPM (δ), 80 MHz

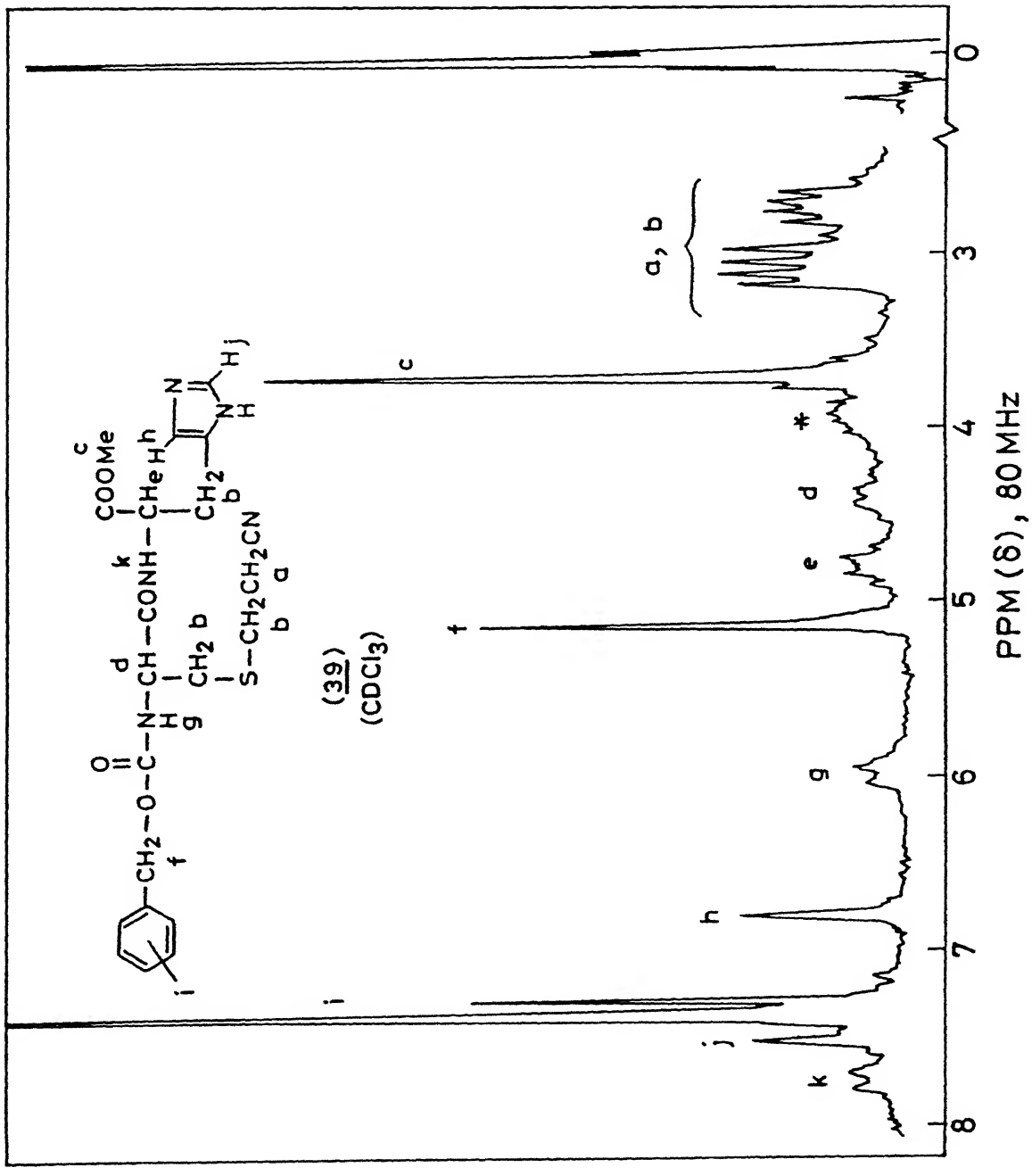
(39)
(CDCl3)
PPM (δ), 80 MHz
0
3
4
5
6
7
8
a, b
c
d
e
f
g
h
i
j
k
*

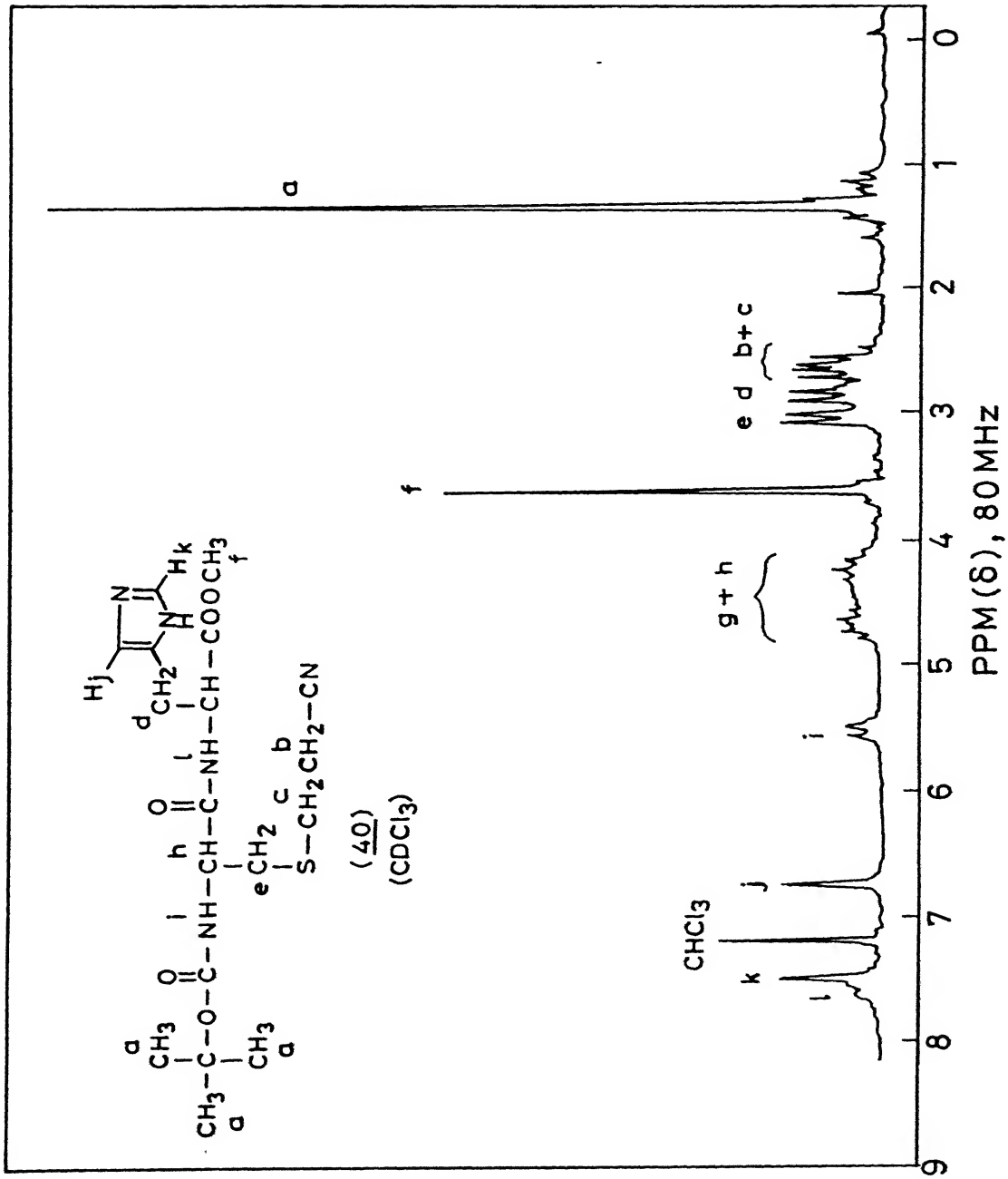
(40)
(CDCl3)
CHCl3
PPM(δ), 80 MHz

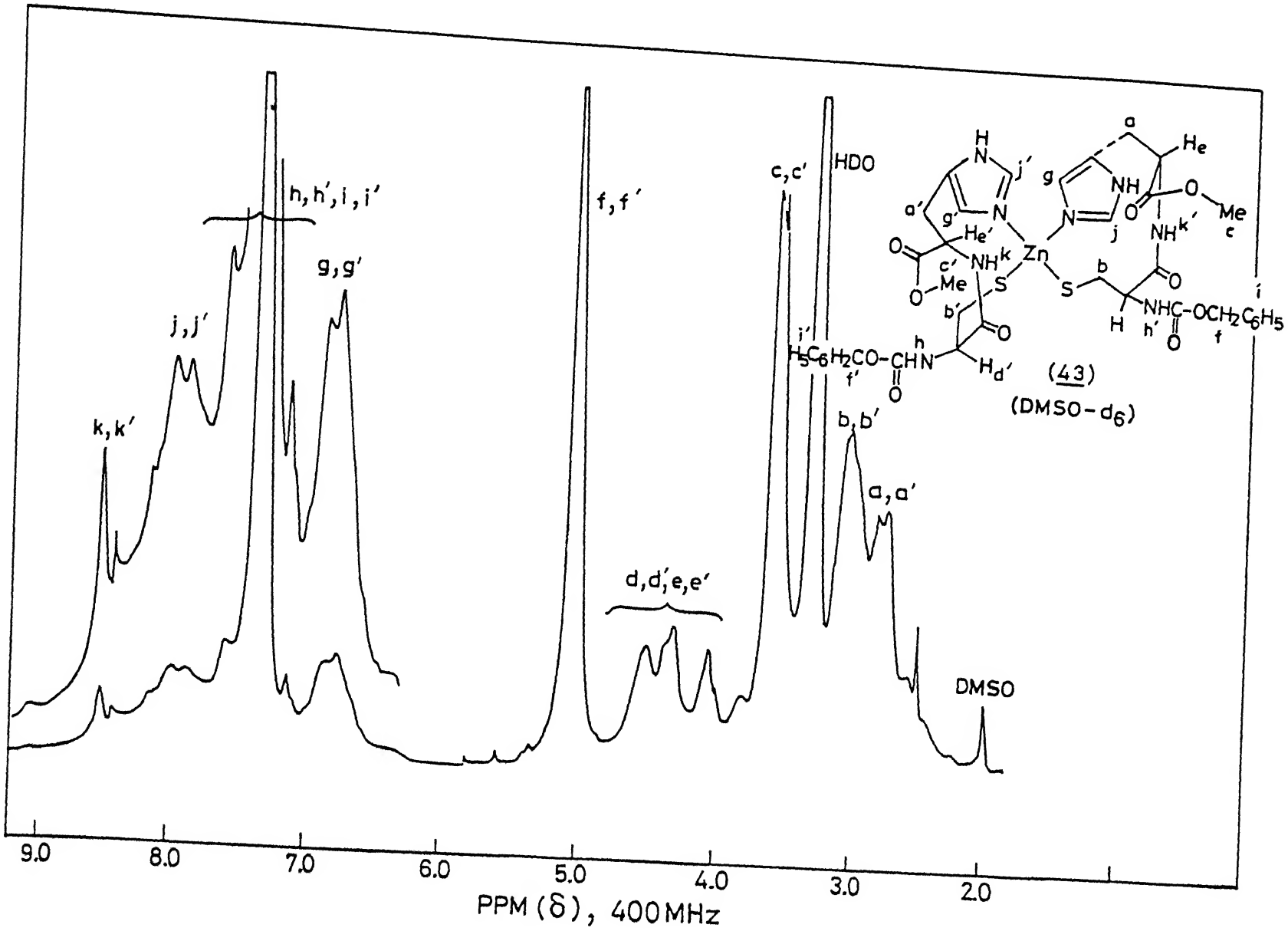
k,k′
j,j′
h,h′,i,i′
g,g′
f,f′
d,d′,e,e′
c,c′
HDO
b,b′
a,a′
DMSO
9.0
8.0
7.0
6.0
5.0
4.0
3.0
2.0
PPM (δ), 400MHz
(43)
(DMSO-d6)

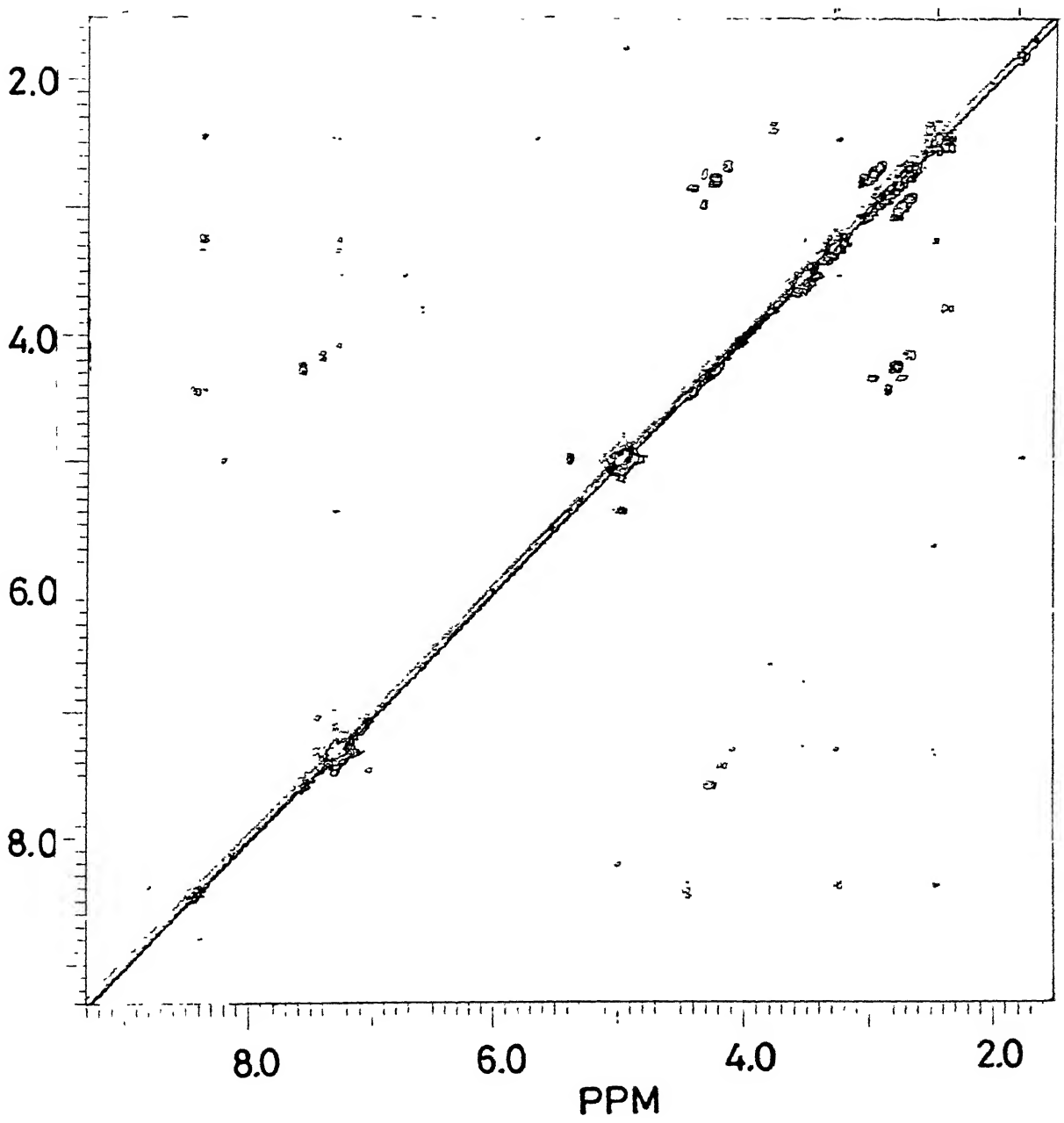

COSY Spectrum of (400MHz) of $(Z\text{-Cys-His-OMe})_2Zn^{II}$ (43) in DMSO-d_6

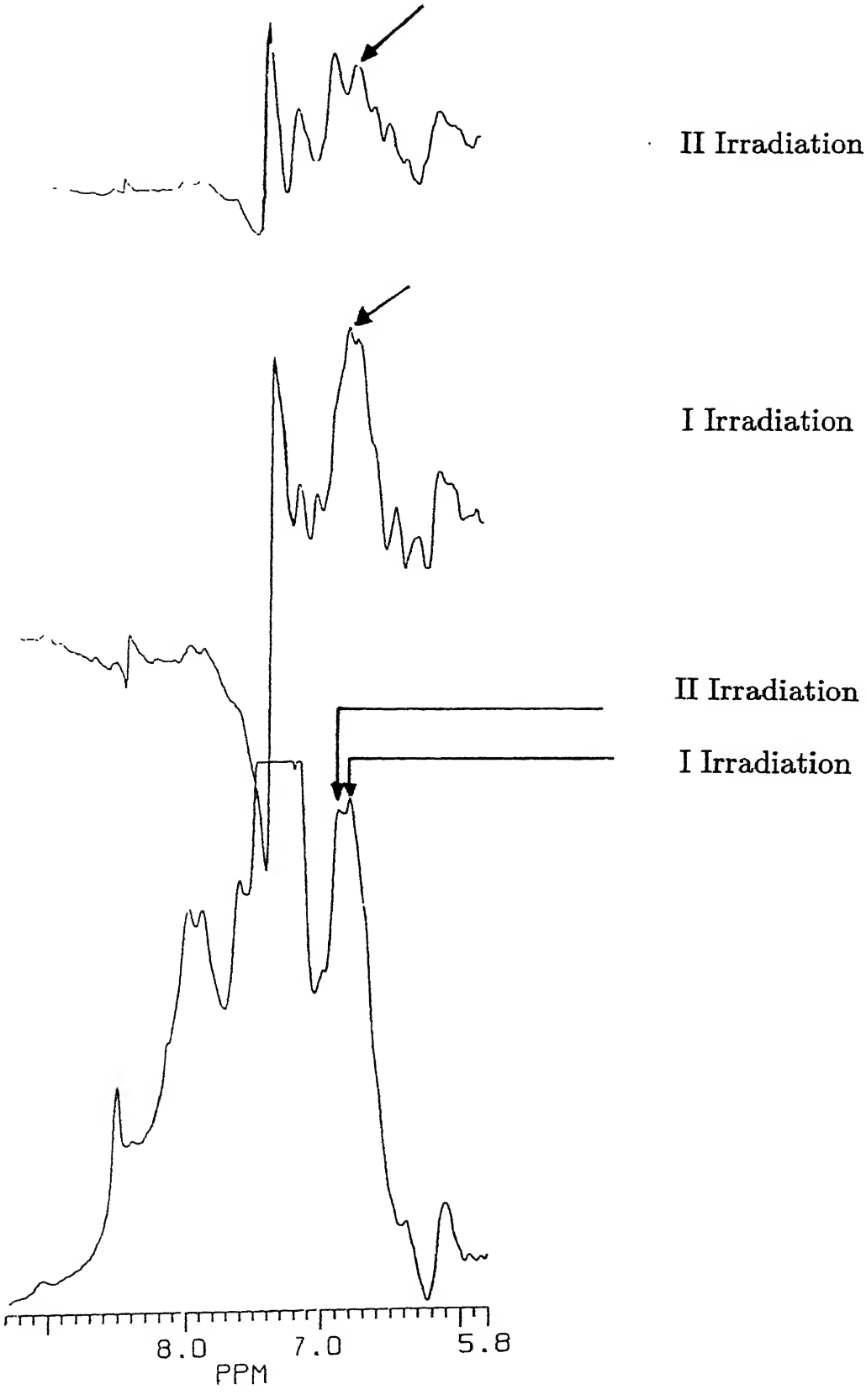

NOe Difference spectrum of (Z-Cys-His-OMe)$_2$Zn^{II} complex (43). The irradiated protons are denoted in the normal spectrum. The arrows in the difference spectrum denote the enhancement protons.

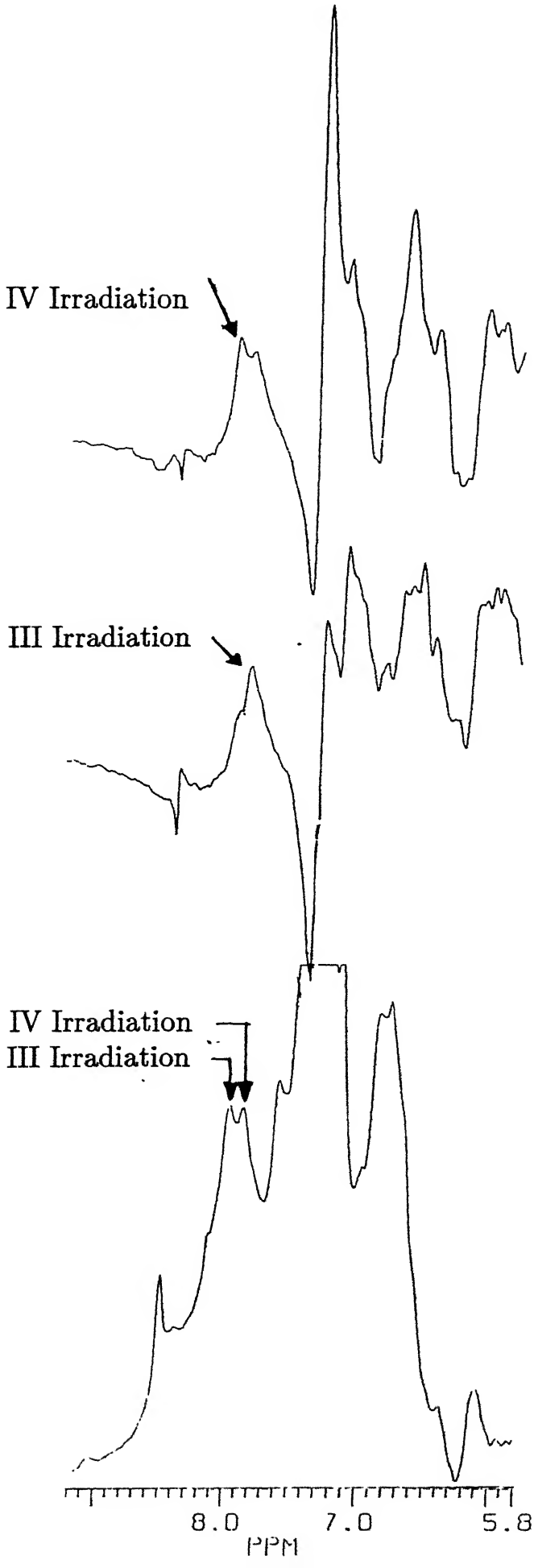
IV Irradiation
III Irradiation
IV Irradiation
III Irradiation
8.0
7.0
5.8
PPM

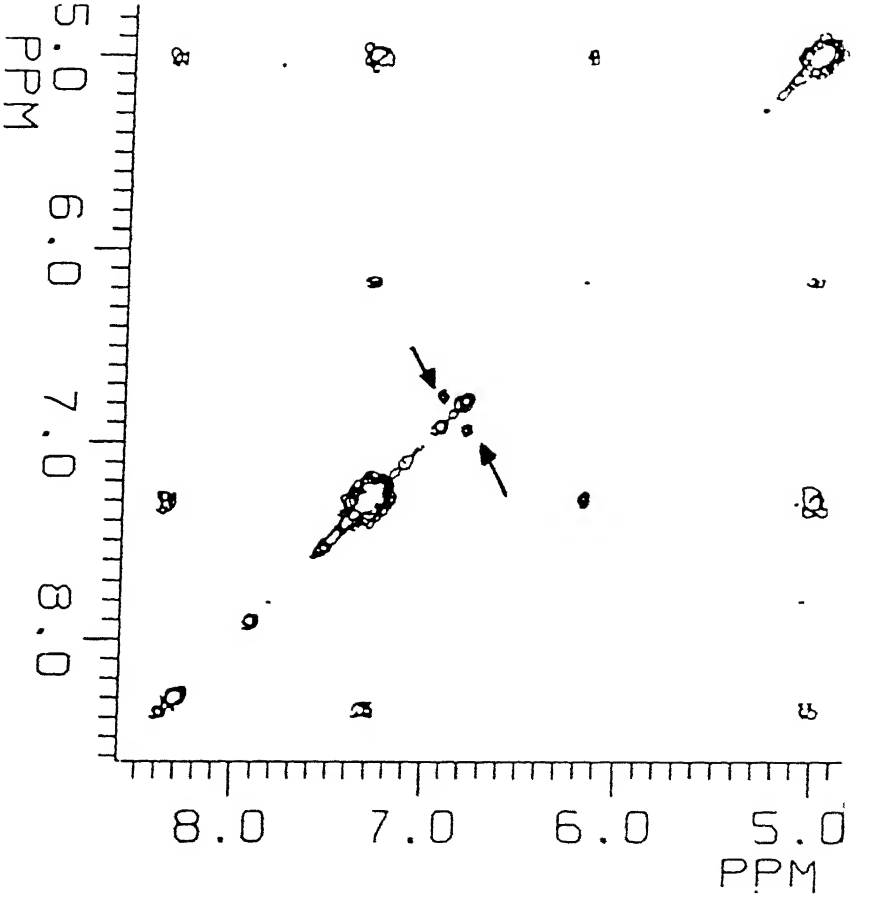

NOESY Spectrum (400MHz) of (Z-Cys-His-OMe)$_2$Zn^{II} (<u>43</u>) in DMSO-d$_6$. The arrows indicate the observed NOESY cross peaks, corresponding to the 4,4'- His protons

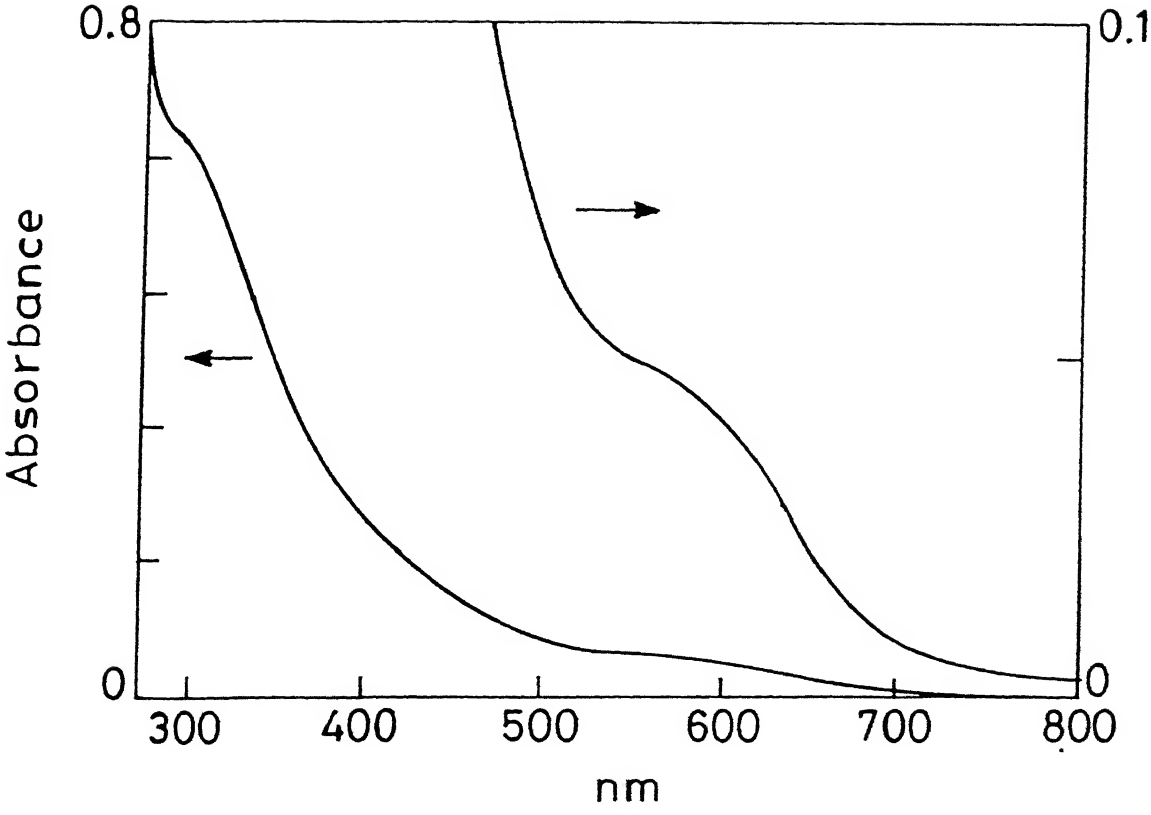

UV Spectrum of $(Z\text{-Cys-His-OMe})_2Co^{II}$ complex (44) in DMF

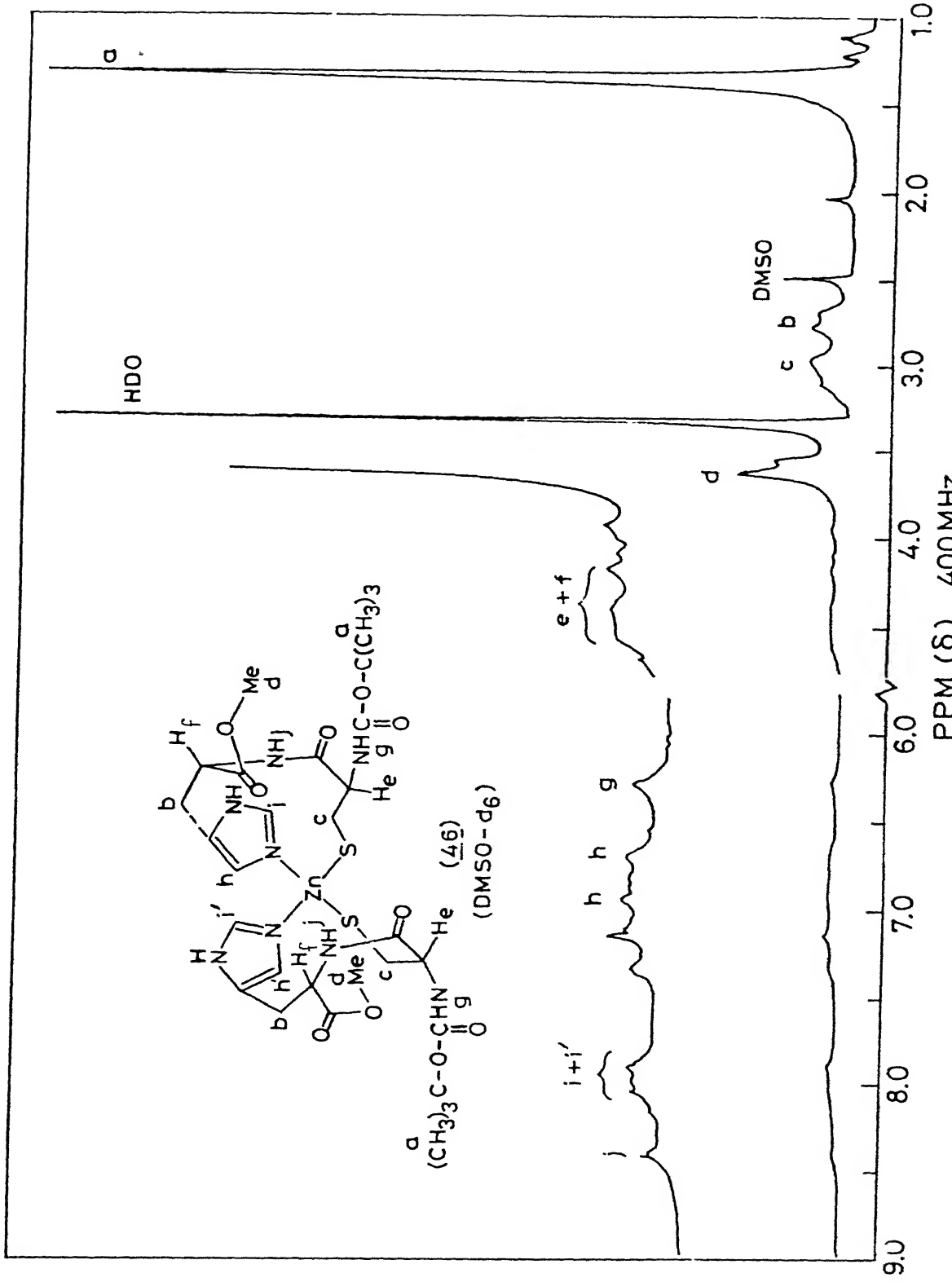
HDO
DMSO
PPM (δ), 400MHz
1.0
2.0
3.0
4.0
6.0
7.0
8.0
9.0
(4b)
(DMSO-d6)

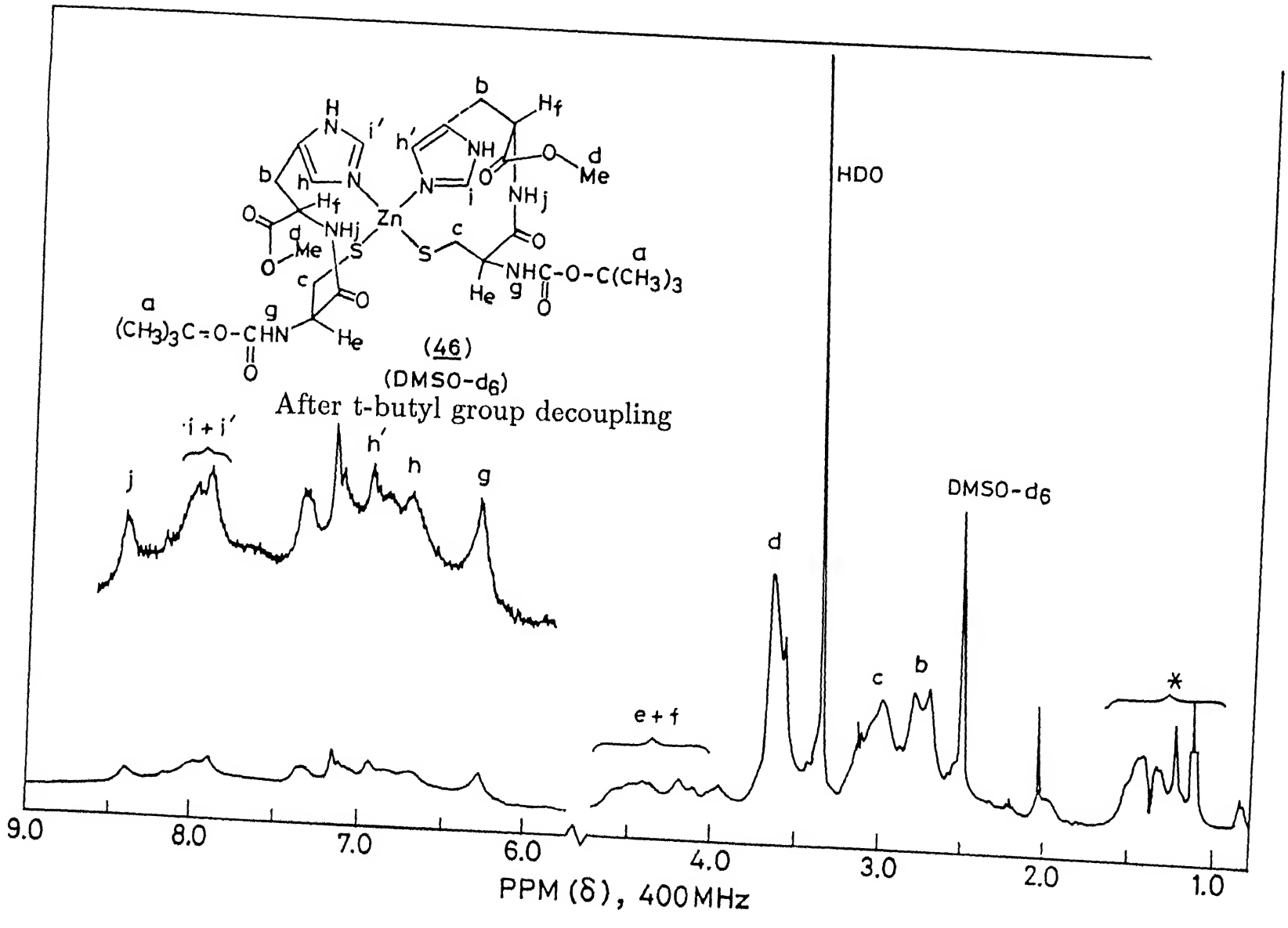
HDO
DMSO-d6
(46)
(DMSO-d6)
After t-butyl group decoupling
i + i′
j
h′
h
g
d
c
b
e + f
*
9.0
8.0
7.0
6.0
4.0
3.0
2.0
1.0
PPM (δ), 400MHz

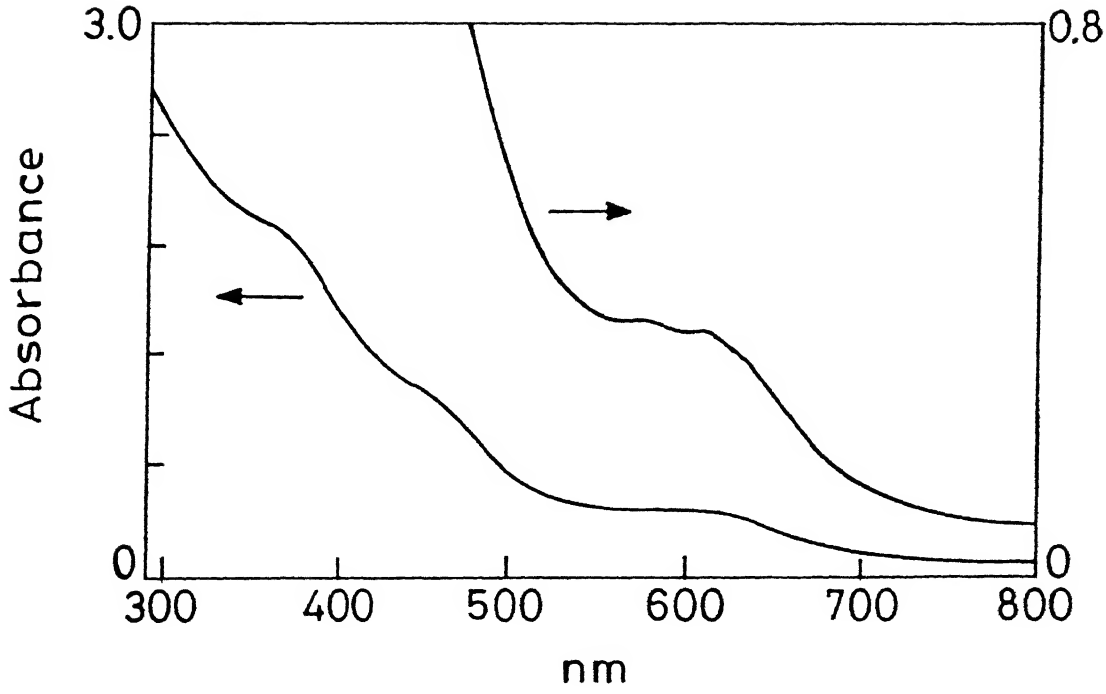

UV Spectrum of $(Boc\text{-}Cys\text{-}His\text{-}OMe)_2Co^{II}$ complex (47) in DMF

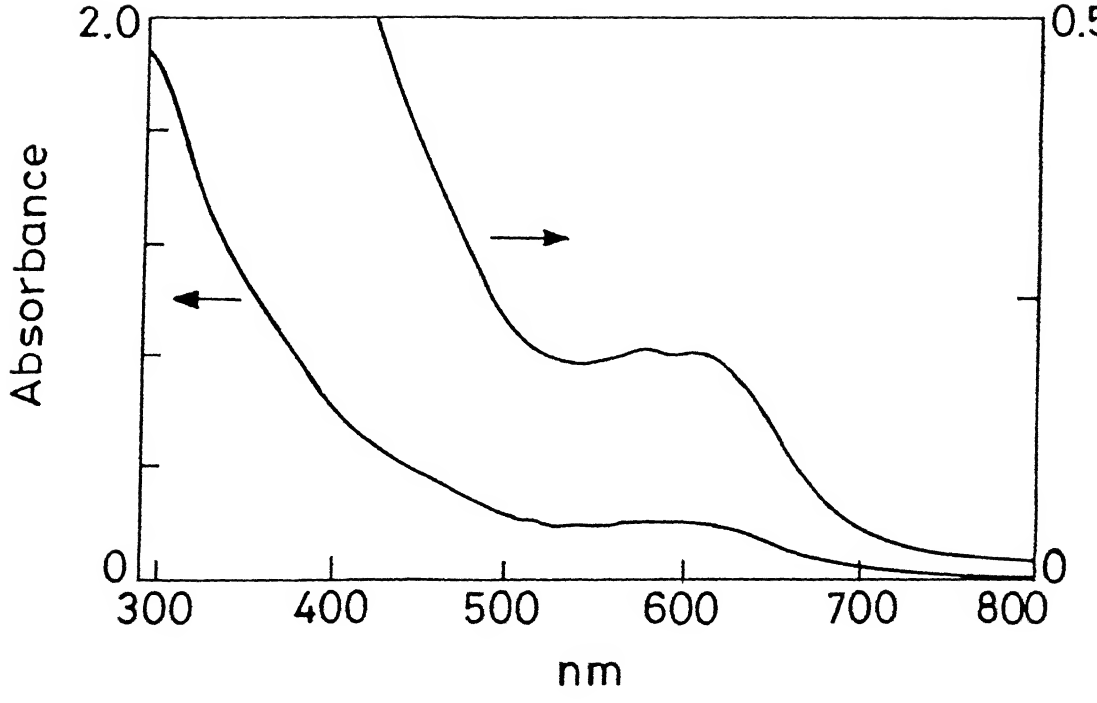

UV Spectrum of (Boc-His-Cys-OMe)$_2$Co^{II} complex (50) in DMF

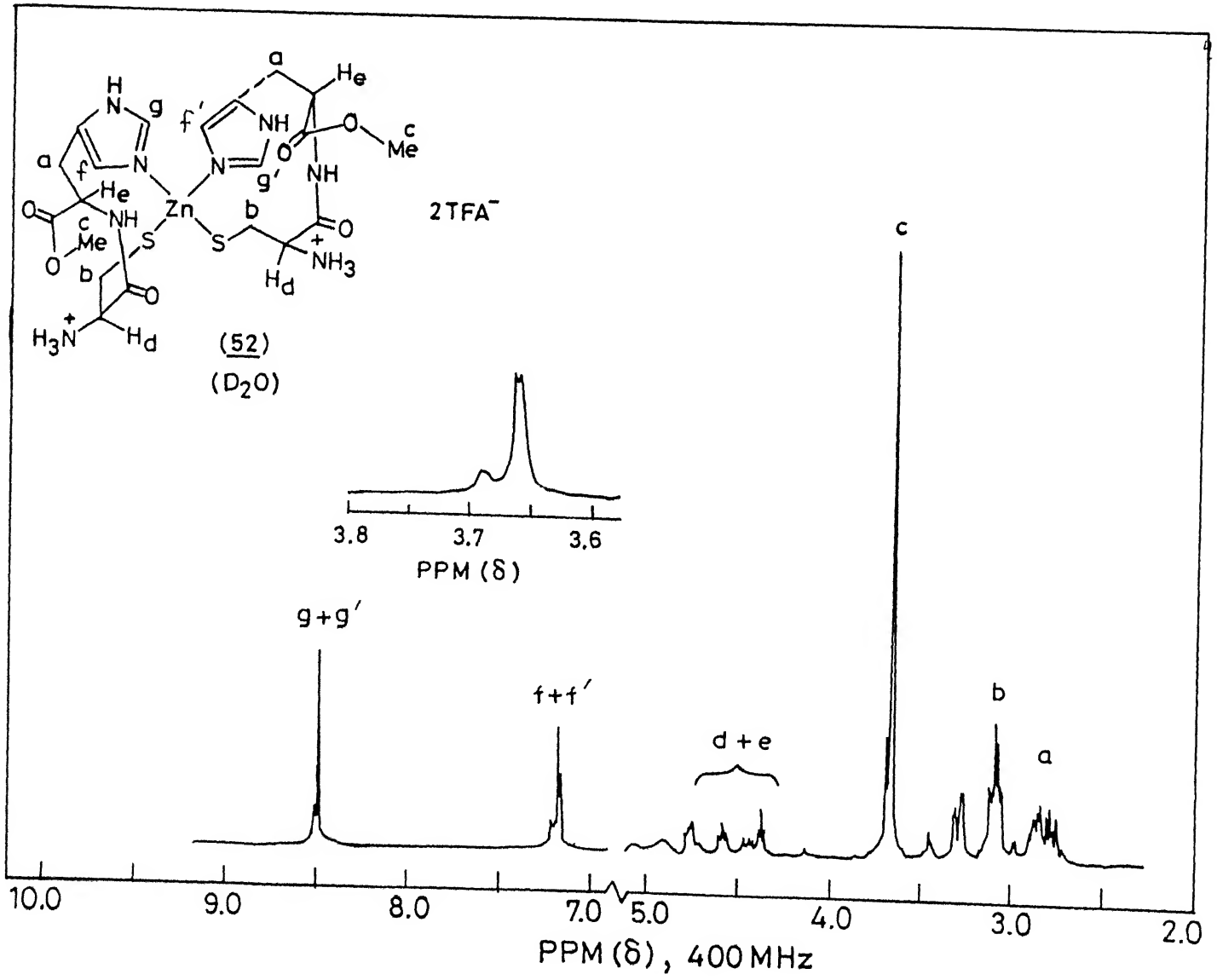
2TFA⁻
(52)
(D2O)
3.8
3.7
3.6
PPM (δ)
g+g′
f+f′
d + e
c
b
a
10.0
9.0
8.0
7.0
5.0
4.0
3.0
2.0
PPM (δ), 400 MHz

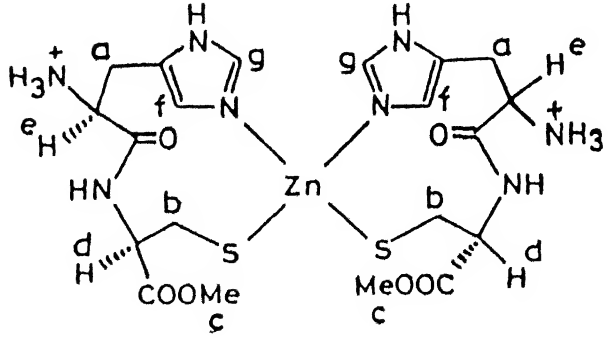
H
N
a
g
H_3N^+
f
N
e
H
O
HN
b
Zn
d
H
S
COOMe
c
g
f
a
H^e
NH_3^+
NH
MeOOC
2TFA⁻

(53)

(D_2O)

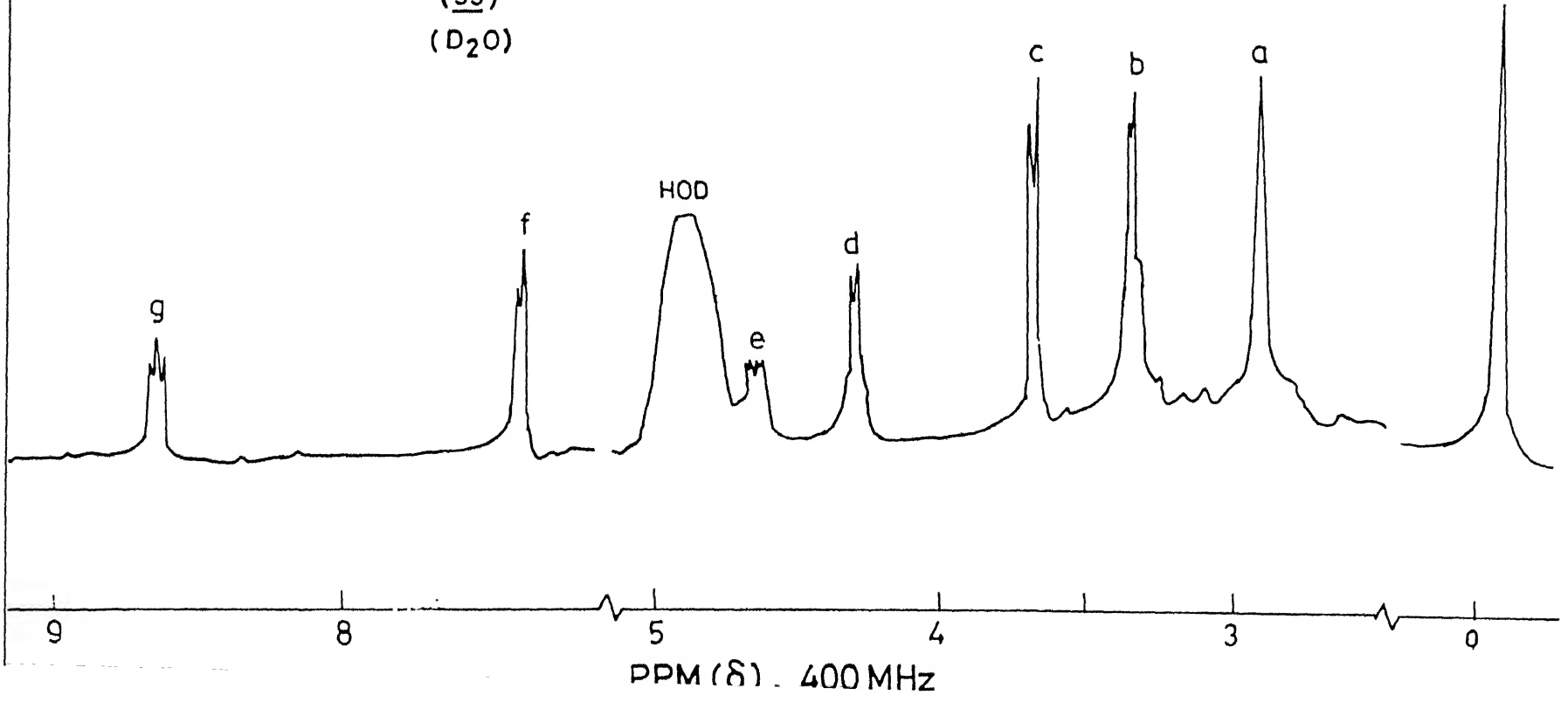
g
f
HOD
e
d
c
b
a
9
8
5
4
3
0
PPM (δ) . 400 MHz

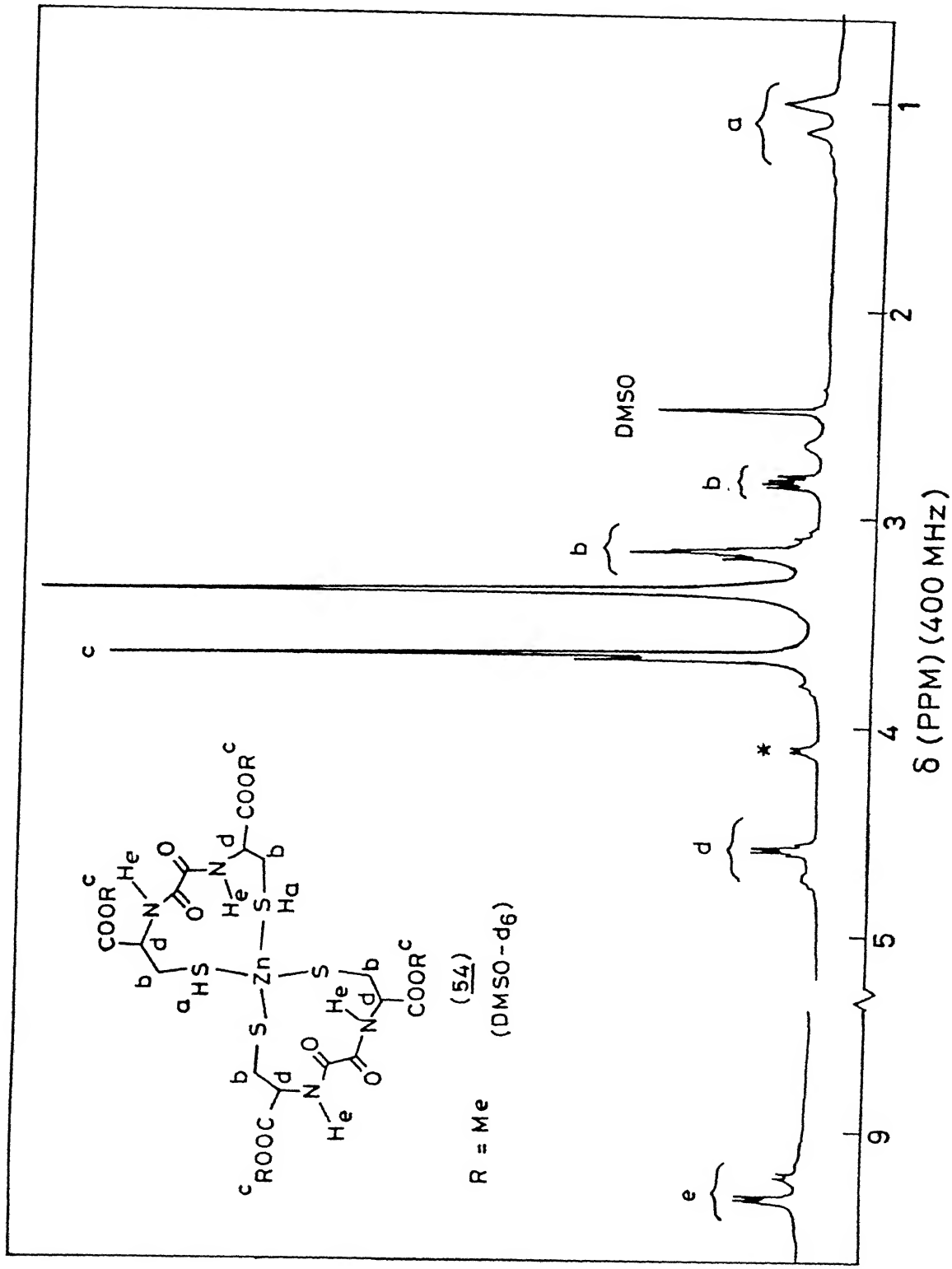
δ (PPM) (400 MHz)
DMSO
R = Me
(54)
(DMSO-d6)

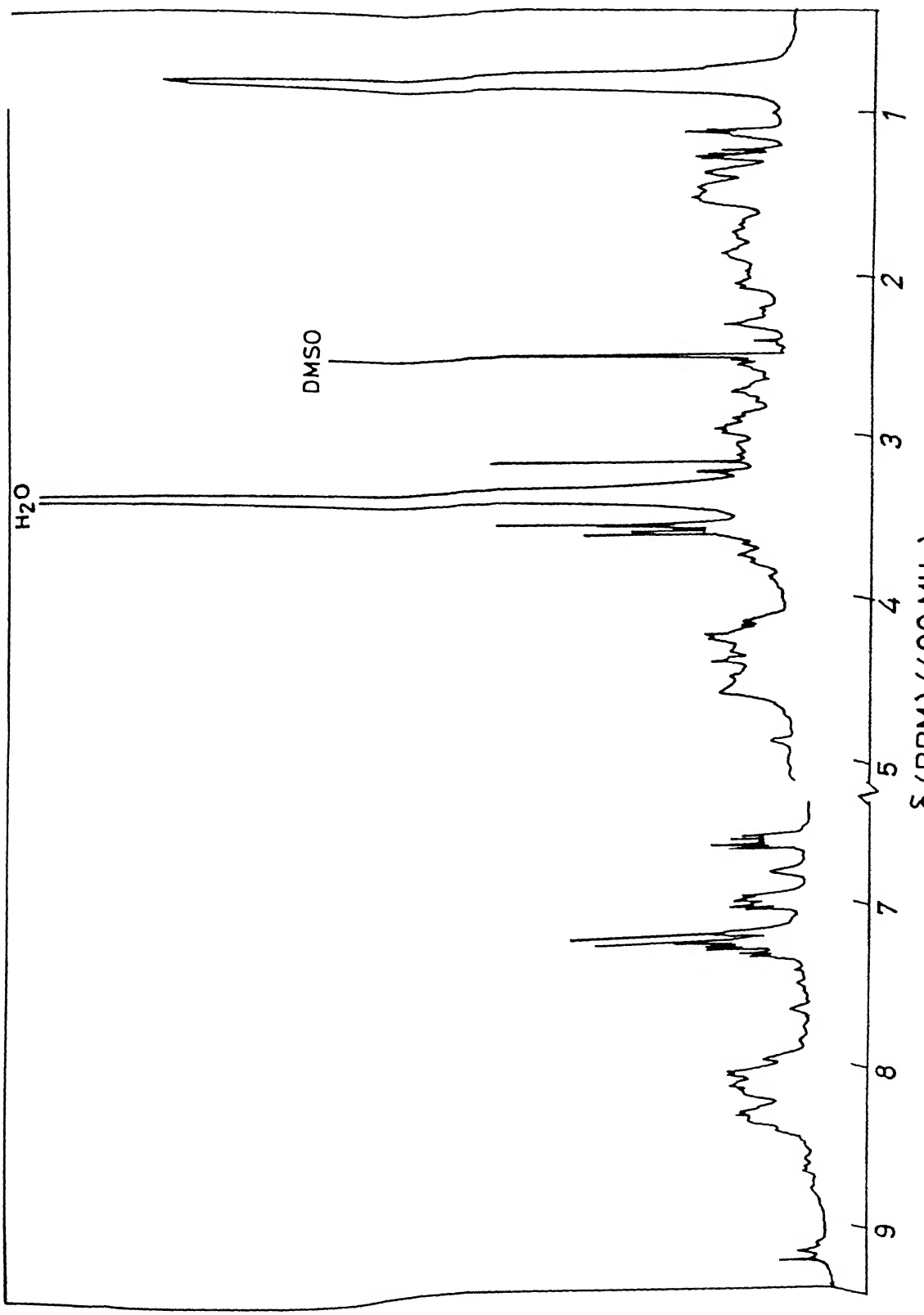

400 MHz NMR spectrum of insulin.6-OMe in DMSO-d_6

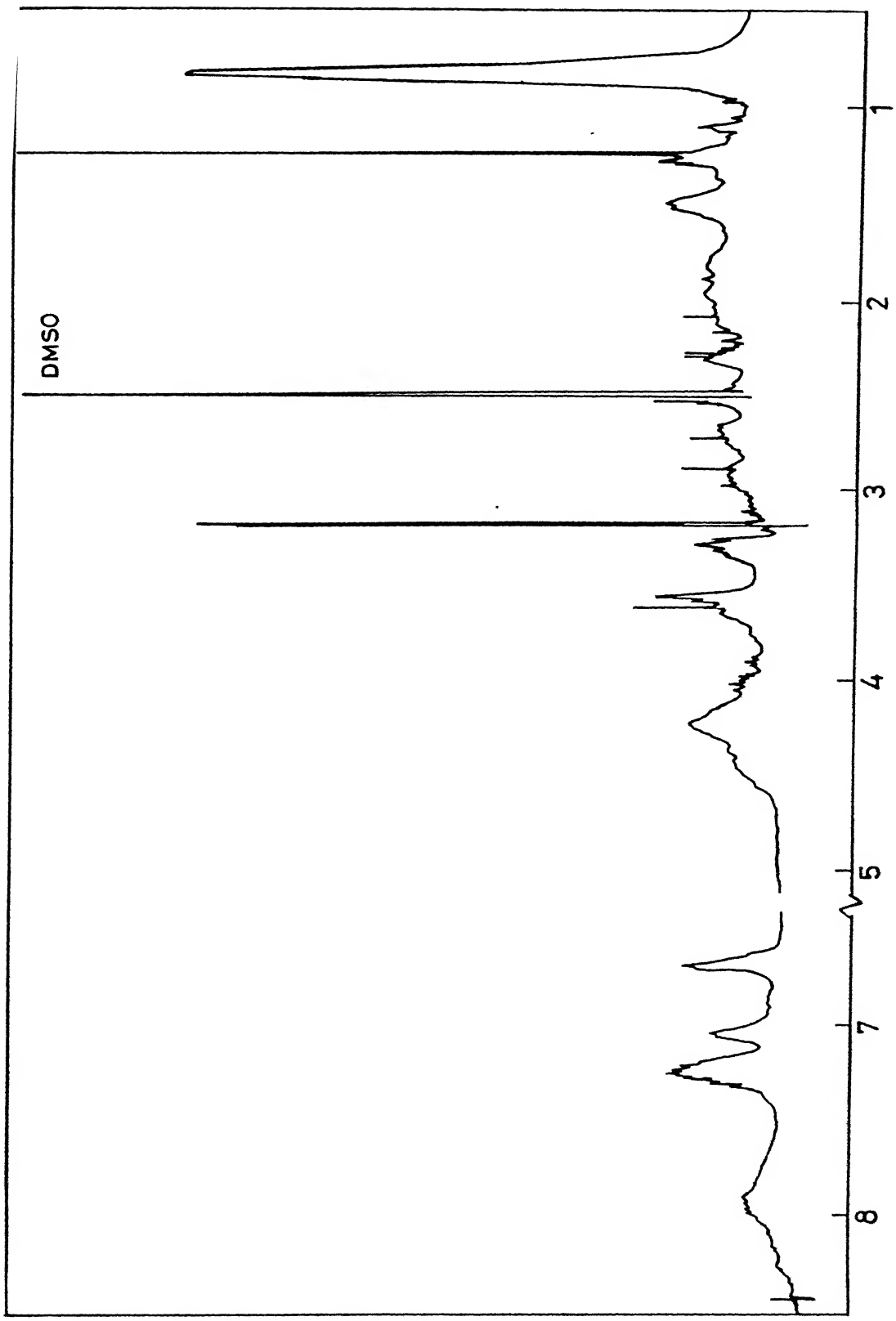

400 MHz NMR spectrum of insulin.6-OMe - zinc finger complex in DMSO-d_6

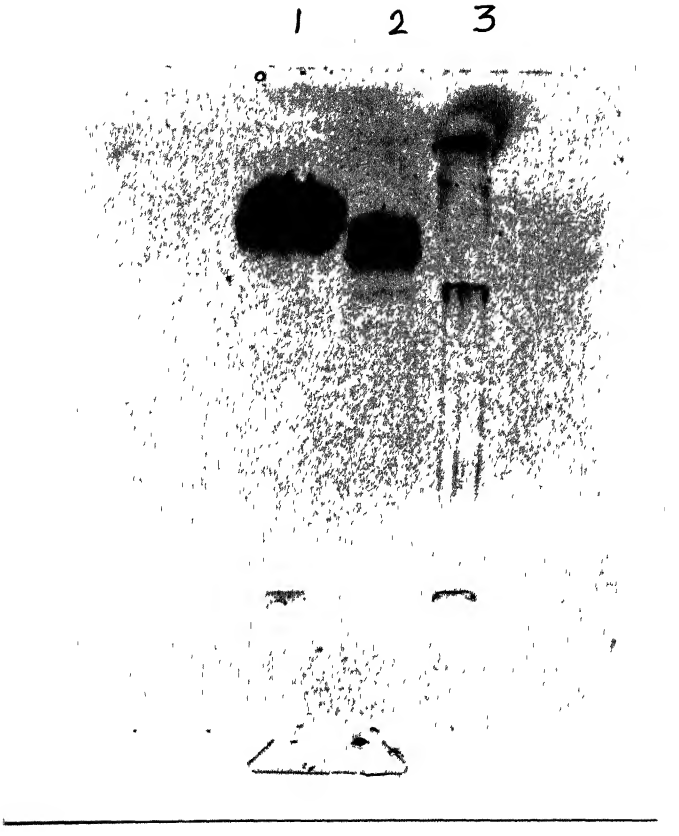

Polyacrylamide gel electrophoretic analysis of insulin - zinc finger complex. 1. insulin.6-OMe ; 2. insulin.6-OMe - zinc finger complex; 3. Molecular weight marker

E. EXPERIMENTAL

All amino acids used were of L - configuration. IR spectra were recorded on PE 580 / 1600 FT instruments. 1D proton nmr were recorded on WP80 / WM400 / AM300 / Varian500 / R 600 instruments. 2D proton nmr were obtained in WM400/ Varian500 instruments. UV spectra were secured using a PE - Lambda 2 UV / Visible spectrophotometer. Optical rotations were measured using an automatic JASCO digital polarimeter. FAB mass spectra were recorded on a Jeol SX 102 / DA - 6000 mass spectrometer / data system using argon (6KV, 10ma) as the FAB gas. The accelerating voltage was 10KV and the spectra were recorded at room temperature. m-Nitrobenzyl alcohol (NBA) was used as the matrix. Zinc analyses were done using EDTA titration with standard controls. Silica gel was used for tlc and column chromatography (100 - 200 mesh). Reactions were monitered wherever possible by tlc. The organic extracts were invariably dried over anhydrous $MgSO_4$ and solvents evaporated in vacuo.

I. Cystine diOMe.2HCl (1):

To a suspension of L-cystine (4.15g, 17.30mmol) in dry MeOH (125ml), a steady stream of dry HCl was passed for 4h, solvents evaporated to 30ml, refrigerated, filtered, dried and crystallised (MeOH) to afford 4.68g (1), mp 170°-171°C (lit[23] .173°C).

II. L-Cystine-di-t-Butyl Ester [Cystine-di-O^{t}Bu][26] (2):[24]

Isobutylene was prepared by heating t-butanol with about one third of its weight

by hydrated oxalic acid. The reaction proceeded smoothly at 87° - 100° C, giving isobutylene in quantitative yields.

In a Parr steel reaction vessel was placed THF (25ml) and Conc. H_2SO_4 (0.5ml), chilled in ice-salt, and admixed, under stirring, with cystine (3.0g, 12.50mmol) slowly. The resulting clear solution was admixed with liquid isobutylene (~ 30ml), the reaction vessel sealed, left stirred at room temperature for 40h, chilled in ice-salt, opened carefully and the contents poured on to water (60ml), neutralised, adjusted pH to ~10 with 1N NaOH, extracted with EtOAc (3x20ml), washed with water (2x10ml), dried ($MgSO_4$), filtered, evaporated and dried thoroughly to give Cystine-di-O^{t}Bu (2) as an yellow oily compound, yield: 1.40g (32%).

ir: ν_{max} (neat) cm^{-1} : 3376, 1730, 1155, 1035.

nmr: δ ($CDCl_3$) (60MHz) : 1.50(s, 18H, t-butyl), 2.95(t, 4H, Cys β-CH_2-), 3.65(b, 2H, Cys α-CH).

III. Bis-N-benzyloxycarbonyl Cystine [bis-Z-Cystine](3) :

To an ice-cooled and stirred solution of cystine (2.4g, 10mmol) in 1N NaOH (20ml) was added, in drops, a toluene solution of carbobenzoxy chloride (Z-Cl) (50% v/v) (8.54ml, 30mmol), maintaining the pH throughout at 9-10 by addition of 1N NaOH. The reaction was left stirred for 4h at 0° C, washed with ether (2x25ml), the pH adjusted to 3 with 6N HCl, filtered and the filtrate extracted with EtOAc (3x15ml). The initially precipitated material was dissolved in warm EtOAc, the combined extracts washed with 0.6N HCl (2x25ml), water (2x25ml), dried ($MgSO_4$), evaporated and the resulting yellow oily product crystallised from chloroform; mp 112°-115°C (lit.[25] 114°C), yield: 3.5g (68.9%)

ir: ν_{max} (KBr) cm^{-1}: 3310, 1690, 1530, 1060.

nmr: δ ($CDCl_3$): 3.22(d, 4H), 4.59(q, 2H), 5.13(s, 4H), 6.00(d, 2H), 7.41(s, 10H).

$[\alpha]_D^{25}$ = -151°(c=1, MeOH).

IV. Bis-N-t-Butuyloxycarbonyl Cystine [Bis-Boc-Cystine] (4):

To a stirred solution of cystine (2.4g, 10mmol) in 1N NaOH (22ml) was added slowly di-t-butyl dicarbonate (4.46g, 20mmol) for 2h, left stirred overnight. The resulting milky solution was extracted with petroleum ether (4x15ml), the organic layer extracted with saturated $NaHCO_3$ (4x15 ml), the combined aqueous layers adjusted to pH 1 by careful addition of $KHSO_4$ (8.96g in 60 ml)(CO_2 !!), extracted with EtOAC (4x30ml), washed with water (3x20ml), dried ($MgSO_4$), evaporated with bath temperature below 30°C and dried thoroughly *in vacuo* to afford bis-Boc-Cystine (4), mp 145°-146°C (lit.[27] 143°- 145°C), yield: 2.8g (63.9%)

ir: ν_{max} (KBr) cm^{-1}: 3370, 2980, 1720, 1680, 1510.

nmr: δ($CDCl_3$)(80MHz): 1.4(s, 18H), 3.1(d, 4H), 4.6(b, 2H), 5.5(b, 2H).

V. Preparation of N,N'-Di-Benzoyl Cystine: Di-Bz-Cystine (5) :

To a stirred suspension of L-Cystine (4g, 16.8mmol) in water (100ml), was added 10% aqueous NaOH solution (25ml), followed by in drops, addition of benzoyl chloride (16.52ml) at 0°C. The reaction mixture was left stirred for 5h -keeping the pH alkaline by addition of required amount of NaOH solution- acidified with dil.HCl, the resulting stiff gel was filtered, refluxed with CCl_4 (50ml) and decanted. The gel was extracted two more times with refluxing CCl_4 (50 ml each). The resulting residue on crystallisation from dilute alcohol gave 6.24g (84%) of (5), mp 197°-198°C (lit.[26] 196°-197°C).

VI. Preparation of Di-Benzyloxycarbonyl Cystine di-OMe

Di-Z-Cystine di-OMe(6):

To an ice cooled and stirred mixture of (1) (2.4g, 7.04mmol) in saturated solution of $NaHCO_3$ (30ml) and $CHCl_3$ (30ml), was added, in drops, over 0.5h Z-Cl (5.66ml, 50% toluene solution). The reaction mixture was left stirred for 3h, separated the aqueous and organic layers, the organic layer was admixed with pyridine (1ml), washed successively with dil.H_2SO_4 (2x25ml), satd. $KHCO_3$ solution (2x15ml), dried ($MgSO_4$), evaporated and the resulting syrupy residue on standing over petroleum ether gave (7) as spongy white precipitate, yield: 1.3g (34.5%), mp 66°-68°C (lit.[23] 73°-75°C).

(ii). Alternatively, the product was also obtained by using ethereal diazomethane:

To bis-Z-Cystine (3) (0.600g) in MeOH (1ml) was added at 0°C, ethereal solution of diazomethane - generated *in situ* by the addition of nitrosomethyl urea to a mixture of 10% NaOH and ether - until a slight yellow colour persisted, refrigerated for 3-4h, excess diazomethane was removed in a stream of N_2 gas, evaporated and triturated with petroleum ether to afford 0.644g of (7)(68.30%), mp. 68°-70°C.

ir:ν_{max} (KBr) cm^{-1}: 3340, 1735, 1695, 1540, 1240

nmr: $\delta(CDCl_3)$ (80MHz): 3.15 (d, 4H), 3.75 (s, 6H), 4.62 (q, 2H), 5.13 (s, 4H), 5.59 (b, 2H), 7.33(s, 10H).

VII. Preparation of Di-Benzoyl Cystine di-OMe [Di-Bz Cystine di-OMe](7):

The preparation was carried out as in the case (7), yield: 52%, mp 169°-171°C, (lit.[23] 177°-178°C).

ir:ν_{max} (KBr) cm^{-1}: 3340, 1750, 1640, 1528.

nmr:δ ($CDCl_3$) (80MHz): 3.30 (d, 4H), 3.76 (s, 6H), 5.0 (q, 2H), 7.74 (m, 10H), 8.45 (d, 2H).

VIII. Bis-N-Benzyloxycarbonyl Cystine di p-Nitrophenyl Ester: [Bis-Z-Cystinyl di-ONp] (8):

To an ice-cooled and stirred solution of (3)(1.5g, 2.94mmol) in EtOAc (30ml) was added p-nitrophenol (0.8g, 5.87mmol) followed by , after 0.25h, DCC (1.2g, 5.87mmol). The reaction mixture was left stirred for 4h at 0°C and at room temperature for 48h, filtered and washed with 5% aqueous bicarbonate (3x25ml), water (3x25ml), dried ($MgSO_4$), evaporated and the residue on crystallisation from hot MeOH afforded bis-Z-Cystinyl di-ONp (8), 1.3g (62%), mp 125°-127°C which was used for next step without delay.

nmr: δ ($CDCl_3$) (80 MHz) : 3.34(d, J=5Hz, 4H), 4.88 (q,2H), 5.12 (s, 4H), 5.72(d, 2H), 7.38(br, 14H), 8.25(d, 4H, J=9Hz).

IX. Bis-t-Butyloxycarbonyl Cystine di-p-Nitrophenyl Ester [Bis-Boc Cystine di-ONp (9)]:

To a stirred solution of (4) (1.5g, 3.42mmol) in EtOAc (35ml), at 0°C, was added p-nitrophenol (0.801g, 6.84mmol), followed by the addition of, after 0.25h, DCC (1.410g, 6.84 mmol). The reaction mixture was stirred at 0°C for 4h and at room temperature for 40h, filtered the precipitated DCU, the filtrate washed with 5% aqueous $NaHCO_3$ (2x15ml), water (2x10ml), dried ($MgSO_4$), evaporated, dried and crystallised to afford the p-nitrophenyl ester (9) as an yellow solid, mp 133°-136°C; yield : 1.44g (64%), .

ir:ν_{max} (KBr) cm^{-1} : 3373, 1772, 1755, 1681, 1520, 1253, 1054.

nmr: δ ($CDCl_3$) (80MHz): 1.47(s, 18H), 3.35(d, 4H), 4.83(q, 2H), 5.51(d, 2H), 7.32, 8.38(d,d, 8H).

X. S-Acetamidomethyl Cysteine hydrochloride [S-Acm-Cys . HCl](10) :

a. N-(Hydroxymethyl)acetamide:

To a clear solution of formalin (37-41% aqueous solution) (13.7g, 170mmol) and anhydrous K_2CO_3 (1g, 170mmol) was added acetamide (15.0g, 150mmol), swirled, heated on a water bath for 5 min., allowed to stand overnight, subjected to a stream of CO_2 gas for 10 min., evaporated under reduced pressure, with heating below 40°C, and thoroughly dried. To the resulting oily residue, which contained some precipitated salt, was added anhydrous Na_2SO_4 (13g) in portions. After 3h, the oily residue was diluted with acetone (20ml), filtered, the filtrate was again dried over anhydrous Na_2SO_4 (5g), filtered, evaporated and dried thoroughly to give N-(hydroxymethyl)acetamide as a colorless hygroscopic oil, yield: 15.30g ($\sim$ 100 %).

b. S-Acetamidomethyl Cysteine Hydrochloride [S-Acm Cys HCl] (10):

A solution of N-(hydroxymethyl)acetamide (12.7g, 143mmol) and L-Cysteine. mono HCl. mono H_2O (22.80g, 130mmol) in water (35ml) was cooled in an ice-bath, admixed with conc.HCl (5ml) slowly during 5min, purged with dry nitrogen, stoppered, left aside for 48h, during which cysteine was largely consumed [tlc (elution medium t-Butanol:Acetic acid:Water::10:2:3),]. The reaction mixture was evaporated below 40°C, the resulting solid, admixed with absolute alcohol (10ml) and evaporated. This entrainment procedure was repeated twice more. The crude product was dissolved in MeOH (25ml), ether was added until a cloudy solution re-

sulted, stoppered and refrigerated for 4 days, filtered, washed with ether and dried thoroughly to afford S-Acm Cys.HCl.H_2O (10), contaminated with minor amounts of Cystine. 2HCl; yield 10.5g (35.4%), mp 157°- 159°C (dec.) (lit.[28] 159°-163°C (dec.).

The above product was taken up in water (12ml), adjusted pH to 6 with aqueous KOH (2.5N), evaporated below 40°C under reduced pressure, dissolved in hot water (10ml), admixed with absolute alcohol (30ml), stoppered and refrigerated for about one week to secure colorless crystals of pure S-Acm Cys.monoH_2O, yield: 7.2g, mp 187°-190°C (dec.) (lit.[28] 187°C (dec.)).

ir: ν_{max} (KBr) cm^{-1} : 3238, 1727, 1602, 1560.

nmr: δ (D_2O) (80MHz): 2.0(s, 3H, Ac-), 3.09(m, 2H, cys β- CH_2), 3.92(m, 1H, cys α-CH), 4.15(m, 2H, -CH_2NHAc).

XI. N-Benzyloxycarbonyl-S-Acetamidomethyl Cysteine [Z-S-Acm Cys] (11) :

To an ice-cooled and stirred suspension of (10)(3.0g, 12.20mmol) in aqueous NaOH (2N) (25ml) was added, in drop, Z-Cl (4.82ml, 45% in toluene, 15.25mmol), left stirred at 0°C for 4h, maintaining the pH ~ 10 by addition of 2N NaOH, and at room temperature for 6h, extracted with ether (3x15ml), adjusted to pH ~3 with dil.HCl, extracted with EtOAc (4x15ml), dried ($MgSO_4$), filtered, evaporated and dried to give Z-S-Acm Cys (11) as a gummy compound, yield: 3.63g (91.4%).

ir: ν_{max} (neat) cm^{-1} : 3370, 1748, 1650, 1556.

XII. N-t-Boc-S-Acm-Cysteine [Boc-S-Acm-Cys] (12):

Under dry nitrogen blanket, a mixture of (10) (2.2g, 9.65mmol) and DMF (20ml), added TMG (2.22g, 19.30mmol) slowly, followed by the slow addition of

t-butoxycarbonyl azide (1.50g, 10.60mmol) and TMG (1.11g, 9.65mmol). The reaction mixture was stirred for 15h, concentrated in vacuo at below 35°C, admixed with water (7ml), washed with EtOAc (2x10ml), the aqueous layer adjusted to pH 3, under cooling with 50% aqueous citric acid, saturated with brine (2x15ml), extracted with EtOAc (3x20ml), dried ($MgSO_4$), evaporated, dried thoroughly, triturated with warm ether (25ml), and allowed to stand overnight to yield 0.950g (32%) of (12) as a white spongy product, mp 104°-106°C (lit.[29] 110°-112°C).

ir: ν_{max} (KBr)cm^{-1}: 3359, 1718, 1700, 1527, 1164.

nmr:δ ($CDCl_3$ (80MHz): 1.43 (s, 9H, $(CH_3)_3C$-), 2.00 (s, 3H, Ac-), 3.07 (2H, m, β-CH_2), 4.46 (b-m, 3H, α-CH-, -S-CH_2-NH-), 5.61 (b, 1H, -O-CO-NH-), 8.82 (b, 1H, -CH_2-NH-CO-).

XIII. S-Acm-Cys-OMe (13):

Thionyl chloride (0.86ml, 11.82mmol) was added to an ice-cooled, stirred suspension of (10) (2.0g, 9.52mmol) in MeOH (10ml). The reaction mixture was left stirred at 0°C for 3h, left aside at room temperature overnight, filtered and the filtrate evaporated to get S-Acm-Cys-OMe HCl (13) as a foamy solid, yield: 2.086g (90.3%). ir: ν_{max} (KBr) cm^{-1} : 1732, 1250.

XIV. Z-S-Acm Cys ONp (14):

To an ice-cooled and stirred solution of (11) (1.60g, 4.91mmol) in EtOAc (25ml) was added, in small amounts, p-nitrophenol (0.695g, 5.0mmol), followed by DCC (1.03g, 5.0mmol). The reaction mixture was left stirred at 0°C for 4h, at room temperature for 48h, filtered to remove the DCU, the filtrate was treated with EtOAc (20ml), washed with 5% aqueous $NaHCO_3$ (3x10ml), water (2x10ml), dried ($MgSO_4$), filtered, evaporated and dried thoroughly and crystallised from MeOH to afford Z-S-Acm Cys ONp (14) as a white solid, yield: 1.94g (88.4%), mp 102°-105°C,

which was taken for the next step immediately.

ir: ν_{max} (KBr) cm^{-1} : 3320, 1720, 1692, 1533, 1347.

XV. Boc-S-Acm-Cys-ONp (15):

To an ice-cooled and stirred solution of Boc-S-Acm-Cys (12) (1.0g, 3.60mmol in EtOAc (30ml), at 0°C, was added in small amounts p-nitrophenol (0.556g, 4mmol), followed by DCC (0.824g, 4mmol). The reaction mixture was stirred at 0°C for 4h, at room temperature for 48h, diluted with EtOAc (25ml), washed with 5% aqueous NaHCO (3x10ml), water (2x10ml), dried ($MgSO_4$), filtered, evaporated and dried thoroughly. The resulting oily compound was taken up in MeOH (10ml) and allowed to stand overnight in the refrigerator and filtered to afford Boc-S-Acm-Cys-ONp (15) yield: 1.150g, (78%), mp 88° - 90° C.

ir: ν_{max} (KBr) cm^{-1} : 3338, 1771, 1685, 1534, 1517, 1345,1152, 1064.

XVI. Histidine Methyl Ester Dihydrochloride [His-OMe.2HCl] (16):

A stirred solution of L-histidine.HCl.H_2O (3g, 14.35mmol) in dry MeOH (28ml) was admixed with conc.H_2SO_4 (0.8ml), refluxed for 2.5h, subjected to a stream of dry HCl for 3h, towards the end of which the product started separating as a white precipitate. The reaction mixture was refrigerated for 4h, filtered, the residue washed with hot MeOH (15ml) under protection from moisture, filtered, and the filtrate refrigerated overnight and the resulting His-OMe.2HCl (16) filtered and dried; yield: 1.5g (43%); mp 204°-206°C (lit.[30] 200°-202°C).

ir: ν_{max} (KBr) cm^{-1}: 1760.

nmr: δ (D_2O)(80MHz) : 3.38(d, 2H, His β-CH_2-), 3.78(s, 3H, ester), 7.59(s, 1H, His4H), 8.69(s, 1H, His2H).

XVII. Preparation of N-t-butyloxycarbonyl histidine methyl ester [N-t-Boc His-OMe] (18):

To a solution of His-OMe (17) (1.63g, 9.66mmol) - prepared by, passing a steady stream of NH_3 gas, at 0°C, to His-OMe.2HCl in $CHCl_3$ (30ml) for 0.5h, filtration of NH_4Cl and evaporation of the solvents and drying - in pyridine (3.3ml), was added, in small lots, di-t-butyl di-carbonate (2.44g, 10.97mmol). The reaction mixture was stoppered and kept at rt for 72h, evaporated, admixed with EtOAc (30ml), washed with water (2x10ml) and extracted with citric acid (0.5M) (3x15ml). The EtOAc layer was processed as described in the following paragraph. The aqueous layer was adjusted to pH 8 with solid $NaHCO_3$, extractred with EtOAc (3x15ml), washed with brine (2x10ml), dried ($MgSO_4$), evaporated and dried thoroughly to give 0.846g of (18), mp 113° - 115° C.

The EtOAc layer mentioned above was washed with citric acid (0.25M) (2x10ml), satd. $NaHCO_3$ (2x10ml), brine (2x10ml), dried ($MgSO_4$), evaporated and dried to give, as an oil, N^{α},N^{ω} - di Boc-His-OMe (19), which on standing over diiso-propyl ether for about 1 d underwent N^{ω}-deprotection to afford N^{α}-His-OMe (18), combined yield: 1.691g (93.43%), mp 118°-120°C (lit.[32] 125.5° - 126° C).

ir : ν_{max} (KBr) cm^{-1}: 3326, 3239, 1675, 1524, 1168, 1052.

nmr: ($CDCl_3$) (80MHz): 1.45 (s, 9H, $(CH_3)_3C$-), 3.14 (d, 2H, β-CH_2), 3.73(s, 3H, ester), 4.53 (q, 1H, α-CH), 5.82 (d, -CONH-, 1H), 6.90(s, 1H, im4-H), 7.61 (s, 1H, im2H).

XVIII. N-t-Butyloxycarbonyl Histidine Hydrazide [Boc-His Hydrazide] (20):

Hydrazine hydrate (0.352ml, 11.35mmol) was added to a stirred solution of (18)

(0.540g, 2.01mmol) in MeOH (2.5ml), refrigerated for 48h, evaporated, triturated with hexane (3x5ml each) and hexane : $CHCl_3$ (7:3) (3x5ml), and dried thoroughly to give Boc-His hydrazide (20), 0.500g (93%), mp 75°-80° C.

XIX. Preparation of Tryptophan methyl ester. 2HCl [Trp-OMe.2HCl] (21):

To an ice-cooled and stirred mixture of $SOCl_2$ (2.38ml, 28.6mmol) and MeOH (30ml), L-tryptophan (2.5g, 12mmol) was added, left stirred at the same temperature for 5h and then at rt overnight, concentrated, admixed dry ether (10ml), refrigerated, filtered and crystallised from MeOH to give Trp-OMe.2HCl (21); mp. 210° - 215° C (lit.[33] 213.5° - 214° C), yield 2.8g (88.3%).

XX. N-Benzoyl Tryptophan Methyl Ester [Bz-Trp-OMe] (22):

To an ice-salt cooled and stirred solution of (21) (2.55g, 10mmol) in satd. $NaHCO_3$ (150ml), was added in drops, benzoyl chloride (1.2ml, 10.34mmol). The reaction mixture was left stirred at 0° C for 4h, admixed with benzene (20ml), left stirred overnight, extracted with EtOAc (3x30ml), washed with water (2x10ml), dried ($MgSO_4$), evaporated and dried thoroughly to get Bz-Trp-OMe (22), yield: 1.80g (56%).

ir: ν_{max} (KBr) cm^{-1} : 3370, 1740, 1640, 1523, 1025.

nmr: δ ($CDCl_3$) (80MHz): 3.53 (d, 2H), 3.76 (s, 3H), 5.15 (q, 1H), 6.86 (d, 1H), 7.45(m, 10H), 8.63 (b, 1H).

XXI. Preparation of 2,2'-dithio bis-(Bz-Trp-OMe) (23):

(a). Preparation of S_2Cl_2 :[34]

In a reaction flask equipped with a gas inlet and the outlet reaching inside an-

other receiver flask with an outlet was placed sulfur powder (4 g), melted, cooled and held at 50° - 80° C (flame!) and subjected to a stream of a steady stream of chlorine gas. The crude S_2Cl_2 condensed in the cooled receiver flask. It was redistilled after addition of a small amounts of sulfur powder, at atmospheric pressure. The portion which distilled above 137°C was refractionated over sulfur at $\sim$ 15 mm, in an apparatus with ground glass joints to give pure S_2Cl_2 as a golden yellow oily compound. bp 29° - 30° C/15 torr

(b). Reaction of S_2Cl_2 with Bz-Trp-OMe (22):

To an ice-cooled and stirred solution of (22) (3.22g, 10mmol) in alcohol-free dry $CHCl_3$ (35ml), was added, in drops, a solution of S_2Cl_2 (0.67g, 4.96mmol) in $CHCl_3$ (15ml); the reaction was accompanied by evolution of HCl gas, and the odour of S_2Cl_2 was absent after 4h. The reaction mixture left stirred overnight, shaken with satd.$NaHCO_3$ (2x10ml), dried ($MgSO_4$), evaporated and chromatographed on silica gel. Elution with benzene:EtOAc (85:15) gave (23) as a yellow compound, mp 122°-125°C; Yield: 0.78g (24%).

ir: ν_{max} (KBr) cm^{-1}: 3372, 1736, 1650, 1516, 1034.

nmr: δ ($CDCl_3$) (80MHz): 3.27 (m, 4H), 3.80 (s, 6H), 5.30 (m, 2H), 7.03, 7.42 (m, 18H), 9.32 (b, 2H).

ms: (FAB) m/z : 707 $(MH)^+$, 353 (2-thio-(Bz)-Trp-OMe)

Anal.: Calcd. for $C_{38}H_{34}O_6N_4S_2$: C, 64.59; H, 4.82; N, 7.93 %

Found : C, 63.58; H, 4.92; N, 7.10

XXII. Condensation of bis-Z-Cystinyl di-ONp with His-OMe.2HCl

Preparation of bis-Z-Cystinyl di-His-OMe (24):[35]

To an ice-cooled and stirred suspension of (16) (1.01g, 4.2mmol) in dry DMF (15ml), was added Et_3N (1.2ml, 8.4mmol), followed by (8) (1.3g, 1.73mmol). The reaction mixture was left stirred at room temperature for 48h, diluted with EtOAC (30ml), filtered, the filtrate washed with 5% aqueous ammonia (4x25ml), water (4x25ml), dried ($MgSO_4$), evaporated and the residue on crystallisation from hot MeOH afforded 1.25g (89%) of bis-Z-Cystinyl di-His-OMe (24) , mp 154° - 156° C.

ir: ν_{max} (KBr) cm^{-1} : 3307, 1734, 1695,1654, 1540.

nmr: δ (DMSO-d_6) (400MHz): 2.83, 3.08(q,q, 4H, Cystine β-CH_2), 2.93 (m, 4H, His β-CH_2), 3.55(s, 6H, ester), 4.32(q, 2H, Cystine α-CH), 4.47(q, 2H, His α-CH), 5.04(s, 4H, Ar-CH_2), 6.83(s, 2H, His4H), 7.33(m, 10H, Ar), 7.52(s, 2H, His2H), 7.56(d, 2H, Cystine NH), 8.5(d, 2H, HisNH).

ms: (FAB) m/z : 811 $(M+H)^+$, 407 (Z-Cys-His-OMe + H)$^+$.

$[\alpha]_D^{25}$ = -78.77 (c = 0.9, MeOH).

Anal. : Calcd. for $C_{36}H_{42}N_8O_{10}S_2$: C, 53.3; H, 5.19, N, 13.83 %

Found: C, 52.6; H, 5.29, N, 13.89

XXIII. Preparation of bis-Boc-Cystinyl di His-OMe (25):

To an ice cooled and stirred suspension of (16) (1.24g, 5.10mmol) in DMF (15ml), was added Et_3N (1.42ml, 10.20mmol), followed by, after 0.5h, (9) (1.73g, 2.54mmol) in DMF (5ml). The reaction mixture was left stirred at 0° C for 4h, and then at rt for 30h, admixed with with 5% aqueous ammonia solution (3x15ml), water (3x15ml), dried ($MgSO_4$), evaporated, dried thoroughly and chromatographed on silica gel.

Elution with $CHCl_3$:MeOH (92 : 8) afforded bis-Boc-Cystinyl di-His-OMe(25, mp 142°-145°C; Yield: 0.50g (67%).

ir: ν_{max} (KBr) cm^{-1} : 3327, 1737, 1691, 1657, 1521, 1171, 1047.

nmr: δ($CDCl_3$ + $DMSO_6$) (80MHz) : 1.43 (s, 18H), 3.14 (b, 8H,Cystine β-CH_2 , His β-CH_2) 3.69 (s, 6H), 4.65 (b, 4H, Cystine α-CH, His α-CH), 6.26 (d, 2H, Cystine NH), 6.88 (s, 2H, His 4H), 7.74 (s, 2H, His2H), 8.06(d, 2H, His NH).

ms: (FAB) m/z : 743 $(M+H)^+$, 372 (Boc-Cys His-OMe+ H)$^+$.

$[\alpha]_D^{25}$ = -73.30 (c, 0.232, MeOH).

XXIV. Preparation of Bis-Boc-His Cystine- di-OMe (26):

To an ice cooled and stirred solution of (20) (0.725g, 2.70mmol) in 2N HCl (4ml), was added, in small lots, $NaNO_2$ (0.20g, 2.90mmol). The resulting yellow reaction mixture was admixed with, after 0.25h, chilled EtOAc (8ml) followed by 50% aqueous K_2CO_3 (4.48ml, 16.2mmol). The EtOAc layer was separated and the aqueous phase extracted with chilled EtOAc (2x4ml). The combined EtOAc extracts were dried $MgSO_4$ at 0° C and admixed with, at 0°C, a solution of Cystine di-OMe - prepared from its dihydrochloride (1) (0.443g, 1.3mmol) in CH_2Cl_2 (15ml) and Et_3N (0.37ml, 2.7mmol), by stirring at 0° C for 0.5h, filtration and evaporation - in EtOAc (5ml). The reaction mixture was left stirred at 0° C for 2h and refrigerated for 24h, kept at rt for 15h, evaporated and the crude product chromatographed on silica gel. Elution with $CHCl_3$:MeOH (93 : 7) gave bis-Boc-His Cystine-di-OMe (26), mp 125°-128° C (with initial softening ~ 95 °-100° C); Yield: 0.210g(21%).

ir: ν_{max} (KBr) cm^{-1} : 3304, 1746, 1679, 1521, 1167, 1049.

nmr: δ ($CDCl_3$) (80MHz): 1.44(s, 18H, $(CH_3)_3$-), 3.09(b, 8H, Cystine β-CH_2 ,

His β-CH_2), 3.75(s, 3H, ester), 4.64(b, 4H, Cystine α-CH, His α-CH), 6.36(d, 2H, HisNH), 6.86(s, 2H, His4H), 7.64(s, 2H, His2H), 7.76(d, 2H, Cystine NH).

ms: (FAB) m/z : 743 $(M+H)^+$; 372 (Boc-His Cys OMe+H)$^+$.

$[\alpha]_D^{25}$ = -70.1 (c, 0.291, MeOH)

XXV. N-Benzyloxycarbonyl S-Acetamidomethyl Cysteinyl Histidine Methyl Ester: [Z-S-Acm-Cys His-OMe] (27):[36]

To an ice cooled and stirred suspension of (16) (1.09g, 4.50mmol) in CH_2Cl_2 (25ml), was added Et_3N (1.28ml, 9.20mmol), followed by, after 0.5h, a solution of (14) (1.91g, 4.27mmol) in CH_2Cl_2 (20ml). The reaction mixture was left stirred at 0° C for 3h, then at rt for 40h, evaporated, taken up in EtOAc (60ml), washed with water (2x5ml), dried ($MgSO_4$) and evaporated, triturated with ether (3x5 ml) and dried thoroughly to give Z-S-Acm Cys His-OMe (27), mp 110°-112° C; yield: 0.833g (40.8%).

ir: ν (KBr) cm^{-1} : 3309, 1743, 1692, 1644, 1526, 1262,1048.

nmr: δ($CDCl_3$ -DMSO-d_6) (80MHz): 1.98(s, 3H, Ac-), 2.88, 3.13 (d,d, 4H, Cys β-CH_2 , His β-CH_2), 3.75(s, 3H, ester), 4.38, 4.66(m, Cysα-CH, His α-CH), 5.16(s, 2H, $ArCH_2$-), 6.47(d, 1H, CysNH-), 6.84(s, 1H, His4H), 7.41(s, 5H, Ar-), 7.69(b-m, 2H, His2H, HisNH), 8.0(d, 1H, AcNH).

ms: (FAB) m/z: 478 (M+1). $[\alpha]_D^{23}$ = -22.96° (c, 0.527, MeOH).

Anal.: Calcd. for $C_{21}H_{27}O_6N_5S$: C, 52.83, H, 5.66, N, 14.68 %

Found : C, 52.89, H, 5.60, N, 14.30.

XXVI. N-t-Butyloxycarbonyl-S-Acetamidomethyl Cysteinyl Histidine Methyl Ester : [Boc-S-Acm-Cys His-OMe] (28):

To an ice cooled and stirred suspension of (16)(0.532g, 2.2mmol) in CH_2Cl_2 (25ml), was added Et_3N (0.62ml, 4.4mmol), followed by, after 0.5h, a solution of (15) (0.726g, 1.76mmol) in CH_2Cl_2 (20ml). The reaction mixture was left stirred at 0° C for 4h, then at rt for 48h, filtered, evaporated, taken up in EtOAc (30ml), washed with 5% aqueous ammonia solution (2x10ml), water (2x5ml), dried ($MgSO_4$), evaporated, dried thoroughly and chromatographed on a silica gel. Elution with $CHCl_3$: MeOH (90 : 10) afforded Boc-S-Acm-Cys HisOMe (28), mp 128°-130° C (with initial softening at ~ 80° - 85° C); yield: 0.250g (41%).

ir: ν_{max} (KBr) cm^{-1}: 3298, 1745, 1662, 1540, 1257, 1168, 1050

nmr: δ ($CDCl_3$) (80MHz): 1.38(s, 9H, t-Butyl), 2.83 (t, 2H, Cys β-CH_2), 3.1(t, 2H, His β-CH_2), 3.66(s, 3H, ester), 4.70(m, 2H, Cys α-CH, His α-CH), 5.78(d, 1H, CysNH), 6.78(s, 1H, His4H), 7.59(b, 2H, His2H, HisNH), 7.77(d, 1H, AcNH).

ms: (FAB) m/z : 444 $(M+1)^+$.

$[\alpha]_D^{23}$: -14.86 (c, 1.05, MeOH).

XXVII. Cyclo[Bis-Oxalyl Cystine di OMe] (29):[37]

Triethylamine (1.63 ml, 11.74 mmol) was added to ice cooled and stirred suspension of (1) (2.0g,5.87 mmol) in CH_2Cl_2 (25ml), left stirred for 0.5h, admixed with ether (15ml), filtered, evaporated, dried, dissolved in dry benzene (75ml) and this solution was added simultaneously with a solution of oxalyl chloride (0.51ml, 5.87mmol) in dry benzene (75ml), very slowly, during 8h, to dry benzene (100ml) admixed with Et_3N (1.63ml, 11.74mmol). The reaction mixture was left stirred for 12h, filtered, washed with water (20ml), MeOH (10ml) and dried to afford 0.954g

(53%) of crude (25), mp 180°- 185° C, which was placed in Sohxlet thimble and extracted with EtOAc for 40h, followed by $CHCl_3$:MeOH::85:15 for 40h. The combined organic extracts on evaporation in vacuo gave 0.540g (30%) of pure (29) which on crystallisation from EtOAc-$CHCl_3$ afforded (29), fine needles, mp 195°-197° C .

ir: ν_{max} (KBr) cm^{-1}: 3288, 1743, 1660, 1510.

ms: (FAB) m/z : 645 $(M+1)^+$.

$[\alpha]_D^{25}$ = -33.8 (c = 0.142, $CHCl_3$).

Anal.: Calcd. for $C_{20}H_{28}O_{12}N_4S_4$: C, 37.28; H, 4.35 ; N, 8.70 %

Found: C, 36.62 ; H, 4.19 ; N, 8.08

^{1}H NMR (400 MHz) studies on (29):

^{1}H NMR (δ):

$CDCl_3$, 24° C: 3.22, 3.26 (4H, d,d, J = 16Hz,8Hz);3.30, 3.34 (4H,d,d, J = 16Hz, 8Hz) (β-CH_2), 3.80(12H, s) (ester), 4.87(4H, t, J = 8.5Hz) (α-CH), 8.13 (4H d, J = 8Hz), (NH).

ii. DMSO-d_6 , 24°C: 2.82, 2.86 (4H, d,d, J = 16Hz, 8Hz); 3.15, 3.10 (4H, d,d, J = 16Hz, 8Hz) (β-CH_2), 3.65 (12H,s)(ester), 4.59 (4H, d,d J = 8Hz) (α-CH), 8.34 (4H, d, J = 8.48Hz)(NH).

iii.Pyridine-d_5 , 24°C: 3.41 (8H,d,d J = 8Hz,8Hz)(β -CH_2), 3.60(12H, s)(ester), 5.39 (4H,d,d J= 8Hz,8Hz) (α-CH), 10.57 (4H, d, J = 8 Hz)(NH).

NH shift from solvent titration (gradient $CDCl_3$: DMSO-d_6):

δ (% DMSO-d_6): 8.14 (0), 8.27 (2), 8.40 (4), 8.50 (6), 8.58 (8), 8.64 (10), 8.83 (18), 8.90 (20), 9.08 (40); shift Σ 0.94.

Temperature dependent NH shift in DMSO-d_6: δ (°C):

9.34 (24), 9.28 (30), 9.22 (40), 9.15 (50), 9.08 (60), 9.0 (70); dδ/dT ppb/K -7.18.

^{13}C NMR (100 MHz), $CDCl_3$, 50° C : 29.69 (β-CH_2), 52.85,52.97 (α-CH), 41.38 (OCH_3), 159.16,159.53 (COOMe), 159.64 (NHCO).

XXVIII. Cyclo[Bis-Oxalyl Cystine di-O^{t}Bu] (30):

A solution of (2) (1.03g, 2.9 mmol) in dry benzene (60 ml) was added simultaneously with a solution of oxalyl chloride (0.25 ml, 2.9 mmol) in dry benzene (60ml), very slowly, over a period of $\sim$ 6h, to dry benzene (50 ml) admixed with Et_3N (1.0 ml, 7.25 mmol). The reaction mixture was left stirred for 8h, concentrated, washed with dil.HCl (2x10 ml), dried, evaporated and chromatographed on a silica gel. Elution with hexane and benzene (1:1) yielded (30) as a yellow foamy compound, yield: 30%.

ir: ν_{max} (KBr) cm^{-1}: 3384, 1737, 1682, 1513, 1154.

nmr: δ ($CDCl_3$) (80MHz) : 1.5(s, 36H, $(CH_3)_3C$-), 3.23(b-m, 8H, β-CH_2), 4.73(b, 4H, α-CH), 8.09(b, 4H, -NH-).

ms: (FAB) m/z : 589 (M - ^{t}butyl + H)$^+$.

XXIX. Bis[Oxalyl S-Acetamidomethyl-Cysteine Methyl Ester]:
Bis[Oxalyl-S-Acm-Cys-OMe] (31):

To an ice cooled and stirred solution of (13) (2.0g, 8.26mmol) in CH_2Cl_2 (35ml), was added Et_3N (1.25ml, 9mmol), followed by, after 0.5h, a further lot of Et_3N (2.53ml, 18.17mmol), and in drops a solution of oxalyl chloride (0.36ml, 4.13mmol) in CH_2Cl_2 (12ml). The reaction mixture was left stirred at 0° C for 3h, then at rt for 30h, the precipitated Et_3N.HCl filtered,the filtrate washed with water (3x5ml),

dried ($MgSO_4$), evaporated, dried thoroughly and chromatographed on silica gel. Elution with EtOAc:MeOH (88:12) gave Bis[oxalyl S-Acm-Cys-OMe] (31), mp. 154° - 156° C; yield: 0.302g (15.7%)

ir: ν_{max} (KBr) cm^{-1} : 3277, 1744, 1660, 1530, 1020.

nmr: δ ($CDCl_3$) (400MHz): 2.02(s, 6H, Ac-), 3.14 (m, 4H, Cys β-CH_2), 3.8(s, ester), 4.39(m, 4H, AcNH-CH_2-), 4.85(b-m, 2H, Cys α-CH), 6.58(b, 2H, AcNH-), 8.17(d, 2H, oxamideNH).

ms: (FAB) m/z: 467 $(M+1)^+$.

XXX. Preparation of Cyclo Succinyl Cystine diOMe (32):

Triethylamine (3.28ml, 23.48mmol) was added to an ice cooled and stirred suspension of cystine di-OMe. 2HCl (1) (4g, 11.74mmol) in CH_2Cl_2 (25ml), left stirred for 0.5h, admixed with ether (20ml), filtered, evaporated, dried, dissolved in dry benzene (150ml) and this solution was added simultaneously to a solution of succinyl chloride (1.26ml, 11.4mmol) in dry benzene (150ml), very slowly, during 12h, to dry benzene (200ml) admixed with Et_3N (3.28ml, 23.48mmol). The reaction mixture was left stirred overnight, filtered, washed the precipitate with benzene, water (25ml), dried thoroughly, powdered, taken in a Soxhlet thimble and extracted with benzene (125ml), with $CHCl_3$:MeOH :: 80:20 (100ml) for 48h, solvents evaporated, dried thoroughly to give cyclo succinyl cystine diOMe (32), mp 235° -240° C, with initial softening at 225° -230° C; yield: 1.07g (26%).

ir: ν_{max} (KBr) cm^{-1} : 3317, 3292, 1742, 1647, 1541, 1035.

ms: (FAB), m/z: 351 $(M+1)^+$.

$[\alpha]_D^{25}$: -62.75° (c, 0.153 , $CHCl_3$).

Anal. : calc. for $C_{12}H_{18}O_6N_2S_2$: C, 41.14 H, 5,14 N, 8.0 %

Found: C, 40.84 H, 5.23 N, 7.72

^{1}H NMR (400MHz) studies on 32:

^{1}H NMR (δ):

i. $CDCl_3$, 24° C: 2.5(4H,d,d)(succinyl), 2.8(4H,d, J=14.2Hz) (βCH_2), 3.80(6H,s) (ester), 4.85(2H,q) (α-CH), 8.20(2H,d) (NH).

ii. DMSO-d_6, 24°C: 2.55(4H,d,d)(succinyl), 2.89(4H,d)(βCH_2), 3.63(6H,s)(ester), 4.62(2H,q)(α-CH), 8.20(2H,d)(NH).

NH shift from solvent titration (gradient $CDCl_3$: DMSO-d_6):

6.65(0), 6.76(2), 6.85(4), 6.97(10), 7.17(20), 7.33(40); shift Σ 0.72.

Temperature dependent NH shift in DMSO-d_6, δ (° C):

8.196(25), 8.17(30), 8.14(35), 8.11(40), 8.07(45), 8.06(50), 8.03(55);

dδ /dt ppb/K -9.5.

XXXI. Treatment of bis-Boc-Cystinyl di-His-OMe (25 with TFAA-H_2O:

Preparation of 2 TFA^- NH_3Cystine di-HisOMe (33):

A solution of (25) (0.100g, 0.14mmol) in water (1ml) was cooled in ice, admixed with TFAA (0.45ml), stoppered left aside overnight, evaporated and dried thoroughly to give 2 TFA^- NH_3Cystine di-HisOMe (33).

nmr (D_2O)(400MHz): 3.04(m, 4H, His β-CH_2), 3.18(m, 4H Cys β-CH_2), 3.56(s, 6H, ester), 4.16(t, 2H, Cys α-CH), 4.68 (t, 2H, His α-CH), 7.14(s, 2H, His 4,4'H), 8.42(s, 2H, His 2,2'H).

ms: (FAB) m/z : 543 $[M\text{-}2Boc\text{-}2TFA^- + 1]^+$, 271 $[(M\text{-}2Boc\text{-}2TFA^-)/2]^+$.

XXXII. Treatment of bis-Boc-His Cystine-di-OMe (26), with TFAA-H_2O: Preparation of 2 TFA^- NH_3His Cystine-di-OMe: (34):

A solution of (26) (0.100g,) in water (1ml) was cooled in ice, admixed with TFAA (0.45ml), stoppered left aside overnight, evaporated and dried thoroughly to give 2 TFA^- NH_3His Cystine-di-OMe (34)

nmr (D_2O)(400MHz): 2.86(m, 4H, His β-CH_2), 3.04(m, 4H Cys β-CH_2), 3.58(s, 6H, ester), 4.08(t, 2H, Cys α-CH), 4.24 (His α-CH), 7.16(d, 2H, His 4,4'H), 8.30(d, 2H, His 2,2'H).

ms: (FAB) m/z : 543 $[M\text{-}2Boc\text{-}2TFA^-+1]^+$.

XXXIII. Reaction of Di-Z-Cystine-di-OMe with PDT followed by acrylonitrile addition: Preparation of Z-S-Cyanoethyl Cys-OMe (36): [50]

Under nitrogen blanket and stirring a solution of (7) (0.322g, 0.6mmol) in MeOH (10ml), was admixed with neat PDT (0.08ml, 0.8mmol), left stirred for 6h, admixed with acrylonitrile (0.170ml, 2.40 mmol), left stirred for 5h, solvents evaporated, washed with petroleum ether (2x5ml), dried thoroughly. Preparative TLC on silica gel using benzene:CHCl::85:15 as developer afforded (36) as a gummy compound; yield: 0.187g (48%).

ir: ν_{max} (neat) cm^{-1} : 3330, 2240, 1745, 1720, 1525, 1220, 1060.

nmr: $\delta(CDCl_3)$ (80MHz): 2.7 (m, 4H, -$SCH_2CH-2CN$), 3.1 (q, 2H, -CH_2S-), 3.85(s, 3H, ester), 4.65 (m, 1H, α-CH), 5.16 (s, 2H, Ar-CH_2-), 5.60(b, 1H, -CONH-), 7.43 (s, 5H, Ar-).

Anal.: Calcd. for $C_{15}H_{18}O_4N_2S$: C, 55.9 H, 5.6 %

Found : C, 56.24 H, 6.01

XXXIV. Reaction of Di-Bz-Cystine-di-OMe with PDT followed by acrylonitrile addition: Preparation of Bz-S-Cyanoethyl Cys-OMe (37):

The reaction of bis-Bz-Cystine-di-OMe (7)(0.200g, 0.420mmol), precisely as described above, with PDT followed by acrylonitrile addition afforded 0.100g (40%) of (36) as an oil.

ir: ν_{max} (neat) cm^{-1} : 3320, 2265, 1740, 1650, 1540, 1030.

nmr: $\delta(CDCl_3)$ (80MHz): 2.69 (m, 4H, -SCH_2CH_2-), 3.22 (q, 2H, -CH_2S-), 3.85(s, 3H, ester), 5.0 (m, 1H, α-CH), 7.09 (d, 1H, -CONH-), 7.49, 7.82 (m, 5H, Ar-).

Anal. : Calcd. for $C_{14}H_{16}O_3N_2S$: C , 57.5 H, 5.5 %

Found : C, 58.02 H, 5.72.

XXXV. Reaction of bis-Z-Cystinyl di-His-OMe (24) with Propane-1,3- dithiol (PDT) Followed by Acrylonitrile addition:
Preparation of S(β-Cyanoethyl)-Z-Cysteinyl Histidine Methyl Ester [Z-Cys(S-β-Cyanoethyl) HisOMe] (39):[50]

All the operations were carried out under dry oxygen-free nitrogen blanket and dry degassed solvents were used. To a stirred solution of (24) (0.081g, 0.1mmol) in dry MeOH (20ml) was added 0.14M methanolic PDT (1ml, 0.14mmol). The reaction mixture was left stirred for 8h, admixed with 0.3M methanolic acrylonitrile (1.4ml, 0.43mmol), left stirred for 6h, solvents evaporated, the residue triturated with petroleum ether (40°-60°C) (2x10ml), dried, extracted the residue with EtOAC (2x10ml) and evaporated. The crude product on preparative tlc using $CHCl_3$:MeOH :: 80:20 as developer afforded Z-Cys(S-β-Cyanoethyl)His-OMe (37) as a white compound, mp 99°-101° C; yield: 0.033g (overall yield 36%).

ir: ν_{max} (KBr) cm^{-1} : 3300, 2240, 1740, 1690, 1640, 1520.

nmr: $\delta(CDCl_3)$ (80MHz): 3.0(m,8H, Cys β-CH_2, His β-CH_2, -SCH_2CH_2-), 3.75(s,3H, ester), 4.44(m, 1H, Cys α-CH), 4.8(q, 1H, His α-CH), 5.16(s, 2H, Ar-CH_2), 6.00(b-d, 1H, CysNH), 6.81(s, 1H, His4H), 7.44(s, 5H), 7.56(s, 1H, His2H), 7.78(d, 1H CysNH).

$[\alpha]_D^{26}$ = -37.97 (c = 1.33, MeOH).

XXXVI. Reaction of bis-Boc Cystinyl di His-OMe (25) with PDT followed by Acrylonitrile Addition: Preparation of Boc-Cys(S-β-Cyanoethyl) His-OMe (40):

The reaction of (25)(0.100g, 0.135mmol) with PDT followed by acrylonitrile addition, precisely as described above gave 0.085g (74%) of (40), as a foamy solid.

ir: ν_{max} (KBr) cm^{-1} : 3340, 2254, 1746, 1661, 1516, 1257, 1168, 1047.

nmr: $\delta(CDCl_3)$ (80MHz): 1.43(s, 9H,$(CH_3)_3$-), 2.80(m, 8H, -SCH_2CH_2-, Cys β-CH_2 , His β-CH_2), 3.70 (s, ester), 4.35(q, 1H, Cys α-CH), 4.75(q, 1H, His α-CH), 5.60(d, 1H, CysNH), 6.83(s, 1H, His4H), 7.56(s, 1H, His2H), 7.66(d, 1H, HisNH).

ms: (FAB) m/z : 426 $(M + H)^+$.

$[\alpha]_D^{27}$ = -30.0^o (c, 0.41, MeOH).

Anal. : Calcd. for : $C_{18}H_{27}O_5N_5S.H_2O$: C, 48.76, H, 6.09, N, 15.80 %

Found : C, 48.19, H, 6.14, N, 14.89.

XXXVII. Reaction of oxytocin with PDT followed by addition of acrylonitrile: Demonstration of -S-S- $\rightarrow$ -2SH Change

To a stirred solution of oxytocin acetate salt (0.001g, 0.940 μmol), in dry and degassed MeOH (3ml), under argon atmosphere, was added 0.29mM methanolic

PDT (0.096ml, 1.90 μmol), The reaction mixture was left stirred for 6h, admixed with 0.294M methanolic acrylonitrile (0.065ml, 0.0190 μmol), stirred for 30min., solvents evaporated, washed with dry benzene (2 x 5ml) and dried thoroughly under high vacuum. Amino acid analysis on an automated amino acid analyser and comparison with starting material revealed complete reduction of the S-S bridge.

XXXVIII. Reaction of insulin with PDT follwed by addition of acrylonitrile: Demonstration of 3 S-S $\longrightarrow$ 2 -SH Change

To stirred bovine insulin (0.006g, 1 μmol) in triple distilled water (1.2ml), under argon atmosphere was added 0.12M methanolic PDT (0.083ml, 0.01mmol), stirred for 6h, admixed with 0.15M methanolic acrylonitrile (0.53ml, 0.08mmol), stirred for 30min., solvents evaporated, washed with benzene (2x5ml) and dried thoroughly. Aminoacid analysis revealed reduction of 2 of the three S-S bridges of insulin.

XXXIX Reaction of c-lysozyme with PDT followed by addition of acrylonitrile : Demonstration of 4 S-S $\longrightarrow$ 2 -SH Change

Under a dry nitrogen blanket, c-lysozyme (1 μmol) was mixed with PDT (93 μmol). After 0.5h stirring, additional PDT (50 μmol) was added and stirring continued for 8h. The mixture was triturated with dry hexane (1x3ml), mixed with 0.5ml of urea (6 mol dm^{-3}) followed by acrylonitrile (60 μmol), left stirred for 5h, evaporated, dried, taken up in distilled water, dialysed and the clear solution lyophilysed to give the product as a white powder. Electrophoresis on SDS-PAGE against starting material showed no fragmentation of the enzyme.

XL Reaction of cystine with PDT followed by addition of acrylonitrile: Isolation of S-β-Cyanoethyl Cysteine

To a stirred suspension of cystine (0.120g, 0.5mmol) in MeOH : pH 8.0 phosphate buffer solution (1:10) (10ml) was added 0.6M methanolic PDT (1.2ml, 0.7mmol), shaken for 40h, filtered, the filtrate extracted with benzene (2x10ml), admixed with 1.06M methanolic acrylonitrile (0.5ml, 0.5mmol), left stirred under nitrogen atmosphere for 10h, and evaporated to give 0.079g (63%) of S-β-Cyanoethyl Cysteine, mp 172° - 175° C which was in all respects identical to that of an authentic sample.

XLI. Reaction of bis-Z-Cystinyl di-His-OMe (24) with PDT Followed by $ZnCl_2$ Addition: Preparation of Zinc-Finger Template (43): [35]

All operations were carried out under dry oxygen-free nitrogen atmosphere and dry, degassed solvents were used. To a stirred solution of bis-Z-Cystinyl di-His-OMe (24) (0.630g, 0.778mmol) in dry MeOH(48ml) was added 0.06M methanolic PDT (2ml, 1.2mmol). The reaction mixture was left stirred for 8h, evaporated, triturated the residue with petroleum ether (2x10 ml) and benzene (2x10 ml), dried thoroughly, dissolved in MeOH (45ml), cooled to 0° C, admixed with Et_3N (0.22ml, 1.58mmol) and left stirred for 0.75h. Addition of $ZnCl_2$ (99.99%) (0.105g, 0.773mmol) resulted in the immediate precipitation of the zinc template. The reaction mixture was further left stirred at 0° C for 0.75h, centrifuged, washed with hot MeOH (2x5ml) and dried to afford 0.50g of (43); mp 188°-192° C (dec.); (overall yield: 73.5%).

ir: ν_{max} (KBr) cm^{-1} : 3308, 1718, 1674, 1508.

nmr: δ (DMSO-d_6) (400MHz): 2.75,3.05(m, 4H, His β-CH_2), 2.83, 3.10(m, 4H, Cys β-CH_2), 3.55, 3.63(s,s, 6H, ester), 4.08, 4.35(b-d, 2H, Cys α-CH), 4.40,4.52(b-d, 2H,

His α-CH), 5.05(s, 4H, $ArCH_2$-), 6.78(s)6.85 (s)(2H, His 4,4'H), 7.38(s, 10H,Ar), 7.6(b, 2H, CysNH), 7.85(s) 7.98(s) (2H, His2,2'H), 8.45(m, 2H, His NH).

ms: (FAB) m/z: 875 $(M)^+$; 911 $(M+2H_2O+H)^+$

$[\alpha]_D^{25}$ = -21.15 (c=1.04, DMF).

Anal. : Calcd. for $C_{36}H_{42}N_8O_{10}S_2Zn.2H_2O$: C,47.39; H,5.08; N,12.28; Zn,7.16 %

Found : C,46.34; H,4.64; N,11.28; Zn,7.17 and 7.96.

XLII. Reaction of (27) with $ZnCl_2$: Conversion of (27) to (43):[36]

To a solution of (27) (0.150g, 0.314mmol) in MeOH (7ml), under argon atmosphere, was added 0.2M methanolic $ZnCl_2$ (3.12ml, 0.628mmol), stirred for 15h, neutralised with 5% aqueous ammonia to pH$\sim$ 9, centrifuged the precipitated product, washed with water (2x5ml), MeOH (2x5ml) and dried thoroughly to afford the zinc complex (43), 0.053g (38%), mp 190°-195° C (dec.) whose properties were identical in all respects to that secured from the previous experiment.

XLIII. Reaction of bis-Z-Cystinyl di-His-OMe (24) with PDT Followed by $CoCl_2 . 6H_2O$ Addition: Preparation of Cobalt-Finger Template (44):

All operations were carried out under dry, oxygen free nitrogen blanket and dry, degassed solvents were used. To a stirred solution of (24) (0.200g, 0.250mmol) in MeOH(20ml) was added 0.3M methanolic PDT (1.27ml, 0.375mmol), the reaction mixture left stirred for 7h, evaporated, the residue triturated with petroleum ether (2x10ml), benzene (2x10ml), dried thoroughly, dissolved in MeOH (15ml), cooled at 0° C, admixed with 0.5M methanolic Et_3N (1ml, 0.50mmol) and left stirred for 0.75h at 0° C. Addition of $CoCl_2.6H_2O$ (0.052g, 0.22mmol) resulted in the immediate

precipitation of the Cobalt-Template (44). The mixture was left stirred at 0°C for additional 0.25h, centrifuged, washed with hot MeOH (2x5ml) and dried thoroughly to yield 0.087g (overall yield from bis-Z-Cystine : 40%) of (44) as a bluish green solid; mp 175°-180° C (dec).

UV: λ_{max} nm (c, 2x10^{-4} M, DMF): 595 (sh) ($\epsilon = 225 M^{-1}cm^{-1}$), 280 (sh)($\epsilon = 3400$ $M^{-1}cm^{-1}$).

ms: (FAB) m/z: 868 $(M-1)^+$; 905 $(M + 2H_2O)^+$.

XLIV. Reaction of bis-Z-Cystinyl di-His-OMe (24) with PDT followed by the addition of $CdCl_2$.2 1/2 . H_2O:

Preparation of the cadmium analog (45) of zinc finger motif:

To a stirred solution of (24) (0.110g, 0.135mmol) in MeOH 15(ml), under nitrogen blanket was added 0.8M methanolic PDT (0.29ml, 0.203mmol). The reaction mixture was left stirred for 6h, solvents evaporated, washed with petroleum ether (2x5ml), benzene (2x5ml), dried thoroughly, taken in MeOH (15ml), cooled at 0° C, admixed with 0.5M methanolic Et_3N (0.534ml) followed by after 0.75h, at 0° C, $CdCl_2$. 21/2.H_2O (0.025g, 0.135mmol). Immediate precipitation occured. The mixture was left stirred for next 0.5h, refrigerated overnight, centrifuged, washed the precipitate with hot MeOH (2x5ml) and dried thoroughly to afford (45) as white powder, mp 170°-172° C; yield: 0.076g (61%).

ir: ν_{max} (KBr) cm^{-1}: 3311, 1730, 1681, 1518.

nmr: ($CDCl_3$ + DMSO-d_6) (80MHz) : 3.33(b-m, 8H, Cys β-CH_2, His β-CH_2), 3.68(s, ester), 4.35(b-m, 2H, Cys α-CH), 4.73(b-m, 2H, His α-CH), 5.01(s, 2H, -CH_2Ar), 6.9(b, 2H, His 4,4'H), 7.38(b, 12H, Ar-, CysNH), 7.75(b-m, 4H, His 2,2'H, HisNH).

XLV. Reaction of Bis-Boc Cystinyl di-His-OMe (25) with PDT followed by $ZnCl_2$ Addition: Preparation of Zinc Finger Template (46):

To a stirred solution of (25) (0.250g, 0.34mmol) in MeOH (15ml), under dry, oxygen - free nitrogen blanket, was added 0.6M methanolic PDT (0.85ml, 0.51mmol). The reaction mixture was left stirred for 8h, solvents evaporated, dried thoroughly, dissolved in MeOH (25ml), cooled to 0^o C, admixed with 0.29M methanolic Et_3N (0.104ml, 0.748mmol), left stirred for 0.5h, and then admixed with 0.23M methanolic $ZnCl_2$ (1.41ml, 0.32mmol). The mixture was stirred for 1h at 0°C, refrigerated overnight, filtered, washed with hot MeOH (2x5ml), dried thoroughly to get Boc Zinc Finger Template (46) as a white powder, yield: 0.098g (overall yield from bis-Boc-Cystine : 36%), mp 255^o - 265^o C (dec.).

ir: ν_{max} (KBr) cm^{-1} : 3368, 1740, 1676, 1508, 1167, 1049.

nmr: δ(DMSO-d_6) (400MHz): 1.5 (s, 18H, $(CH_3)_3$-), 2.74 (b, 4H, His β-CH_2), 3.0 (b, 4H, Cys β-CH_2), 3.59 (b-d, 6H, ester), 4.38 (b, 4H, Cys α-CH, His α-CH), 6.28(b, 2H, Cys NH), 6.72(b-d, 2H, His4,4'H), 7.92 (b-d, 2H, His2,2'H), 8.40(b, 2H, HisNH).

ms: (FAB) m/z: 843 $(M + 2H_2O)^+$, 807 $(M)^+$.

$[\alpha]_D^{23} = 21.0^o$ (c, 0.250, DMF).

Anal.: Calcd. for $C_{30}H_{46}O_{10}N_8S_2$ Zn.$2H_2$ O : C, 42.7 H, 5.46 %

Found : C, 41.89 H, 5.69

XLVI. Reaction of Boc-S-Acm-Cys-His-OMe (28) with $ZnCl_2$:

Conversion of Boc-S-Acm-Cys-His-OMe (28) to Zinc Finger Template (46):

To a stirred solution of (28) (0.100g, 0.226mmol) in MeOH (5ml), under argon atmosphere, was added 0.123M methanolic $ZnCl_2$ (3.66ml, 0.452mmol). The reaction mixture was left stirred for 7h, adjusted pH to 9 with 5% aqueous ammonia solution, refrigerated for 3h, centrifuged, washed with water (2x5ml), MeOH (2x5ml) and dried thoroughly to afford the zinc complex (46), mp 255°-260° C; yield: 0.040g (37%), which was identical in all respects to sample reported previously (Experiment XLV)

XLVII. Reaction of bis-Boc-Cystinyl di-His-OMe (25) with PDT Followed by $CoCl_2.6H_2O$ Addition: Preparation of Cobalt-Finger Template (47):

To a stirred solution of (25) (0.200g, 0.27mmol) in MeOH (15ml), was added, under dry, oxygen - free nitrogen atmosphere, 0.6M methanolic PDT (0.68ml, 0.405mmol), the mixture left stirred for 8h, solvents evaporated , washed with petroleum ether (2x5ml) , benzene (2x5ml), dried thoroughly, dissolved in MeOH (15ml), cooled to 0° C, admixed with 0.72M methanolic Et_3N (0.76ml, 0.55mmol), followed by, after 0.5h, $CoCl_2$. H_2O (0.038g, 0.26mmol). The reaction mixture left stirred for 1h, refrigerated overnight, filtered washed with hot MeOH (2x5ml) and dried thoroughly to give (Boc-Cys His-OMe)Co complex as a green powder (47), mp 185°-187° C; yield: 45%.

ir: ν_{max} (KBr) cm^{-1} : 3362, 1735, 1685, 1507, 1250, 1166, 1021.

UV: λ_{max}(nm) (c, 1.039 x 10^{-3}M, DMF): 612.8(sh) (ϵ 339$M^{-1}cm^{-1}$), 576.6 (sh) (ϵ 359$M^{-1}cm^{-1}$).

ms: (FAB) m/z : 800 $(M-1)^+$, 836 (M-1 + $2H_2O$).

XLVIII. Reaction of bis-Boc-Cystinyl di-His-OMe (25) with PDT followed by the addition of $CdCl_2.21/2\ H_2O$: Preparation of the cadmium analog (48) of zinc finger motif:

The reaction of (25)(0.090g, 0.121mmol) with PDT followed by metal complexation precisely as described in experiment XLVI gave 0.018g of (48), mp 225°-230° C (dec.); yield: 27%.

ir: ν_{max} (KBr) cm^{-1} : 3332, 1740, 1676, 1517.

nmr: δ ($CDCl_3$ + DMSO-d_6) (80MHz) : 1.36(s, 18H, $(CH_3)_3C$-), 2.82(b-m, 8H, Cys β-CH_2, Hisβ-CH_2), 3.66(s, 6H, ester), 4.05(b, 2H, Cys α-CH), 4.48(b, 2H, His α-CH), 6.39(b, 2H, BocNH-), 7.06(b, 2H, His 4,4'H), 7.84(b, 4H, His 2,2'H, CysNH).

XLIX. Reaction of Bis-Boc His Cystine di-OMe (26)with PDT followed by $ZnCl_2$ addition : Preparation of Zinc Finger Template 'anti sense' analog (49):

To a stirred solution of (26) (0.300g, 0.404mmol) in MeOH (12ml), was added 0.6M methanolic PDT (1.01ml, 0.606mmol), under total nitrogen blanket, left stirred for 8h , solvents evaporated , washed with petroleum ether (2x5ml), benzene (2x5ml), dried thoroughly, dissolved in MeOH (10ml), cooled to 0° C, admixed with 0.72M methanolic Et_3N (1.2ml, 0.86mmol),followed by, after 0.5h stirring at 0°C, 0.153M methanolic $ZnCl_2$ (2.6ml, 0.396mmol).The reaction mixture was left stirred for 1h, refrigerated for 6h, filtered, washed with hot MeOH (2x5ml), dried thoroughly to give (Boc-His Cys-OMe)$_2$Zn complex (49) as white granules, mp 250°-255° C (dec.); yield: 0.170g (52%).

ir: ν_{max} (KBr) cm^{-1} : 3358, 1733, 1674, 1507, 1166, 1051.

nmr: δ (DMSO-d_6) (400MHz) : 1.38(s, 18H, $(CH_3)_3C$-), 2.85 (b, 8H, Cys β-CH_2 His β-CH_2), 3.65(s, 6H, ester), 4.29(b, 4H, Cys α-CH, His α-CH), 6.87(b, 2H, His4,4'H), 7.12(b, 2H, HisNH), 7.84(b, 2H, His2,2'H), 7.96(b, 2H, CysNH).

ms: (FAB) m/z : 807 $(M)^+$, 843(M^++2H_2O).

$[\alpha]_D^{27} = +8.3^o$ (c, 0.325, DMF).

L. Reaction of Bis-Boc His Cystine di-OMe (26) with PDT followed by addition of $CoCl_2.6H_2O$: Preparation of Cobalt Template Reverse analog (50):

To a stirred solution of (26) (0.090g, 0.121mmol) in MeOH (5ml), was added, under dry, oxygen-free nitrogen blanket, 0.6M methanolic PDT (0.30ml, 0.182mmol), left stirred for 8h, evaporated, washed with petroleum ether (2x5ml), benzene (2x5ml), dried thoroughly, dissolved in MeOH (8ml), cooled to 0^o C, admixed with 0.43M methanolic Et_3N (0.20ml, 0.14mmol) and then after 0.5h stirring, 0.72M methanolic $CoCl_2.6H_2O$ (0.028g, 0.118mmol). The reaction mixture was left stirred for 2h, filtered, washed with hot MeOH (2x5ml) and dried thoroughly to give (Boc-His Cys-OMe)$_2$Co complex (50) as a dark green powder, yield: 0.065g (67%), mp 220^o-225^oC (dec.).

ir: ν_{max} (KBr) cm^{-1} : 3382, 1728, 1674, 1507, 1166, 1049.

UV: λ_{max}(nm) (c, 7.65 x 10^{-3} M, DMF): 608.5(sh) (ϵ = 282 $M^{-1}cm^{-1}$), 583 (ϵ = 272 $M^{-1}cm^{-1}$).

ms: (FAB) m/z : 801 (M^+).

LI. Reaction of bis-Boc-His Cystine-di-OMe (26) with PDT followed by the addition of $CdCl_2$.2 1/2 H_2O: Preparation of Cadmium Template Reverse Analog (51) of zinc finger motif:

Bis-Boc-His-Cystine-di-OMe (26)(0.090g, 0.121mmmol) was processed, precisely as described in Experiment XLVI to afford 0.018gg (19%) of (51), mp 235°-240° C (dec.).

ir: ν_{max} (KBr) cm^{-1} : 3322, 1728, 1674, 1507.

LII. Treatment of Boc Zinc Finger Template (46), with TFAA-H_2O: Preparation of (TFA^- NH_3Cys HisOMe)$_2$Zn complex (52):

A solution of (46) (0.100g,) in water (1ml) was cooled in ice, admixed with TFAA (0.45ml), stoppered left aside overnight, evaporated and dried thoroughly to give (Cys His-OMe)$_2$Zn complex (52) mp 235°-240° C; yield: 0.101g (98%).

nmr: $\delta(D_2O)$ (400MHz): 2.81 (m, 4H, His β-CH_2), 3.08(m, 4H, Cys β-CH_2), 3.68(d, 6H, ester), 4.42(m , 2H, Cys α-CH), 4.75(m, 2H, His α-CH), 7.17(d, 2H, His4,4'H), 8.49 (d, 2H, His2,2'H).

ms: (FAB) m/z : 762 $[M\text{-}2Boc+TFA^-+2]^+$, 648 $[M\text{-}2Boc\text{-}2TFA^-+2H_2O]^+$, 605[M-2BOc-2]$^+$, 325 $[M+2H_2O/2\text{-}2Boc\text{-}2TFA^-]^+$.

LIII. Treatment of Boc Zinc Finger Template 'anti sense' (49), with TFAA-H_2O: Preparation of (H_3N^+-His Cys-OMe)$_2Zn^{II}$ TFA^- complex (53):

A solution of (49) (0.100g,) in water (1ml) was cooled in ice, admixed with TFAA (0.45ml), stoppered left aside overnight, evaporated and dried thoroughly to give (H_3N^+-His Cys-OMe)$_2Zn^{II}$ TFA^- complex (53) (53); yield: 0.101g (98%).

nmr: $\delta(D_2O)$ (400MHz): 2.90(b, 4H, His β-CH_2), 3.40(b, 4H, Cys β-CH_2), 3.72(d,

6H, ester), 4.32(b,2H, Cys α-CH), 4.66 (b, 2H, His α-CH), 7.40(d, 2H, His 4,4'H), 8.60(m, 2H, His 2,2'H).

ms: (FAB) m/z : 606[M-2Boc-1]$^+$, 301[(M-2Boc)/2 - 2]$^+$.

LIV. Reaction of cyclo[bisoxalyl cystine diOMe] with PDT followed by $ZnCl_2$ Complexation:

Preparation of (Oxalyl bis Cysteine Methyl Ester) $_{29}$ Zinc Complex (54):

To a stirred solution of (29) (0.087g, 0.135mmol) in MeOH (20ml) was added, 0.6M methanolic PDT (0.68ml, 0.406mmol). The reaction mixture was left stirred for 8h, filtered to remove undissolved materials, filtrate evaporated, thoroughly washed with benzene (3x5ml) to remove dithiolane polymer, dried to afford 0.055g (62.5%; 0.169mmol) of the thiol, mp 175°-177° C, which was taken up in MeOH (15ml), admixed with 0.72M methanolic solution of Et_3N (0.52ml, 0.372mmol), stirrred for 0.5h, admixed 0.067M methanolic $ZnCl_2$ of 99.99% purity (1.20ml, 0.080mmol) followed by $(Et_4)N$ Br (0.027g, 0.165mmol), stirred for 0.75h, refrigerated overnight, centrifuged, the residue thoroughly washed with MeOH (2x10ml) to remove all extraneous compounds, and dried to afford 0.035g (overall yield : 35.6% from (29)) of (54) as a microcrystalline solid, mp 275°-280° C, which gave analytical data in good agreement with expected values.

ir: ν_{max} (KBr) cm^{-1} : 3376, 1740, 1683, 1575, 1506.

nmr: δ (DMSO-d_6) (400MHz): 1.01 (b, 2H)(-SH), 2.82 (m, 4H) 3.17 (m, 4H)(β-CH_2), 3.64 (s, 12H)(ester), 4.58 (m, 4H)(α-CH), 9.28 (d, J=8Hz, 4H)(-NH-).

ms: (FAB) m/z: 712 $(MH)^+$.

LV. Preparation of "Insulin-Zinc Finger":

a. Zinc-Free Insulin[58]:

The pH of a suspension of commercial insulin (0.200g) in triple distilled (Quartz glass distilled) water (5ml) was adjusted to 2 with 2N HCl. To the resulting clear solution, was added, in drops, 15% aqueous NaCl (AR grade). Whilst the pH stabilised at 1.87, precipitation occurred. The reaction mixture was left aside overnight, centrifuged, washed with 15% NaCl solution (2x3ml), the wet precipitate was taken once again in triple distilled water and the above process repeated two times. Finally the precipitate was thorougly dried to get 0.120g of zinc-free Insulin.

b. Insulin Hexa Methyl Ester . 3HCl[59]:

To stirred and ice cooled solution of zinc-free insulin (0.070g) in EtOH:1.33N HCl :: 90:10 (10ml) (pH 2.10), was added, in drops, distilled ethereal diazomethane, maintaining the pH$\sim$ 4-5 with 0.6N HCl, until the light yellow color of the reagent persisted. The reaction mixture was refrigerated overnight, evaporated in vacuo (50°C) after addition of absolute EtOH (2x3ml) and dried thoroughly, to give insulin hexa methyl ester.3HCl, yield: 0.076g.

c. Insulin Hexa Methyl Ester Free Base:

To an ice cooled and stirred solution of insulin hexa methyl ester . 3HCl (0.060g, 9.68μmol) in MeOH (5ml), was added 0.102M methanolic Et_3N (1.4ml, 100mmol). The reaction mixture was stirred for $\sim$ 1h and evaporated to give 0.062g of insulin hexa methyl ester.

d. Treatment of Insulin Hexa Methyl Ester with PDT Followed by $ZnCl_2$ addition: Preparation of "Insulin-Zinc Finger":

Under nitrogen, to a stirred solution of the free base insulin hexa methyl ester (0.062g, 10.37 μmol) in MeOH:H_2O (85:15 v/v) (8ml), was added 0.100M methanolic solution of PDT (1ml, 100μmol), left stirred for 8h, solvents evaporated, washed with benzene (3x7ml), dried thoroughly, taken up in MeOH:H_2O:EtOH :: 85:15:10 (v/v) (10ml), cooled to 0° C, admixed with 0.144M methanolic Et_3N (0.01ml, 100μmol), left stirred for 40min., admixed with 0.102M methanolic $ZnCl_2$ (0.35ml, 35μmol), left stirred for 1h at 0° C, left aside under stirring at rt overnight, centrifuged, washed with water (quartz glass triple distilled) (3x4ml), dried thoroughly to give 0.040g of "insulin zinc free" as a white powder, whose electrophoretic profile showed that the disulfide bridges linking A and B chains were intact and that metal has been incorporated.

References

[1] (i). P.H. von Hippel, and O.G. Berg, Proc.Natl.Acad.Sci.U.S.A., 1986, *83*, 1608. (ii). P.H. von Hippel and O.G. Berg in Protein - Nucleic Acid Interaction (W. Saenger, ed.), Chapter 1, Macmillan, 1989, London.

[2] N.C. Seeman, J.M. Rosenberg and A. Rich, Proc.Natl.Acad.Sci.U.S.A., 1976, *73*, 804.

[3] D.D. Brown, Cell, 1984, *73*, 804.

[4] B. Picard and M. Wegnez, Proc.Natl.Acad.Sci.U.S.A., 1979, *76*, 241.

[5] A.M. Ginsberg, B.O. King and R.G. Roeder, Cell, 1984, *39*, 479.

[6] J. Miller, A.D. McLachlan and A. Klug, EMBO J., 1985, *4*, 1609.

[7] K. Nagai, Y. Nakaseko, K. Nasymuth and D. Rhodes, Nature, 1988, *332*, 284.

[8] (i). J.M. Berg, Proc.Natl.Acad.Sci.U.S.A., 1988, *85*, 99. (ii). T.J. Gibson, J.P.M. Postma, R.S. Brown and P. Argos, Prot.Eng. 1988, *2*, 209.

[9] (i). G. Parraga, S.J. Horvath, A. Eisen, W.E. Taylor, L. Hood, E.T. Young and R.E. Klevit, Science, 1988, *241*, 1489. (ii). M.S. Lee, G.P. Gippert, K.V. Soman, D.A. Case and P.E. Wright, Science, 1989, *245*, 635.

[10] N.P. Pavletich and C.O. Pabo, Science, 1991, *252*, 809.

[11] (i). J. Kuhawara and J.E. Coleman, Biochemistry, 1990, *29*, 8627; (ii). R.W. Kriwacki, S.E. Schultz, T.A. Steitz and J.P. Caradonna, Proc.Natl.Acad.Sci.U.S.A., 1992, *89*, 9759.

[12] B.A. Krizek, B.T. Amann, V.J. Kilfoil, D.L. Merkle and J.M. Berg, J.Am.Chem.Soc., 1991, *113*, 4518.

[13] J.R. Desjarlais and J.M. Berg, Proc.Natl.Acad.Sci.U.S.A., 1992, *89*, 7345.

[14] B.F. Luisi, W.X. Xu, Z. Otwinowski, L.P. Freedman, K.R. Yamamoto, and P.B. Sigler, Nature, 1991, *352*, 497.

[15] R. Marmorstein, M. Carey, M. Ptashne and S.C. Harrison, Nature, 1992, *356*, 408.

[16] J.M. Berg, Science, 1986, *232*, 485.

[17] T.L. South, B. Kim and M.F. Summers, J.Am.Chem.Soc., 1989, *111*,395.

[18] M.F. Summers, T.L. South, B.Kim and D.R. Hare, Biochemistry, 1990, *27*, 329.

[19] L.M. Green and J.M. Berg, Proc.Natl.Acad.Sci.U.S.A., 1989, *86*, 4047.

[20] B.C. Cunningham and M.G. Mulkerrin and J.A. Wells, Science, 1991, *253*, 545.

[21] H. Ogoshi, H. Hatakeyama, J. Kotani, A. Kawashima and K. Yasuhisa, J.Am.Chem.Soc., 1991, *113*, 8181.

[22] (i). Harrison, S.C. Nature, 1991, *353*, 715; (ii). Steitz, T.A. Q.Rev.Biophys. 1990 *23*, 205; (iii). Pabo, C.O.; Sauer, R.T. Annu.Rev.Biochem. 1992, *61*, 1053; (iv). Klug, A.; Rhodes, D. Trends Biochem. 1987, *12*, 464; (v). Pavletich, N.P.;Pabo,

C.O. Science, 1991, *252*, 809; (vi). Vallee, B.L.; Coleman, J.E.; Auld, D.S. Proc.Natl.Acad.Sci. U.S.A. 1991, *88*, 999; (vii). Marmorstein, R.; Carey, M.; Ptashne, M.; Harrison, S.C. Nature, 1992, *356*, 408; (viii). Kraulis, P.J.; Raine, A.R.C.; Gadhavi, P.L.; Lane, E.D. Nature, 1992 *356*, 448; (ix). Baleja, J.P.; Marmorstein, R.; Harrison, S.C.; Wagner, G. Nature, 1992, *356, 450*

[23] L.Zervas and I. Photaki, J.Am.Chem.Soc., 1962, *84*, 3887.

[24] (i). Davies, J.Am.Chem.Soc., 1928, *50*, 2778; (ii). J.G. Wilson, L.A. Cohen, ibid., 1963, *85*, 560.

[25] V. Du Vigneaud and G.L. Miller, Biochem.Prep., 1952, *2*, 74.

[26] J. Greenstein and Winitz, Amino Acids and Peptides, John-Wiley, Vol.2, p. 1269.

[27] O. Keller, W.E. Keller, G. Van Look and G. Wersin, Org.Syn. *63*, 167.

[28] J.D. Milkowski, D.F. Veber and R. Hirschmann, Org.Syn. Coll.Vol.6, Ed. Noland, John-Wiley p.5.

[29] D.F. Veber, J.D. Milkowski, S.L. Verga, R.G. Denkewalter and R. Hirschmann, J.Am.Chem.Soc., 1972, *74*, 5456.

[30] N.C. Davies, J.Biol.Chem. 1956, *223*, 935.

[31] J. Greenstein and M. Winitz, Amino Acids and Peptides, John-Wiley, Vol.2, p. 1061

[32] B.O. Hanford, T.A. Hylton, K.T. Wang and B. Weinstein, J.Org.Chem., 1968, *33*, 4251.

[33] H. Peter, M. Brugger, J. Schreiber and A. Eschenmoser, Helv. Chim. Acta, 1963, *46*, 577

[34] G. Brauer,Inorg.Chem.Prep. (Ed.) Academic Press, N.Y. , 2nd edition, 1963, Vol.1, p.371.

[35] S. Ranganathan and N. Jayaraman, Tetrahedron, 1992, *48*, 931.

[36] S. Ranganathan and N. Jayaraman, Tett. Lett., 1992, *33*, 6681.

[37] S. Ranganathan, N. Jayaraman, R. Roy and K.P. Madhusudanan, Communicated.

[38] H. Kessler, D.F. Mierke, D. Donald and M. Furber, Angew. chem. Int. Ed. Engl., 1991, *30*, 954.

[39] B. Donzel, B. Kamber, K. Wuthrich and R. Schwyzer, Helv. Chim. Acta, 1972, *55*, 947 ;

[40] (i). J.R. Kalman, T.J. Blake, D.H. Williams, J. Feenay and G.C.K. Roberts, J.Chem.Soc., Perkin Trans. I, 1979,1313 ; (ii). E. Hyde, J.R. Kalman, D.H. Williams, J. Feenay and R.R. Olsen, J.Chem.Soc., Perkin Trans.I, 1982, 1041.

[41] R.L. Baxter, S.S.B. Glover, E.M. Gordon, R.O. Gould, M.C. McKie, A.I. Scott and M.D. Walkinshaw , J.Chem.Soc. Perkin Trans. I, 1988,365.

[42] (i) B. Panijpan, J.Chem.Educ., 1977, *54*, 670 ; (ii). B.V.V. Prasod, A. Ravi and P. Balaram, Biochim.Biophys. Res.Commun., 1981, *103*, 1138.

[43] N. Srinivasan, R. Sowdhamini, C. Ramakrishnan and P. Balaram, Int.J.Peptide Protein Res. 1990, *36*, 147.

[44] S.L. Schreiber, Science, 1991, *251*, 283; S.L. Schreiber, J. Liu, M.W. Albers, M.K. Rosen, R.F. Standaert, T.J. Wandless and P.K. Somers, Tetrahedron, 1992,*48*, 2545.

[45] G.D. van Duyne, R.F. Standaert, S.L. Schreiber and J. Clardy , J.Am.Chem.Soc., 1991, *113*, 7433.

[46] S. Ranganathan, D. Ranganathan, S. Bamezai, W.P. Singh D. Bhattacharryya, G.P. Singh, R. Rathi, S. Saini, N. Jayaraman and B.K. Patel, Pure & Appl. Chem., 1990, *62*, 1437.

[47] A. Dabre, Practical Protein Chemistry - A Hand Book, Wiley, N.Y, 1986, p. 71.

[48] M. Caserio and J.J. Kim, Phosphorus and Sulfur, 1985, 304.

[49] L. Weil and T.S. Seibles, Arch. Biochem. Biophys., 1961, *95*, 470.

[50] S. Ranganathan and N. Jayaraman, J. Chem. Soc. Chem. Commun., 1991, 934.

[51] G. Jung, C. Carrera, H. Bruckner and W.G. Bessler, Ann., 1983, 1608.

[52] K.S. Iyer and W.A. Klee, J.Biol.Chem., 1973, *248*, 707.

[53] Yu.M. Torchinsky, Sulfur in Proteins, Pergamon, Oxford, 1981, p. 202.

[54] L. Regan and N.D. Clarke, Biochemistry, 1990, *29*, 10878.

[55] J. Diaz, R. Guegan, M. Beaumont, J. Benost, J. Clement, C. Fauchard, D. Galties, J. Millan, C. Muneaux, Y. Muneaux, M. Vedel and R. Schwyzer, Bioorg. Chem., 1979, *8*, 429.

[56] T.L. Blundal and L.N. Johnson in Protein Crystallography, Academic Press, 1976, p.24.

[57] (i). Micheal Kochoyan and M.A. Weiss, Nature, 1991, *354*, 238 ; (ii). A.D. Kline and R.M. Justice, Jr., Biochemistry, 1990, *29*, 2906.

[58] J. Schlichtkrull, Acta. Chem. Scand., 1956, *10*, 1455.

[59] M.A. Ruttenberg, Science, 1972, *177*, 623.

[60] (i). C.R. Cantor and P.R. Schimmel, Biophysical Chemistry, W.H. Freeman and Co., San Francisco, 1980, Part II, p.412.

[61] T. Maniatis, E.F. Fritsch and J. Sambrook, Molecular Cloning: A Laboratory Manual, Cold Spring Harbor Laboratory, 1982.

[62] D. Chatterji and U.S. Nandi, J.Sci.Indust.Res. 1978, *37*, 449

[63] A. Rich, A. Nordheim and A.H.-J. Wang, . Annu.Rev.Biochem. 1984, *53*, 791;

[64] V.I. Ivanov, L.E. Minchenkova, A.K. Schyolkina and A.I. Poletayev, Biopolymers, 1973, *12*, 89; R.K. Mishra, P.K. Latha and S.K. Brahmachari, Nucl.Acids.Res., 1988, *16*, 588.

[65] Y.A. Shin and G.L. Eichhorn, Biochemistry, 1968, *7*, 1026

[66] The incursion of DNA aggregation - which has a connotation of irreversibility - on addition of A is clearly ruled out. The stoichiometry and cooperativity could be explained only on the basis of selectivity and formation of well defined structures. In the case of complex formation with poly d(G-C), the formation of

well-defined structure is facilitated by initial interaction between NHs of imidazoles and negatively charged phosphodiester group, followed by an interaction between the free amino group and -C^6=O and N^7 of guanine residues. Since the latter possibility do not exist in the case of poly d(A-T), the interaction with A is found to be non-specific interaction.

The results of the present intermolecular association since no drastic changes in the pattern or λ_{max} peaks either in UV or in CD were seen. (Brahms et.al. Biochem. 1969, *8* (8) 3269-3278). and the study was carried-out at room temperature, low ionic strength and at micromolar concentrations, which are unfavourable for any interaction leading to aggregation or precipitation.

[67] S. Ranganathan and N. Jayaraman, Communicated, 1993.

VITAE

I, N. Jayaraman, born in Pudukkottai, Tamil Nadu, on 25th of May, 1964. I did my B.Sc.(Chemistry) from University of Madras in 1984, and after about one and half years of employment in a pharmaceutical company, I joined M.Sc.(Chemistry) in Annamalai University in 1986 and subsequently joined for the Ph. D., programme in the Department of Chemistry, IIT Kanpur in 1988. At present, I am Senior Research Fellow.

List of Publications:

(1) Chemical Approaches to the Re-structuring of Proteins
S. Ranganathan, D. Ranganathan, S. Bamezai, W.P. Singh, D. Bhattacharyya, G.P. Singh, R. Rathi, S. Saini, N. Jayaraman and B.K. Patel, Pure & Appl. Chem., 1990, *62*, 1437.

(2) Highly Efficient Propane-1,3-dithiol Mediated Thiol - Disulfide Interchange: A Facile and Clean Methodology for S-S Reduction in Peptides
S. Ranganathan and N. Jayaraman, J. Chem. Soc. Chem. Commun., 1991, 934.

(3) Synthesis of "Zinc Finger" Template
S. Ranganathan and N. Jayaraman, Tetrahedron, 1992, *48*, 931.

(4) A General and Versatile Route to "Zinc Finger" Templates
S. Ranganathan and N. Jayaraman, Tett. Lett., 1992, *33*, 6681.

(5) A Short Serendipitous Synthesis of Minimal Glucocorticoid Receptor Zinc Template

S. Ranganathan, N. Jayaraman, R. Roy and K.P. Madhusudanan, Communicated, 1993.

(6) Specific Interaction Between Minimal Zinc Finger Motif and DNA

S. Ranganathan, N. Jayaraman and D. Chatterji, Communicated, 1993.

Symposium Proceedings:

(1) Manifestations of Molecular Recognition in the Genesis of Information - Function Composites

S. Ranganathan, G.P. Singh, H. Rastogi, D. Kundu , N. Jayaraman and D. Chatterji, Discussion Meeting on: Molecular Recognition, Chemical and Biological Aspects, Indian Institute of Science, Bangalore, India, Oct. 1992.

(2) Zinc Finger Template Prototypes: Synthesis and DNA Interaction Studies with Template Prototypes

Invited Talk,

Third National Organic Symposium Trust Conference, Bhubeneshwar, India, Dec. 1992.